Université catholique de Louvain
Faculté d'Ingénierie Biologique, Agronomique et Environnementale
Institut des Sciences de la Vie
Groupe de Physiologie Moléculaire (FYMO)

Endoplasmic Reticulum-Associated Degradation of mutated forms of yeast ABC-transporter Pdr5

Thèse présentée par Nathalie Campagnolo en vue de l'obtention du grade de Docteur en Sciences Agronomiques et Ingénierie Biologique

Supervisor:
Prof. Michel Ghislain

President of the jury:
Prof. Jacques Fastrez

Members of the jury :
Prof. Anabelle Decottignies
Prof. Damien Hermand
Prof. Jacques Mahillon
Prof. Micheline Vandenbol

July 2011

Ces quatre années de thèse n'auraient pu aboutir sans le soutien, l'intervention et la présence de nombreuses personnes.

Tout d'abord, je souhaiterais remercier mon promoteur pour m'avoir donné l'opportunité de faire un doctorat ainsi que pour ses nombreux conseils et remarques avisées.

Aussi, je remercie vivement mes lecteurs de thèse pour leurs aides et leurs commentaires qui ont permis d'aboutir à ce travail.

Je voudrais également remercier tous les membres passés et présents du groupe FYSA/FYMO pour leurs aides, leurs soutiens, leurs discussions intéressantes et l'excellente atmosphère de travail. Un merci tout particulier à la «Polish Team» et plus spécifiquement à my dear Aga pour tous ces bons moments partagés et les souvenirs inoubliables accumulés, ce fut un vrai plaisir de travailler à ses côtés durant ces 4 années!

Enfin, je souhaiterais remercier mes parents, ma famille et mes amis pour leurs soutiens divers, leurs compréhensions (de mes nombreuses absences et retards..), leurs encouragements, leurs soirées divertissements, leurs capacités d'écoute et pour beaucoup d'autres choses encore, ce qui a contribué grandement à l'accomplissement de ce travail colossal. Merci à vous!

Table of contents

Abbreviations

Summary

Introduction.....1

1. ABC transporter proteins.....4
1.1. Structure of ABC transporter proteins.....4
1.2. Yeast ABC proteins.....5
1.3. Transport mechanisms of ABC transporter proteins.....7
2. Pleiotropic Drug Resistance ABC-transporter Pdr5.....10
2.1. Membrane topology of Pdr5p.....10
2.2. Substrate specificity of Pdr5p.....12
2.3. Transcriptional regulation of the *PDR5* gene.....14
3. Degradation of proteins.....17
3.1. ER-associated degradation.....17
3.1.1. Recognition of aberrant proteins in ER.....20
3.1.2. ER-associated ubiquitylation.....24
3.1.2.1. The Hrd1p complex.....26
3.1.2.2. The Doa10p complex.....29
3.1.3. Model ERAD substrates are degraded through distinct ERAD pathways.....30
3.1.3.1. Model ERAD substrates.....30
3.1.3.1.1. Soluble luminal proteins.....32
3.1.3.1.2. Soluble cytosolic protein.....33
3.1.3.1.3. Membrane protein with a misfolded cytosolic domain.....33
3.1.3.1.4. Membrane proteins with a luminal lesion.....34
3.1.3.1.5. Membrane protein with a misfolded domains facing the ER lumen and the cytosol.....35
3.1.3.2. Distinct ERAD pathways.....35
3.1.4. Retro-translocation into the cytosol and delivery to the 26S proteasome.....37
3.1.4.1. Retro-translocon.....37
3.1.4.2. The Cdc48p/Ufd1p/Npl4p complex.....39
3.1.4.3. Delivery to the proteasome.....39
3.1.4.4. The 26S proteasome.....40
3.1.5. The Unfolded Protein Response.....42
3.1.6. Accumulation of unfolded proteins in subcellular compartments.....42
3.2. Vacuolar degradation.....44

3.2.1. Transport pathways to the vacuole....45
3.2.2. Ubiquitin as an endocytosis signal for plasma membrane proteins....47
4. Role of the secretory pathway in ERAD....48
4.1. ER-to-Golgi transport....48
4.2. Golgi-to-ER transport....51

Aim of the study....55

Results....61

1. Drug sensitivity phenotype of yeast strains expressing Pdr5p variants....66
1.1. The three mutated forms of Pdr5p....66
1.2. The three C-truncated variants of Pdr5p....73
2. Expression levels of Pdr5p variants....76
2.1. Western blot analysis....76
2.2. Northern blot analysis....82
3. Turnover of mutated Pdr5p forms....83
3.1. The three mutated forms of Pdr5p....85
3.2. The three C-truncated variants of Pdr5p....87
4. Effect of mutations in ER-associated Ub-ligases on degradation of Pdr5p variants....88
4.1. Western blot analysis....88
4.2. Pulse-chase analysis....90
5. Implication of the putative Der1p retro-translocon in degradation of Pdr5p variants....96
6. Effect of a mutation impairing vacuolar degradation on stability of Pdr5p variants....98
7. Effect of mutations in ER-associated Ub-ligases on subcellular localization of mutated Pdr5p forms....99
8. Role of Sar1p/COPII machinery and ER-to-Golgi transport in degradation of the three mutated forms of Pdr5p....103
8.1. Pulse-chase analysis....104
8.1.1. Effect of inactivation of the Sar1p/COPII machinery....104
8.1.2. ER-to-Golgi and Golgi-to-ER transports....107
8.2. Subcellular localization of Pdr5p variants in strains impaired in the early steps of the secretory pathway and in Golgi-to-ER transport 113
9. Degradation of C-terminally truncated forms of Pdr5p....118
9.1. Implication of the ERAD-C pathway in degradation of $Pdr5^{TM1-6}$....118
9.2. $Pdr5^{TM1-8}$ is a long-lived protein....127

9.3. Vacuolar and ER-associated degradation of Pdr5^{TM1-10}.....134
10. Response of the UPR pathway to the expression of Pdr5p variants.....144

Discussion and perspectives.....151

1. Degradation of Pdr5^{TM1-6}.....154
2. Degradation of Pdr5^{TM1-8}.....157
3. Degradation of Pdr5^{TM1-10}.....158
4. Degradation of Pdr5$^{L183P+C1427Y}$.....162
5. Degradation of Pdr5^{L183P} and Pdr5^{C1427Y}.....163
6. Protein sorting according to misfolded domain location.....165
7. Perspectives.....168

Materiels and Methods.....173

1. Strains and media.....175
1.1. *Escherichia coli*.....175
1.2. *Saccharomyces cerevisiae*.....175
2. DNA constructs and oligonucleotides.....177
3. Antibodies.....182
4. Drug resistance assays.....183
5. Protein analysis.....184
5.1. Preparation of yeast whole-cell extracts.....184
5.2. Protein quantification.....184
5.3. Proteins separation and detection.....185
5.3.1. SDS-polyacrylamide gel electrophoresis (PAGE).....185
5.3.2. Western blot.....186
6. RNA.....187
6.1. RNA extraction.....187
6.2. RNA quantification.....188
6.3. Northern blot.....188
7. Pulse-chase analysis.....190
8. β-galactosidase activity measurements.....191
9. Fluorescence microscopy.....192

References.....195
Titres récents de la collection.....215

Annex (Pulse-Chase summary table).....225

β-gal	beta-galactosidase	E2	Ubiquitin-conjugating enzyme
ABC	ATP Binding Cassette	E3	Ubiquitin protein ligase
Amp	Ampicillin	E4	Ubiquitin chain elongase
C/Cys	Cysteine	EDTA	EthyleneDinitriloTetra Acetic acid, disodic salt
CFTR	Cystic Fibrosis Transmembrane conductance Regulator	EDEM	ER degradation-enhancing 1,2-mannosidase-like protein
CNX	Calnexin	ER	Endoplasmic Reticulum
COPI	COat Protein complex I	ERAC	ER-Associated Compartment
COPII	COat Protein complex II	ERAD	ER-Associated Degradation
CPY	CarboxyPeptidase Y	ERAD-C	cytosolic ERAD
CRT	Calreticulin	ERAD-L	luminal ERAD
dNTP	DesoxyriboNucleotide TriPhosphate	ERAD-M	membranous ERAD
DTT	DiThioThreitol	Gal	Galactose
E1	Ubiquitin-activating enzyme	GFP	Green Fluorescent Protein

HEPES	N-2-HydroxyEthylPiperazine-N'-2-Ethane-Sulfonic acid	ONPG	O-NitroPhenyl-β-D-Galactopyranoside
His	Histidine	ori	origin of replication
Hsp	Heat Shock protein	P/Pro	Proline
K/Lys	Lysine	PCR	Polymerase Chain reaction
L/Leu	Leucine	PDR	Pleiotropic Drug Resistance
Lac	Lactose	PDRE	PDR Element
lacZ	the gene for beta-galactosidase	PMSF	PhenylMethylSulfonyl Fluoride
LB	Luria-Bertani	rpm	rotation by minute
MDR	Multiple Drug Resitance	SDS	Sodium DodecylSulfate
MIC	Minimal Inhibitor Concentration	PAGE	PolyAcrylamyde Gel Electrophoresis
NBD	Nucleotide Binding Domain	$t_{1/2}$	protein's half-life
OD_{230} OD_{260} OD_{280} OD_{420} OD_{595} OD_{600}	Optical density absorbance at a wavelength of 230, 260, 280, 420, 595 and 600 nm.	TE	Tris/EDTA buffer

TM	Transmembrane	UBX	Ubiquitin regulatory X
TMD	TM Domain	UGGT	UDP-glucose:glycoprotein glucosyltransferase
TMS	TM Span or Segment	UPR	Unfolded Protein Response
Trp	Tryptophane	UPRE	UPR Element
Tris	Trishydroxymethyl aminomethane	Ura	Uracil
Ub	Ubiquitin	wt	wild-type
UBA	ubiquitin-associated	Y/Tyr	Tyrosine
UBL	ubiquitin-like		

Summary

One of the research activity in our laboratory focuses on the quality control and degradation of mutated versions of the yeast plasma membrane ABC-transporter Pdr5. The main objective of the doctoral work was to ascertain the veracity of the ERAD model established with engineered fusion proteins featuring how newly synthesized membrane proteins are targeted for degradation by the proteasome. Depending of the localization of the mutated domain, ER lumen versus the cytosol, the ERAD model predicts that misfolded proteins are degraded via different pathways (Carvalho et al. 2006; Vashist et al. 2001; Vashist and Ng 2004). To ascertain the model, we have contructed 3 protein variants, $Pdr5^{L183P}$, $Pdr5^{C1427Y}$ and $Pdr5^{L183P+C1427Y}$. According to the model, $Pdr5^{L183P}$ that is misfolded as the result of a mutation in a cytosolic region should be ubiquitylated by the Ub-ligase Doa10p (ERAD-C pathway) and transported back to the cytosol in a Der1p and Sec61p-independent process. In contrast, $Pdr5^{C1427Y}$ with a misfolded region facing the ER lumen should be ubiquitylated by Hrd1p (ERAD-L pathway) and required Der1p and/or Sec61p for its degradation. $Pdr5^{L183P+C1427Y}$ variant that combines the cytosolic and luminal substitutions should be targeted by the ERAD-C pathway for degradation as this pathway predominates the ERAD-L pathway. The importance of the ER-to-Golgi transport (post-ER quality control) for proteasome-mediated degradation of mutated variants have been also tested. An other objective of this work is the identification of amino-acid determinants in the Pdr5 sequence which trigger the quality control system and subsequent degradation using C-truncated variants.

Introduction

Introduction of antibiotics in medical practice in the 1940s led to the emergence of antibiotic resistance. Various organisms (first showed in mammalian cells) developped multiple resistances against a range of drugs, a phenomenon called multiple drug resistance (MDR). MDR had an impact on cancer treatments but also on the development of effective therapies. Some cases of MDR are associated with the overexpression of membrane proteins of the ATP Binding Cassette (ABC) family, which pump the drugs out of the cell. The first characterized MDR transporters were eukaryotic members of the ABC superfamily, the mammalian P-glycoprotein (MDR1) and the multidrug resistance-associated protein 1 (MRP1) (Cole et al. 1992; Lubelski et al. 2007; Riordan et al. 1985).

Research work in our laboratory focuses on the mechanisms by which yeast develops resistance to naturally occuring cytotoxic compounds and xenobiotics. In particular, we are interested in degradation of the plasma membrane ABC transporter Pdr5p by the ubiquitin/proteasome system. Pdr5p is homologous to human MDR and cystic fibrosis transmembrane conductance regulator (CFTR) ABC-transporters and is a major MDR determinant in yeast. Understanding the mechanisms by which a nascent misfolded ABC-transporter protein is recognized by the quality control system in the ER and degraded by the proteasome could be the way to cure human diseases that are caused by a dysfunction of the quality control system (cystic fibrosis, Parkinson's, Huntington's, Alzheimer's) (Selkoe 2003).

1. ABC transporter proteins

The ABC transporter family is present in all living organisms (e.g. 71 members in bacterium *Escherichia coli*, 31 members in yeast *Saccharomyces cerevisae*, 48 members in *Homo sapiens* and 113 members in plant *Arabidopsis thaliana*) (Moussatova et al. 2008). The majority of ABC proteins are active transporters which couple ATP hydrolysis to the transport of substrates across biological membranes. They have been shown to be involved not only in the export but also in the import of a wide variety of compounds. «ABC exporters» in prokaryotes and eukaryotes mediate the extrusion of toxic substances whereas «ABC importers» in prokaryotes allow essentiel nutrients to be taken up (Lubelski et al. 2007).

1.1. Structure of ABC transporter proteins

ABC transporters have a characteristic modular structure consisting of a hydrophobic transmembrane domain (TMD) and a cytosolic hydrophilic nucleotide-binding domain (NBD). This module is repeated twice in some proteins. The TMD consists of six membrane-spanning α-helices, or transmembrane spans (TMS), and forms the channel through which the substrates cross the membrane. The NBD (≃ 250 amino acids) contains the Walker A ($GX_4GK[S/T]$) and B ($[\text{hydrophobic residues}]_4D$) motifs involved in ATP binding and hydrolysis. The NBD also contains the ABC signature sequence LSGGQ (Michaelis and Berkower 1995). Even between ABC proteins sharing a relative high sequence identity, the TMDs are highly

divergent in comparison to the NBDs. This divergence might be responsible for the substrate specificity.

1.2. Yeast ABC proteins

Different classification schemes for ABC proteins from the yeast *S. cerevisiae* have been proposed (Bouige et al. 2002; Dassa and Bouige 2001; Jungwirth and Kuchler 2006). The classification presented here separate full-sized transporters from half-sized transporters and soluble ABC proteins (Figure 1).

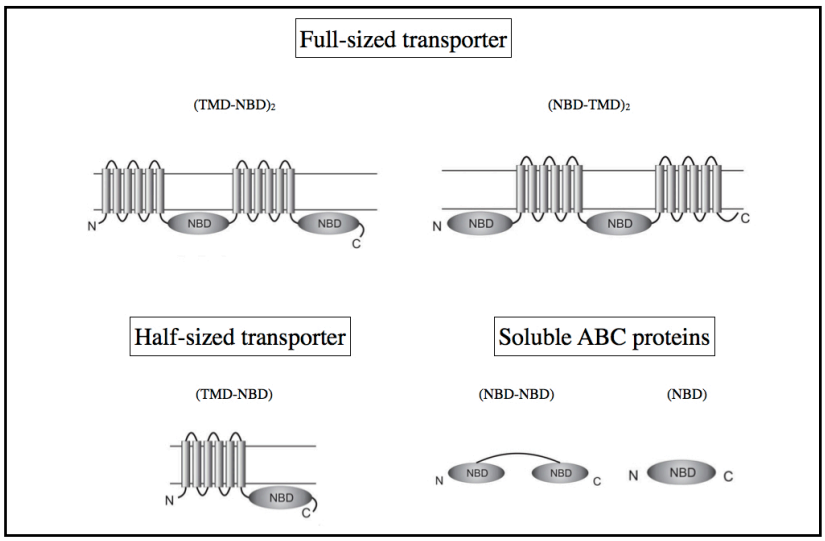

Figure 1. Membrane topology of yeast ABC transporters (modified from Kovalchuk and Driessen 2010). ABC proteins can be divided into full-sized transporters consisting of 2 modules of (TMD-NBD) or (NBD-TMD), half-sized transporters with a (TMD-NBD) conformation and TMD-lacking soluble polypeptides with a NBD or $(NBD)_2$ topology.

The full-sized ABC transporters can adopt two distinct topologies : (NBD-TMD)$_2$ or (TMD-NBD)$_2$ (Bauer et al. 1999; Decottignies and Goffeau 1997).

The (NBD-TMD)$_2$ topology is illustrated by members of the PDR subfamily including Pdr5p, Pdr10p, Pdr11p, Pdr12p, Pdr15p and Snq2p. Pdr5p and Snq2p are responsible for the resistance to a large variety of structurally unrelated xenobiotics (Kolaczkowski et al. 1998). Snq2p shares 40% amino acid identity with Pdr5p and mediates specifically the transport of benomyl whereas Pdr5p mediates the transport of cycloheximide or itraconazole (the function of Pdr5p is detailed in §2). Pdr10p and Pdr15p share 66 and 74% sequence identity with Pdr5p. Pdr15p is a stress response factor responsible for the efflux of chloramphenicol and polyoxyethylene-9-lauryl (Giaever et al. 2002; Rogers et al. 2001; Wolfger et al. 1997; Wolfger et al. 2004). Pdr10p is believed to play a role in pleiotropic drug resistance by virtue of its resemblance to Pdr5p (Abolmaali et al. 2008; Decottignies et al. 1998). Experimental evidence supporting such a role is lacking. Pdr11p (31% identity with Pdr5p) is involved in the transport of sterols when cells are grown in the absence of oxygen (Wilcox et al. 2002). Pdr12p (39% identity with Pdr5p) exports organic acids such as sorbate, benzoate, acetate and propionate (Piper et al. 1998; Schuller et al. 2004).

The (TMD-NBD)$_2$ topology is illustrated by members of the MRP (multidrug resistance-associated protein) and MDR subfamilies, including Yor1p, Ycf1p and Ste6p. Yor1p and Ycf1p are members of the MRP subfamily and are the closest yeast homologues of human CFTR. Yor1p is

involved in the efflux of erythromycin and oligomycin across the plasma membrane. Ycf1p is localized in the vacuolar membrane and confers resistance to cadmium and arsenite (Katzmann et al. 1995; Li et al. 1996). The MDR subfamily consists of members which are not associated with drug resistance. Ste6p is member of the MDR subfamily and mediates the export of a sexual pheromone (McGrath and Varshavsky 1989).

Half-sized transporters with a $(TMD\text{-}NBD)_1$ topology include Atm1p, Mdl1p and Mdl2p. These proteins extrude iron-sulfur clusters or peptides outside the mitochondria (Kispal et al. 1999; Young et al. 2001).

Caf16p and Yef3p are soluble ABC proteins consisting of one and 2 NBDs, respectively. Caf16p is involved in transcription initiation and mRNA elongation and degradation (Liu et al. 2001). Yef3p is a translation elongation factor facilitating the release of deacylated tRNA from the ribosome (Triana-Alonso et al. 1995).

1.3. Transport mechanisms of ABC transporter proteins

Our understanding of the molecular mechanisms of substrate transport is limited by the lack of structural information due to the difficulty in crystallizing membrane proteins. A 1.5-Å X-ray structure of a bacterial histine permease (HisP) NBD was published in 1998 (Hung et al. 1998). High-resolution X-ray structures of NBDs from bacterial MutS (Lamers et al. 2000; Obmolova et al. 2000), MalK (Diederichs et al. 2000) and Rad50 (Hopfner et al. 2000) confirmed the structure published by Hung and co-

workers (1998). The X-ray structure of a soluble full-length ABC transporter is available for vitamin B12 importer BtuCD from *E. coli* (Locher et al. 2002) and for lipid flippase MsbA from *E. coli* (Chang and Roth 2001) and *Vibrio cholerae* (Chang 2003), the latter being a close homologous to mammalian P-glycoprotein (P-gp). BtuCD forms a dimeric complex with the ATP-binding sites facing each other at the interface between the NBDs («closed» dimer conformation) whereas dimeric MsbA shows the NBDs in a «open» conformation (see Figure 2). The 3-D structure of *Vibrio cholerae* MsbA presents the ATP-binding sites facing each other in contrast to the *E. coli* MsbA structure (Chang and Roth 2001; Chang 2003). These differences could reflect different conformational states during the catalytic cycle.

Higgins and Linton (2004; 2007) have proposed the so-called «ATP-switch model» illustrated in Figure 2. In this model, the switch between the «open» and «closed» conformations of the NBDs results in a directional transport of the substrate, via a conformational change of the TMDs. In the «open» conformation (basal state, Figure 2, top left), the NBDs are able to rotate freely relative to the TMDs. A high-affinity binding site for the transport substrate on the TMDs is accessible from the cytoplasmic face of the membrane. The transport cycle is initiated by the binding of the substrate to its high-affinity binding site on the TMDs. This induces a conformational change which is transmitted to the NBDs, faciliting ATP binding and transition from the «open» to «closed» NBD dimer conformation (Figure 2, StepII). ATP binding induces changes in the substrate-binding site affinity of the TMDs, resulting in the release of the substrate in the extracellular

medium. In StepIII, ATP hydrolysis induces the destabilization of the transporter to the original state but not yet its restoration. The substrate-binding site remains exposed to the extracellular face of the membrane and the conformation of the TMDs is still distinct from that of the nucleotide-free state. Sequential release of P_i and ADP resets the transporter to its basal «open» dimer conformation ready to initiate another transport cycle (Figure 2, StepIV). It seems that only one ATP molecule is required for some ABC transporters.

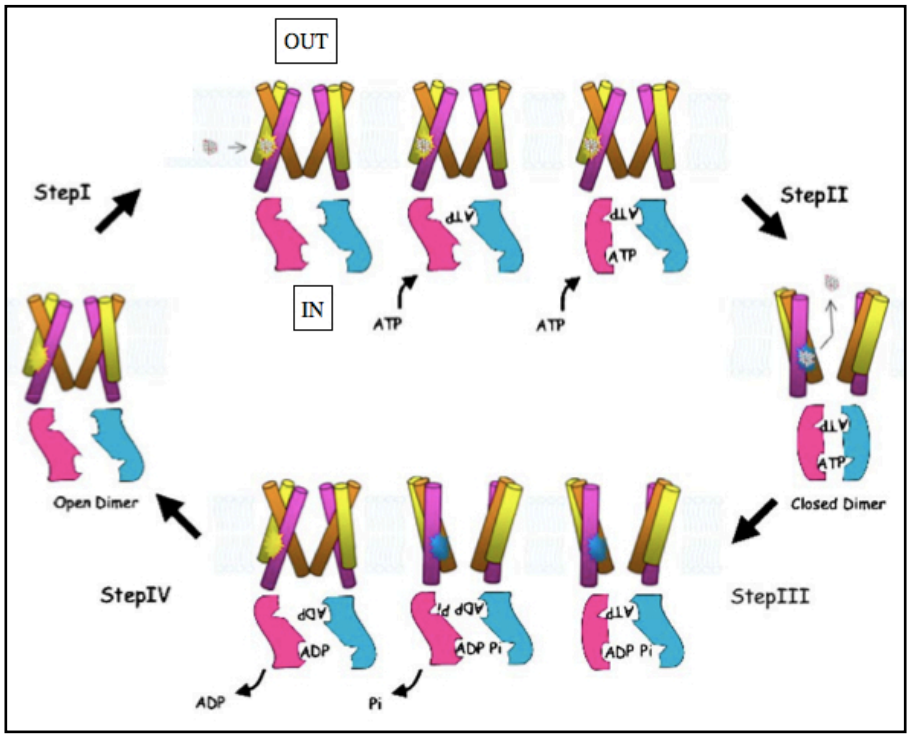

Figure 2. The «ATP-switch model» illustrating the mechanism of the transport cycle of an ABC transporter (modified from Higgins and Linton 2007). TMDs are shown as «cylinders» associated with globular NBDs at the cytoplasmic side of the membrane. See text for details.

2. Pleiotropic Drug Resistance ABC-transporter Pdr5

The Pdr5 protein from *S. cerevisiae* is a 165 kDa (1511 amino acids) ABC-transporter localized in the plasma membrane (Balzi et al. 1994; Meyers et al. 1992). The *PDR5* gene was independently identified by four laboratories using different genetic approaches (Balzi et al. 1994; Bissinger and Kuchler 1994; Hirata et al. 1994; Kralli et al. 1995). Pdr5p is a stable protein (Decottignies et al. 1999) with less than 10% degradation seen over a 180-minute incubation in the presence of protein synthesis inhibitors.

2.1. Membrane topology of Pdr5p

Pdr5p has a $(NBD\text{-}TMD)_2$ topology (Figure 3). The Walker A motif of the first NBD (NBD1) has the lysine residue replaced by a cysteine ($GX_4G\underline{C}T$) whereas the Walker B motif lacks the 4 hydrophobic residues preceding the conserved aspartate residue. On this NBD1 the histidine of the H-loop is missing. The NBD2 presents an incomplete ABC signature (LNVEQ) (Balzi et al. 1994). The presence of variant residues in the NBDs supports the model in which two Pdr5p molecules associate with each other, via the NBDs, to form a functional transporter complex.

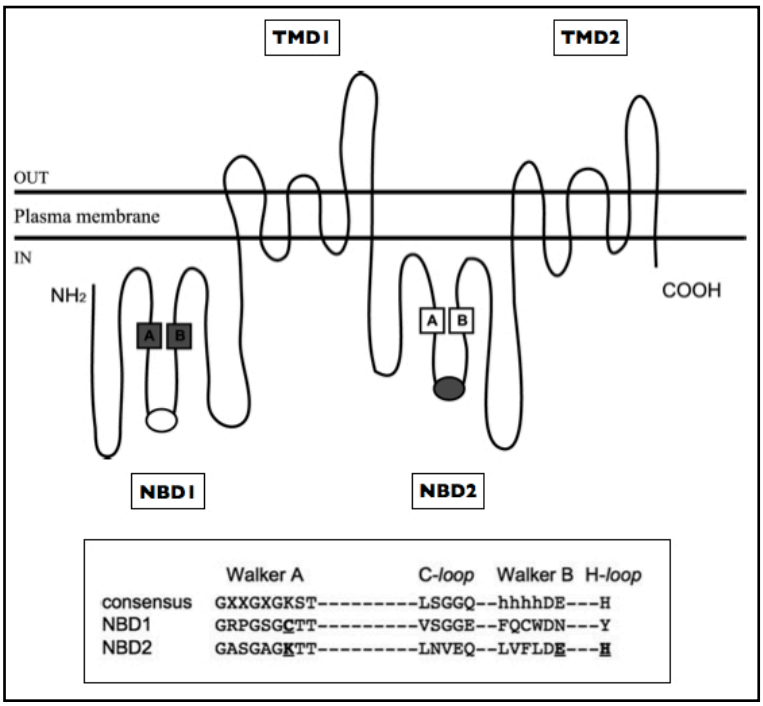

Figure 3. (NBD-TMD)$_2$ topology of Pdr5p (modified from de Thozee 2006 and Ernst et al. 2008). The grey squares in the NBD1 represent the variant Walker A and B motifs. The grey oval in the NBD2 represents the incomplete ABC signature. The sequences of the Walker A and B motifs and the C-and H-loops are shown for NBD1 and NBD2.

A three-dimensional structure at 25 Å resolution was obtained by computer-aided assembly of electron microscopy of 2-D crystals (Ferreira-Pereira et al. 2003) (Figure 4). Pdr5p assembles into a dimeric complex in which each subunit forms two lobes connected to the membrane by a stalk domain. NBD1 and NBD2 are oriented perpendicularly and appear spatially close. During the catalytic cycle, the NBDs rotate around the axis formed by the stalk. Using a yeast two-hybrid assay, Subba Rao et al. (2002) have shown an interaction between two NBD1 domains, consistent with Pdr5p

oligomerisation. The formation of dimeric complexes is also predicted for human ABC transporters CFTR, P-gp and MRP1 (Boscoboinik et al. 1990; Marshall et al. 1994; Naito and Tsuruo 1992; Soszynski et al. 1998; Wang et al. 2000).

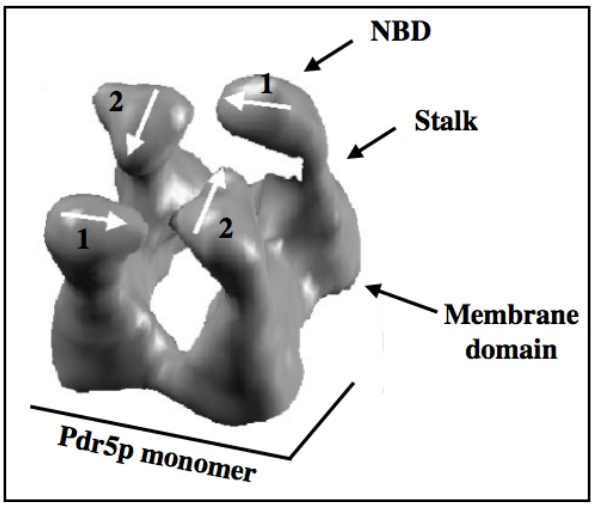

Figure 4. Three-dimensional structure of Pdr5p dimer at 25 Å resolution (modified from Ferreira-Pereira et al 2003). Three regions are clearly seen : the membrane domains, the stalk domains and the NBDs. Arrows show the different orientations of the NBD1s and NBD2s.

2.2. Substrate specificity of Pdr5p

Pdr5p mediates the ATP-driven efflux of hundreds of cytotoxic compounds from unrelated classes, including antibiotics (cycloheximide, chloramphenicol), anti-cancer drugs like Tamoxifen which is also transported by P-gp, fungicides (azoles derivatives) and steroids (Kolaczkowski et al. 1996). It also transports phospholipids and

sphingolipids (Decottignies et al. 1998; Kihara and Igarashi 2004; Kolaczkowski et al. 1996; Pohl et al. 2005). Overexpression of Pdr5p induces a PDR phenotype (Balzi et al. 1987; Decottignies et al. 1994; Kolaczkowski et al. 1996) and its loss a drug sensitivity phenotype (Bissinger and Kuchler 1994; Egner et al. 2000; Kolaczkowski et al. 1998). To have an efficient transport, key residues of the TMD act in the recognition and accomodation of the substrate in the drug chamber, whereas other key residues of the NBDs are required for ATP hydrolysis and energy coupling to the transport (Egner et al. 1998; Egner et al. 2000; Moody et al. 2002; Neyfakh 2002).

Golin and collaborators have shown that the size, but not hydrophophicity, of the substrates is an important factor determining the transport specificity (Golin et al. 2000; Golin et al. 2003). It has been proposed that the TMDs form a large intramembrane chamber containing at least 3 substrate-binding sites depending on the chemical properties of the transported molecules (Golin et al. 2007). No obvious unifying chemical feature is specific to the binding site 1 in comparison with sites 2 and 3 (Golin et al. 2007). Rhodamine 6G, ^{125}iodoarylazidoprazosin and clotrimazole define transport site 1. Hydrophobic residues at site 2 form a number of van der Waal's interactions with the substrate whereas charged residues at site 3 form electrostatic attractions with the substrate. The transport sites for several substrates may overlap (Golin et al. 2007).

Mutational analysis has shown the role of TM span 10 (TMS10) in drug recognition (Egner et al. 1998; Egner et al. 2000). Several mutagenesis

studies on human P-gp have shown a role of TMS1, TMS5/6 and TMS11/12 in substrate recognition and transport (Loo and Clarke 1996, 1997b, 1997a). The H-loop has been shown to play a role in the specific transport of Rhodamine 6G (Ernst et al. 2008). Drug transport is also impaired by mutations of NBD residues which affect ATP hydrolysis or conformational changes between the NBDs and TMDs (Hoof et al. 1994).

2.3. Transcriptional regulation of the *PDR5* gene

A complex network of transcription factors control the expression of multiple drug transporters in yeast. The transcription factors Pdr1p and Pdr3p control the expression of the *PDR5* gene via the binding to at least 3 conserved pleitropic drug response elements (PDREs), TCCGCGGA, in the promoter region (Balzi et al. 1994; DeRisi et al. 2000; Katzmann et al. 1994). These motifs contribute equally to regulation of *PDR5* (Katzmann et al. 1996). Note that the *PDR5* promoter region contains 4 PDREs but the function of only 3 PDREs has been investigated.

Pdr1p and Pdr3p belong to the bi-nuclear Gal4p-like family which is characterized by a $Zn(II)_2Cys_6$ DNA-binding motif. The zinc finger domain of Gal4p recognizes DNA binding sites in the target genes. The DNA-binding domain of Pdr1p and Pdr3p is located at the N-terminus (Figure 5). It is followed by a short linker region and a coiled-coil dimerization element (Kolaczkowska and Goffeau 1999) which participates in the formation of homo- and heterodimers, explaning the distinct regulation of Pdr1p and Pdr3p targets (Mamnun et al. 2002). The central region of Pdr1p and Pdr3p

contains eight conserved hydrophobic motifs (MI to MVIII). The deletion of the small region surrounding motifs I and II in Pdr1p leads to a transcription factor that is much more active compared to the wild-type protein (Kolaczkowska et al. 2002). This region is referred to as the inhibitory domain (ID). The activation region (AR) is located at the C-terminus of Pdr1p and Pdr3p and interacts with Ngg1p and Ada2p which, together with Gcn5p, constitue the transcriptional adaptor complex responsible for Gal4p inhibition (Martens et al. 1996; Simonics et al. 2000). Unlike Pdr1p, Pdr3p contains a second activation region at the N-terminus (Delaveau et al. 1994). Pdr3p lacks the nuclear localization signal (NLS) found in Pdr1p, altough both proteins are found in the nucleus (Delahodde et al. 1995).

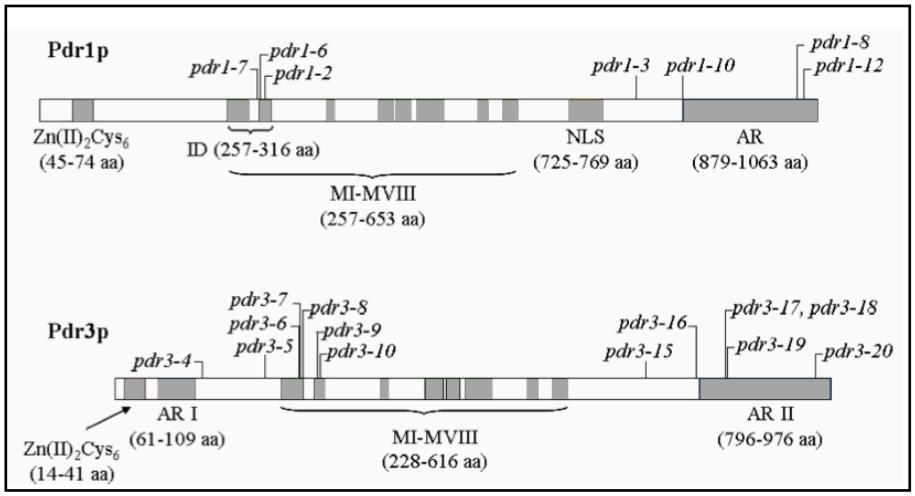

Figure 5. Conserved motifs in Pdr1p and Pdr3p (based on picture from Kalaczkowska and Goffeau, 1999). The zinc finger motif is denoted as $Zn(II)_2Cys_6$, the inhibitory domain as ID, the conserved hydrophobic motifs as MI to MVIII, the nuclear localization sequence as NLS and the activation regions as AR. Gain-of-function mutations of Pdr1p and Pdr3p are indicated in italic.

Despite a 36% overall amino acid sequence identity between Pdr1p and Pdr3p, these transcription factors play distinct roles. The loss of Pdr1p has a more pronounced effect on drug sensitivity than that of Pdr3p (Mahe et al. 1996). However, the sensitivity to Rhodamine 6G and diazaborine is more affected by Pdr3p loss (Kolaczkowska and Goffeau 1999). The *PDR3* promoter has two PDREs, indicating an autoregulatory loop in addition to the regulation by Pdr1p (Delahodde et al. 1995). Gain-of-function mutations that upregulate the expression of Pdr5p and several other ABC transporters, including Snq2p, Yor1p, Pdr10p and Pdr15p, have been isolated (Carvajal et al. 1997; Ogawa et al. 1998; van den Hazel et al. 1999). The *PDR1-3* mutation is a F815S substitution near the carboxyl-terminal activation domain. The level of Pdr5p expression is increased 15-fold in *PDR1-3* cells compared to wild-type *PDR1* cells, an increase similar to that obtained with a multi-copy plasmid containing the *PDR5* gene (Decottignies et al. 1999).

The amount of Pdr5p molecules decreases rapidly when the cells enter the stationary phase or when glucose or nitrogen are depleted. The decrease in Pdr5p level results from reduced transcription of the *PDR5* gene (Mamnun et al. 2004). An explanation for this regulatory effect is that the detoxification role of Pdr5p is no more required during the stationary phase of growth.

3. Degradation of proteins

Proteins destined for the secretory pathway are synthesized on cytosolic ribosomes and transported, either co- or post-translationally, to the endoplasmic reticulum (ER) (Brodsky 1996). The ER is endowed with a quality control system that monitors newly synthesized proteins for correct chain folding and modification, as well as assembly into functional macromolecular complexes (Ellgaard and Helenius 2003; Kopito 1997; Sitia and Braakman 2003). Aberrant and misfolded proteins are retro-translocated to the cytosol, where they are ubiquitylated and eliminated by the 26S proteasome (Hampton 2002; Kostova and Wolf 2003; McCracken and Brodsky 2003; Meusser et al. 2005; Plemper and Wolf 1999; Werner et al. 1996). The 26S proteasome is a large multi-subunit complex composed of two outer 19S caps and one inner 20S catalytic core (see §3.1.4.4.). The ubiquitin-proteasome system is one of the main proteolytic pathway with the vacuole (see §3.2.).

3.1. ER-associated degradation

ER-associated protein degradation (ERAD) comprises at least three steps: (i) the recognition of a misfolded or unassembled polypeptide by the quality control system, (ii) its retro-translocation (or dislocation) into the cytosol across the ER membrane and (iii) ubiquitin-mediated degradation by the proteasome (Figure 6).

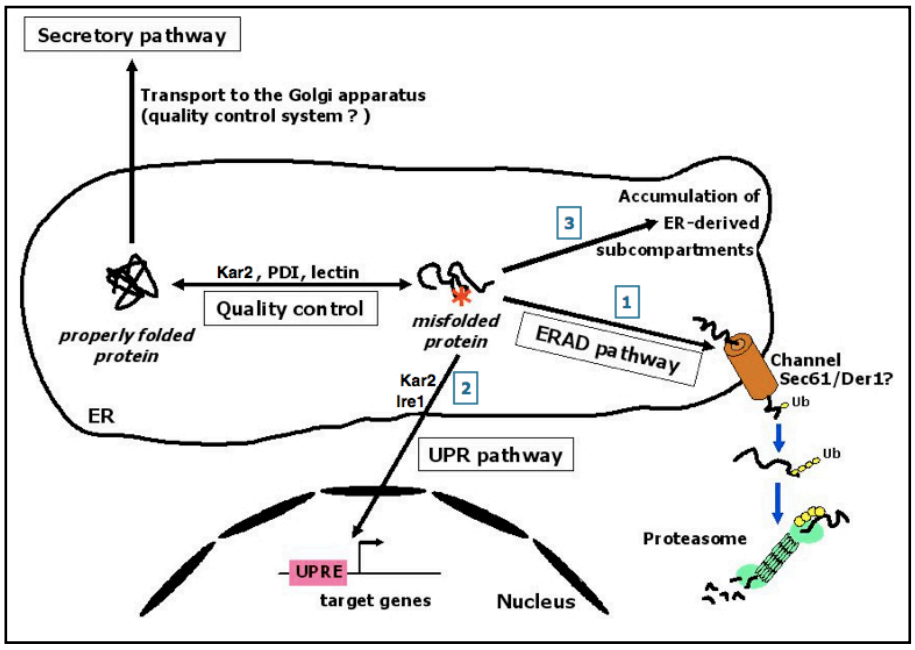

Figure 6. Overview of ER protein quality control and proteasome-mediated degradation. Newly synthesized secretory proteins are monitored for non-native conformation by a quality control system consisting of various ER folding sensors (Kar2p, PDI and lectin-like chaperones). **(1)** Unfolded or misfolded proteins are transported across the ER membrane into the cytosol, where they are marked for proteasomal elimination by E3 ligase-mediated conjugation to ubiquitin (Ub) (details not shown). **(2)** The accumulation of unfolded and misfolded proteins in the ER induces UPR (unfolded protein response), resulting in the activation of genes coding for ER chaperones and proteins involved in the secretory and ERAD pathways. **(3)** Another mechanism for overcoming the toxicity linked to elevated amounts of misfolded proteins is their sequestration into ER-derived subcompartments like ERACs (ER-Associated Compartments).

A second mechanism for dealing with misfolded proteins beside the ERAD pathway is termed the unfolded protein response (UPR) (see §3.1.5.), which increases the ER folding capacity and may trigger ER-phagy (Bernales et al. 2007; Ron and Walter 2007). A third mechanism is the sequestration of the

misfolded proteins in special ER-derived subcellular compartments (Klionsky 2007) (see §3.1.6.) (Figure 6).

Studies using yeast and mammalian cells have shown that the basic events of the ERAD pathway are conserved in eukaryotes (Gnann et al. 2004; Lenk et al. 2002; Ward et al. 1995) (Table 1).

Table 1. Mammalian counterparts of the yeast ERAD components

Activity/Function	Yeast	Mammalian
Chaperone proteins	Kar2	BiP/GRP78
	Ero1	Ero α and β
	Mnl1 (Htm1)	EDEM1, 2 and 3
	Mns1	ER ManI
	Lhs1	Grp170
	Yos9	OS-9/XTP3-B
Ub-activating enzyme - E1	Uba1	Uba1, Uba6
Ub-conjugating enzymes - E2s	Ubc1	UBE2k
	Ubc6	UBE2J1, UBE2J2
	Ubc7	UBE2G1, UBE2G2
Ub-protein ligases - E3s	Doa10	TEB4
	Hrd1 (Der3)	HRD1 gp78 (AMFR)
	Hrd3	Sel1L
	Rsp5	NEDD4

Activity/Function	Yeast	Mammalian
Ub chain elongation - E4	Ufd2	Ufd2
Dislocation pore	Sec61	Sec61
	Der1	Derlin1, 2 and 3
Cdc48p/Ufd1p/Npl4p complex - extraction of ubiquitylated substrates from the ER membrane	Cdc48	p97 or VCP
	Npl4	Npl4
	Ufd1	Ufd1
Substrate adaptators for the proteasome	Rad23	HR23A, HR23B
	Dsk2	Ubiquilin, Ubql2, Plic2
Cdc48 receptor	Ubx2	UBXD2/ Erasin
Protein associated to E3 with unknown function	Usa1	HERP

3.1.1. Recognition of aberrant proteins in ER

Newly synthesized protein undergoes several post-translational modifications in the ER, including the removal of the signal sequence, disulphide bond formation, *N*-glycosylation and the addition of glycosylphosphatidylinositol. Proteins folding involves ER-resident molecular chaperones of the heat shock protein (Hsp) 70 family called Kar2p in yeast (Kozutsumi et al. 1989; Normington et al. 1989; Rose et al. 1989). Function and specificity of Hsp70 are regulated by co-chaperones

(e.g. Hsp40s) and nucleotide exchange factors (e.g. Lhs1) (Saris et al. 1997; Takeuchi 2006).

Disulphide-bond formation is catalysed by protein disulphide isomerases (PDIs), including Pdi1p, four other non-essential Pdi-related proteins (Norgaard et al. 2001) and Ero1p (Fassio and Sitia 2002; Gross et al. 2006). These oxidoreductases ensure that irreversible formation of disulphide bonds does not occur until protein folding is complete. However, no significant effects on ERAD are seen in various *PDI*-deleted strains (Norgaard et al. 2001).

Degradation of misfolded glycoproteins is triggered by a mannose timer-based mechanism (Ellgaard and Helenius 2003; Jakob et al. 1998; Nakatsukasa et al. 2001). The attachment of *N*-linked carbohydrates is essential for the maturation of secretory and membrane proteins (Figure 7). After transfer of the core oligosaccharide ($Glc_3Man_9GlcNAc_2$) onto an Asn residue in the consensus Asn-X-Ser/Thr motif (X represents any amino acid), the three glucose residues are removed by glucosidases 1 and 2. Correctly folded glycoproteins exit the ER and reach their final destinations. The terminal mannose residue of the $Man_9GlcNAC_2$ oligosaccharide on nascent glycosylated proteins is removed by α-1,2-mannosidase I (Mns1p). The mannosidase reaction is slow, so only terminally misfolded proteins that spend an excessive amount of time in the ER will be trimmed. The $Man_8GlcNAC_2$ oligossacharide is trimmed more extensively by ER α-mannosidase-like lectins (Mnl1p or Htm1p) which enhance degradation of N-glycosylated misfolded proteins. However, as all folded glycoproteins

also contain a Man_8 oligosaccharide, it seems likely that the signal for ERAD consists of a polypeptide determinant in addition to the glycan structure (Byrd et al. 1982; Spear and Ng 2005). The lectin-like protein Yos9p has a proof-reading function in scanning for the Man_7 determinant in substrates ready to be translocated back to the cytosol for degradation (Denic et al. 2006; Gauss et al. 2006b; Hirsch et al. 2006).

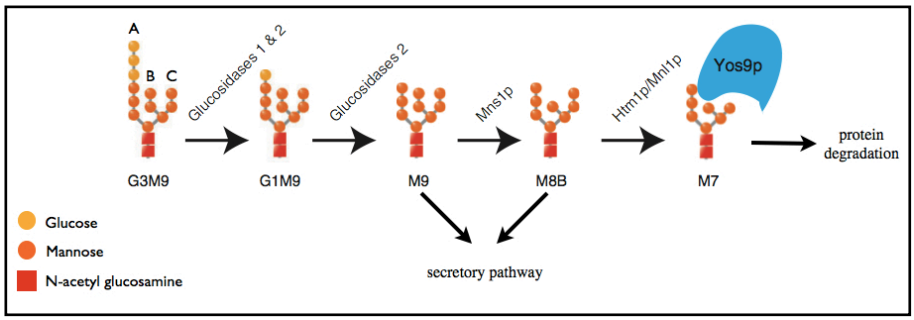

Figure 7. Quality control by lectin-like proteins in yeast (modified from Hoseki et al 2010). Oligosaccharyltransferase transfers $Glc_3Man_9GlcNAC_2$ (G3M9) oligosaccharides to an asparigine residue from the Asn-X-Ser/Thr motif in nascent polypeptides. Glucosidases 1 and 2 remove the two outer glucose residues giving $Glc_1Man_9GlcNAC_2$ (G1M9). Glucosidase 2 removes the last glucose residue giving $Man_9GlcNAC_2$ (M9). The ER Mns1 α-mannosidase trims the mannose moiety of the B branch of misfolded proteins, giving $Man_8GlcNAC_2$ (M8B). Htm1p processes the C branch, giving M7 ($Man_7GlcNAC_2$), which is recognized by Yos9p as a degradation signal.

As folding sensors, ER luminal Hsp70s, lectins and PDIs are key components of the quality control system (Bukau et al. 2006). These molecular chaperones monitor the stability of non-native proteins and the presence of unpaired cysteine residues or immature glycans (Krebs et al.

2004; Sitia and Braakman 2003). Folding or assembly intermediates are retained in the ER and allowed to undergo further folding attempts. It is still not clear how molecules that have not had the time to fold are distinguished from those that have failed to fold after many attempts and must therefore be eliminated.

The ubiquitin-proteasome system can recognize a wide variety of proteins through the presence of specific degradation signals or degrons (Ravid and Hochstrasser 2008). A degron refers to a peptide region that is sufficient for the recognition by a proteolytic machinery. An important property of the degron is its transferability. Genetically engineered attachment of the degron confers metabolic instability on otherwise long-lived proteins (Hochstrasser 1996).

A degron can occur either at the N or C-terminal region, these are called N-degrons or C-degrons respectively. The N-degron can be illustrated by the Matα2 transcriptionnal regulator protein that presents a degradation signal in the first N-terminal 67 residues called *Deg1* signal (Chen et al. 1993; Johnson et al. 1998). The ubiquitin-proteasome system can also recognized a specific residue at the N-terminus of a protein. This degradation pathway is termed the «N-end rule pathway» and states that the half-life of a protein is determined by the nature of its N-terminal residue (Bachmair et al. 1986; Bartel et al. 1990). Varshavsky and co-workers systematically changed the N-terminal residue in an otherwise identical series of *E. coli* β-galactosidase test substrates and expressed them in yeast, where they displayed a remarkable range of degradation rates (half-lives ranged from a few minutes to greater than 20 hours) (Bachmair et al. 1986).

In addition to N- and C- degrons, the presence of a «distributed degron» has been detected in the 3-hydroxy-3methylglutaryl Coenzyme A (HmgCoA) reductase isoform, Hmg2. Effectively, Hmg2 has the information necessary for degradation dispersed throughout the 500 residues of its TMD (Gardner and Hampton 1999).

In most cases, the degron is hidden inside the protein and must be revealed as a consequence of protein unfolding. Alternatively, post-translational modifications, including phosphorylation, ensure that the degron is actived correctly. Degradation induced by phosphorylation is referred as phosphodegron. The mechanism by wich phosphorylation drives substrate to degradation is under investigation. The best characterized of such phosphodegrons are the ones involved in the ordered elimination of specific cyclins and cyclin-dependent kinase inhibitors by the ubiquitin system (reviewed in Tyers and Jorgensen 2000; Ang and Harper 2004).

3.1.2. ER-associated ubiquitylation

Ubiquitin (Ub) is a 76-residue polypeptide which is covalently and reversibly conjugated to proteins, via an isopeptide bond between the carboxyl-terminal glycine of Ub and a lysine residue on the target protein. Only three residues differ between yeast and human. Ub has seven lysine residues that can be involved in the formation of polyUb chains *in vitro* or *in vivo* (Peng et al. 2003).

Ub-mediated degradation requires the sequential action of E1 Ub-activating enzyme, E2 Ub-conjugating (Ubc) enzymes, E3 Ub-protein ligases that enable the physical interaction of the E2 and its substrate and, in some cases, E4 Ub chain elongation factor (e.g. Ufd2p) (Figure 8) (Koegl et al. 1999; Nakatsukasa et al. 2008; Richly et al. 2005).

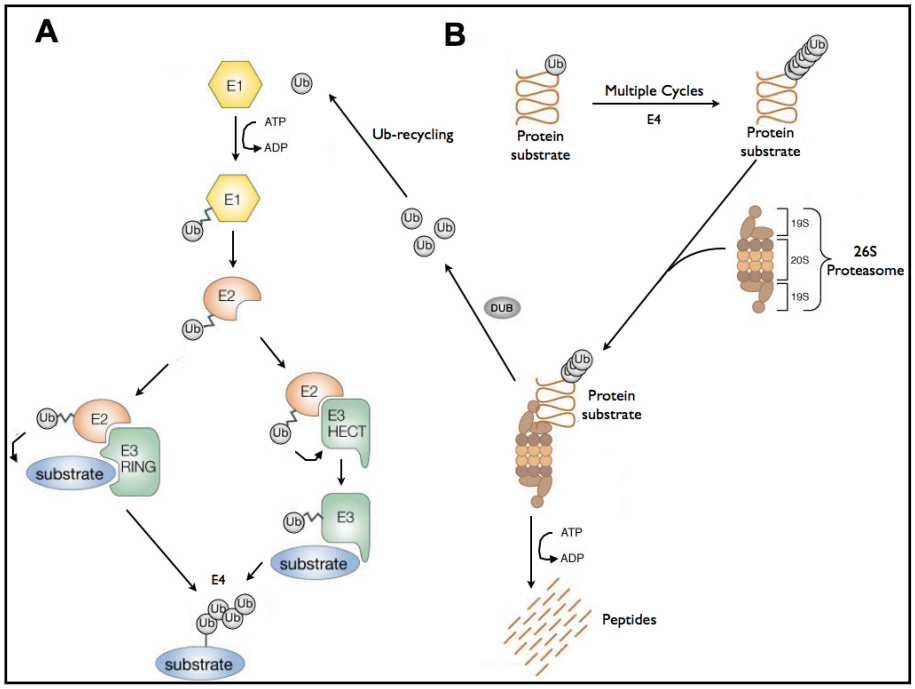

Figure 8. The ubiquitylation machinery. **(A)** The E1 enzyme activates Ub at the expense of ATP. The Ub is then transferred to E2 enzymes. With the help of a substrate-specific E3, the Ub is conjugated to the target protein. E3s with a HECT domain have the property to receive the Ub moiety from E2s before transferring it to the substrate and E3s with a RING domain favour the direct transfer of Ub from E2s to the target protein. Enzymes specialized in the poly-Ub chain elongation (e.g. Ufd2p) are also referred as E4. **(B)** Ubiquitylated protein substrate is digested by the 26S proteasome and de-ubiquitylation enzymes (DUB) recycle the Ub.

Yeast has only one E1 enzyme that activates Ub at the expense of ATP. The activated Ub is then transferred to ERAD E2s, Ubc6p, Ubc7p and Ubc1p (Hiller et al. 1996). The ERAD E3s are named Hrd1p and Doa10p (Hampton et al. 1996; Huyer et al. 2004b; Plemper et al. 1998). These enzymes contain a zinc finger domain of the RING (really interesting new gene) type and act as scaffolds for the assembly of the machinery involved in substrate recognition and ubiquitylation. Note that some E3s not involved in ERAD contain a HECT (homologous to E6-associated protein C-terminus) domain instead of the RING domain. E3s with a HECT domain have the property to receive the Ub moiety from E2s before transferring it to the substrate. In contrast, E3s with a RING finger domain favour the direct transfer of Ub from E2s to the target protein.

3.1.2.1. The Hrd1p complex

The HmgCoA reductase degradation (Hrd) protein 1, also named Der3p for Degradation in the ER, consists of 551 amino acids forming six TMSs and two terminal cytosolic loops (Deak and Wolf 2001; Gardner et al. 2000) (Figure 9). Hrd1p was identified by genetic screens for factors involved in the regulation of 3-hydroxy-3-methylglutaryl coenzyme A (HMG-CoA) reductase protein (Hampton et al. 1996) and in the degradation of mutated forms of Pdr5p ($Pdr5^{C1427Y}$ or Pdr5*) and vacuolar carboxypeptidase Y (CPY*) (Plemper et al. 1998).

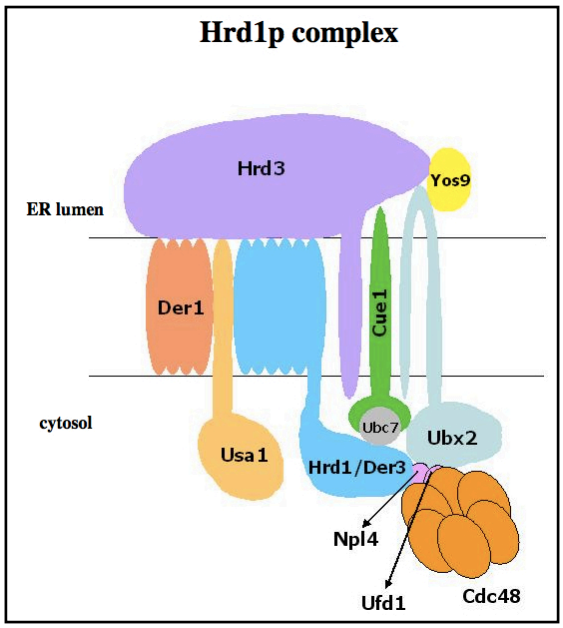

Figure 9. Subunit composition of the Hrd1p complex. The protein complex contains a large ER luminal region (Hrd3p and Yos9p) which may serve as a substrate receptor site. Usa1p interacts with Der1p, a putative constituent of the retro-translocation pore. Ubx2p acts as a membrane anchor of the Cdc48p/Ufd1p/Npl4p complex, which is involved in the extraction of ubiquitylated substrates from the ER membrane.

Hrd1p assembles with the Ubc7p-Cue1p dimeric complex in a RING finger-dependent manner (Friedlander et al. 2000; Hampton et al. 1996). Cue1p is a ER membrane protein that recruits the Ub-conjugating enzyme. Physical association with Ubc1p and Ubc6p has also been reported (Bays et al. 2001b). Hrd1p also interacts with Hdr3p and the Cdc48p/Ufd1p/Npl4p complex which is involved in the extraction of ubiquitylated substrates from the ER membrane (see §3.1.4.2.). Hdr3p is a membrane protein with a large ER-luminal domain that functions as a substrate receptor (Gardner et al.

2000; Hampton et al. 1996). In the absence of Hrd3p, Hrd1p is rapidly degraded by the ubiquitin-proteasome system (Gardner et al. 2000; Plemper et al. 1999). The interaction between Hrd1p and the Cdc48p/Ufd1p/Npl4p complex requires the membrane Ubx2 protein, which contains a N-terminal Ub-associated (UBA) domain, known to bind the Ub chain of ERAD substrates, and a C-terminal Ub-like (UBX) domain, which binds Cdc48p (Decottignies et al. 2004; Neuber et al. 2005; Schuberth et al. 2004).

The transmembrane Der1 protein is linked to Hrd1p via Hrd3p and Usa1p (U1-Snp1 associating protein 1), a protein of unknown function with a Ub-like (UBL) domain which is recognized by the proteasome (Carvalho et al. 2006; Gauss et al. 2006a). Usa1p was identified through the interaction with Snp1, a small nuclear ribonucleoprotein involved in pre-mRNA splicing (Awasthi et al. 2001). The deletion of the *USA1* gene is synthetically lethal with the deletion of *IRE1*, which encodes a key player in the UPR (see §3.1.5.) (Carvalho et al. 2006). Der1p is involved in the degradation of CPY* and PrA*, a mutated form of proteinase A (Knop et al. 1996). The lectin-like Yos9p physically and mechanistically interacts with Hrd1p by binding to Kar2p and to a luminal domain of Hrd3p (Carvalho et al. 2006; Denic et al. 2006; Gauss et al. 2006b). The Kar2p-Yos9p-Hrd3p complex is not disrupted by the loss of Hrd1p, but this complex no longer interacts with the Cdc48p/Ufd1p/Npl4p complex (Carvalho et al. 2006; Denic et al. 2006).

3.1.2.2. The Doa10p complex

Doa10p was identified in a screen for genes complementing the growth phenotype of a *Deg1*-fusion protein (Swanson et al. 2001). *Deg1* is a degradation signal found in the first 67 residues at the N-terminus of the Matα2 transcriptionnal regulator (Chen et al. 1993; Johnson et al. 1998). Doa10p is a 14-TMS protein from the ER/nuclear envelope, with the N- and C-termini facing the cytosol (Kreft et al. 2006; Swanson et al. 2001) (Figure 10).

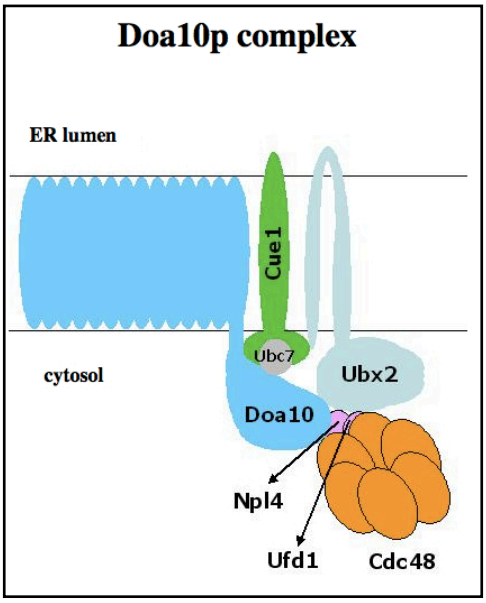

Figure 10. Subunit composition of the Doa10p complex. The protein complex is composed of the Doa10p E3 Ub-ligase, the Ubc7p E2 Ub-conjugating enzyme which binds to the membrane anchoring factor Cue1p. Ubx2p acts as a membrane anchor of the Cdc48p/Ufd1p/Npl4p complex.

The Ub-ligase is part of a complex that includes Ubc7p, which is tethered to the ER membrane via its association with Cue1p (Biederer et al. 1997), and the Cdc48p/Ufd1p/Npl4p complex, which is recruited to the membrane via Ubx2p (Neuber et al. 2005; Schuberth et al. 2004). Ubc6p is anchored to the ER membrane through a C-terminal hydrophobic tail. Doa10p is required for the degradation of soluble proteins including the cytosolic Ura3p-CL1 fusion protein (a soluble cytosolic Ura3p protein with a transplantable degradation signal) and nuclear Matα2p. Doa10p also targets membranous ABC-transporter variant Ste6-Q1249-X for proteasomal degradation (Metzger et al. 2008). The Cdc48p/Ufd1p/Npl4p complex facilitates the degradation of membrane-embedded Doa10 substrates and is not required for degradation of soluble cytosolic proteins. So both membrane and soluble cytosolic proteins are ubiquitylated by Doa10p but the pathways leading to the proteasome are distinct (Ravid et al. 2006).

3.1.3. Model ERAD substrates are degraded through distinct ERAD pathways

3.1.3.1. Model ERAD substrates

Key factors in ERAD have been identified by using wild-type ER resident proteins (HMG-CoA reductase) and mutated forms of secretory (CPY*) and membrane proteins (Pdr5*, Ste6-Q1249X) as ERAD substrates (Figure 11 ; Table 2). Protein fusions have also been constructed that expose misfolded segments to the cytosolic and/or the luminal side of the ER membrane (KWW, CTG*, KSS) (Taxis et al. 2003; Vashist and Ng 2004).

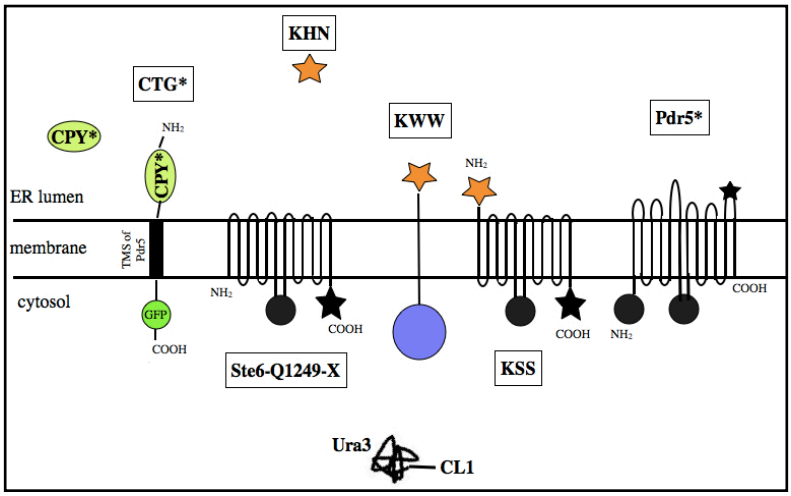

Figure 11. Model ERAD substrates. NBDs are represented by black circles. Residue substitutions and nonsense mutations are represented by a black star. See text and Table 2 for details.

Table 2. List of model ERAD substrates.

Soluble luminal proteins

Substrat	Description	Factors required
CPY*	Mutant form of vacuolar carboxypeptidase Y	Kar2p, Hsp40 co-chaperones Jem1p and Scj1p, Der1p, Ubc1p, Ubc7p, Hrd1p-Hrd3p.
KHN	Yeast Kar2p signal sequence fused to simian virus 5 HA-neuraminidase ectodomain	ER α-mannosidase-like lectins Htm1p (Mnl1p), Cue1p, Der1p, Hrd1p-Hrd3p.

Soluble cytosolic protein

Substrat	Description	Factors required
Ura3p-CL1	Cytosolic soluble protein (Ura3) with a transplantable 16-residue degron (CL1)	Hsp70 chaperone SSa1p, Hsp40 co-chaperone Ydj1p, Ubc6p, Ubc7p, Doa10p.

Membrane protein with a misfolded cytosolic domain

Substrat	Description	Factors required
Ste6-Q1249-X	C-terminally truncated form of Ste6p	Hsp70 chaperone SSa1p, Hsp40 co-chaperones Ydj1p and Hlj1p, Doa10p.

Membrane proteins with a luminal lesion

Substrat	Description	Factors required
Pdr5* or $Pdr5^{C1427Y}$	Mutant form Pdr5-C1427Y	ER α-mannosidase-like lectins Htm1p, Hrd1p-Hrd3p.
CTG*	CPY* fused to the GFP via a transmembrane segment (TMS) from Pdr5p	Hsp70 chaperone Ssa1p, Hsp40 co-chaperone Hlj1p, Cwc23p and Jid1p, Ubc1p, Ubc7p, Hrd1p-Hrd3p.
KWW	KHN luminal domain, Wsc1p (yeast cell wall integrity and stress response component 1) TMS and cytosolic domain	ER α-mannosidase-like lectins Htm1p (Mnl1p), Cue1p, Der1p, Hrd1p-Hrd3p.

Membrane protein with misfolded domains facing the ER lumen and the cytosol

Substrat	Description	Factors required
KSS	KHN luminal domain fused to the second TMS of Ste6p transmembrane domain, Ste6*p (Q1249-X) cytosolic mutant domain	ER α-mannosidase-like lectins Htm1p (Mnl1p), Doa10p.

3.1.3.1.1. Soluble luminal proteins (Figure 11 and Table 2)

CPY* is rapidly degraded by the ubiquitin-proteasome system via Hrd1p-Hrd3p, Ubc1p and Ubc7p (Finger et al. 1993; Hiller et al. 1996). Retro-translocation of CPY* depends on Der1p, Kar2p and the Hsp40 co-chaperones Jem1p and Scj1p (Nishikawa et al. 2001; Plemper et al. 1997).

CPY* degradation is impaired by mutation of glucosidases I and II (Hitt and Wolf 2004b; Jakob et al. 1998) or the α-mannosidase-like lectin (Mnl1p or Htm1p) (Jakob et al. 2001; Nakatsukasa et al. 2001).

KHN degradation is dependent of Hrd1p-Hrd3p, Cue1p, Der1p and the α-mannosidase-like lectin (Mnl1p or Htm1p) (Vashist et al. 2001).

3.1.3.1.2. Soluble cytosolic protein (Figure 11 and Table 2)

Degradation of Ura3p-CL1 is dependent of a cytosolic Hsp70 chaperone, Ssa1p, and its Hsp40 co-chaperone, Ydj1p, but not Hlj1p, an other co-chaperone of Ssa1p (Metzger et al. 2008). As its degradation also requires the ER-localized E2s Ubc6p and Ubc7p and E3 Doa10p, it is likely that the cytosolic facing leaflet of the ER membrane serves as a platform for Ura3-CL1 degradation (Metzger et al. 2008).

3.1.3.1.3. Membrane protein with a misfolded cytosolic domain (Figure 11 and Table 2)

Ste6-Q1249-X form is retained in the ER and ubiquitylated by Doa10p (Loayza et al. 1998). The Hsp70 co-chaperone, Ssa1p, and its Hsp40 co-chaperones Ydj1p and Hlj1p are required for degradation of Ste6-Q1249-X (Huyer et al. 2004b). The luminal Kar2p chaperone is not required in this process.

3.1.3.1.4. Membrane proteins with a luminal lesion (Figure 11 and Table 2)

Pdr5* is retained in the ER membrane and targeted for proteasomal degradation by Hrd1p-Hrd3p (Egner et al. 1998; Plemper et al. 1998). The role of the E3 Doa10p has not been investigated. The evidence for Pdr5* misfolding is a glycosylation pattern different from that of intact Pdr5p (Plemper et al. 1998). The C1427Y substitution may impair the formation of disulphide bonds with cysteine residues facing the ER lumen (Plemper et al. 1998). Unlike Kar2p, the luminal chaperone lectin Htm1p is required for Pdr5* degradation (Gnann et al. 2004; Jakob et al. 2001; Plemper et al. 1998).

The CTG* fusion protein (CPY*-TMS^{Pdr5}-GFP) is ubiquitylated by Hrd1p-Hrd3p (Taxis et al. 2003). CTG* degradation is independent of Kar2p. The cytosolic Hsp70 chaperones Ssa1p and Hsp40 co-chaperones Hlj1p, Cwc23p and Jid1p are required for degradation. The implication of cytosolic chaperones is surprising as CTG* contains a luminal lesion which should be recognized by luminal chaperones.

KWW is a short-lived membrane protein and its degradation depends on ER-resident proteins Htm1p, Cue1p, Der1p and Hrd1p (Vashist and Ng 2004).

3.1.3.1.5. Membrane protein with misfolded domains facing the ER lumen and the cytosol (Figure 11 and Table 2)

KSS is ubiquitylated by Doa10p and its degradation depends on the luminal chaperone lectin Htm1p/Mnl1p (Vashist and Ng 2004).

3.1.3.2. Distinct ERAD pathways

The use of these substrates (Figure 11, Table 2) has led to the identification of different ERAD pathways according to the localization of the misfolded lesion (Figure 12) (Ahner and Brodsky 2004; Vashist and Ng 2004). ER luminal proteins and membrane proteins with lesions in a luminal domain are recognized by a set of specific chaperones that are linked to the Hrd1p complex defining the so-called ERAD-L pathway. Whereas, membrane proteins with cytosolic lesions are recognized by another set of chaperones linked to the Doa10p complex defining the ERAD-C pathway. The ERAD-M pathway targets membrane proteins with intra-membrane lesions for degradation, a process that is independent of Usa1p and Der1p (Carvalho et al. 2006).

The use of KSS, a misfolded membrane protein with misfolded domains facing the ER and the cytosol, has shown that nascent transmembrane proteins are monitored by a two-step quality control system as KSS is only ubiquitylated by Doa10p. The first ERAD-C checkpoint relies on the inspection of cytosolic face of the ER membrane. If a lesion is detected, the

membrane protein is targeted for proteasome-mediated degradation via Doa10p. If the cytosolic domain are found to be correctly folded, the transmembrane protein is inspected by ERAD-L checkpoint, which targets misfolded proteins for degradation through a pathway shared by soluble secretory proteins and involving Hrd1p (Vashist and Ng 2004).

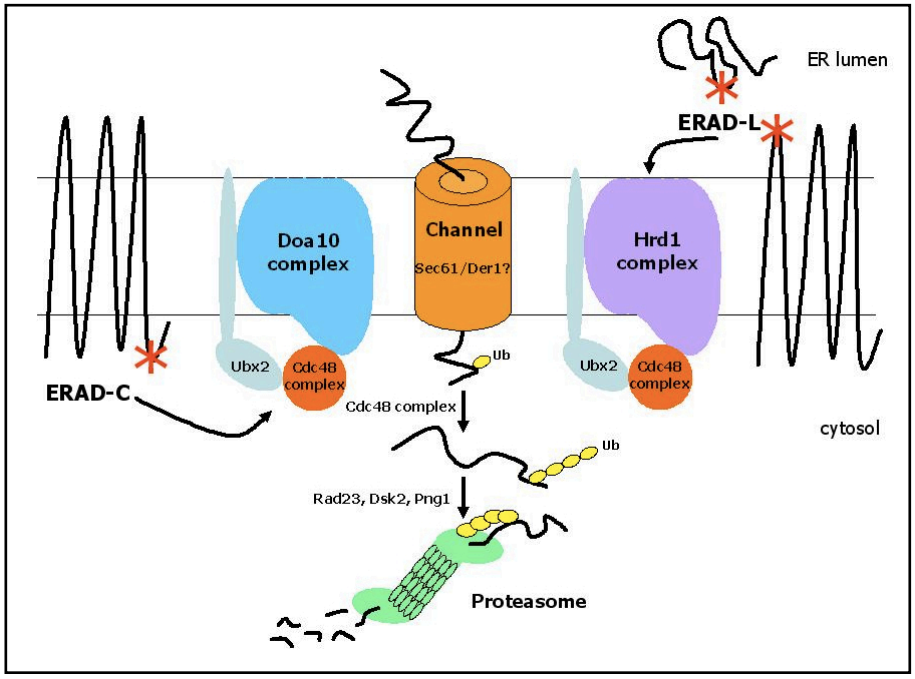

Figure 12. Proteins with luminal and cytosolic lesions are targeted for proteasome-mediated degradation through distinct protein-Ub ligase complexes. Membrane proteins with misfolded cytosolic domains (red star) are substrates of the Ub-ligase Doa10p (ERAD-C pathway), whereas membrane and soluble proteins with luminal misfolded domains (red stars) are substrates of the Ub-ligase Hrd1p (ERAD-L pathway). The third ERAD-M checkpoint which relies on the inspection of transmembrane domains and activates Hrd1p is not represented.

3.1.4. Retro-translocation into the cytosol and delivery to the 26S proteasome

3.1.4.1. Retro-translocon

Proteasome-mediated degradation of proteins located in the ER compartment requires their retro-translocation back to the cytosol. The identity of the channel components responsible for retro-translocation is still debated, the potential candidates being the Sec61p translocon, Der1p (component of the Hrd1p complex) and Doa10p (Nakatsukasa and Brodsky 2008).

Sec61p is an obvious candidate for the retro-translocon because of its role in the translocation of newly synthesized proteins in the ER. Studies used *sec61-2* mutant cells indicate that the Sec61 channel functions in retrograde transport of CPY* and Pdr5* to the cytosol for proteasomal degradation (Pilon et al. 1997; Plemper et al. 1997; Plemper et al. 1998; Willer et al. 2008). However, the interpretation of these data is complicated by the fact that the *sec61-2* strain is also defective in translocation. Recent data of co-translationally imported CPY* derivatives in a *sec61-3* mutant strain, which is specifically impaired in the retro-translocation indicate that a functional Sec61p is essential for the elimination of CPY* (Willer et al. 2008). The role of Sec61 in the retrograde transport is also based on the finding that Sec61p interacts with Hrd3p (Schafer and Wolf 2009) and with the proteasome 19S particle (Ng et al. 2007). The ubiquitylation and retro-translocation of CPY* is impaired by the loss of Hrd1p although the interaction with Sec61p is not (Schafer and Wolf 2009). These results

suggest that the role of Sec61p might be the delivery of CPY* to the Hrd1p complex, which forms the retro-translocon. It is also possible that Sec61p and Hrd1p complex are components of the same channel.

The formation of a disulphide-linked intermediate complex between Sec61p and a transmembrane ERAD substrate (Deg1-Sec62 fusion protein) has been reported (Scott and Schekman 2008) supporting the view that Sec61p acts directly in the retro-translocation or indirectly in remodelling membrane proteins before they are retro-translocated via a separate ER channel.

An other candidate for the retro-translocon is Der1p. This 4 TMSs protein associates to Hrd1p and Hrd3p (Carvalho et al. 2006; Hitt and Wolf 2004a; Knop et al. 1996) and might form a pore in the ER membrane. Der1p intervenes in the degradation of KWW, KHN, CPY* but not CTG* (Hitt and Wolf 2004a; Huyer et al. 2004b; Knop et al. 1996; Taxis et al. 2003; Vashist and Ng 2004).

Ste6-Q1249-X and the engineered KSS protein do not require Der1p or Sec61p for ER-associated degradation (Kreft et al. 2006; Vashist and Ng 2004; Walter et al. 2001). Since these substrates are ubiquitylated by Doa10p and not by Hrd1p, it has been proposed that the retro-translocation channel consists of Doa10 TMSs (Kreft et al. 2006).

3.1.4.2. The Cdc48p/Ufd1p/Npl4p complex

Ubiquitylated ERAD substrates are released from the ER by a cytosolic Ub-specific chaperone complex consisting of Cdc48p, Ufd1p and Npl4p (Bays et al. 2001a; S. Braun et al. 2002; Hitchcock et al. 2001; Jarosch et al. 2002; Rabinovich et al. 2002; Ye et al. 2001). Cdc48p has two ATP-binding domains and two Second Regions of Homology (SRH) motifs (Frohlich et al. 1991). X-ray crystallographic studies have shown six subunits assembled into a ring, the overall shape of which changes during the ATPase catalytic cycle (DeLaBarre and Brunger 2003; Dreveny et al. 2004). A nucleotide-dependent conformational switch may apply tension to bound proteins, thereby allowing unfolding of the polypeptide chain (Bukau et al. 2006). Cdc48p binds to the C-terminal domain of Ufd1p and to the N-terminus of Npl4p, a protein with a zinc-binding motif (Bruderer et al. 2004; Meyer et al. 2000; Rape et al. 2001). The N-terminal domain of Ufd1p and the zinc finger motif of Npl4p bind to Ub (Alam et al. 2004; Park et al. 2005). The Cdc48p/Ufd1p/Npl4p complex is recruited to the ER membrane by the UBX (Ub-regulatory X) domain of Ubx2p (Carvalho et al. 2006). Ubx2p also contains a Ub-associated (UBA) domain that binds Ub chains and may transport the ERAD substrates to Cdc48p (Neuber et al. 2005; Schuberth et al. 2004).

3.1.4.3. Delivery to the proteasome

After retro-translocation to the cytosol, the (poly)ubiquitylated substrates are delivered to the proteasome by Rad23p and Dsk2p (Chen and Madura 2002;

Funakoshi et al. 2002; Medicherla et al. 2004). These proteins contain single or multiple repeats of the UBA domain in addition to a Ub-like (UBL) domain, which is recognized by the proteasome (see §3.1.4.4.) (Elsasser et al. 2002). The 26S proteasome and the Ub chain elongation factor Ufd2p associate with the Rad23 UBL domain in a mutually exclusive manner (Kim et al. 2004). Rad23p and Cdc48p have been shown to interact with a conserved peptide *N*-glycanase, Pgn1p, which is required for the deglycosylation of misfolded glycoproteins during proteasome-dependent degradation (Hirsch et al. 2004; Nita-Lazar and Lennarz 2005; Suzuki et al. 2000).

The poly-ubiquitylated versus de-ubiquitylated state of an ERAD substrate and its subsequent targeting to the proteasome are determined by a subtle balance between Ufd2p and Doa1p (a WD40 repeat protein controlling the cellular free Ub concentration) and Otu1p (a de-ubiquitinating enzyme). Doa1p and Otu1p bind to Cdc48p, enhancing their inhibitory effect on Ufd2p (Richly et al. 2005; Rumpf and Jentsch 2006). As the C-terminal end of Doa1p interacts with the UBX domain, it is possible that the binding of Ubx2p to Cdc48p is also inhibited by Doa1p (Decottignies et al. 2004).

3.1.4.4. The 26S proteasome

The 26S proteasome is a large multi-subunit complex composed of two outer 19S caps and one inner 20S catalytic core (reviewed in Lupas et al. 1993) (Figure 13).

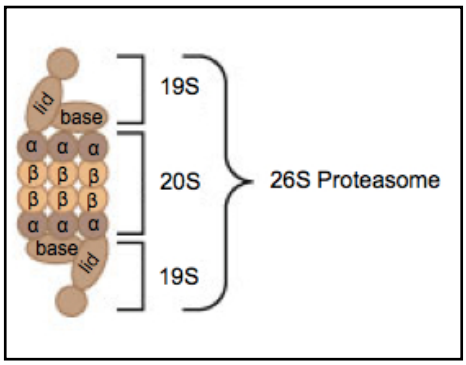

Figure 13. 26S proteasome. The 26S proteasome is composed of two outer 19 caps and one inner 20S catalytic core. The organisation of the α- and β-subunits within the catalytic core is shown. The 19S cap is composed of a lid and a base.

The lid of the 19S cap is composed of eight proteins (Rpn3, 5, 6, 7, 8, 9, 11, 12) which recognize poly-Ub conjugate substrates and trim Ub-chain of substrates into mono-Ub. The base consists of six AAA-ATPases (Rpt1-6p) which catalyse ATP hydrolysis to maintain the protein substrate in an unfolded state and to open the pore leading to the proteolytic core (Braun et al. 1999; Strickland et al. 2000). Two other components of the base, Rpn1p and Rpn2p, are involved in protein-protein interactions and recruit Dsk2p and Rad23p (Elsasser et al. 2002). The 20S particle is composed of 2 α outer and 2 β inner rings, each composed of seven distinct subunits (Groll et al. 1997). The outer rings have no proteolytic activities and may play a structural role. The inner rings possess three types of proteolytic activities : a chymotrypsin-like activity, a trypsin-like activity and a peptidylglutamyl peptide hydrolysing activity (Arendt and Hochstrasser 1997; Chen and Hochstrasser 1996; Enenkel et al. 1994).

3.1.5. The Unfolded Protein Response

Accumulation of unfolded proteins in the lumen of the ER induces a signaling pathway called UPR for Unfolded Protein Response (Chapman et al. 1998; Shamu et al. 1994; Sidrauski et al. 1998). Ire1p is a conserved membrane kinase containing a luminal domain responsible for sensing misfolded proteins, a cytosolic kinase domain and a ribonuclease domain (Hampton 2003). In yeast, under normal growing conditions, monomeric Ire1p is bound to Kar2p in an inactive complex. High amounts of unfolded or misfolded proteins provoke the release of Kar2p from the complex and the assembly of Ire1p into an oligomeric active kinase complex (Shamu and Walter 1996). Ire1p autophosphorylation activates the C-terminal endoribonuclease activity and promotes the splicing of an intron in the *HAC1* pre-mRNA. The mature mRNA is then translated into a transcription factor which induces the expression of target genes by binding to a conserved UPR Element (UPRE) in the promoter regions (Cox and Walter 1996). The UPR alleviates stress by upregulating the expression of ER chaperones (Kar2p), proteins involved in the secretory pathway (Sec12p) and components of the ERAD pathway (Ubc7p and Hrd1p) (Travers et al. 2000).

3.1.6. Accumulation of unfolded proteins in subcellular compartments

Formation of tubulo-vesicular structures, known as ER-associated compartments (ERACs) (Figure 14A) (Huyer et al. 2004a), is induced by mutated forms of the plasma membrane H^+-ATPase (Pma1-D378N) (de

Kerchove d'Exaerde et al. 1995; Harris et al. 1994; Supply et al. 1993), Pdr5 ($Pdr5^{L183P}$) (de Thozee et al. 2007) and ABC-transporters Ste6p (Loayza et al. 1998). These structures are different from karmellae, which consist of stacked ER membrane pairs surrounding the nuclear envelope in cells overexpressing HMG-CoA reductase (Wright et al. 1988) (Figure 14B). ERACs and karmellae increase the volume of the ER, which may help the accomodation of overexpressed or misfolded membrane proteins and prevent the aggregation of unfolded proteins by reducing their concentration.

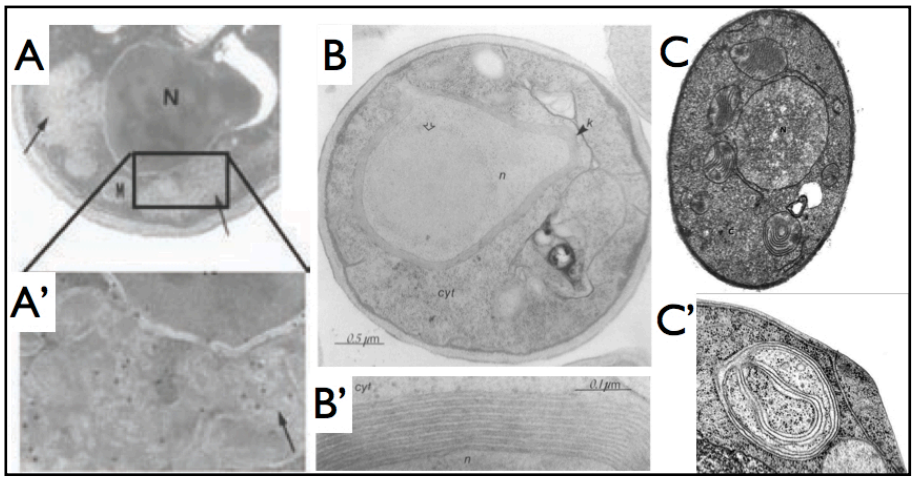

Figure 14. Electron micrographs of yeast cells showing different ER-derived subcompartments at low (top) or high (bottom) magnification. (A, A') Cells expressing a mutated form of the plasma membrane H^+-ATPase (Pma1-D378N) show ERACs that are marked by gold-linked antibodies raised against Kar2p (black dots). n, nucleus ; m, mitochondria ; and vacuoles can be seen (reviewed in Campagnolo and Ghislain 2010). **(B, B')** Cells overexpressing HMG-CoA reductase show karmellae (k), that are stacked membranes around the nucleus (n) in the cytoplasm (cyt) (Wright et al. 1988). **(C, C')** UPR-induced cells show ER-containing autophagosomes. n, nuclei ; c, cytoplasm. High-pressure freezing/freeze substitution image by Bernales et al. 2007.

In yeast, activation of the UPR pathway induces the formation of autophagosomes that selectively include ER membranes, their delimiting double membranes also being partially derived from the ER (Figure 14C) (Bernales et al. 2007). This so-called ER-phagy can remove damaged parts of the ER and participate in reducing the size of the ER back to normal once the folding stress is gone. ER-phagy could therefore represent an important degradative function of the UPR and be an integral player in achieving homeostatic control (Bernales et al. 2007).

The recently identified juxta-nuclear quality control (JUNQ) compartment serves as a temporary storage site for misfolded ubiquitylated proteins that cannot be folded or degraded because of the limited capacity of the ubiquitin-proteasome system under certain stress conditions (Kaganovich et al. 2008).

3.2. Vacuolar degradation

The main proteolytic compartment is the vacuole which represents 25% of the yeast cell volume. The vacuole contains a variety of degradative enzymes, including endo- and exo-proteases, ribonucleases, polyphosphatases, α-mannosidase, trehalase and alkaline phosphatase. Vacuolar proteases are synthesized as inactive proproteins. The N-terminal sequence of the proproteins is removed by vacuolar proteinase A (Pep4p) and/or proteinase B (Prb1p) resulting in active proteins (Van Den Hazel et al. 1996). The vacuole also serves as a storage site for amino acids, purines,

polyamines, polyphosphates and various toxic substances. The multi-subunit membrane H^+-ATPase mediates vacuole acidification which is required for intracellular pH homeostasis and osmotic regulation besides protein degradation.

3.2.1. Transport pathways to the vacuole

Several different transport pathways converge to the vacuole (Figure 15). Vacuolar proteins are transported from the ER to the Golgi, via the COPII vesicles (see §4.1) and diverted to the vacuole via the CPY pathway. Proteins from the cell surface are transported to the vacuole for degradation through the endocytic pathway. These two pathways join at the multivesicular body (MVB), prevacuolar or late endosomal compartment. The alkaline phosphatase (ALP) pathway is an other pathway that bypasses the MVB. The cytosol-to-vacuole targeting (Cvt) pathway is used by hydrolase aminopeptidase I (API) and is distinct from autophagy which nonselectively delivers cytosolic proteins and organelles to the vacuole for degradation and recycling.

The proteasomal/ERAD and autophagic pathways function together to eliminate misfolded proteins (Bernales et al. 2007; Fu and Sztul 2009). Using a real-time imaging approach, Fu and Sztul (2009) have shown that a marker of pre-autophagosomes co-localizes with ERACs, the formation of which is induced by expression of CFTR in yeast. The ERACs have also been shown to be temporally and spatially adjacent to the vacuolar compartment (Fu and Sztul 2009). As previously mentioned, the

accumulation of misfolded proteins in the ER activates the UPR, inducing the formation of autophagosomes (Bernales et al. 2007).

ER-associated degradation of the misfolded Pma1-D138T form is increased upon overexpression of the Cvt pathway component, Atg19p, supporting the view that Cvt and ERAD pathways are linked (Mazon et al. 2007).

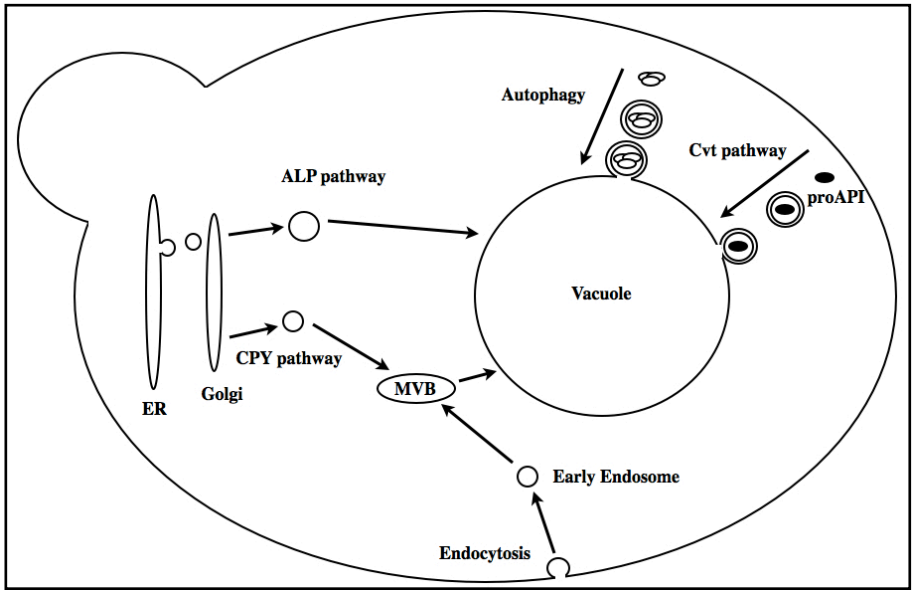

Figure 15. Transport pathways to the vacuole. Vacuolar proteins in the late-Golgi compartment are sorted in vesicles that are addressed to the vacuole. Soluble CPY is delivered to the vacuole via the MultiVesicular Body (MVB) pathway whereas alkaline phosphatase (ALP) bypasses it. Proteins that are endocytosed from the cell surface are transported to the vacuole via the MVB pathway. The cytoplasm-to-vacuole pathway (Cvt) taken by aminopeptidase I (API) and autophagy are also shown.

3.2.2. Ubiquitin as an endocytosis signal for plasma membrane proteins

The link between Ub and membrane trafficking was discovered 15 years ago by Kölling and Hollenberg (1994). They observed that ubiquitylated Ste6p forms accumulated at the plasma membrane in mutants impaired in endocytosis. Hicke and Riezman (1996) showed that the ubiquitylation of the α pheromone receptor, Ste2p, was required for its internalization via endocytosis. The Rsp5 Ub-ligase (HECT domain) is a main determinant of Ub-dependent internalization of several plasma membrane proteins (Hein et al. 1995; Huibregtse et al. 1995), and its role in protein's ubiquitylation was first identified in the case of the Fur4 uracil permease (Galan et al. 1996). Other proteins subject to Ub-dependent endocytosis are Pdr5p (Egner and Kuchler 1996) and the general amino acid permease, Gap1p (Helliwell et al. 2001; Leon et al. 2008; Soetens et al. 2001; Springael et al. 1999).

4. Role of the secretory pathway in ERAD

4.1. ER-to-Golgi transport

The COat Protein complex II (COPII) vesicles mediate the transport of newly synthesized proteins from the ER to the Golgi apparatus (Figure 16, left frame). The process begins with the conversion of soluble Sar1-GDP into membrane-embedded Sar1-GTP, through a transient interaction with the ER-located GDP/GTP exchange factor, Sec12p (Barlowe et al. 1994). Then, Sar1-GTP recruits the Sec23/24 heterodimer complex to form a prebudding complex, which binds Sec13p/Sec31p and facilitates the formation of a scaffold complex leading to vesicle budding and sorting out of the ER membrane.

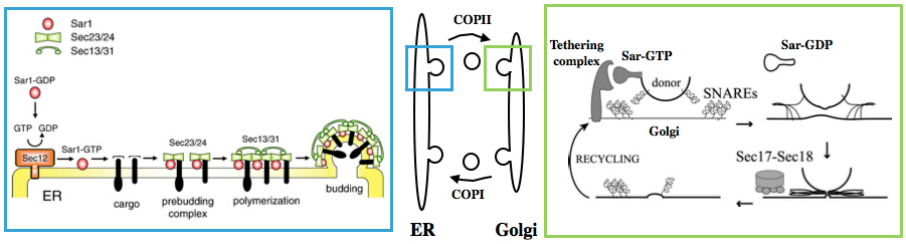

Figure 16. COPII vesicle formation (modified from Sato and Nakano 2007) and vesicle tethering and fusion with Golgi membrane (modified from de Thozee et al. 2007). See text for details.

Before the fusion step involving SNAREs (see below), there is a tethering step (Figure 16, right frame). The tethering is the first interaction of a vesicle and the membrane of an acceptor compartment. Proteins and protein

complexes involved in this step are called tethers or tethering complexes. The tethering step is crucial because it determines the specificity of vesicle targeting. The tethering complexes are Rab effectors, they bind to specific activated GTP- bound Rab GTPases and this allows the tethering of the vesicle to the acceptor membrane. The interaction promotes GTP hydrolysis and Rab-GDP release from the vesicle membrane (Grosshans et al. 2006).

The last step of vesicular transport is fusion. The fusion of vesicles with acceptor compartment is mediated by a special set of proteins called SNAREs (Bonifacino and Glick 2004; Cai et al. 2007). Two categories of SNAREs are distinguished: v-SNAREs are carried by the transport vesicles and t-SNAREs are present on the target membrane. Most SNAREs are transmembrane proteins with a cytosolic N-terminal domain containing the «SNARE motif», which forms a coilded-coil structure after the interaction with other SNAREs (Bock et al. 2001). Usually one SNARE protein, present on one membrane, interacts with three SNARE proteins present on the other. After membrane fusion, Sec17p and Sec18p AAA-ATPase are recruited to disassemble the four interacting SNAREs that are lying on the same membrane (Mayer et al. 1996).

Erv29p and Erv14p are members of the ER vesicle (ERV) family. These membrane proteins receptors load soluble protein cargos into the COPII vesicles (Caldwell et al. 2001; Vashist et al. 2001). Their mutation results in the stabilization of CPY* and PrA* (Vashist et al. 2001). ERADication of Sec61p and misfolded vacuolar H^+-ATPase subunit Vph1p* is not affected by the loss of Erv29p and Erv14p (Biederer et al. 1996; Brodsky and

McCracken 1997). It is likely that membrane protein cargos do not require the receptors as they may interact physically with the coat proteins.

Mutations in the *SEC12* and *SEC18* genes cause stabilization of most soluble (CPY*, PrA* and KHN) and membranous (KWW) ERAD substrates analysed (see Figure 11) (Caldwell et al. 2001; Vashist et al. 2001; Vashist and Ng 2004). From those studies, it seems that the degradation of membrane proteins with a cytosolic lesion does not require Sec12p and Sec18p. To explain the requirement of ER-to-Golgi transport in ERAD, an hypothetical post-ER quality control system which would detect the misfolded proteins that have escaped the ER is assumed. Incomplete glycosylation in the Golgi may be a determining step in targeting the misfolded proteins back to the ER for proteasomal degradation.

A direct contribution of ER-to-Golgi transport in ERAD is the subject of controversy as the *sec18* mutation leads to the depletion of luminal chaperone proteins (e.g. Kar2p) in the ER as the consequence of its accumulation in COPII vesicles and the stabilization of damaged ER luminal proteins. This effect explains why degradation of membrane proteins with a cytosolic mutation is independent of Sec18p as Kar2p is not required.

CFTR is used as an ERAD substrate in yeast. Pulse-chase analysis of CFTR degradation indicates a role of the Sar1p/COPII machinery which is independent of its function in ER-to-Golgi traffic as CFTR is not stabilized in *sec18* mutant strains (Fu and Sztul 2003). The Sar1p/COPII machinery

might mediate the sorting of CFTR into specific ER compartments (ERACs), which constitue the entry to the proteasomal degradation pathway.

4.2. Golgi-to-ER transport

Retrograde transport of proteins from the Golgi to ER is mediated by another complex of coat proteins, called COPI (COat Protein complex I). The main component of the COPI coat is a heptameric complex consisting of two subcomplexes (Figure 17) (reviewed in Beck et al., 2009; Hsu and Yang, 2009). The F subcomplex contains the β (Sec26p), γ (Sec21p), δ (Ret2p) and ζ (Ret3p) subunits and the B subcomplex, the α (Cop1p/Sec33p), β' (Sec27p) and ε (Sec28p) subunits. The initiation of COPI vesicle formation is controlled by Arf1p, a small GTPase. The inactive form of Arf1p (GDP-bound) is recruited to the membrane via the p24 complex. The activation of Arf1p depends on the GDP/GTP exchange factors, Gea1p and Gea2p (Peyroche et al. 1996; Spang et al. 2001). Then, the activated Arf1p-GTP recruites the coatomer to the membrane leading to vesicle budding and sorting out of the Golgi membrane.

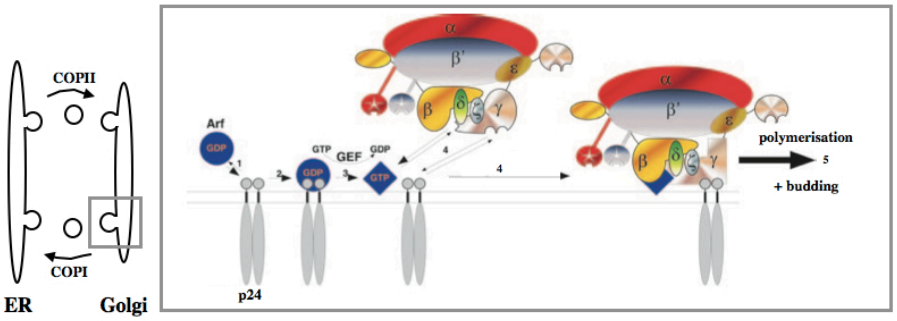

Figure 17. COPI formation (modified from Bethune et al. 2006). (1-2) The inactive form of Arf1p (GDP-bound) is recruited to the membrane via the p24 complex. **(3)** A GDP/GTP exchange factor (Gea1p or Gea2p) catalyzed the exchange of GDP into GFP. **(4)** Activated Arf1p-GTP recruites the coatamer to the membrane. **(5)** Then, Golgi membrane starts to deform and the vesicle buds.

Mutations impairing COPI-mediated retrograde transport have never been used to analyse the requirement of ER-to-Golgi transport for ERAD as these mutations may lead to depletion of the COPII components and proteins, that escape the ER and need to be transported back to the ER.

Aim of the Study

The main objective of the doctoral work was to ascertain the veracity of models featuring how newly synthesized membrane proteins are targeted for degradation by the proteasome. According to the widely accepted model of ERAD (Ahner and Brodsky 2004; Vashist and Ng 2004), a membrane protein that is misfolded as the result of a mutation in a cytosolic region is ubiquitylated by the ER protein Ub-ligase Doa10p (ERAD-C pathway) and transported back to the cytosol in a Der1p and Sec61p-independent process. In contrast, a membrane protein with a misfolded region facing the ER lumen is ubiquitylated by Hrd1p (ERAD-L pathway) and requires Der1p and/or Sec61p for degradation. The ERAD-C and ERAD-L pathways have been identified by using membrane proteins with cytosolic lesions or luminal mutated proteins, respectively. However some proteins used for the validation are engineered fusions consisting of fragments of luminal and cytosolic proteins that are linked by an exogenous transmembrane span (e.g. CTG* in Figure 11 and Table 2). The suitability of those artificial test proteins is therefore questionable.

We have shown that the $Pdr5^{L183P}$ variant having a mutation in a cytosolic loop is targeted for ERAD (de Thozee et al. 2007). This mutated form is predicted to be degraded through the ERAD-C pathway. In contrast, the $Pdr5^{C1427Y}$ variant (Plemper et al. 1998) having a mutation in a luminal loop is predicted to be targeted for proteasomal degradation via the ERAD-L pathway. The availability of these mutated forms of Pdr5p allowed us to test the current model by using yeast strains impaired in key components of the ERAD pathways (Hrd1p, Doa10p and Der1p).

Degradation of a transmembrane protein fusion having lesions in cytosolic and luminal loops (KSS) has been shown to require the ERAD-C components for degradation, as if the ERAD-C pathway predominates over the ERAD-L pathway (Vashist and Ng 2004). To confirm this finding, we constructed a mutated form of Pdr5p that contains a proline residue at position 183 and a tyrosine residue at position 1427 and assessed the requirement of the ERAD-C and -L components for Pdr5$^{L183P+C1427Y}$ degradation.

Mutated forms of CPY and PrA and engineered KHN and KWW proteins require the transport between ER and Golgi to be degraded by the Ub-proteasome system (Caldwell et al. 2001; Vashist et al. 2001). To assess the importance of the ER-to-Golgi transport for degradation of the mutated Pdr5 forms, we used strains that are impaired in Sec12p, Sec18p and Ret3p. If the ER-to-Golgi transport is required, a stabilization in *sec12*, *sec18* and *ret3* mutant strains should be seen. The Sar1p/COPII machinery mediates the sorting of CFTR into ER subdomains, a function independent of its role in ER-to-Golgi traffic (Fu and Sztul 2003). To assess the independent function of Sar1p/COPII machinery in ER-to-Golgi transport, we used strains impaired in Sec12p and Sec18p. If the hypothesis is correct, we should see a stabilizing effect of the *sec12* mutation, but not *sec18*.

A second objective of this doctoral work was the identification of amino-acid determinants in the Pdr5 sequence which trigger the quality control system and subsequent degradation. Three C-truncated variants of Pdr5p that lack the last 2, 4 or 6 TMSs were constructed to underline these degradation

determinants but also to determine which proteolytic system (vacuolar versus proteasomal) is used.

It has been shown that several mutated/truncated proteins accumulate in ERACs (de Kerchove d'Exaerde et al. 1995; de Thozee et al. 2007; Harris et al. 1994; Huyer et al. 2004a; Loayza et al. 1998; Supply et al. 1993; Wright et al. 1988) or karmellae (Wright et al. 1988) (see Introduction §3.1.5.). It is possible that a specific polypeptide conformation induces the formation of these subcellular compartments. To see if the mutated/truncated Pdr5 variants form intracellular vesicles, we fused the GFP to the mutated versions of Pdr5p, analysed their localization by fluorescence microscopy and tried to establish a correlation between a specific polypeptide conformation and the formation of these subcellular compartments.

The accumulation of mutated/truncated proteins in the ER lumen induces the UPR pathway (Chapman et al. 1998; de Thozee et al. 2007; Shamu et al. 1994; Sidrauski et al. 1998), resulting in increased expression of ER chaperones (Kar2p) and proteins involved in the secretory (Sec12p) and ERAD (Hrd1p) pathways. We therefore analysed the effect of the expression of the mutated Pdr5p forms on the activation of the β-galactosidase gene (*lacZ*) placed under the control of the *KAR2* UPRE-containing promoter.

Results

The first step of the projet was the construction of various mutated versions of Pdr5p (Figure 1 and Table 1).

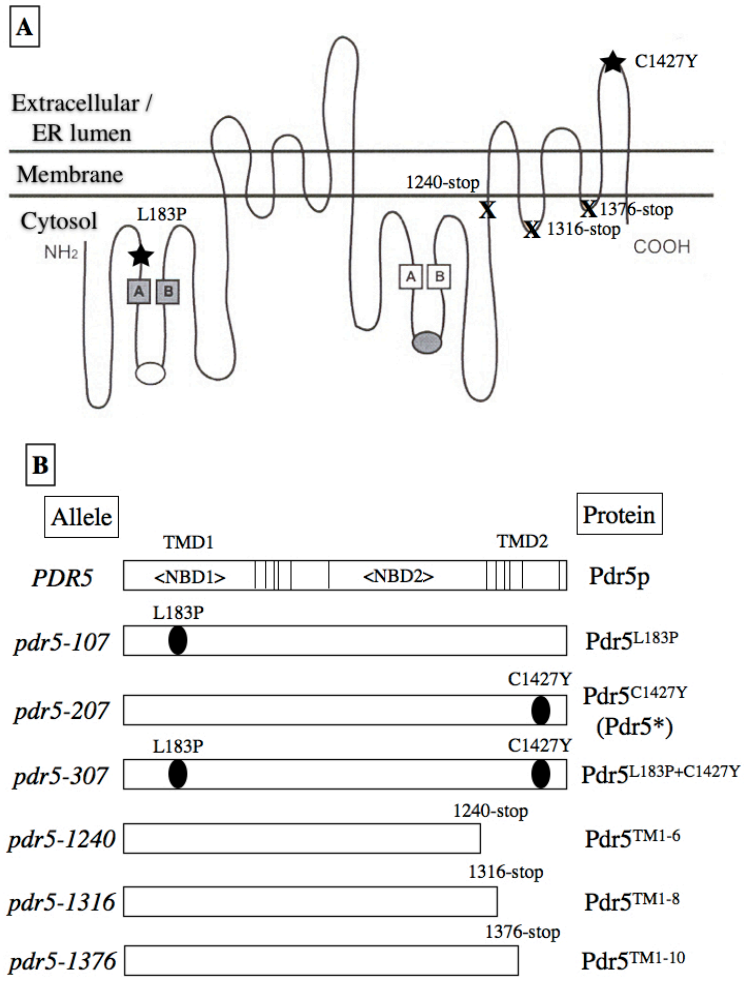

Figure 1. Schematic views of Pdr5p and its mutated/truncated versions. (A) Amino-acid substitutions are indicated with a black star and the nonsense mutations resulting in the formation of truncated variants with a cross. **(B)** Schematic representation of Pdr5p showing the position of the changes in the *pdr5-107*, *pdr5-207*, *pdr5-307*, *pdr5-1240*, *pdr5-1316* and *pdr5-1376* alleles and corresponding mutated forms. Amino-acid substitutions are indicated with a black circle. The NBDs and TMDs are highlighted.

The protein variant designated Pdr5^{L183P} has a leucine residue replaced by a proline at position 183 in the N-terminal cytosolic domain. This mutation has been identified in a screen for mutant strains showing increased drug sensitivity (de Thozee et al. 2007). Using a PCR-based strategy, we introduced the L183P mutation in the *PDR5* gene on the multicopy pRS426 plasmid (origin of replication from the yeast endogenous 2µ plasmid).

The mutated Pdr5^{C1427Y} form contains a tyrosine instead of a cysteine at position 1427 in the C-terminal extracellular loop. This mutated form was identified by Egner et al. (1998) in a screen for mutants impaired in drug transport and used by Plemper et al. (1998) to dissect the ERAD pathway.

We constructed the Pdr5$^{L183P+C1427Y}$ variant by combining the two amino-acid substitutions described above.

The truncated Pdr5^{TM1-10} version contains a C-terminal deletion of 135 amino-acids, removing the last 2 transmembrane spans (TMSs). Pdr5^{TM1-8} and Pdr5^{TM1-6} lack 4 and 6 TMSs as a consequence of the deletion of 195 and 271 residues, respectively.

The mutated and truncated forms of Pdr5p were expressed from the *PDR5* promoter cloned on the multicopy pRS426 plasmid.

Two shorter versions of Pdr5^{TM1-6} lacking the last 353 (Pdr5^{1157}) or 467 amino-acids (Pdr5^{1043}) have been constructed by de Thozee et al. (2007) (chromosomal constructions) (Figure 2 and Table 1).

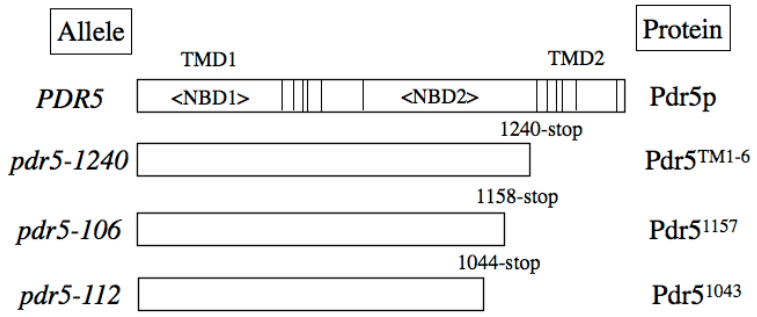

Figure 2. Shematic representation of Pdr5p showing the position of the changes in the *pdr5-1240*, *pdr5-106* and *pdr5-112* mutants. The NBD and TMD are highlighted.

Table 1. Mutant *pdr5* alleles and the encoded protein forms.

Allele	Protein	Reference
PDR5	Pdr5p	Wild-type protein
pdr5-107	Pdr5^{L183P}	de Thozee et al. 2007
pdr5-207	Pdr5^{C1427Y} (Pdr5*)	Egner et al. 1998
pdr5-307	Pdr5$^{L183P+C1427Y}$	This study
pdr5-1240	Pdr5^{TM1-6}	This study
pdr5-1316	Pdr5^{TM1-8}	This study
pdr5-1376	Pdr5^{TM1-10}	This study

Allele	Protein	Reference
pdr5-106	$Pdr5^{1157}$	de Thozee et al. 2007
pdr5-112	$Pdr5^{1043}$	de Thozee et al. 2007

1. Drug sensitivity phenotype of yeast strains expressing Pdr5p variants

1.1. The three mutated forms of Pdr5p

The effect of the $Pdr5^{L183P}$ mutation on drug transport has been analysed using cells that express the mutated ABC-transporter protein from a chromosomal copy (de Thozee et al. 2007). The effect of the $Pdr5^{C1427Y}$ mutation was reported by Kuchler and collaborators (Plemper et al. 1998) who showed that wild-type Pdr5p is a moderately short-lived protein ($t_{1/2} \simeq$ 90 min) in contrast to our results (this work; Decottignies et al. 1999). This discrepancy could be explained by the difference in the yeast strains or in the expression system used (plasmid versus chromosomal copy of the *PDR5* gene). That is why we decided to confirm the effects of the $Pdr5^{L183P}$, $Pdr5^{C1427Y}$ and $Pdr5^{L183P+C1427Y}$ using the expression system designed in this work.

The Pdr5p variants were tested for the ability to confer resistance to cycloheximide (a protein synthesis inhibitor) and itraconazole (an ergosterol synthesis inhibitor). These drugs are specifically transported by Pdr5p and previously used by de Thozee et al. (2007) and Egner et al. (1998) for cells expressing $Pdr5^{L183P}$ and $Pdr5^{C1427Y}$, respectively. Note that the binding site (s) for these drugs have not been identified. We also assayed the resistance to Rhodamine 6G which has not been used in previous studies on $Pdr5^{L183P}$ and $Pdr5^{C1427Y}$. Rhodamine 6G binds to site 1 in Pdr5p and is used as a fluorescent substrate in transport assays.

The *pdr5Δ* (FYMK1/1) strain was transformed with the plasmids expressing Pdr5p, $Pdr5^{L183P}$, $Pdr5^{C1427Y}$ or $Pdr5^{L183P+C1427Y}$. Exponential phase cultures of appropriate transformants in minimal SD medium were diluted to an OD_{600} of 10^{-1}, 10^{-2}, 10^{-3} and 10^{-4}, and 7 µl of each diluted culture were spotted onto SD minimal plates containing 0.01-1.5 µg/mL of cycloheximide, 0.05-6 µg/mL of itraconazole (Figure 3) or 5-200 µg/mL of Rhodamine 6G (Figure 5).

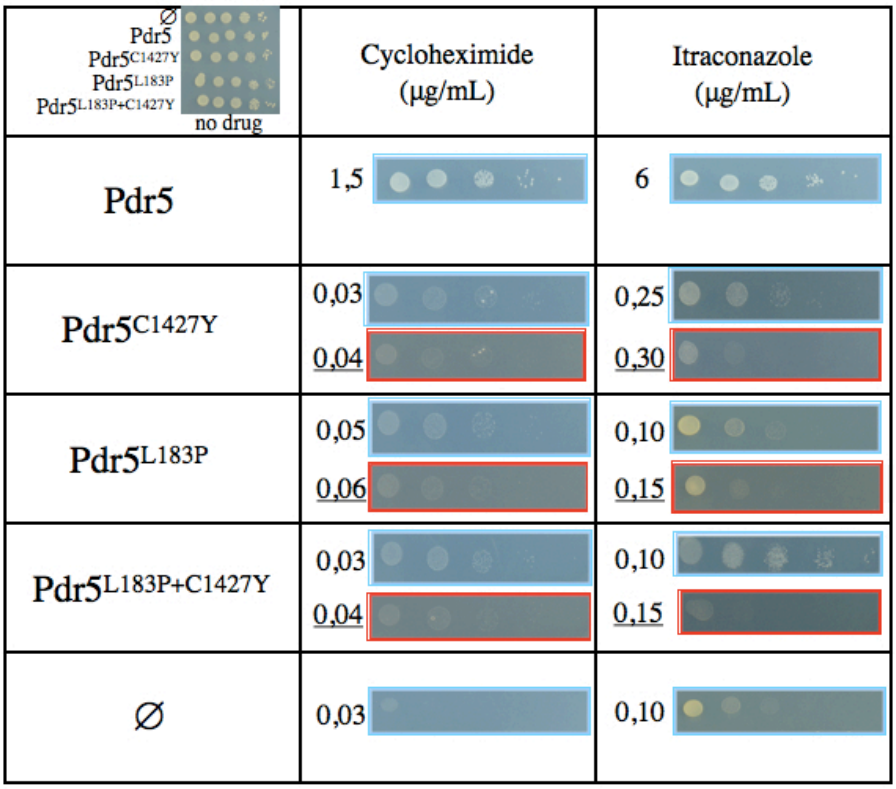

Figure 3. Drug sensitivity phenotype of cells expressing Pdr5 variants. *pdr5Δ* cells (FYMK1/1) transformed with an empty pRS426 plasmid (∅) or a plasmid expressing the indicated wild-type or mutated forms of Pdr5p were grown in SD medium. 7 µl of the cultures diluted 10, 100, 1000 or 10 000 times were spotted onto agar plates containing various concentrations of cycloheximide or itraconazole and the plates were incubated at 28°C for 3 days. The minimal inhibitory concentration (MIC) is underlined. The growth in the absence of the drugs is shown on the top left corner.

As shown in Figure 3, cells expressing wild-type Pdr5p were able to tolerate 1.5 µg/mL of cycloheximide and 6 µg/mL of itraconazole. In contrast, cells expressing Pdr5^{L183P}, Pdr5^{C1427Y} or Pdr5$^{L183P+C1427Y}$ failed to grow in the presence of 0.04-0.06 µg/mL of cycloheximide and 0.15-0.30 µg/mL of

itraconazole. These MIC values are the average of 3 independent assays done with 3 different clones.

In conclusion, the phenotypic analysis confirmed that the L183P and C1427Y substitutions impair cells resistance to cycloheximide and itraconazole as shown by de Thozee et al. (2007) and Egner et al. (1998) despite the differences in the strains and expression systems used. As expected, $Pdr5^{L183P+C1427Y}$ is unable to confer resistance to these drugs, indicating the absence of intragenic suppression of one mutation by the second one.

A more precise determination of drug sensitivity using exponential (rather than stationary) cultures grown in liquid media to keep the drug concentration constant during the assay was carried out. Drug concentration causing 50% growth inhibition (IC_{50}) was determined by adding cycloheximide (0-1.5 μg/mL) or itraconazole (0-6 μg/mL) to liquid cultures. When the cells expressing Pdr5p reached an OD_{600} of 0.8-1 (wild-type control), the incubation was stopped and OD_{600} was measured for the mutant cultures. Relative growth was expressed as the percentage of the OD_{600} value obtained for the *PDR5* cells. Figure 4 shows the average values from 2 independent growth assays using 2 different clones.

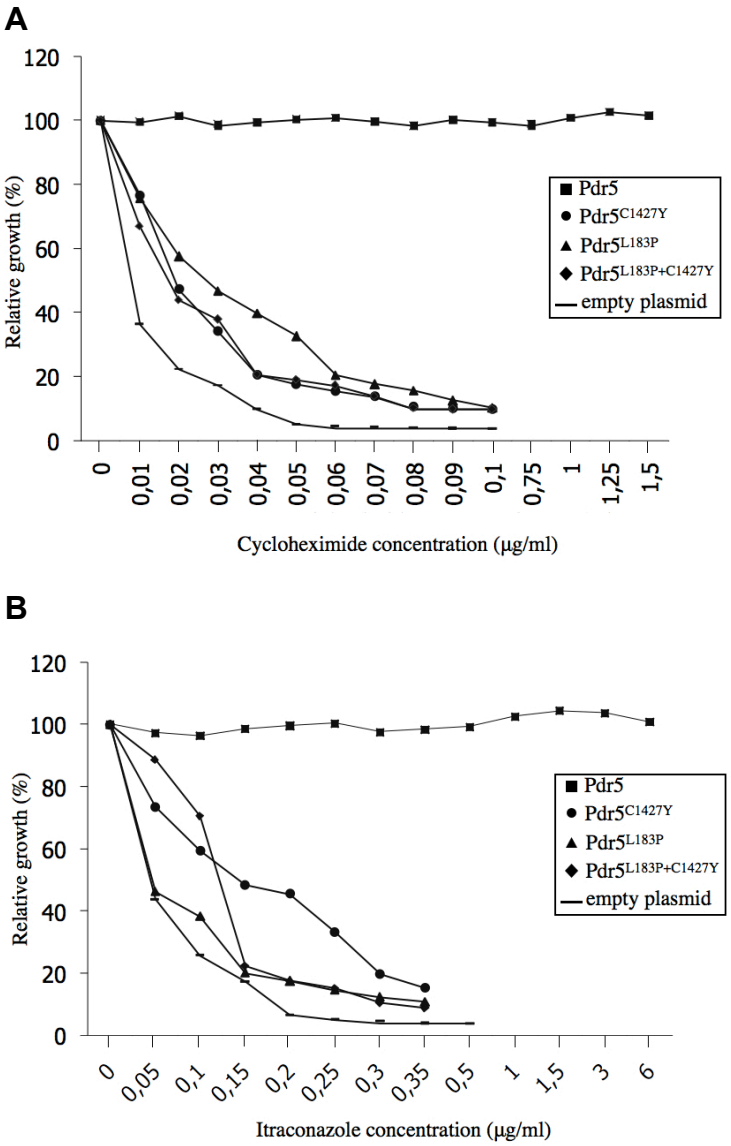

Figure 4. Relative drug sensitivity of cells expressing wt or various mutant forms of Pdr5p. Equal amount of exponentially growing cells were added to SD medium containing the indicated concentrations of cycloheximide **(A)** or itraconazole **(B)** and incubated at 28°C. Once the wild-type *PDR5* cells reached an OD_{600} of 0.8-1, incubation was stopped and the OD_{600} for the mutant cells was expressed as a percentage of the value measured for the wild-type cells.

Cycloheximide IC_{50} values are 0.01-0.02 ug/mL for $Pdr5^{C1427Y}$ and $Pdr^{L183P+C1427Y}$ and 0.02-0.03 µg/mL for $Pdr5^{L183P}$ (Figure 4A).
Itraconazole IC_{50} values are ≈ 0.05 µg/mL for $Pdr5^{L183P}$ and 0.10-0.15 µg/mL for $Pdr5^{C1427Y}$ and $Pdr5^{L183P+C1427Y}$ (Figure 4B).

In comparison to cells expressing $Pdr5^{L183P}$, the cells expressing $Pdr5^{C1427Y}$ showed an increased sensitivity to cycloheximide, but a decreased sensitivity to itraconazole. These results suggest a specific role of Leu183 in the efflux of itraconazole whereas Cys1427 is important for cycloheximide transport. Note that Leu183 is a relatively well conserved residue in other ABC proteins and is close to the Walker A motif in the first NBD. The Leu183 homologous residue of the *E. coli* vitamin B12 transporter BtuCD (Locher et al. 2002) is part of a conserved β-strand. Considering the localization of proline, the L183P substitution is likely to disturb the fold of Pdr5p NBD1 and so the ATP hydrolysis. The mutation might also impair ABC-transporter dimer formation. In conclusion, the cycloheximide or itraconazole sensitivity phenotype observed for $Pdr5^{L183P}$ could be due to a failure of ATP hydrolysis or dimer formation.

As shown in Figure 5, cells expressing wild-type Pdr5p were able to grow in the presence of 200 µg/mL of Rhodamine 6G. In contrast, cells expressing the mutated Pdr5 forms failed to grow in the presence of 15 µg/mL ($Pdr5^{C1427Y}$), 20 µg/mL ($Pdr5^{L183P}$) and 10 µg/mL ($Pdr5^{L183P+C1427Y}$) of Rhodamine 6G suggesting that Leu183 and Cys1427 are important for Rhodamine 6G transport.

Figure 5. Rhodamine 6G sensitivity of cells expressing Pdr5 variants. *pdr5Δ* cells (FYMK1/1) transformed with an empty pRS426 plasmid (∅) or a plasmid expressing the indicated wild-type or mutated forms of Pdr5p were grown in SD medium. 7 µl of the cultures diluted 10, 100, 1000 or 10 000 times were spotted onto agar plates containing various concentrations of Rhodamine 6G and the plates were incubated at 28°C for 3 days. The minimal inhibitory concentration (MIC) is underlined. The growth in the absence of the drugs is shown on the top left corner.

The plasmids expressing the various Pdr5p mutated forms were also transformed into *PDR1 PDR5* (FY1679-28C), *PDR1-3 PDR5* (FYM26/8-5C) and *PDR1-3 pdr5Δ* (FYMK26/8-5077) strains. *PDR5* strains were used to ascertain that the possibility of dimer formations

between mutated and wild-type Pdr5p do not influence the drug sensitivity phenotype. The *PDR1-3* allele encoding a hyperactive form of Pdr1p was used to determine the effect of increased amount of the mutated Pdr5p forms on the drug sensitivity phenotype. A comparable level of drug hypersensitivity was observed whatever the construct or the strain analysed (data not shown) indicating no influence of the endogenous *PDR5* gene or the increased expression of the mutated Pdr5p variants.

1.2. The three C-truncated variants of Pdr5p

To analyse the effects of C-terminal truncations on Pdr5p function, we introduced high copy plasmids expressing Pdr5p and the truncated $Pdr5^{TM1-6}$, $Pdr5^{TM1-8}$ and $Pdr5^{TM1-10}$ into the *pdr5Δ* (FYMK1/1) strain and we analysed the growth of the transformants in the presence of cycloheximide, itraconazole and Rhodamine 6G.

Exponential phase cultures in minimal SD medium were diluted to an OD_{600} of 10^{-1}, 10^{-2}, 10^{-3} and 10^{-4}, and 7 µl of each diluted culture were spotted onto SD minimal plates containing 0.01-1.5 µg/mL of cycloheximide, 0.05-6 µg/mL of itraconazole (Figure 6) or 5-200 µg/mL of Rhodamine 6G (Figure 7).

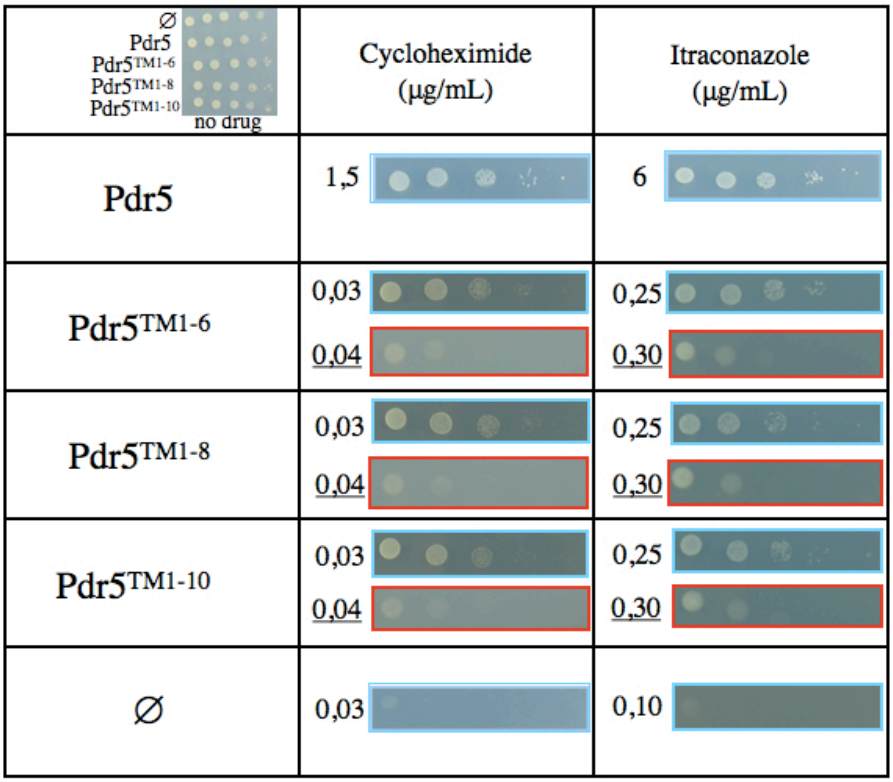

Figure 6. Drug sensitivity phenotype of *pdr5Δ (FYMK1/1)* cells expressing C-terminally truncated forms of Pdr5p. Growth assay was performed as described in Figure 3. Note that the pictures shown for wt Pdr5 is identical to those shown in Figure 3.

The truncation of 2, 4 and 6 TMS impair similarly the growth in the presence of 0.04 µg/mL of cycloheximide (Figure 6), 0.30 µg/mL of itraconazole (Figure 6) and 15 µg/mL of Rhodamine 6G (Figure 7). These MIC values are the average of 3 independent assays realized with 3 different clones.

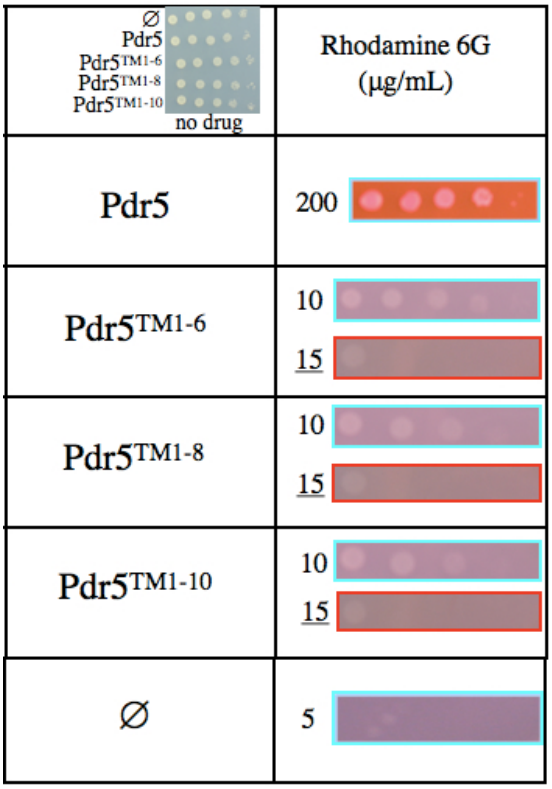

Figure 7. Rhodamine 6G sensitivity of *pdr5Δ (FYMK1/1)* cells expressing various C-terminally truncated forms of Pdr5p. Growth assay in the presence of the indicated concentrations of Rhodamine 6G was performed as described in Figure 5. The results for wt Pdr5p has been taken from Figure 6.

Note that two shorter versions of Pdr5^{TM1-6} (Pdr5^{1157} and Pdr5^{1043}, see Figure 2) have been shown to confer no resistance to cycloheximide and itraconazole (de Thozee et al. 2007).

Compared to Pdr5$^{L183P+C1427Y}$, the truncated forms confer increased Rhodamine 6G resistance (MIC values of 0,15 µg/mL versus 0,10 µg/mL).

Compared to $Pdr5^{L183P}$ or $Pdr5^{L183P+C1427Y}$, the truncated Pdr5p forms confer increased resistance to itraconazole (MIC values of 0,30 µg/mL versus 0,15 µg/mL). $Pdr5^{1157}$ and $Pdr5^{1043}$ variants are also less slightly affected in their ability to confer resistance to the itraconazole, when compared to $Pdr5^{L183P}$ (de Thozee et al. 2007). This results can be explained if the C-terminal truncations had a smaller effect on the protein's expression levels and/or the addressing of the ABC-transporter to the plasma membrane. An other explanation is the lack of ATP hydrolysis, as suggested by localization of the mutated residue in the NBD1,

2. Expression levels of Pdr5p variants

2.1. Western blot analysis

Decreased cell tolerance to drugs may result from decreased amounts of the Pdr5p variants. Indeed, reduced metabolic stability of $Pdr5^{L183P}$ has been shown (de Thozee et al. 2007).

The expression levels of the wild-type and mutated forms of Pdr5p in *PDR1 pdr5Δ* (FYM1679-28C) and *PDR1-3 pdr5Δ* (FYMK26/8-5077) strains were compared by Western blot analysis. The *PDR1-3* allele was used to determine whether the expression levels of the wild-type and mutated versions of Pdr5p is affected by an upregulation at the transition to the stationary phase of growth. Whole-cell extracts were prepared from exponential (OD_{600} = 0.5-0.7 and OD_{600} = 0.8-1), stationary (OD_{600} = 1.6-2) and late stationary (OD_{600} = 2.2-2.5) cultures grown in minimal SD medium.

Proteins (10 µg) were separated by SDS-polyacrylamide gel electrophoresis (PAGE), tranferred onto a nitrocellulose membrane and incubated with antibodies against Pdr5p and Cdc48p, the latter being used for control of equal sample loading. The results obtained with the *PDR1* cells are shown in Figure 8 for the mutated forms and in Figure 9 for the truncated forms.

A 165-kDa band corresponding to Pdr5p was detected in exponentially growing *PDR1* cells (Figures 8, panels A and B). Surprisingly, the expression levels of $Pdr5^{C1427Y}$ were increased compared to those of the wild-type ABC transporter (panel B). The expression levels of Pdr5p and $Pdr5^{L183P}$ were comparable, whereas those of $Pdr5^{L183P+C1427Y}$ were reduced (panel B). At the transition to the stationary phase, $Pdr5^{L183P}$ and $Pdr5^{L183P+C1427Y}$ were no more detected and the expression levels of Pdr5p and $Pdr5^{C1427Y}$ were comparable (panel C). No band for Pdr5p and the variants were seen in stationary phase cultures (panel D). The signal for Cdc48p was identical between the various strains examined, indicating that identical protein amounts were analysed. Western blot analysis was repeated 4 times, with independently prepared extracts giving similar results.

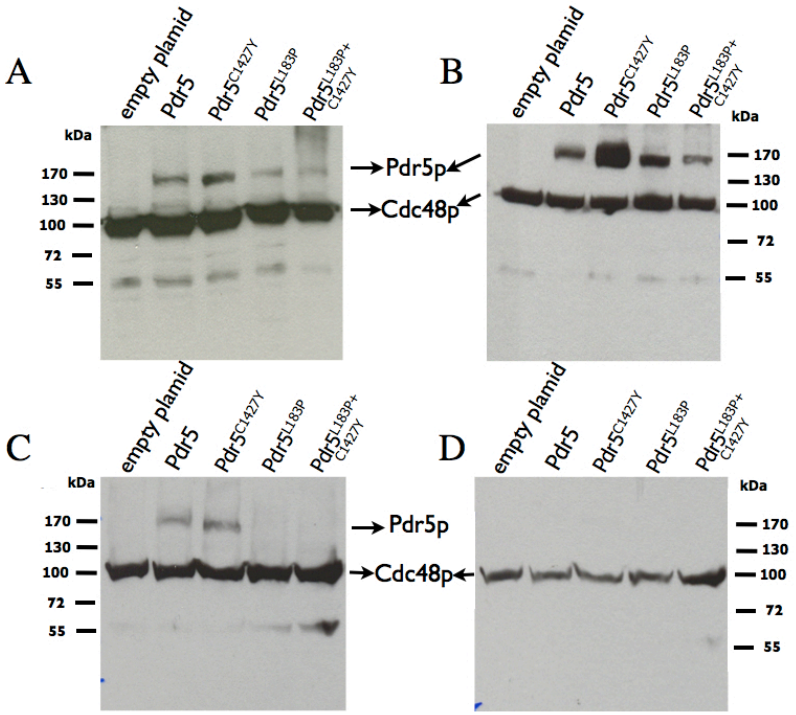

Figure 8. Western blot analysis of wild-type and mutated versions of Pdr5p in *PDR1 pdr5Δ* cells. Whole-cell extracts were prepared from cultures harvested at an OD_{600} of 0.5-0.7 **(A)**, 0.8-1 **(B)**, 1.6-2 **(C)** and 2.2-2.5 **(D)**. Cells were broken by vigorous agitation using glass beads in the presence of protease inhibitors. Proteins (10 µg) were analysed by SDS-PAGE and Western blot using antibodies against Pdr5p (1/2000 dilution) or the cytosolic protein Cdc48p (1/9000 dilution). The size of Pdr5p and Cdc48p are indicated. The membrane was exposed to a Kodak XAR film for 35 min (A-B) or 16 h (C-D).

In exponentially growing *PDR1* cells, $Pdr5^{TM1-10}$ and $Pdr5^{TM1-8}$ were detected as a band of 151 kDa and 145 kDa respectively (Figure 9, panels A and B). The amount of $Pdr5^{TM1-8}$ is comparable to that of Pdr5p whereas that of $Pdr5^{TM1-10}$ is decreased. No signal was detected for $Pdr5^{TM1-6}$ (predicted molecular mass of 138 kDa). At the transition to the stationary

phase, the expression levels of Pdr5^{TM1-8} increased compared to those seen for the wild-type version (panel C). Pdr5^{TM1-8} and wild-type Pdr5p are no more detected in stationary phase cultures (panel D). Cdc48p is expressed to comparable levels between the various strains, indicating that identical protein amounts were analysed. Western blot analysis was repeated 3 times using independently prepared extracts. Similar results were obtained each time. The 55-kDa and 72-kDa bands are unknown proteins that cross react with the Cdc48p antibodies.

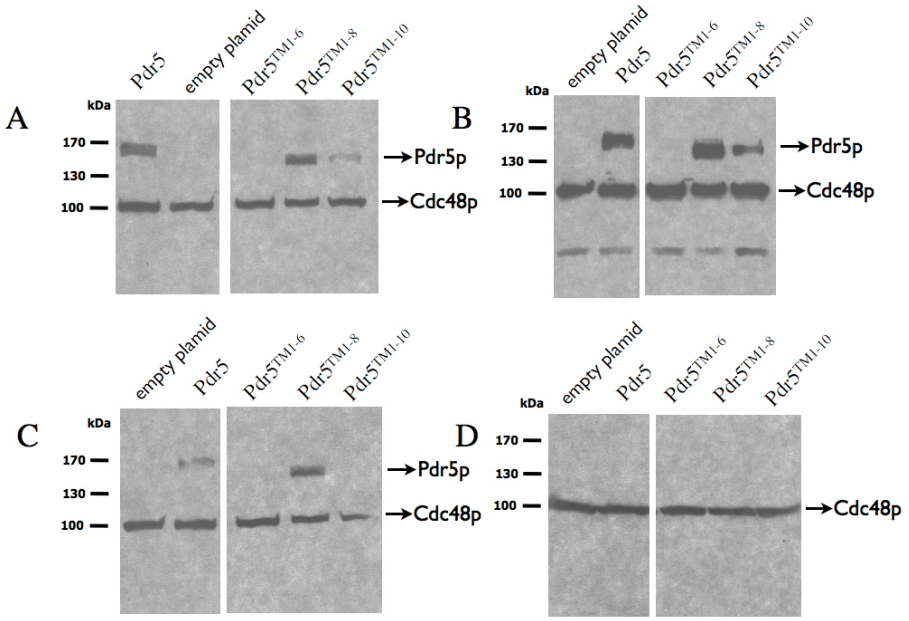

Figure 9. Expression levels of C-terminally truncated versions of Pdr5p in *PDR1 pdr5Δ* cells. See Figure 8 for details. The membrane was exposed to a Kodak XAR film for 30 min.

In conclusion, the L183P mutation and the truncation of 2 or 6 TMSs reduced the expression levels of the ABC-transporter. Reduced amounts of Pdr5p and the variants were observed in cells reaching the stationary phase, indicating an effect of the growth phase on the regulation of protein synthesis or on metabolic stability.

We repeated the Western blot analysis, using whole-cell extracts prepared from *PDR1-3* cells (Figure 10). Exponentially growing *PDR1-3* cells showed an increased levels of $Pdr5^{C1427Y}$ compared to Pdr5p (Figure 10, panels A and B) as previously showed with the *PDR1* cells (Figure 8). The expression levels of $Pdr5^{L183P}$ and $Pdr5^{L183P+C1427Y}$ were comparable to those of Pdr5p (panel A). One cell division later, $Pdr5^{L183P+C1427Y}$ is more abundant and $Pdr5^{L183P}$ less abundant compared to Pdr5p (Figure 10, panel B). An opposite expression pattern is observed in *PDR1* cells, with $Pdr5^{L183P+C1427Y}$ being less abundant compared to Pdr5p (see Figure 8, panel B). At the transition to the stationary phase, the expression levels of Pdr5p and $Pdr5^{C1427Y}$ were comparable, whereas the levels of $Pdr5^{L183P}$ and $Pdr5^{L183P+C1427Y}$ decreased (Figure 10, panel C). The wild-type and mutated forms of Pdr5 were no more detected in late stationary phase (panel D). The Cdc48p band was similar in intensity between the various strains examined, indicating that equal amount of proteins were loaded. Western blot analysis was repeated 2 times, with independent extracts giving similar results. In conclusion, compared to the *PDR1* allele, the *PDR1-3* allele does not lead to a visible increase in the amounts of the wild-type and mutated versions of Pdr5p during the stationary phase of growth.

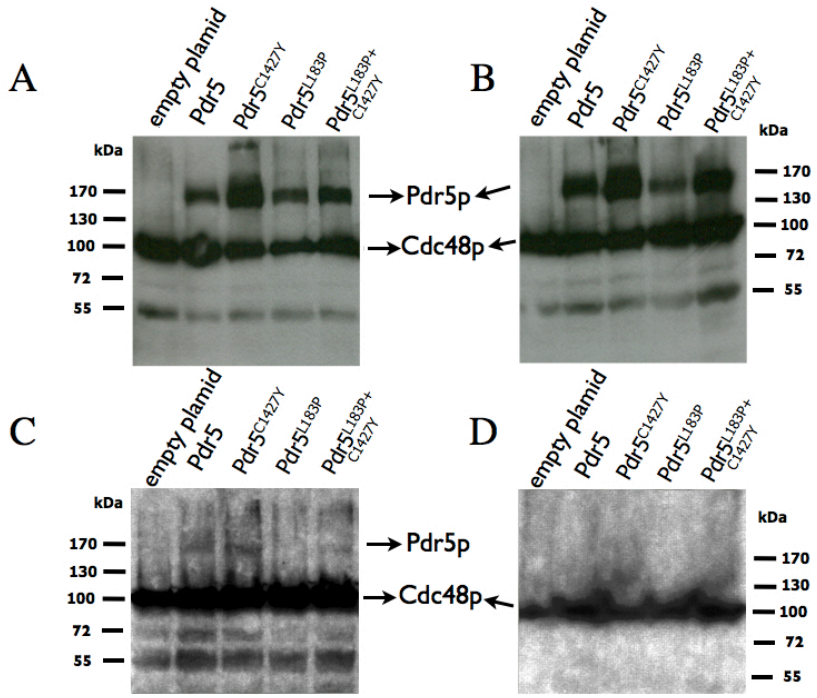

Figure 10. Expression levels of different mutated versions of Pdr5p in *PDR1-3 pdr5Δ* cells. See Figure 8 for details. The membrane was exposed to a Kodak film for 10 sec.

The results obtained with Pdr5^{C1427Y} are striking as this mutated form is rapidly degraded by the proteasome (Plemper et al. 1998) (see Figures 8 and 10). A possibility is that the mRNA levels of Pdr5^{C1427Y} differ from those observed for Pdr5p. This possibility is also conceivable for Pdr5^{L183P}, Pdr5$^{L183P+C1427Y}$, Pdr5^{TM1-6} and Pdr5^{TM1-10}. The presence of an undesirable mutation in the promoter region increasing the amount of proteins is also possible.

2.2. Northern blot analysis

To rule out the possibility that reduced amounts of the Pdr5 variants resulted from decreased transcription levels, the mRNA encoding the various Pdr5p forms was analysed by Northern blot (Figure 11). Total RNA was prepared from exponential (OD_{600} 0.8-1) or stationary (OD_{600} 2.2-2.5) phase cultures of *pdr5Δ* cells expressing the Pdr5 variants from a multicopy pRS426 plasmid. After electrophoresis on a formaldehyde-agarose gel and transfer onto a nylon membrane, total RNA (35 µg) was probed with a [^{32}P]-labelled DNA fragment of *PDR5* or the actin gene (*ACT1*).

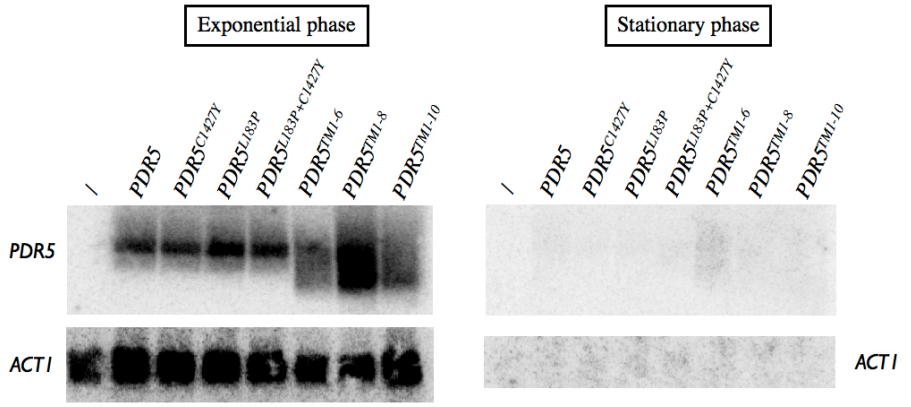

Figure 11. Northern blot analysis of *PDR5* mRNA. Total RNA was extracted from *pdr5Δ* cells from the exponential (left panel) or stationary (right panel) phase. RNA (35 µg) was electrophoresed on a formaldehyde-agarose gel, transferred onto a nylon membrane and hybridized to a [^{32}P]-labelled fragment of *PDR5* (upper panel) or *ACT1* (bottom panel) as a loading control. The membrane was exposed to a phosphor screen for 4 days.

Transcription levels of the 3 mutated *pdr5* alleles are comparable to those of *PDR5*. The levels of the mRNA encoding the truncated forms of Pdr5p are difficult to analyse as more diffuse bands were detected. It seems that the levels of the mRNA encoding Pdr5^{TM1-6} and Pdr5^{TM1-10} are comparable to those of *PDR5* mRNA, whereas the mRNA encoding Pdr5^{TM1-8} is higher. *ACT1* mRNA bands have comparable intensity between the various strains indicating that the same amount of mRNA was analysed. No *ACT1* and *PDR5* transcripts were detected in stationary phase cultures (Figure 11, right panel).

The results of the Northern blot analysis indicate that the difference in the protein amounts between the various mutated forms of Pdr5p is not explained by the mRNA levels of the corresponding mutated alleles as a consequence of modified mRNA turnover or the presence of an undesirable mutation in the promoter region. The lower amounts of Pdr5$^{L183P+C1427Y}$, Pdr5^{TM1-6} and Pdr5^{TM1-10} may therefore resulted from an increased turnover compared to that of Pdr5p. As the mRNA levels of Pdr5^{C1427Y} and wild-type Pdr5p are similar, we have no explanation for the higher amount of Pdr5^{C1427Y} in *pdr5Δ* cells (see Figures 8 and 10).

3. Turnover of mutated Pdr5p forms

As the low amounts of Pdr5$^{L183P+C1427Y}$, Pdr5^{TM1-6} and Pdr5^{TM1-10} may result from degradation, metabolic stability of the various mutated versions of Pdr5p was analysed by pulse-chase analysis. A typical gel and data

quantification for wild-type Pdr5p expressed in wild-type BY4742 strain are shown in Figure 12.

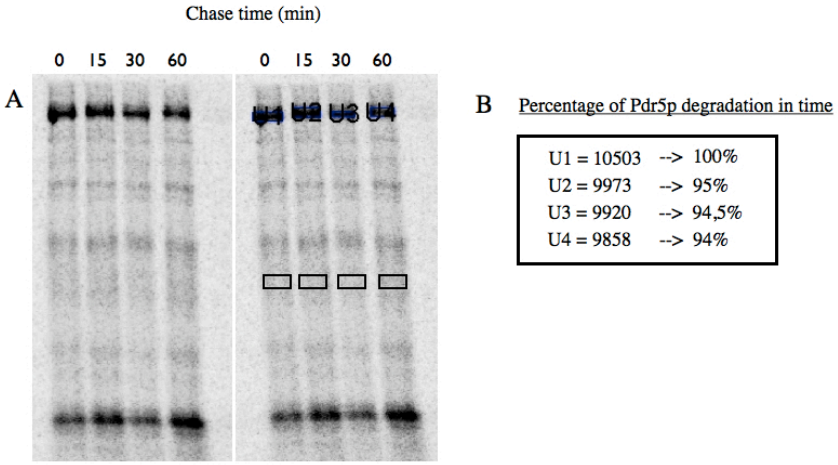

Figure 12. Quantification of Pdr5 bands by using the Phosphor Imager in wt BY4742 cells. **(A)** The wild-type BY4742 strain was transformed with high copy plasmid containing the *PDR5* gene. Exponentially growing cells were incubated in the presence of [^{35}S]-methionine and cysteine for 10 min (pulse). Cells were centrifuged to remove the labelled amino-acids and incubated in SD medium containing unlabelled methionine and cycloheximide for 15, 30 or 60 minutes (chase). Cells samples were transferred to a cryotube containing glass beads, a lysis buffer and SDS and agitated vigorously for 3 min. The lysates were clarified and dilued 4 times with the immunoprecipitation buffer. Polyclonal anti-Pdr5p antibodies were added to the supernant and incubated at 4°C for 2 hours. Protein A-agarose beads were then added and the mixture was incubated at 4°C for 1 hour. The immune complexes bound to the protein A-agarose beads were washed 3-4 times and resuspended in Laemmli buffer for SDS-PAGE. The gel was fixed, dried and the relative intensity of the Pdr5p bands at each time point was quantified by phosphor imaging. **(B)** Rectangles were drawed around the bands and the number of pixels in each rectangle was calculated (U1, U2, U3 and U4). Band intensity depends on the number of photons that are released from the phosphor screen during scanning. Global background using empty rectangles of same size was subtracted from the values obtained in U1-U4 and expressed in percentage.

After global background subtraction, the values were expressed as a percentage of the signal seen at time t = 0 min and plotted as a function of time. In Figure 12, no degradation of Pdr5p is detected, in a striking contrast to the results published by Kuchler and colleagues (Plemper et al. 1998). Bands around 55-kDa on the bottom of the gel and faint bands at different size observed on the gel are unknown proteins cross reacting with the Pdr5p antibodies. Only one autoradiogram representative of the behaviour of a Pdr5p variant in a particuliar yeast strain will be shown. Half-life ($t_{1/2}$) values are average ± variation. Note that exponential decay is a theoretical concept seldom found with proteins as once folded, they are less degradable. Analysis of the turnover of the mutated (Figure 13) and truncated (Figure 14) forms of Pdr5 was carried out in wild-type BY4742 cells transformed with plasmids containing the corresponding mutated or truncated alleles. No Pdr5p band was observed in cells containing an empty plasmid (data not shown).

3.1. The three mutated forms of Pdr5p

No degradation for wild-type Pdr5p was seen during the first 60 min of the chase (n=5) (Figures 13 and 14). The number in parenthesis indicates independant pulse-chase analysis giving comparable results. $Pdr5^{C1427Y}$ and $Pdr5^{L183P}$ are degraded with a $t_{1/2}$ of 25 ± 4 min and 33 ± 5 min (n=5) respectively. Similar half-life values for $Pdr5^{C1427Y}$ (≃ 18 min) and for $Pdr5^{L183P}$ (≃ 15 min) were reported by Plemper et al. (1998) and de Thozee et al. (2007). Compared to $Pdr5^{L183P}$ and $Pdr5^{C1427Y}$, $Pdr5^{L183P+C1427Y}$ is more

rapidly degraded ($t_{1/2}$ = 8 ± 3 min) due probably to the presence of both mutations accelerating its recognition by the proteolic pathway.

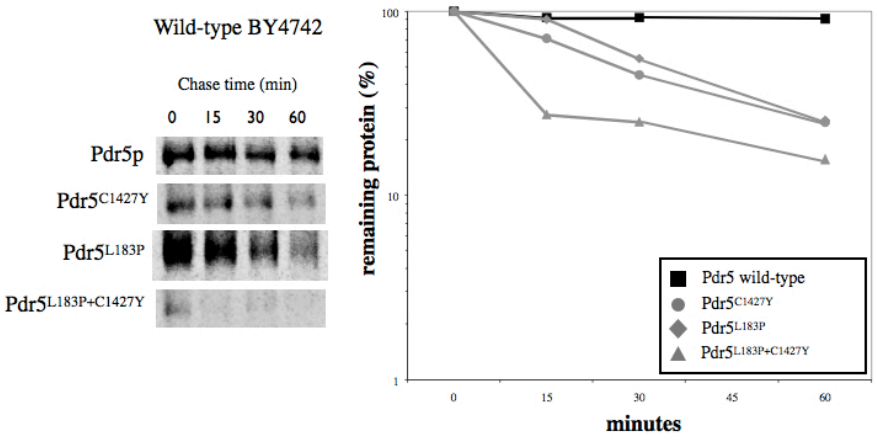

Figure 13. Pulse-chase analysis of wild-type and mutated forms of Pdr5p in BY4742 cells. Exponentially-growing BY4742 cells were incubated with [^{35}S]-methionine for 10 min at 28°C and then washed with an excess of unlabelled methionine and cycloheximide to stop protein synthesis. At the indicated times, an equal amount of cells was lysed and the Pdr5 proteins were purified from the lysates by immunoprecipitation with anti-Pdr5p antibodies and protein-A agarose beads and analysed by SDS-PAGE. Relative band intensity was quantified by phosphor imaging. Protein remaining in percent is represented as a function of time.

3.2. The three C-truncated variants of Pdr5p

As shown in Figure 14, Pdr5^{TM1-6} is a short-lived protein with a $t_{1/2}$ of 9 ± 3 min (n=3), Pdr5^{TM1-8} is a long-lived variant ($t_{1/2}$ > 60 min ; n=3) and Pdr5^{TM1-10} is rapidly degraded with a $t_{1/2}$ of 22 ± 5 min (n=3).

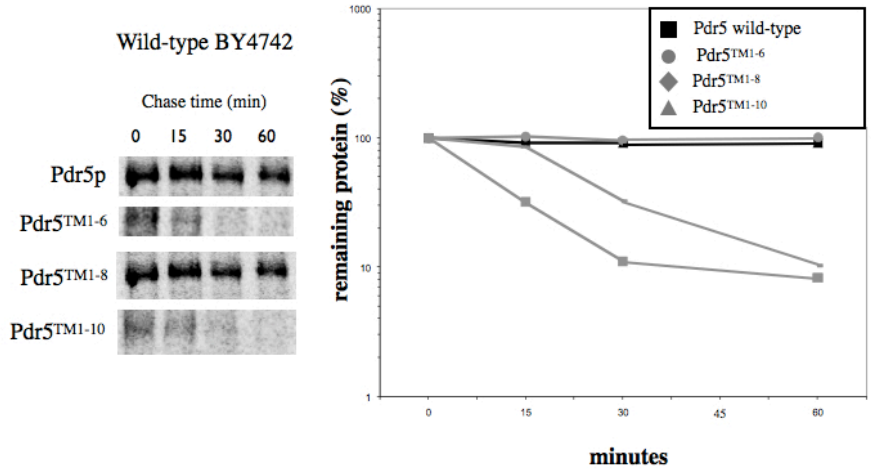

Figure 14. Pulse-chase analysis of wild-type and truncated forms of Pdr5p in BY4742 cells. Protein remaining in percent is represented as a function of time. Note that no significant signal variability was observed along the chase for Pdr5p and Pdr5^{TM1-8}. See Figure 13 for experimental details.

In conclusion, the results of the pulse-chase analysis indicate that the steady-state amounts of Pdr5^{L183P}, Pdr5$^{L183P+C1427Y}$, Pdr5^{TM1-6} and Pdr5^{TM1-10} are low as a consequence of an increased turnover of these variants compared to the wild-type form. Despite the truncation of 4 TMSs, Pdr5^{TM1-8} is a long-lived protein. This result explains why comparable amounts of this variant and Pdr5p were detected by Western blot analysis (see Figure 9).

4. Effect of mutations in ER-associated Ub-ligases on degradation of Pdr5p variants

According to the current ERAD model (Vashist and Ng 2004), $Pdr5^{L183P}$ containing a cytosolic mutation is predicted to be ubiquitylated by the major Ub-ligase of the ERAD-C pathway, Doa10p. In contrast, $Pdr5^{C1427Y}$ having a luminal mutation is predicted to be ubiquitylated by the Ub-ligase of the ERAD-L pathway, Hrd1p. $Pdr5^{L183P+C1427Y}$ having both mutations is predicted to be targeted by the ERAD-C pathway for degradation as this pathway would predominate the ERAD-L pathway. Plemper et al. (1998) showed that $Pdr5^{C1427Y}$ requires Hrd1p for degradation. However, this study did not assess the role of Doa10p. $Pdr5^{L183P}$ is targeted for degradation by the proteasome through the ERAD pathway. The Ub-ligase involved in this process has not been identified (de Thozee et al. 2007).

4.1. Western blot analysis

Various plasmids expressing $Pdr5^{L183P}$, $Pdr5^{C1427Y}$ and $Pdr5^{L183P+C1427Y}$ were introduced into a mutated strain lacking Doa10p (*doa10Δ*) or Hrd1p (*hrd1Δ*) and in the wild-type parental BY4742 strain. Whole-cell extracts were prepared from appropriate transformants and analyzed by Western blot using anti-Pdr5p antibodies to determine whether the loss of Doa10p or Hrd1p results in an increase in the steady-state levels of the Pdr5p variants. In this analysis, Cdc48p serves as a control of equal sample loading (Figure 15).

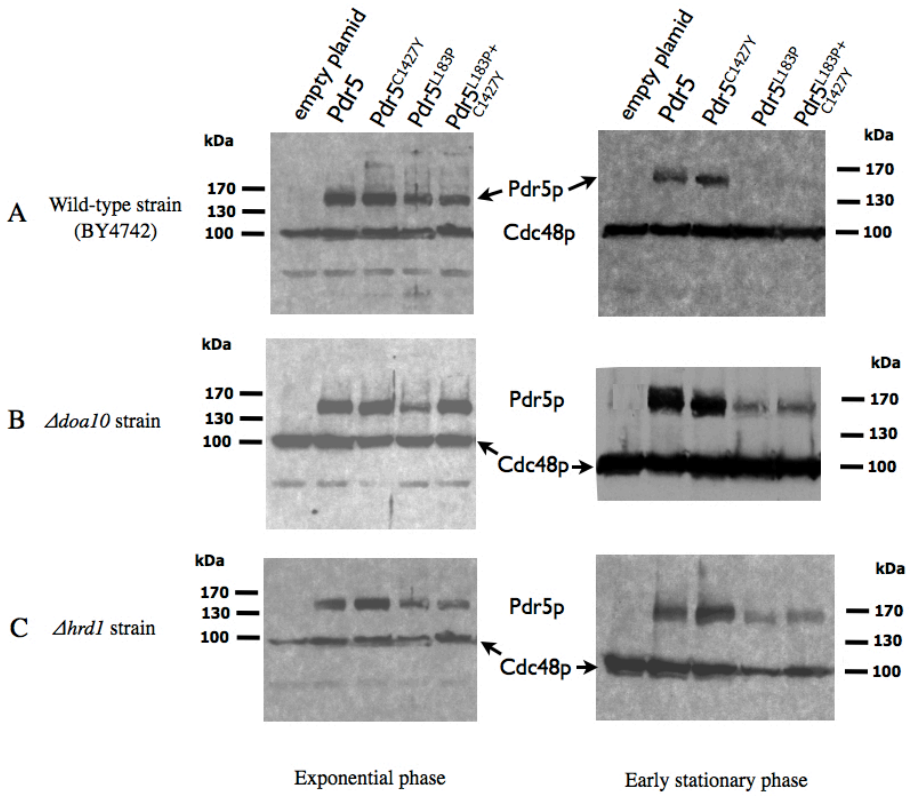

Figure 15. Effect of mutations in ER-associated Ub-ligases on the steady-state levels of Pdr5 variants. Whole-cell extracts were prepared from exponential (OD_{600} 0.8-1, left panels) or early stationary (OD_{600} 1.6-2, right panels) phase cultures of wild-type BY4742 strain **(A)** and *doa10Δ* **(B)** or *hrd1Δ* **(C)** mutated strains. Total protein (10 μg) was analysed by SDS-PAGE and immunoblotting using antibodies against Pdr5p (1/2000 dilution) or Cdc48p (1/9000 dilution). The membrane was exposed to a Kodak XAR film for 30 sec (left panels) or 16 h (right panels).

The loss of Hrd1p (Figure 15, panel C) results in an increased levels of $Pdr5^{L183P}$ (lane 4) and $Pdr5^{L183P+C1427Y}$ (lane 5) compared to the levels seen in the wild-type parental strain at the transition to the stationary phase (right

panel) even if a lower amount of proteins have been loaded on the gel as judged from the decreased intensity of the Cdc48p bands. As no difference in the steady-state levels of Pdr5^{C1427Y} were seen between the wild-type and the mutated strains, we can not determine the Ub-ligase implicated in its degradation. The effects of the *doa10Δ* deletion are more difficult to interpret as more proteins have been loaded on the gel as judged from the increased intensity of the Pdr5p and Cdc48p bands. Western blot analysis was repeated 2 times, with independently prepared extracts giving similar results.

In conclusion, the ERAD-L pathway (Hrd1p) seems to be required for degradation of Pdr5^{L183P} and Pdr5$^{L183P+C1427Y}$.

doa10Δ or *hrd1Δ* cells expressing the Pdr5p variants were tested for their ability to grow in the presence of cycloheximide and itraconazole. None of the strains examined showed an increased tolerance to the drugs, when compared to the wild-type parental cells (data not shown). This result indicates that the deletions of *DOA10* or *HRD1* is not sufficient to restore drug resistance to cells expressing the mutated forms of Pdr5p.

4.2. Pulse-chase analysis

Pulse-chase analysis using the wild-type BY4742 strain has shown that the three mutated versions of Pdr5p were degraded with half-life values of 5-38 min (see Figure 13). As we would like to see the stabilizing effects of the *doa10Δ* and *hrd1Δ* double deletion on Pdr5p variants, plasmids expressing Pdr5^{L183P}, Pdr5^{C1427Y} and Pdr5$^{L183P+C1427Y}$ were introduced into a mutated

strain lacking Doa10p (*doa10Δ*) (Figure 17), Hrd1p (*hrd1Δ*) (Figure 18) or both Ub-ligases (*doa10Δ hrd1Δ*) (Figure 19). Since the double deleted strain is derived from the MHY501 parental strain, the genetic background of which differs from that of BY4742, this wild-type strain was used as a control (Figure 16). The pulse-chase analysis was repeated using BY4742 cells lacking *DOA10* or *HRD1* (Figures 20 and 21).

No degradation was seen for wild-type Pdr5p during the first 60 min of the chase in the MHY501 wild-type (Figure 16) as well as in the congenic strains deficient for Doa10p (n=2-3) (Figures 17 and 20), Hrd1p (n=2-3) (Figures 18 and 21) or both Ub-ligases (n=2) (Figure 19). Pdr5^{C1427Y} signal seen with MHY501 cells is less intense than the signal seen with BY4742 cells, probably due to a low labelling efficiency or a faster degradation in MHY501 cells.

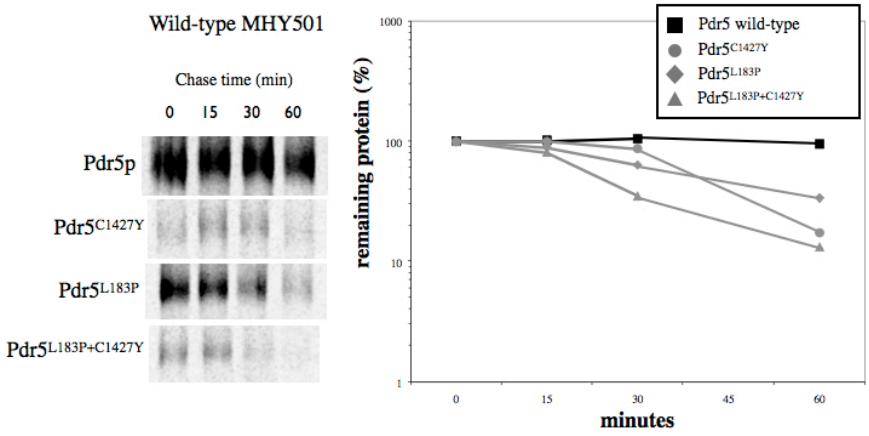

Figure 16. Turnover analysis of wild-type and mutated forms of Pdr5p expressed in wild-type MHY501 cells. Protein remaining in percent is represented as a function of time. Identical results were obtained in 3 independent experiments using different transformants. See Figure 13 for experimental details.

Pdr5^{C1427Y} ($t_{1/2}$ = 26 ± 4 min), Pdr5^{L183P} ($t_{1/2}$ = 38 ± 8 min) and Pdr5$^{L183P+C1427Y}$ ($t_{1/2}$ = 23 ± 4 min) are rapidly degraded in the wild-type MHY501 strain (Figure 16). These values are comparable to those seen with the BY4742 cells (see Figure 13).

Interestingly, the degradation of the Pdr5p variants is decreased in MHY501 cells lacking Doa10p (Figure 17). The $t_{1/2}$ of Pdr5^{C1427Y}, Pdr5^{L183P} and Pdr5$^{L183P+C1427Y}$ are > 60 min. Identical results were obtained in 2 experiments using independent transformants. Note that Pdr5$^{L183P+C1427Y}$ is less stabilized than the other variants in this strain, the extrapoled $t_{1/2}$ value is 65 min.

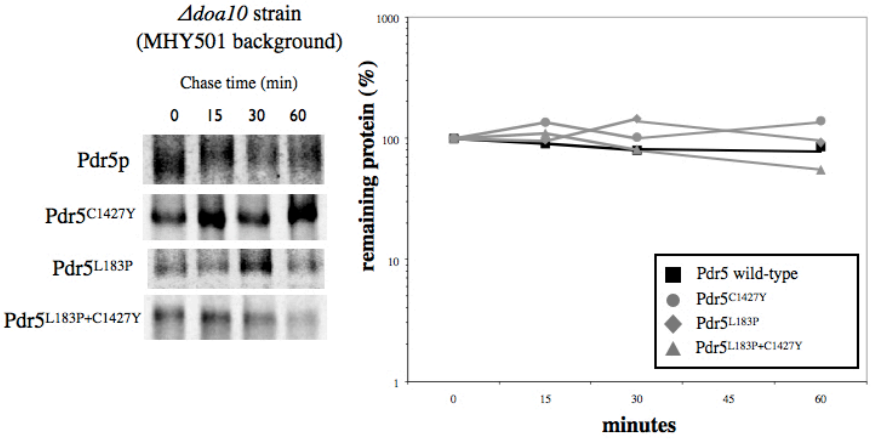

Figure 17. Turnover analysis of wild-type and mutated forms of Pdr5p using MHY501 cells lacking Doa10p. Protein remaining in percent is represented as a function of time. No degradation of Pdr5p is seen in *doa10Δ* cells despite some signal variability. Some signal variability is also observed for Pdr5^{C1427Y} and Pdr5^{L183P} at different time points. See Figure 13 for experimental details.

As shown in Figure 18, the degradation of the mutated ABC-transporters is also decreased in MHY501 cells lacking Hrd1p (n=2), with $t_{1/2} > 60$ min. The intensity of the Pdr5p signal in *hrd1Δ* MHY501 cells varied. $Pdr5^{C1427Y}$ showed some signal variability during the chase despite an overall stabilization. The intensity of the $Pdr5^{L183P}$ band at t = 0 min is weaker than those seen after 15, 30 and 60 min. It is possible that the concentrations of cycloheximide are not sufficient to prevent newly synthesized Pdr5p molecules. It is also possible that [^{35}S]-methonine has not been completely washed off.

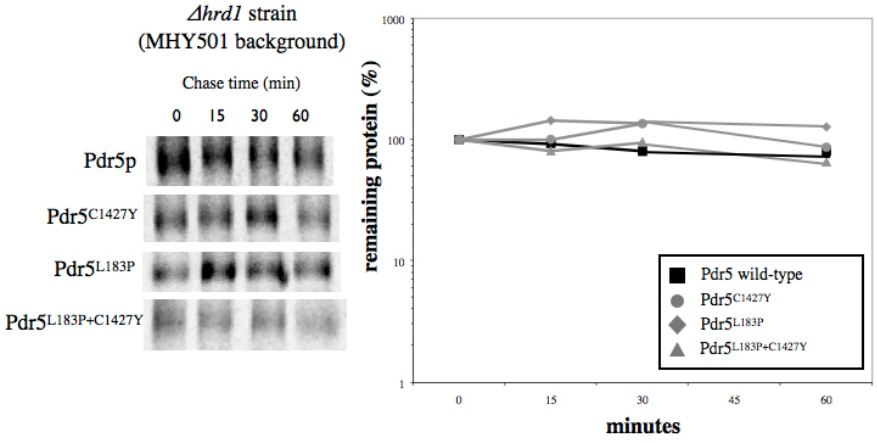

Figure 18. Turnover analysis of wild-type and mutated forms of Pdr5p in MHY501 cells lacking Hrd1p. Protein remaining in percent is represented as a function of time. See Figure 13 for experimental details.

In a mutant cells lacking both Doa10p and Hrd1p (Figure 19), $Pdr5^{C1427Y}$, $Pdr5^{L183P}$ and $Pdr5^{L183P+C1427Y}$ are stabilized with $t_{1/2} > 60$ min (n=2). Despite an overall stability effect in the *doa10Δ hrd1Δ* strain, $Pdr5^{C1427Y}$ and

Pdr5$^{L183P+C1427Y}$ showed some variabilization of signal intensity during the chase. The signals for Pdr5^{L183P} or Pdr5^{C1427Y} observed at t = 0 min is weaker than those seen after 15-60 min like observed in *hrd1Δ* MHY501 cells for Pdr5^{L183P} probably for the same reasons.

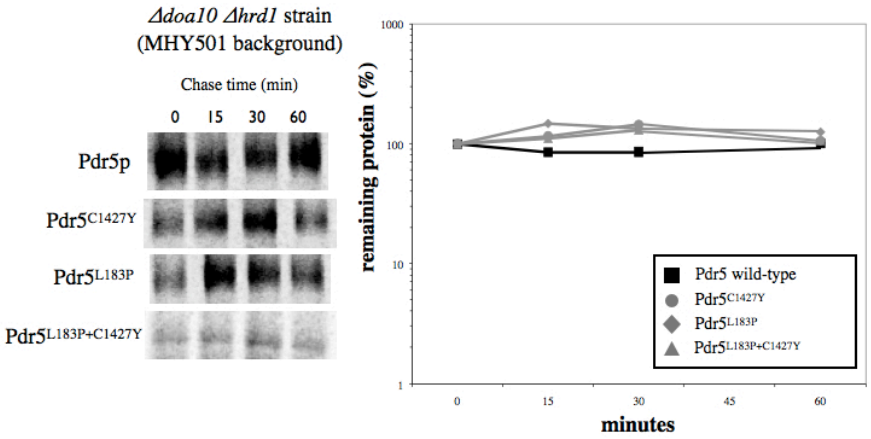

Figure 19. Turnover analysis of wild-type and mutated forms of Pdr5p in MHY501 cells lacking Doa10p and Hrd1p. Protein remaining in percent is represented as a function of time. See Figure 13 for experimental details.

Pdr5^{L183P}, Pdr5^{C1427Y} and Pdr5$^{L183P+C1427Y}$ are stabilized in strains impaired in Doa10p or Hrd1p. This result indicates a cooperation between the Ub-ligases, in contradiction with the ERAD model postulating that only Hrd1p is involved in the recognition of misfolded proteins with a luminal mutation (Pdr5^{C1427Y}) and only Doa10p is involved in the recognition of misfolded proteins with a cytosolic mutation (Pdr5^{L183P}) (Vashist and Ng 2004). Our results indicate that Hrd1p and Doa10p form a complex that catalyses ubiquilylation of misfolded forms of Pdr5p, independently of the localization of the mutated residues. Therefore the predictions based on the utilization of

engineered modular proteins cannot be generalized to a yeast endogenous ERAD substrate. According to the current model, a misfolded protein with a cytosolic and a luminal mutations is predicted to be targeted for degradation by the ERAD-C pathway. This prediction was not confirmed with the Pdr5$^{L183P+C1427Y}$ form as both Ub-ligases are required.

Pulse-chase analysis was repeated using BY4742 cells lacking Doa10p or Hrd1p (Figures 20 and 21) (n=3). No degradation of wild-type Pdr5p and mutated forms is seen in *doa10Δ* cells despite some signal variability (Figure 20). In BY4742 cells lacking Hrd1p, the intensity of the Pdr5p signal varied (Figure 21). The signal increased from 0 to 15 min, then decreased after 30 min to reach the level seen at t = 0 min. Pdr5^{C1427Y} also showed some signal variability in *hrd1Δ* cells during the chase despite an overall stabilization.

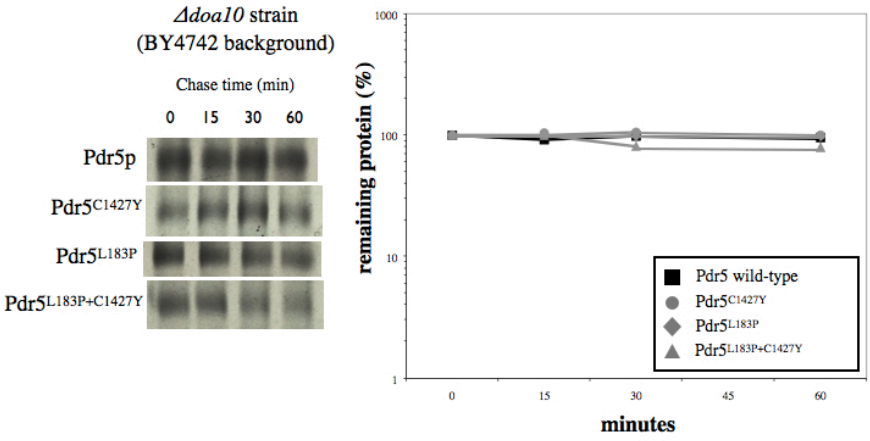

Figure 20. Turnover analysis of wild-type and mutated forms of Pdr5p using BY4742 cells lacking Doa10p. Protein remaining in percent is represented as a function of time. See Figure 13 for experimental details.

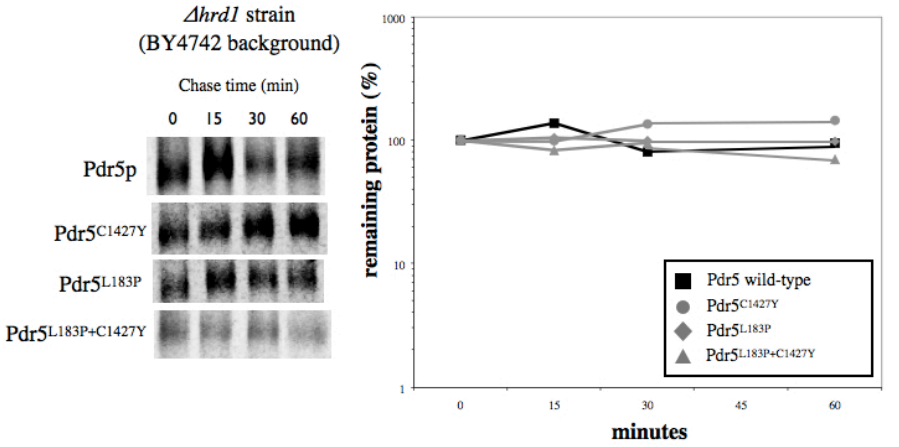

Figure 21. Turnover analysis of wild-type and mutated forms of Pdr5p in BY4742 cells lacking Hrd1p. Protein remaining in percent is represented as a function of time. See Figure 13 for experimental details.

In conclusion, the results obtained with the BY4742 cells are similar to those seen with the MHY501 cells lacking Doa10p or Hrd1p (see Figures 17 and 18). They confirm our finding of the cooperation between the ER Ub-ligases.

5. Implication of the putative Der1p retro-translocon in degradation of Pdr5p variants

According to the current ERAD model (Ahner and Brodsky 2004; Vashist and Ng 2004), a membrane protein with a cytosolic misfolded region is delivered to the proteasome via a Der1-independent process. A membrane protein with luminal misfolded region, however, requires Der1p for degradation. To assess the role of Der1p in the degradation of the Pdr5p

variants, a BY4742 strain containing a *der1Δ* deletion was transformed with high-copy plasmids expressing Pdr5p variants and protein's half-life values were determined by pulse-chase analysis as previously described in Figure 12.

The deletion of the *DER1* gene results in partial stabilization of $Pdr5^{C1427Y}$ and $Pdr5^{L183P+C1427Y}$ and in complete stabilization of $Pdr5^{L183P}$ ($t_{1/2} > 60$ min). Pulse-chase analysis has been repeated 3 times using different transformants and comparable results were obtained each time.

These results suggest that misfolded forms of Pdr5p require Der1p for the transport to the cytosol across the ER membrane in a good agreement with the role of Der1p as a putative channel.

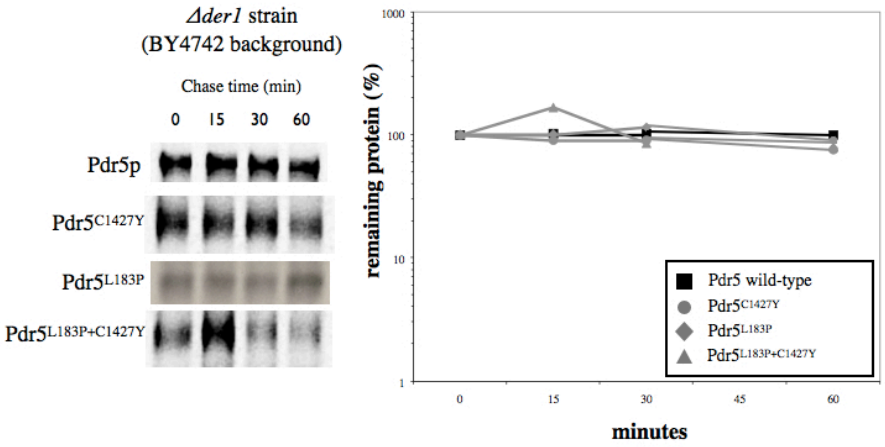

Figure 22. Pulse-chase analysis of the wild-type and mutated forms of Pdr5p in *der1Δ* (BY4742) cells. Protein remaining in percent is represented as a function of time. Signal variabilities are seen for $Pdr5^{L183P+C1427Y}$ as the signal at t = 15 min is probably too strong. See Figure 13 for experimental details.

6. Effect of a mutation impairing vacuolar degradation on stability of Pdr5p variants

ER-associated degradation of Pdr5^{L183P} and Pdr5^{C1427Y} requires the Ub-proteasome system and is independent from the vacuole (de Thozee et al. 2007; Plemper et al. 1998). To confirm those results and determine whether the authors' conclusions also apply to the degradation of Pdr5$^{L183P+C1427Y}$, we used a BY4742 strain impaired in the vacuolar Pep4p maturase/hydrolase.

As shown in Figure 23, Pdr5^{C1427Y}, Pdr5^{L183P} and Pdr5$^{L183P+C1427Y}$ are rapidly degraded with a $t_{1/2}$ of 25 ± 5 min, 22 ± 4 min and 8 ± 3 min, respectively (n=3). This result indicates that their degradation is independent from the vacuolar proteolytic system (compare Figure 23 with Figures 13 and 16).

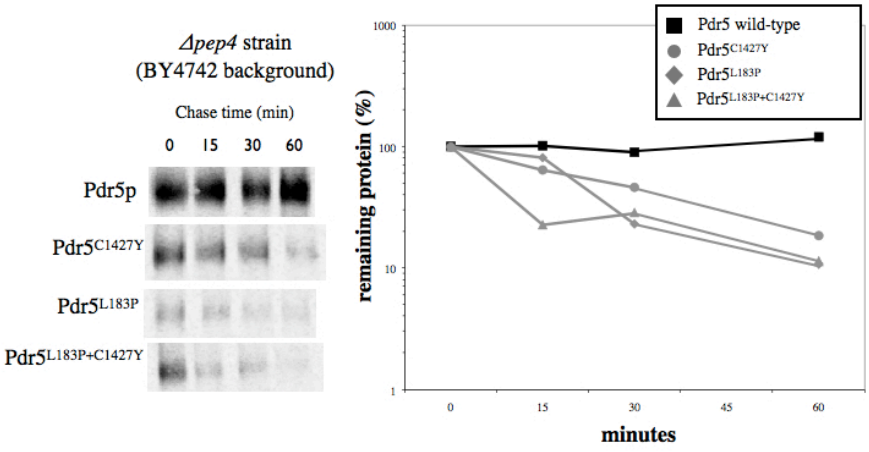

Figure 23. Pulse-chase analysis of the wild-type and mutated forms of Pdr5p in BY4742 cells lacking Pep4p. Protein remaining in percent is represented as a function of time. See Figure 13 for experimental details.

7. Effect of mutations in ER-associated Ub-ligases on subcellular localization of mutated Pdr5p forms

The replacement of a leucine residue by a proline at position 183 affects the plasma membrane localization as the mutated form is found in intracellular vesicles (de Thozee et al. 2007). Similarly, the Pdr5^{C1427Y} variant is found in the ER-perinuclear membrane instead of the plasma membrane (Plemper et al. 1998). To determine which subcellular compartments contain the Pdr5$^{L183P+C1427Y}$ form, we generated a GFP protein fusion and analysed the cells by fluorescence microscopy. The Pdr5^{L183P}-GFP and Pdr5^{C1427Y}-GFP fusions were also constructed to control the suitability of our expression system compared to the one used by de Thozee et al. 2007 (chromosomal construction versus a plasmid in this work) and by Plemper et al. 1998 (different yeast strains). The plasmids expressing the GFP fusions were transformed in wild-type cells and mutant cells impaired in Doa10p and/or Hrd1p to see whether the loss of Ub-ligases allow the mutated Pdr5p forms to reach the plasma membrane.

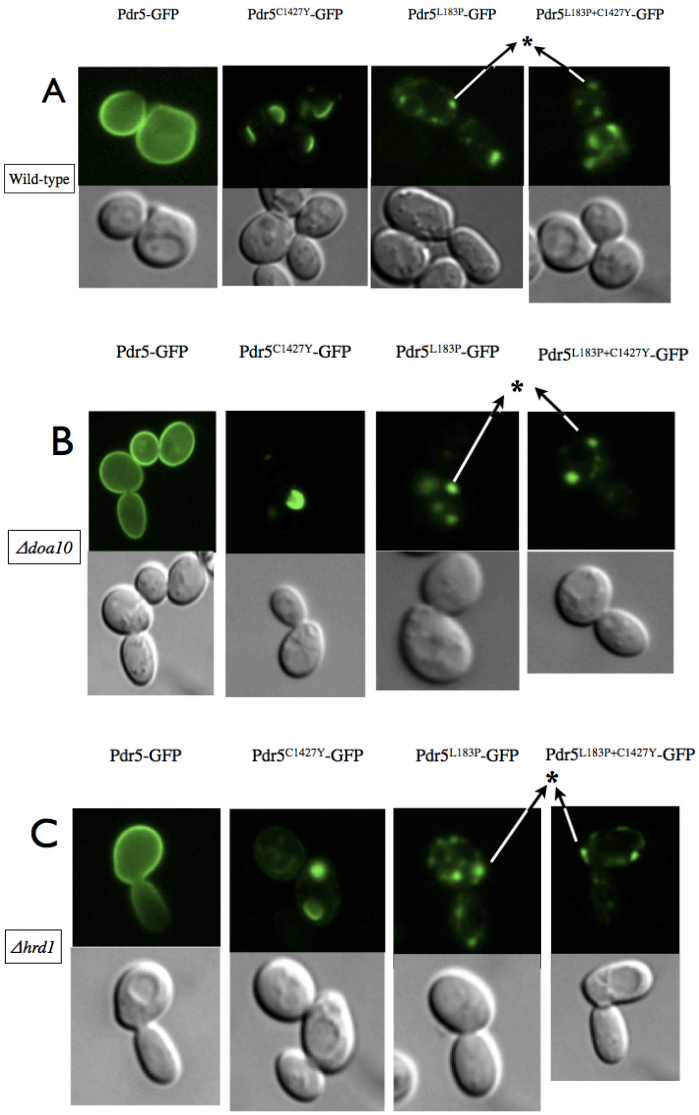

Figure 24. Localization of wild-type and mutated versions of Pdr5p in BY4742 wild-type (A), *doa10Δ* (B) and *hrd1Δ* (C) cells. Cells were transformed with various plasmids expressing Pdr5-GFP, Pdr5^{C1427Y}-GFP, Pdr5^{L183P}-GFP and Pdr5$^{L183P+C1427Y}$-GFP and analysed by fluorescence microscopy. Intracellular vesicles are indicated with an asterisk.

As expected, the Pdr5-GFP protein fusion is located in the plasma membrane in wild-type BY4742 (Figure 24A) or MHY501 (Figure 25A) cells. 90% of the cells examined showed a signal. Pdr5^{C1427Y}-GFP showed an asymetrical localization in the ER-perinuclear membrane, in striking contrast with the symetrical distribution reported by Plemper et al. (1998). Pdr5^{L183P}-GFP accumulated in intracellular vesicles as previously reported (de Thozee et al. 2007). Anti-Kar2p antibodies were not used to confirm that these vesicles are derived from the ER. Therefore, we cannot discard the possibility that Pdr5^{L183P}-GFP accumulated in the Golgi apparatus. Similarly, Pdr5$^{L183P+C1427Y}$-GFP accumulated in intracellular vesicles corresponding to ERACs or the Golgi. Therefore, the L183P substitution is dominant over the C1427Y substitution with respect to the subcellular compartment containing the Pdr5p variant. We found that ≃ 30% of the cells expressing the Pdr5p variants showed no fluorescence.

The plasmids expressing the GFP fusions were transformed in *doa10Δ* (BY4742), *hrd1Δ* (BY4742) and *doa10Δ hrd1Δ* (MHY501) strains. We found that the subcellular localization of the Pdr5p variants was not altered by the loss of Doa10p (Figure 24B), Hrd1p (Figure 24C) or both Ub-protein ligases (Figure 25B). Pdr5^{C1427Y} accumulated asymmetrically in the ER-perinuclear membrane whereas Pdr5^{L183P} and Pdr5$^{L183P+C1427Y}$ accumulated in intracellular vesicles, as previously shown with wild-type BY4742 and MHY501 cells (Figures 24A and 25A). We found that ≃ 30% of the cells expressing the Pdr5p variants showed no fluorescence.

We found that Doa10p and Hrd1p are required for the degradation of Pdr5^{C1427Y}, Pdr5^{L183P} and Pdr5$^{L183P+C1427Y}$. However, their loss does not allow the mutated Pdr5p forms to reach the plasma membrane.

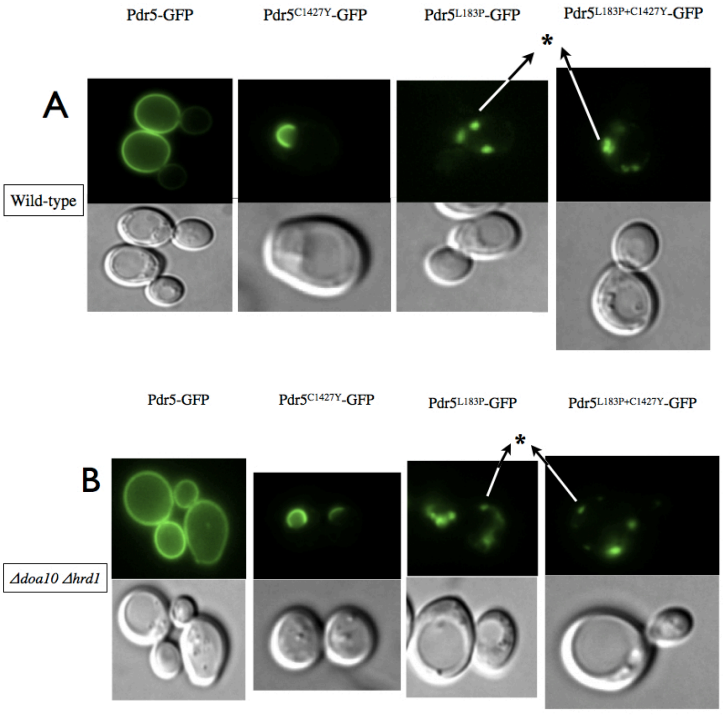

Figure 25. Localization of wild-type and mutated versions of Pdr5p in MHY501 wild-type (A) and *doa10Δ hrd1Δ* cells (B). Cells were transformed with various plasmids expressing Pdr5-GFP, Pdr5^{C1427Y}-GFP, Pdr5^{L183P}-GFP and Pdr5$^{L183P+C1427Y}$-GFP and analysed by fluorescence microscopy. Intracellular vesicles are indicated with an asterisk.

8. Role of Sar1p/COPII machinery and ER-to-Golgi transport in degradation of the three mutated forms of Pdr5p

Several studies have shown a role of the early secretory pathway in proteasome-mediated degradation of ER soluble proteins (CPY*, PrA*, KHN) and membrane proteins with a luminal misfolded domain (KWW) (Caldwell et al. 2001; Vashist et al. 2001). A likely explanation is the existence of a second quality control system in the Golgi, which recognizes the misfolded proteins that have escaped the ER quality control system and redirects them for ER-associated degradation. Interestingly, a recent study on the degradation of heterologously expressed CFTR has shown a role of the Sar1p/COPII machinery, which is independent from its role in the secretory pathway (ER-to-Golgi transport) (Fu and Sztul 2003) as CFTR is stabilized in a *sec12* mutant and not in a *sec18* mutant.

To assess the implication of the Sar1p/COPII machinery in the degradation of the mutated forms of Pdr5p, we used a strain impaired in Sec12p. The *SEC12* gene encodes a GDP/GTP exchange factor that initiates the budding of the COPII vesicles, through Sar1p activation. We also used a *sec18* mutant strain deficient in the ER-to-Golgi traffic. The *SEC18* gene encodes a AAA-ATPase which is essential for membrane fusion between COPII vesicles and the Golgi. A *ret3* mutant was also used to test for the requirement of retrograde Golgi-to-ER transport in the degradation of the Pdr5p variants. The *RET3* gene encodes a coatamer proteins of the COPI

vesicles. The 3 mutant strains have a temperature-sensitive growth defect as the essential proteins become inactivated at 37°C.

8.1. Pulse-chase analysis

8.1.1. Effect of inactivation of the Sar1p/COPII machinery

The plasmids expressing Pdr5p, Pdr5^{C1427Y}, Pdr5^{L183P} and Pdr5$^{L183P+C1427Y}$ were introduced into a *sec12-4* temperature-sensitive strain and the parental *SEC12* (YPM30) strain (n=2). Stability of the Pdr5p variants was determined by pulse-chase analysis using cells incubated at 25°C (permissive temperature) and 37°C (restrictive temperature).

Pdr5p is a long-lived protein in the *SEC12* wild-type (YPM30) and the *sec12-4* mutant strains at 25°C and 37°C (Figure 26). Band intensity in the *sec12-4* cells incubated at 37°C is weaker than the intensity seen at 25°C, which may result from a low labelling efficiency.

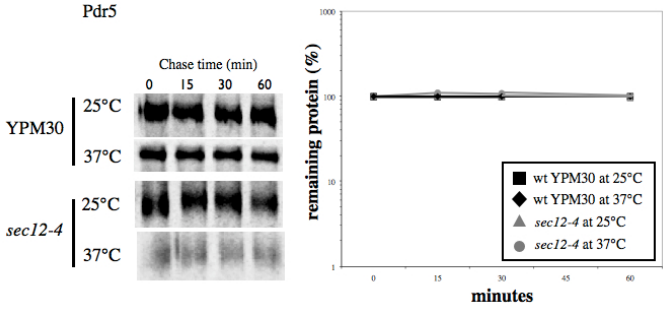

Figure 26. Metabolic stability of Pdr5p in *SEC12* wild-type (YPM30) and *sec12-4* temperature-sensitive strains at 25°C or 37°C. Protein remaining in percent is represented as a function of time. Pulse-chase analysis was carried out as described in Figure 13.

The half-life of Pdr5^{C1427Y} in the *sec12-4* mutant increased from 9 ± 3 min to > 60 min when the cells are transferred from 25°C to 37°C (Figure 27). An increase in the temperature had no effect on the Pdr5^{C1427Y} turnover in the wild-type YPM30 cells, with half-life of 29 ± 5 min and 30 ± 6 min at 25°C and 37°C, respectively. Therefore, Sec12p is required for the degradation of the Pdr5^{C1427Y} variant.

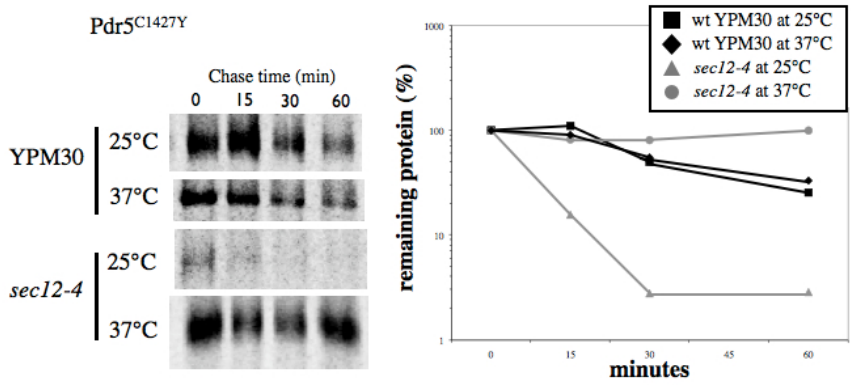

Figure 27. Role of Sec12p in Pdr5^{C1427Y} degradation. Pulse-chase analysis of Pdr5^{C1427Y} degradation was carried out using *SEC12* wild-type (YPM30) and *sec12-4* cells incubated at 25°C or 37°C. Protein remaining in percent is represented as a function of time. See Figure 13 for more detailed experimental conditions.

We also found that Pdr5^{L183P} and Pdr5$^{L183P+C1427Y}$ are stabilized in the *sec12-4* strain when incubated at 37°C, with half-lives increasing from 12 ± 5 min and 16 ± 6 min at 25°C to > 60 min at 37°C (Figures 28 and 29). An increase in the temperature had no effect on the turnover of Pdr5^{L183P} and Pdr5$^{L183P+C1427Y}$ in the wild-type YPM30 cells ($t_{1/2}$ of 24 ± 3 min and 11 ± 3 min at 25°C, and $t_{1/2}$ of 26 ± 6 min and 17 ± 4 min at 37°C, respectively). The stabilization of Pdr5^{L183P} in a *sec12* mutant strain was previously

reported by C. de Thozee and A. Goj in our laboratory (unpublished preliminary data).

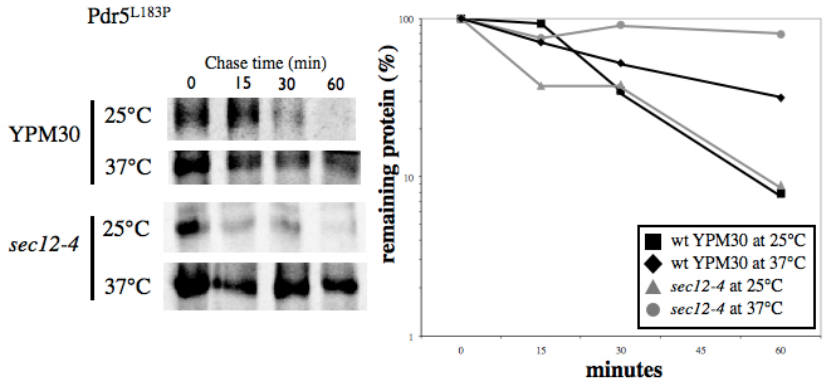

Figure 28. Role of Sec12p in Pdr5^{L183P} degradation. Pulse-chase analysis of Pdr5^{L183P} degradation was carried out using *SEC12* wild-type (YPM30) and *sec12-4* cells incubated at 25°C or 37°C. Protein remaining in percent is represented as a function of time. See Figure 13 for more detailed experimental conditions.

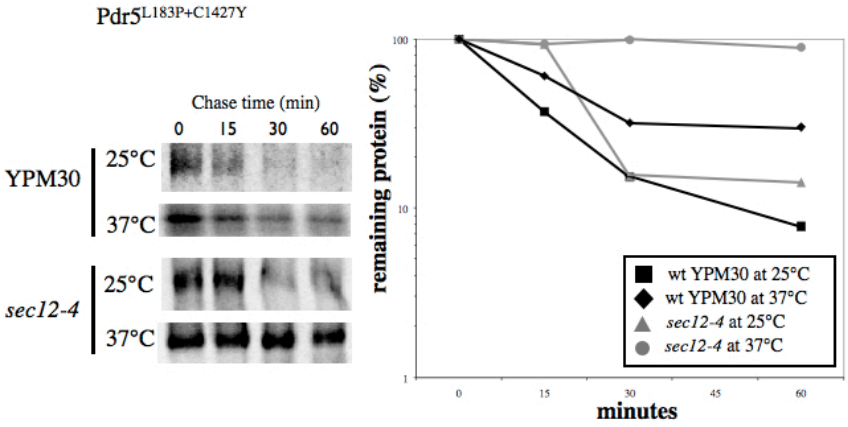

Figure 29. Role of Sec12p in Pdr5$^{L183P+C1427Y}$ degradation. Pulse-chase analysis of Pdr5$^{L183P+C1427Y}$ degradation was carried out using *SEC12* wild-type (YPM30) and *sec12-4* cells incubated at 25°C or 37°C. Protein remaining in percent is represented as a function of time. See Figure 13 for more detailed experimental conditions.

From the results of the pulse-chase analysis we conclude that Pdr5^{C1427Y}, Pdr5^{L183P} and Pdr5$^{L183P+C1427Y}$ require Sec12p and most likely the Sar1p/ COPII machinery to be efficiency degraded. Pdr5^{C1427Y} and Pdr5$^{L183P+C1427Y}$ which possess a luminal mutation are predicted to require an efficient ER-to-Golgi transport to be degraded. Therefore the implication of the Sec12p in their degradation is not surprising. The involvement of Sec12p in Pdr5^{L183P} degradation is more puzzling. This result suggests that Pdr5^{L183P} require the Sar1p/COPII machinery to reach specific ER subcompartments where it is targeted for proteasome-mediated degradation, through the ERAD pathway.

8.1.2. ER-to-Golgi and Golgi-to-ER transports

To determine whether the Pdr5p variants reach the Golgi apparatus, where they are transported back to the ER for ubiquitylation and proteasome-mediated degradation, we analysed the effect of the *sec18* and *ret3* mutations on the degradation. As a control, we firstly checked that Pdr5p is a long-lived protein in the *sec18-1* and *ret3-1* mutant strains and the parental wild-type YPM30 strain at 25°C and 37°C (n=2) (Figure 30).

The Pdr5p variants are rapidly degraded in the *sec18-1* and *ret3-1* mutant strains at the permissive temperature (25°C) (n=2) (Figures 31-33) in good agreement with the results seen with the wild-type parental YPM30 strain.

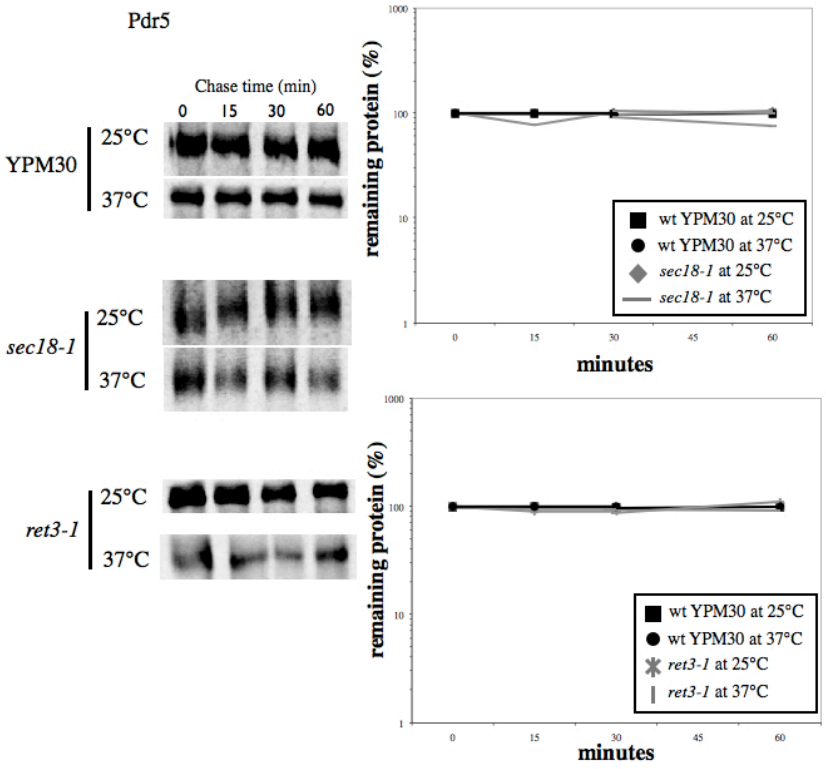

Figure 30. Metabolic stability of Pdr5p in *sec18-1* and *ret3-1* temperature-sensitive mutant strains at 25°C or 37°C. Protein remaining in percent is represented as a function of time. Pulse-chase analysis was carried out as described in Figure 13.

Pdr5^{C1427Y} is stabilized in the *sec18-1* and *ret3-1* strains when incubated at 37°C, with $t_{1/2}$ > 60 min at 37°C versus 16 ± 3 min and 11 ± 2 min at 25°C, respectively (Figure 31). At the permissive temperature, Pdr5^{C1427Y} seems to be more rapidly degraded in the secretory pathway mutants than in the wild-type parental strains examined. This result might be due to the low signal

seen at t = 0 min as a consequence of a poor metabolic incorporation of [^{35}S]-methionine in the mutant strains at 25°C.

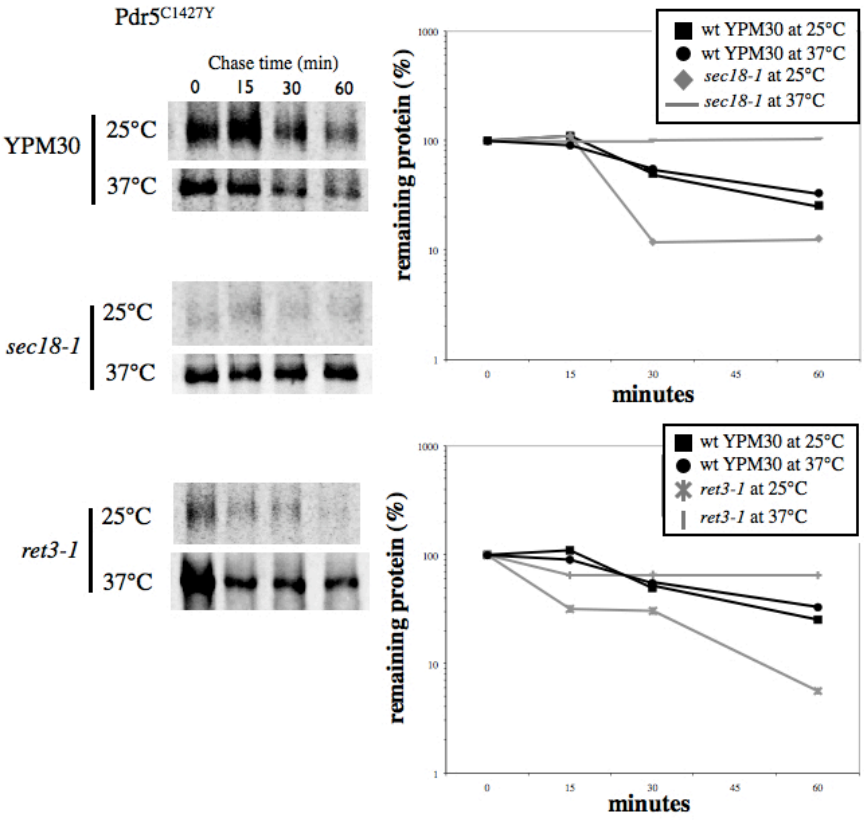

Figure 31. Role of Sec18p and Ret3p in Pdr5^{C1427Y} degradation. Pulse-chase analysis was carried out using wild-type (YPM30), *sec18-1* and *ret3-1* cells incubated at 25°C or 37°C. Protein remaining in percent is represented as a function of time. Pulse-chase analysis was carried out as described in Figure 13.

In contrast to Pdr5^{C1427Y}, Pdr5^{L183P} is not stabilized by mutations in *SEC18* ($t_{1/2}$ of 24 ± 5 min at 25°C and 26 ± 6 min at 37°C) or *RET3* ($t_{1/2}$ of 9 ± 4 min at 25°C and 15 ± 3 min at 37°C) (Figure 32).

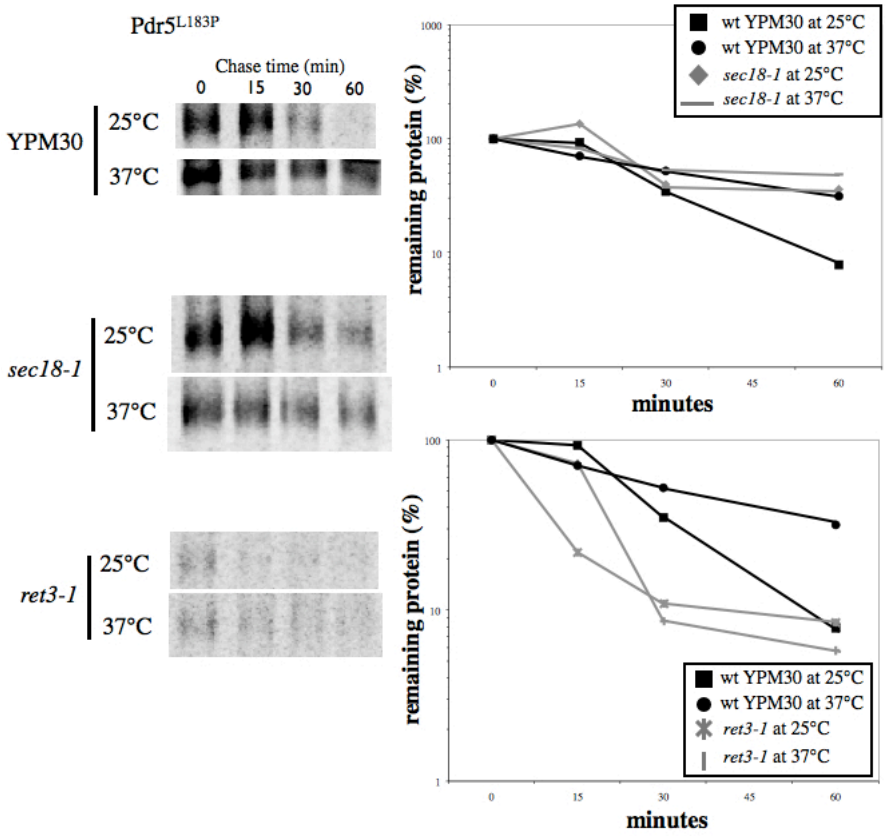

Figure 32. Role of Sec18p and Ret3p in Pdr5^{L183P} degradation. Pulse-chase analysis was carried out using wild-type (YPM30), *sec18-1* and *ret3-1* cells incubated at 25°C or 37°C. Protein remaining in percent is represented as a function of time. Pulse-chase analysis was carried out as described in Figure 13.

The half-life of Pdr5$^{L183P+C1427Y}$ in a *sec18-1* strain increased from 7 ± 4 min at 25°C to > 60 min at 37°C (Figure 33). Pdr5$^{L183P+C1427Y}$ is degraded with a $t_{1/2}$ of 16 ± 6 min in a *ret3-1* at 25°C. At 37°C, Pdr5$^{L183P+C1427Y}$ is stabilized ($t_{1/2}$ > 60 min).

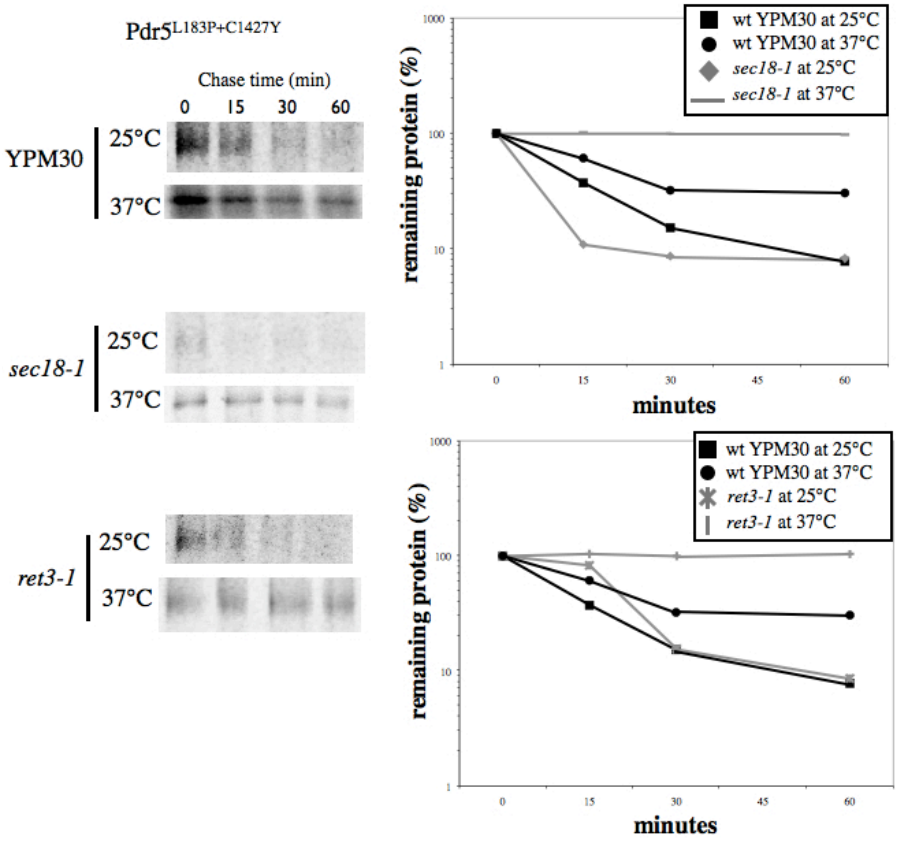

Figure 33. Role of Sec18p and Ret3p in Pdr5$^{L183P+C1427Y}$ degradation. Pulse-chase analysis was carried out using wild-type (YPM30), *sec18-1* and *ret3-1* cells incubated at 25°C or 37°C. Protein remaining in percent is represented as a function of time. Pulse-chase analysis was carried out as described in Figure 13.

We found an effect of the *sec18* mutation on the degradation of Pdr5^{C1427Y} (Figure 31) and Pdr5$^{L183P+C1427Y}$ (Figure 33), but not Pdr5^{L183P} (Figure 32). The effect of the *ret3-1* mutation is hard to interpret due to a [^{35}S]-methionine incorporation problem (in the case of Pdr5^{L183P} or Pdr5$^{L183P+C1427Y}$) or inequal immunoprecipitates recovery (in the case of Pdr5^{C1427Y}).

On the basis of the stabilization of Pdr5^{C1427Y} and Pdr5$^{L183P+C1427Y}$ in the *sec18-1* mutant strain, we conclude that ER-to-Golgi transport (and presumably transport back to the ER) is required for these variants to be efficiency degraded through the ERAD pathway as vacuolar degradation has been discarded. Our results are in good agreement with the model that predicts a role of the secretory pathway in proteasome-mediated degradation of ER soluble proteins and membrane proteins with a luminal misfolded domain. In contrast, the instability of Pdr5^{L183P} in the *sec18-1* strain indicate that vesicle fusion to the Golgi apparatus is not required. Instability of Pdr5^{L183P} in *sec18* and *ret3* mutant strains was previously reported by C. de Thozee and A. Goj in our laboratory (unpublished preliminary data). In the case of Pdr5^{L183P} which is not stabilized in the *sec18* strain, the requirement of Sec12p for Pdr5^{L183P} degradation might be independent of its role in the formation of the COPII vesicles and ER-to-Golgi transport.

8.2. Subcellular localization of Pdr5p variants in strains impaired in the early steps of the secretory pathway and in Golgi-to-ER transport

The results of the pulse-chase analysis indicate that Sec12p is required for the degradation of the Pdr5p variants. The effect of the mutation of Sec12p on subcellular localization was analysed by fluorescence microscopy, using cells expressing GFP fusions. We also analysed the effect of the loss of Ret3p, which impairs Golgi-to-ER retrograde transport.

The *sec12-4* temperature-sensitive mutant strain was transformed with the plasmids expressing Pdr5^{L183P}, Pdr5^{C1427Y} and Pdr5$^{L183P+C1427Y}$ as a protein fusion to the GFP. The *ret3-1* temperature-sensitive mutant strain was transformed with the plasmids expressing Pdr5^{C1427Y}-GFP and Pdr5$^{L183P+C1427Y}$-GFP. The *sec18-1* mutant strain was transformed with the plasmid expressing wild-type Pdr5-GFP. Appropriate transformed cells were grown at 25°C (permissive temperature) and then incubated at 25°C or 37°C (restrictive temperature) before microscopy analysis of GFP fluorescence. We found that incubation at 37°C has to be shorter than 1 h to avoid the loss of the fluorescence signal seen during prolonged incubation.

Pdr5-GFP was found to accumulate in the plasma membrane of *sec12-4*, *sec18-1* and *ret3-1* cells at 25°C (Figure 34). The inactivation of Sec12p and Sec18p at 37°C alters the localization of Pdr5-GFP from the plasma membrane to the ER-perinuclear membrane (asymmetric localization). In

contrast, the inactivation of Ret3p has no effect on the plasma membrane localization of Pdr5p.

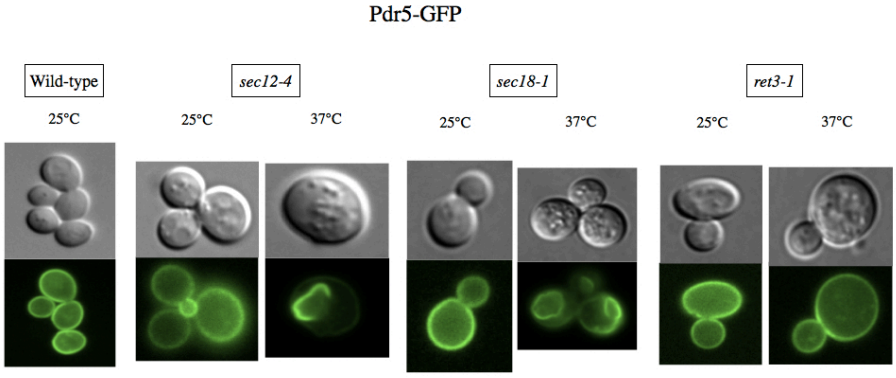

Figure 34. Localization of Pdr5-GFP in wild-type (YPM30), *sec12-4*, *sec18-1* and *ret3-1* cells incubated at 25°C or 37°C. Around 10% of the cells examined showed no fluorescence.

Pdr5^{C1427Y}-GFP accumulates asymmetrically in the ER-perinuclear membrane in wild-type cells and in the *sec12-4* and *ret3-1* mutant cells incubated at 25°C (Figure 35). At 37°C, the accumulation of Pdr5^{C1427Y}-GFP in the ER-perinuclear membrane shows less asymmetry, forming a rim in the *sec12-4* strain, wheres it remains asymmetrically localized in the ER-perinuclear membrane in the *ret3-1* strain.

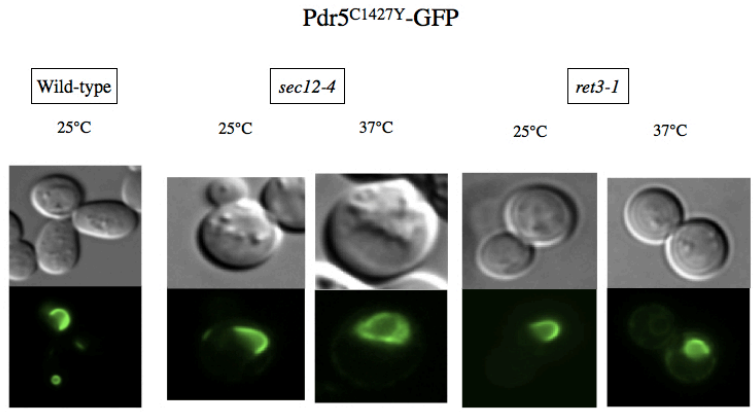

Figure 35. Localization of Pdr5^{C1427Y}-GFP in wild-type (YPM30), *sec12-4* and *ret3-1* cells incubated at 25°C or 37°C. Around 30% of the cells examined showed no fluorescence.

Pdr5^{L183P}-GFP accumulates in intracellular vesicles in *sec12-4* cells grown at 25°C or 37°C (Figure 36).

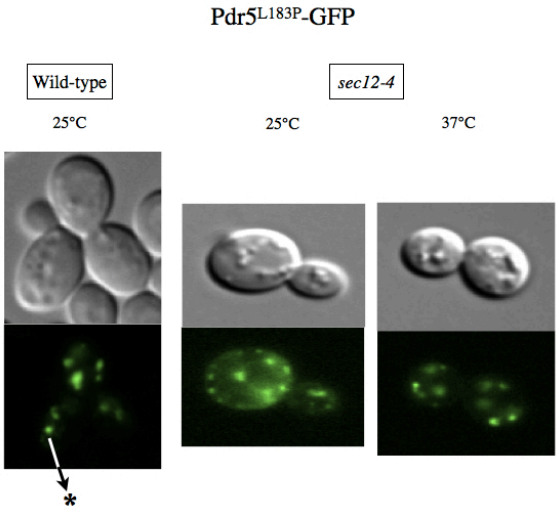

Figure 36. Localization of Pdr5^{L183P}-GFP in wild-type (YPM30) and *sec12-4* cells incubated at 25°C or 37°C. Intracellular vesicles are indicated with an asterisk. Around 30% of the cells examined showed no fluorescence.

Pdr5$^{L183P+C1427Y}$-GFP is found in intracellular vesicles in *sec12-4* and *ret3-1* cells grown at 25°C or 37°C (Figure 37).

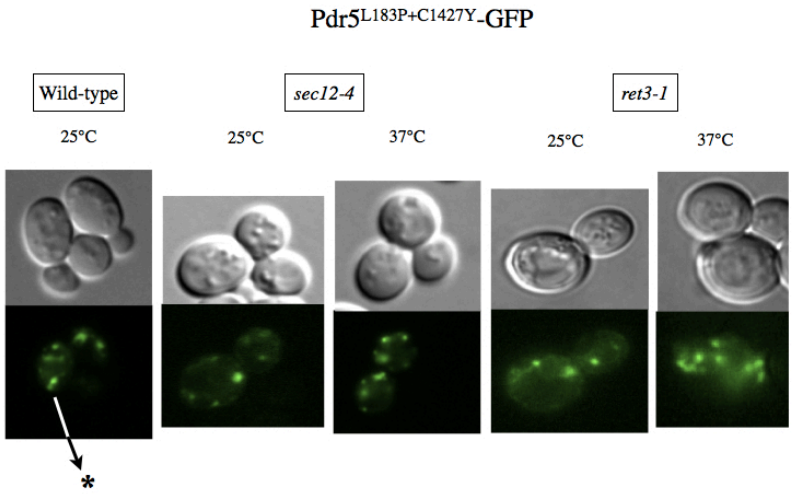

Figure 37. Localization of Pdr5$^{L183P+C1427Y}$-GFP in wild-type (YPM30), *sec12-4* and *ret3-1* cells incubated at 25°C or 37°C. Intracellular vesicles are indicated with an asterisk. Around 30% of the cells examined showed no fluorescence.

The results of fluorescence microscopy analysis indicate that the inactivation of Sec12p had no effect on the localization of Pdr5^{L183P}-GFP or Pdr5$^{L183P+C1427Y}$-GFP in intracellular compartments believed to be ERACs. The exact nature of these compartments requiring the use of anti-Kar2p antibodies.

Sec12p is not involved in the formation of the intracellular vesicles even though it is involved in the degradation of the Pdr5p variants as shown by pulse-chase analysis.

We need to exert some caution when interpreting fluorescence microscopy data. The fluorescence signal may correspond to a stabilized GFP fusion, to GFP alone or to a unstable GFP fusion which is protected from proteasomal degradation or on its way to the proteasome. The fluorescence signal disappeared in cells incubated for more than 60 min, consistent with the degradation of the GFP fusion.

If Sec12p is required to accumulate Pdr5^{L183P}-GFP and Pdr5$^{L183P+C1427Y}$-GFP in intracellular vesicles, a disappearance of these compartments in *sec12* mutant strain at 37°C would be expected. However, the incubation time was probably too short to see a disappearance of «ancient» intracellular vesicles as it takes ≃ 100 min for the disappearance of ERACs formed by CFTR (Fu and Sztul 2009). Note that CFTR has a $t_{1/2}$ ≃ 10-15 min in wild-type cells and a $t_{1/2}$ ≃ 40-45 min in *sec12* cells (Fu and Sztul 2003) so it could be different concerning the disappearance of intracellular vesicles formed by Pdr5p variants. Real-time imaging of the cells expressing the various GFP fusions will be a better approach to observe the appearance and disappearance of fluorescent ERACs.

For these reasons, we are more confident on pulse-chase results and we do believe that the formation of these intracellular vesicles are dependent of the Sar1p/COPII machinery.

9. Degradation of C-terminally truncated forms of Pdr5p

We generated different C-terminally truncated Pdr5p forms that lack 2 ($Pdr5^{TM1-10}$), 4 ($Pdr5^{TM1-8}$) and 6 TMSs ($Pdr5^{TM1-6}$). These constructions were used to determine whether the absence of the C-terminal membrane spanning segments influence the plasma membrane localization and/or stimulates the ER quality control system and proteasome-mediated degradation. It is also possible that the Pdr5p variants escape the ER quality control system and are addressed to the vacuole for degradation. Data on expression levels, subcellular localization and metabolic stability are presented below, using a separate section for each truncated form.

9.1. Implication of the ERAD-C pathway in degradation of $Pdr5^{TM1-6}$

Western blot analysis has shown that the steady-state levels of the $Pdr5^{TM1-6}$ form lacking the C-terminal membrane domain in wild-type BY4742 cells are low (see Figure 9).

To test the hypothesis that low levels of $Pdr5^{TM1-6}$ are the consequence of its degradation via the ERAD pathway, we analysed the effect of the loss of ER Ub-ligases Hrd1p (ERAD-L pathway) and Doa10p (ERAD-C pathway). The results of the Western blot analysis are shown in Figure 38 using antibodies against Pdr5p and Cdc48p (as a control) to compare the steady-state amounts of the truncated ABC-transporter protein.

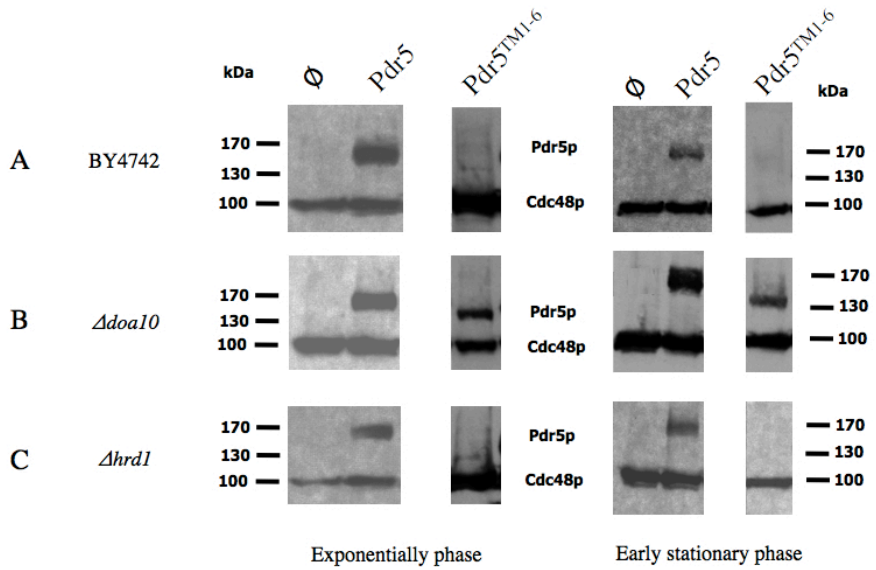

Figure 38. Expression of Pdr5^{TM1-6} in exponentially growing cells and during early stationary phase. Whole-cell extracts were prepared from exponential (OD_{600} 0.8-1, left panels) or early stationary (OD_{600} 1.6-2, right panels) phase cultures of BY4742 **(A)** and congenic *doa10Δ* **(B)** or *hrd1Δ* **(C)** strains. Cells were harvested by centrifugation and lysed with glass beads in the presence of protease inhibitors. An equal amount of whole-cell extract (10 µg) was analysed by SDS-PAGE and immunoblotting using antibodies against Pdr5p (1/2000 dilution) or Cdc48p (1/9000 dilution). The membrane was exposed to a Kodak XAR film for 30 sec (left panels) or left 16 h (right panels). Western blot analysis was repeated 2 times, with independently prepared extracts giving similar results.

No signal was detected in whole-cell extracts prepared from *hrd1Δ* cells (BY4742 background) harvested at the exponential (left panels) or the early stationary (right panels) phases of growth. However, the *doa10Δ* cells showed a 138-kDa band which corresponds to the predicted size of Pdr5^{TM1-6}. No difference in band intensity was seen between cells collected at the exponential phase and cells at the stationary phase.

Our results indicate that Pdr5^{TM1-6} is targeted to degradation through the ERAD-C pathway (Doa10p) and not the ERAD-L pathway (Hrd1p), in good agreement with the current ERAD model (Ahner and Brodsky 2004; Vashist and Ng 2004). The NBD2 of Pdr5^{TM1-6} is no more anchored to the membrane and might be freely accessible to cytosolic chaperone proteins which stimulate the ERAD-C pathway.

To confirm the implication of the ERAD-C pathway (Doa10p) in the degradation of Pdr5^{TM1-6}, pulse-chase analysis were carried out using the *doa10Δ* or *hrd1Δ* mutant BY4742 strains (Figure 39). Pdr5^{TM1-6} degradation is not impaired by the deletion of *HRD1* ($t_{1/2}$ of 4 ± 2 min). However, Pdr5^{TM1-6} is stabilized in the *doa10Δ* mutant strain ($t_{1/2}$ > 60 min). Each pulse-chase analysis was repeated 3 times, giving similar results each time.

The implication of the putative retro-translocon, Der1p, was also tested. As shown in Figure 39, the degradation of Pdr5^{TM1-6} is not impaired by the deletion of *DER1* ($t_{1/2}$ of 4 ± 1 min ; n=3) indicating that this truncated version is degraded in a Der1-independent process, in good agreement with the ERAD model.

The effect of the *PEP4* deletion on the degradation of Pdr5^{TM1-6} was also analysed (Figure 39). The truncated form is not stabilized in the *pep4Δ* strain ($t_{1/2}$ of 7 ± 3 min ; n=3), indicating that Pdr5^{TM1-6} is only degraded by the proteasome, through the ERAD pathway, and not in the vacuole.

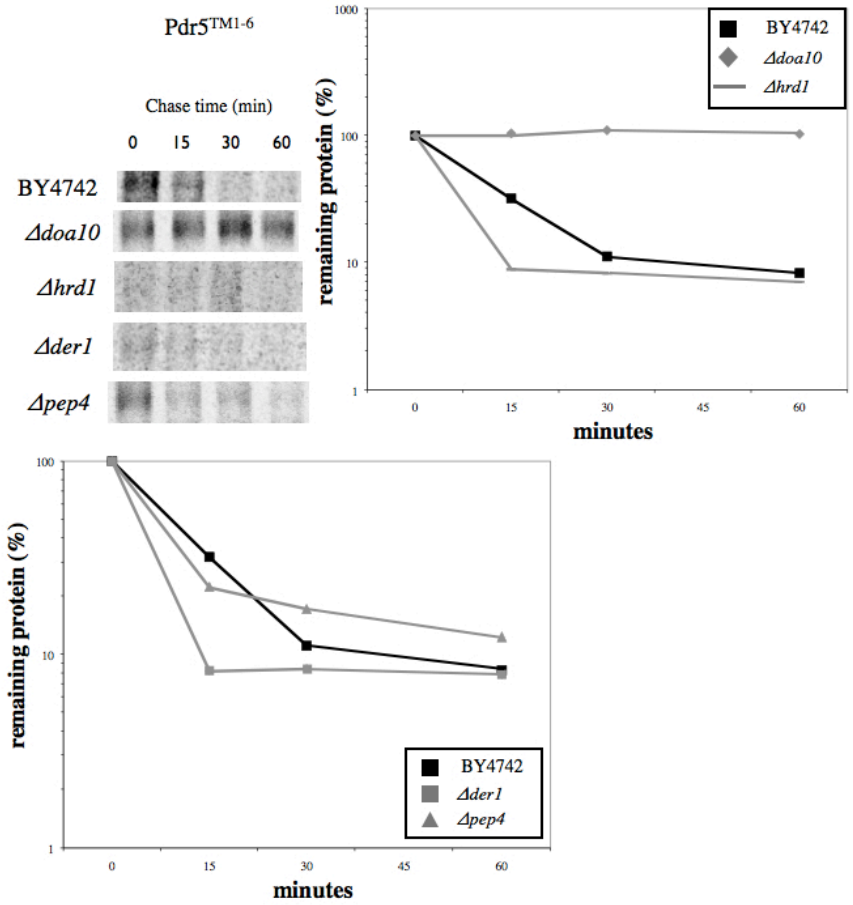

Figure 39. ER-associated degradation of Pdr5^{TM1-6}. Pulse-chase analysis was carried out using wild-type (BY4742), *doa10Δ*, *hrd1Δ*, *der1Δ*, and *pep4Δ* cells. Protein remaining in percent is represented as a function of time. See Figure 13 for detailed experimental conditions.

To determine whether Hrd1p can substitute for the absence of Doa10p, we compared the degradation rate of Pdr5^{TM1-6} between cells lacking Doa10p and cells lacking both Doa10p and Hrd1p using the wild-type MHY501

parent as a control (n=2) (Figure 40). The half-life of Pdr5^{TM1-6} is 8 ± 3 min in the wild-type cells, 16 ± 3 min in congenic *hrd1Δ* cells and > 60 min in congenic *doa10Δ* cells. These results are comparable to those seen with BY4742 cells lacking Doa10p or Hrd1p (see Figure 39). In particular, we confirmed the stabilization of Pdr5^{TM1-6} in cells lacking Doa10p. No further stabilization is seen in cells lacking both Doa10p and Hrd1p (Figure 40). It is therefore unlikely that Hrd1p contributes to the degradation of Pdr5^{TM1-6}.

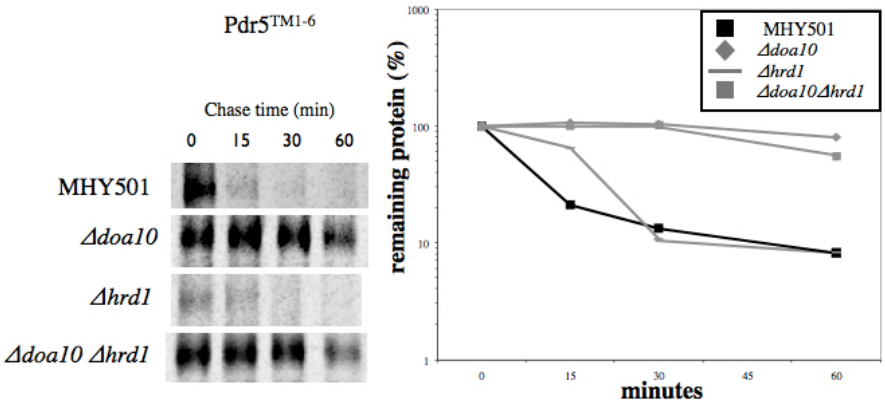

Figure 40. Pulse-chase analysis of Pdr5^{TM1-6} turnover in MHY501 cells impaired in Doa10p and/or Hrd1p. Pulse-chase analysis were carried out using wild-type (MHY501), *doa10Δ*, *hrd1Δ* and *doa10Δ hrd1Δ* cells. Protein remaining in percent is represented as a function of time. See Figure 13 for detailed experimental conditions.

Subcellular localization of Pdr5^{TM1-6} was determined in the wild-type BY4742 and MHY501 strains by fluorescence microscopy, using a GFP protein fusion (Figure 41). The Pdr5^{TM1-6}-GFP was also expressed in strains

impaired in Doa10p, Hrd1p or in both Ub-protein ligases to determine the effect of these mutations on the subcellular localization of Pdr5^{TM1-6} (Figure 41).

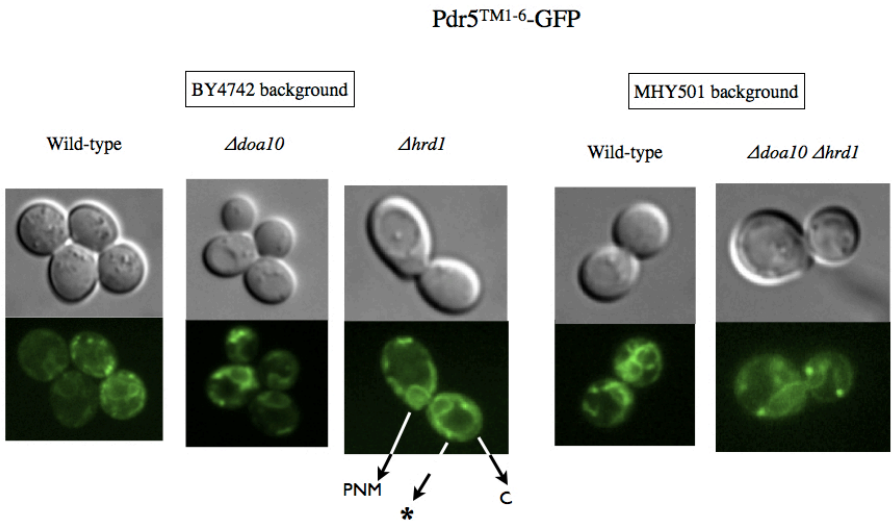

Figure 41. Localization of Pdr5^{TM1-6}-GFP in *doa10Δ*, *hrd1Δ* and *doa10Δ hrd1Δ* cells. Fluorescence microscopy-based images of wild-type (BY4742, MHY501), *doa10Δ*, *hrd1Δ* and *doa10Δ hrd1Δ* cells expressing Pdr5^{TM1-6}-GFP. Intracellular vesicles are indicated with an asterisk. PNM, ER-perinuclear membrane ; C, cortical ER.

Only ≈ 30% of the cells examined showed a fluorescence signal in the ER-perinuclear membrane, cortical ER and intracellular vesicles. The cortical ER is a subcompartment of the ER localized under the plama membrane. Pdr5^{TM1-6} localization was not affected by the deletion of *HRD1* and *DOA10*, alone or in combination.

We need to exert some caution when interpreting fluorescence microscopy data because Pdr5^{TM1-6} was not detected by Western blot analysis. Therefore, the fluorescence signal may correspond to a stabilized GFP

fusion, to GFP alone after fusion cleavage or to an unstable GFP fusion which is protected from proteasomal degradation in specific compartments. Western blot analysis of cells expressing Pdr5^{TM1-6}-GFP will allow us to determine whether the protein fusion is cleaved or not and whether the full-length chimera is a stable protein or not.

The localization of Pdr5^{TM1-6} in intracellular vesicles suggests the requirement of the Sar1p/COPII machinery to be efficiency degraded. To assess its implication, pulse-chase analysis were carried out used a strain impaired in Sec12p. The possibility of the requirement of an efficient ER-to-Golgi transport for the degradation of Pdr5^{TM1-6} was also analysed by pulse-chase. Pdr5^{TM1-6} was expressed in the wild-type parental YPM30 strain and the congenic *sec12-4*, *sec18-1* and *ret3-1* mutant strains (n=2) (Figure 42).

The truncated ABC-transporter protein is rapidly degraded in the wild-type strain at 25°C ($t_{1/2}$ of 13 ± 5 min) or 37°C ($t_{1/2}$ of 6 ± 2 min) as previously shown for the other wild-type BY4742 and MHY501 strains (see Figures 39 and 40). In a *sec12-4* strain grown at the permissive temperature of 25°C, the degradation of Pdr5^{TM1-6} is not affected ($t_{1/2}$ of 7 ± 4 min). At the restrictive temperature of 37°C, however, the truncated ABC-transporter protein is stabilized with a $t_{1/2} > 60$ min. Inactivation of Sec18p failed to stabilize Pdr5^{TM1-6} ($t_{1/2}$ of 6 ± 2 min at 25°C and $t_{1/2}$ of 11 ± 5 min at 37°C). In the same way, inactivation of Ret3p at 37°C failed to stabilize the truncated Pdr5p form ($t_{1/2}$ of 7 ± 4 min at 25°C and 8 ± 5 min at 37°C).

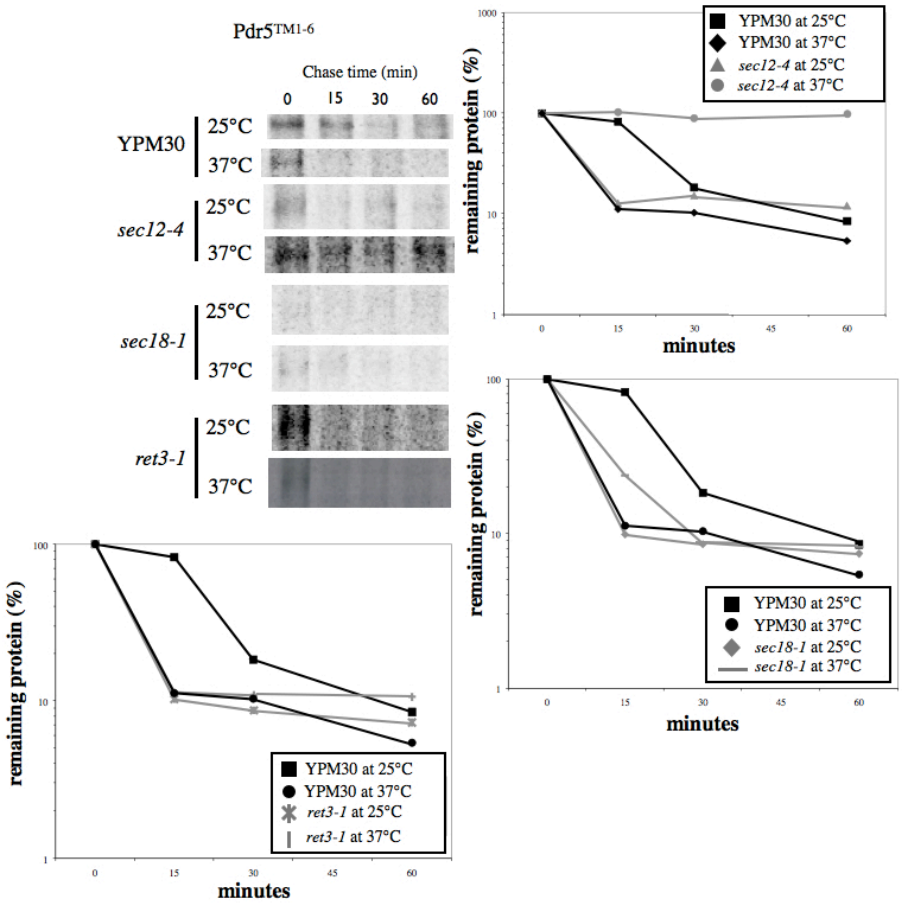

Figure 42. Role of Sec12p, Sec18p and Ret3p in Pdr5^{TM1-6} degradation. Pulse-chase analysis was carried out using wild-type (YPM30), *sec12-4*, *sec18-1* and *ret3-1* cells incubated at 25°C or 37°C. Protein remaining in percent is represented as a function of time. See Figure 13 for detailed experimental conditions.

These results show that only Sec12p is required for Pdr5^{TM1-6} degradation, in a good agreement with the role of the GDP/GTP exchange factor in the degradation of the mutated Pdr5 forms analysed in this work. The loss of Sec18p and Ret3p had no stabilizing effect on Pdr5^{TM1-6} degradation,

suggesting that ER-to-Golgi transport is not required. This finding supports the current ERAD model for membrane proteins lacking misfolded luminal domains.

The effect of the loss of Sec12p on the localization of Pdr5^{TM1-6} in intracellular vesicles, ER-perinuclear membrane and cortical ER was examined by fluorescence microscopy (Figure 43). Only ≈ 30% of cells examined showed a fluorescent signal at 25°C. When transferred to 37°C, only 10% of the cells showed a signal in intracellular vesicles, ER-perinuclear membrane and cortical ER, which was completely gone after an incubation of 30 min.

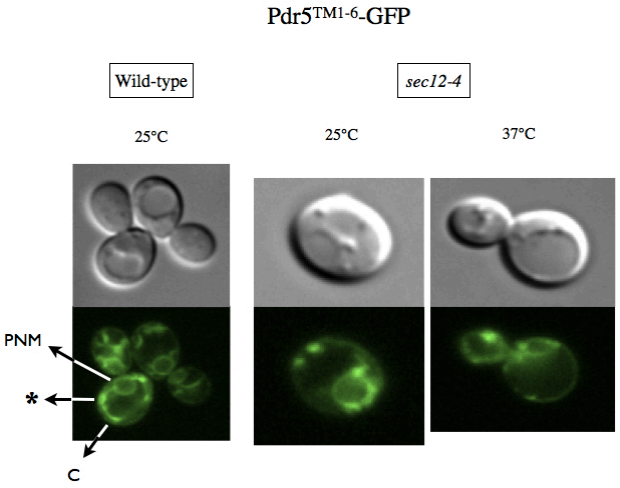

Figure 43. Role of Sec12p in localization of Pdr5^{TM1-6}-GFP. Fluorescence microscopy-based images of wild-type (YPM30) and *sec12-4* cells expressing Pdr5^{TM1-6}-GFP at 25°C and 37°C. Intracellular vesicles corresponding to ERACs, early Golgi or Golgi are indicated with an asterisk. PNM, ER-perinuclear membrane ; C, cortical ER.

Interpretation of fluorescence microscopy data need to be taken with precautions for the same reason as mentioned before. The incubation time was probably too short to see a diseappearence of intracellular vesicles. For these reasons, we are more confident in pulse-chase results and we do believe that the formation of these intracellular vesicles are dependent of the Sar1p/COPII machinery (stability effect in *sec12-4* cells).

9.2. Pdr5^{TM1-8} is a long-lived protein

A plasmid that expresses a C-terminally truncated form lacking the last 4 TMSs, Pdr5^{TM1-8}, was introduced into the wild-type parental BY4742 strain and the congenic *doa10Δ* and *hrd1Δ* null mutant strains. Appropriate transformants were selected and whole-cell extracts were analysed by Western blot using antibodies against Pdr5p (and Cdc48p as a control) to compare the steady-state amounts of the truncated ABC-transporter protein.

A 145-kDa band corresponding to the truncated Pdr5 form was detected in all strains (Figure 44). No difference in the expression levels was seen in wild-type cells compared to cells impaired in ERAD. There was also no effect of the growth phase on the amount of Pdr5^{TM1-8}. These results indicate that, unlike Pdr5^{TM1-6}, Pdr5^{TM1-8} is not subject to degradation and is a stable protein.

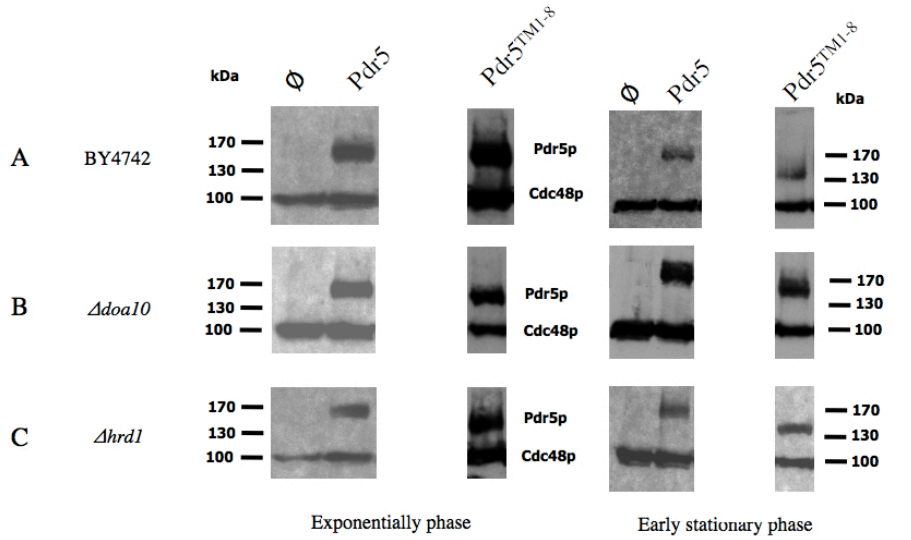

Figure 44. Expression of Pdr5^{TM1-8} in exponentially growing cells and during early stationary phase. Whole-cell extracts were prepared from exponential (OD_{600} 0.8-1, left panels) or early stationary (OD_{600} 1.6-2, right panels) phase cultures of BY4742 **(A)** and congenic *doa10Δ* **(B)** or *hrd1Δ* **(C)** strains. Cells were harvested by centrifugation and lysed with glass beads in the presence of protease inhibitors. An equal amount of whole-cell extract (10 µg) was analysed by SDS-PAGE and immunoblotting using antibodies against Pdr5p (1/2000 dilution) or Cdc48p (1/9000 dilution). The membrane was exposed to a Kodak XAR film for 30 sec (left panels) or left 16 h (right panels). Western blot analysis was repeated 2 times with independently prepared extracts giving similar results.

Pdr5^{TM1-8} stability was assessed by pulse-chase analysis. As shown in Figures 45 and 46, no degradation of Pdr5^{TM1-8} was detected in the wild-type BY4742 and MHY501 strains ($t_{1/2}$ > 60 min ; n=2-3). Obviously the same result was obtained with strains impaired in ERAD or vacuolar degradation (*pep4Δ* strain). We have no explanation for the signal variability between different time points (in particular, the 30 min point for *doa10Δ* BY4742 cells).

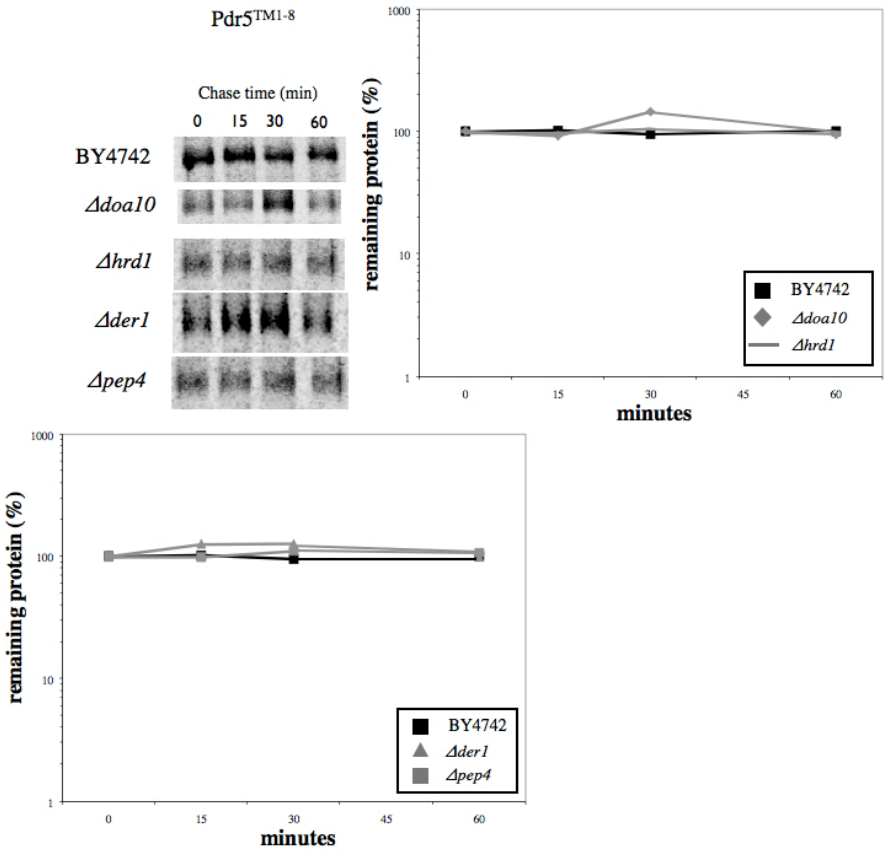

Figure 45. Pulse-chase analysis of Pdr5^{TM1-8}. Pulse-chase analysis was carried out using wild-type (BY4742), *doa10Δ*, *hrd1Δ*, *der1Δ* and *pep4Δ* cells. Protein remaining in percent is represented as a function of time. See Figure 13 for detailed experimental conditions.

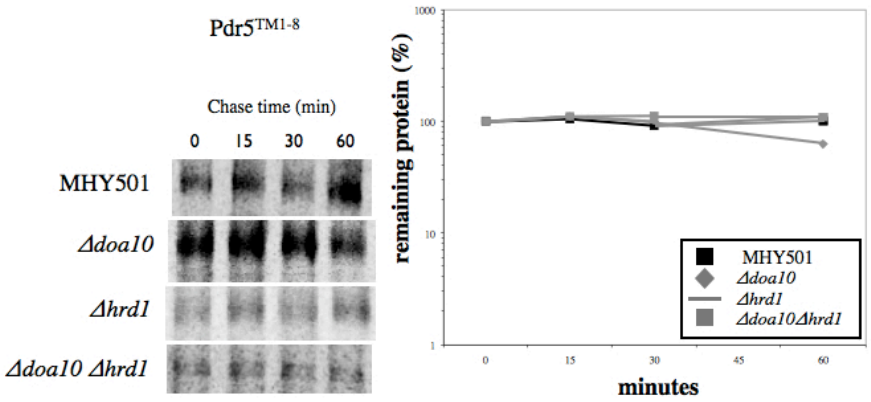

Figure 46. Pulse-chase analysis of Pdr5^{TM1-8} in MHY501 cells lacking Doa10p and/or Hrd1p. Pulse-chase analysis were carried out using wild-type (MHY501), *doa10Δ*, *hrd1Δ* and *doa10Δ hrd1Δ* mutant cells. Protein remaining in percent is represented as a function of time. See Figure 13 for detailed experimental conditions.

The results of the Western blot and pulse-chase analysis indicate that adding two TMSs at the C-terminus of Pdr5^{TM1-6} stabilizes the ABC-transporter protein.

We determined the subcellular localization of Pdr5^{TM1-8} by fluorescence microscopy, using a GFP protein fusion. Pdr5^{TM1-8}-GFP was found in the ER-perinuclear membrane and cortical ER in wild-type cells and mutated cells lacking Hrd1p and/or Doa10p (Figure 47). These results indicate that the truncated variant is not correctly addressed to the plasma membrane, possibly as a consequence of the removal of an adressing sequence at the C-terminus. An other possibility is that Pdr5^{TM1-8} fails to fold correctly and is recognized by the ER quality control system. Lacking a putative C-terminal degron, the truncated variant escapes ubiquitylation and remains in the ER.

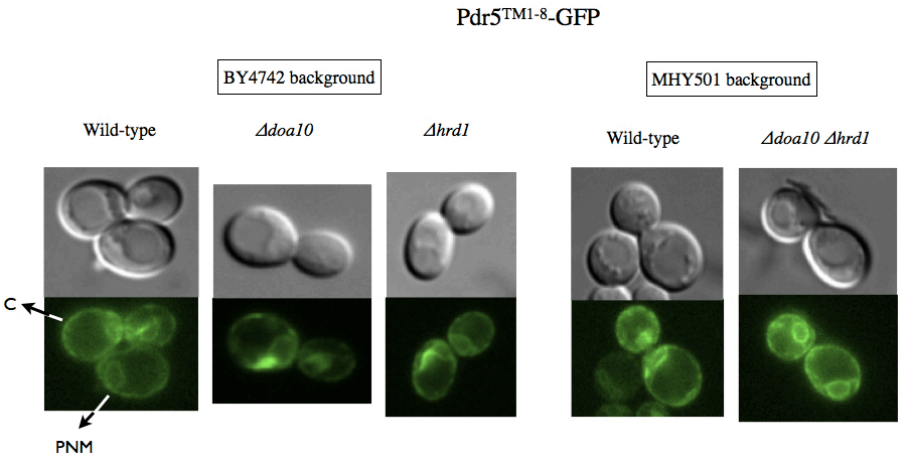

Figure 47. Localization of Pdr5^{TM1-8}-GFP in *doa10Δ*, *hrd1Δ* and *doa10Δ hrd1Δ* cells. Fluorescence microscopy-based images of wild-type (BY4742, MHY501), *doa10Δ*, *hrd1Δ* and *doa10Δ hrd1Δ* cells expressing Pdr5^{TM1-8}-GFP. Around 10% of the cells examined showed no fluorescence. PNM, ER-perinuclear membrane ; C, cortical ER.

If Pdr5^{TM1-8} lacks an important signal sequence required for plasma membrane targeting, the localization in the ER-perinuclear membrane and cortical ER would not be altered by a mutation of *SEC12*. Fluorescence microscopy of *sec12* cells expressing the Pdr5^{TM1-8}-GFP chimera showed a fluorescence signal in the ER-perinuclear membrane and cortical ER at 25°C as seen with the wild-type parental strain (Figure 48). At 37°C, however, the fluorescence signal was concentrated in a high dot, which is believed to correspond to a subcompartment of the ER, and no fluorence was observed in cortical ER.

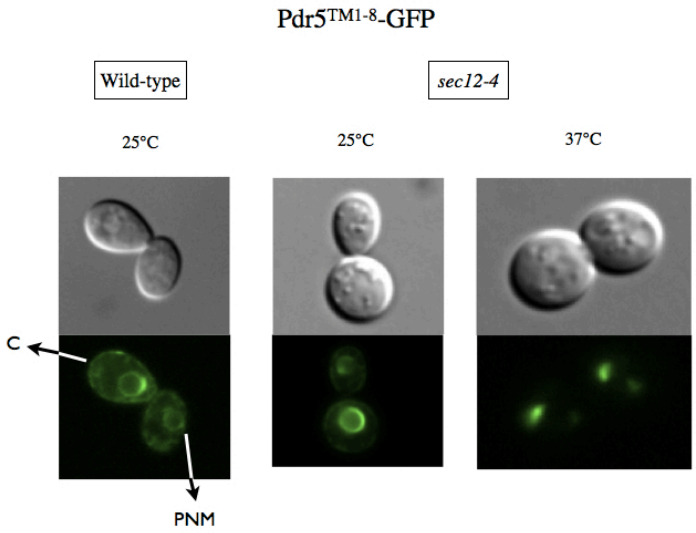

Figure 48. Role of Sec12p in localization of Pdr5^{TM1-8}-GFP. Fluorescence microscopy-based images of wild-type (YPM30) and *sec12-4* cells expressing Pdr5^{TM1-8}-GFP at 25°C and 37°C. Around 10% of the cells examined showed no fluorescence. PNM, ER-perinuclear membrane ; C, Cortical ER.

A minor fraction of Pdr5^{TM1-8} protein might be located in the plasma membrane as a difference of localization was observed in *sec12* cells between 25°C and 37°C (ER-perinuclear membrane and cortical ER at 25°C versus high dot at 37°C). However, the fluorescent signal observed with Pdr5^{TM1-8} in *sec12-4* cells at 37°C is very different from the one seen with the wild-type Pdr5p form in the same mutant strain (see Figure 34). Effectively, in *sec12* strain at 37°C, Pdr5^{TM1-8}-GFP is concentrated in high dot whereas Pdr5-GFP accumulated to the ER-perinuclear membrane (asymmetric localization). It is difficult to differenciate the cortical ER, localized under the plasma membrane, and the plasma membrane by fluorescence microscopy. Co-localization with a plasma membrane marker will help to elucidate this point.

Pulse-chase analysis indicate that Pdr5^{TM1-8} is a long-lived protein in mutant strains impaired in Sec12p, Sec18p or Ret3p ($t_{1/2}$ > 60 min ; n=2) (Figure 49). Some signal variability was observed with the *sec12-4* cells. At 25°C, the Pdr5^{TM1-8} band at t = 60 min is less intense than the bands detected at earlier chase time. This might result from a difference in sample loading.

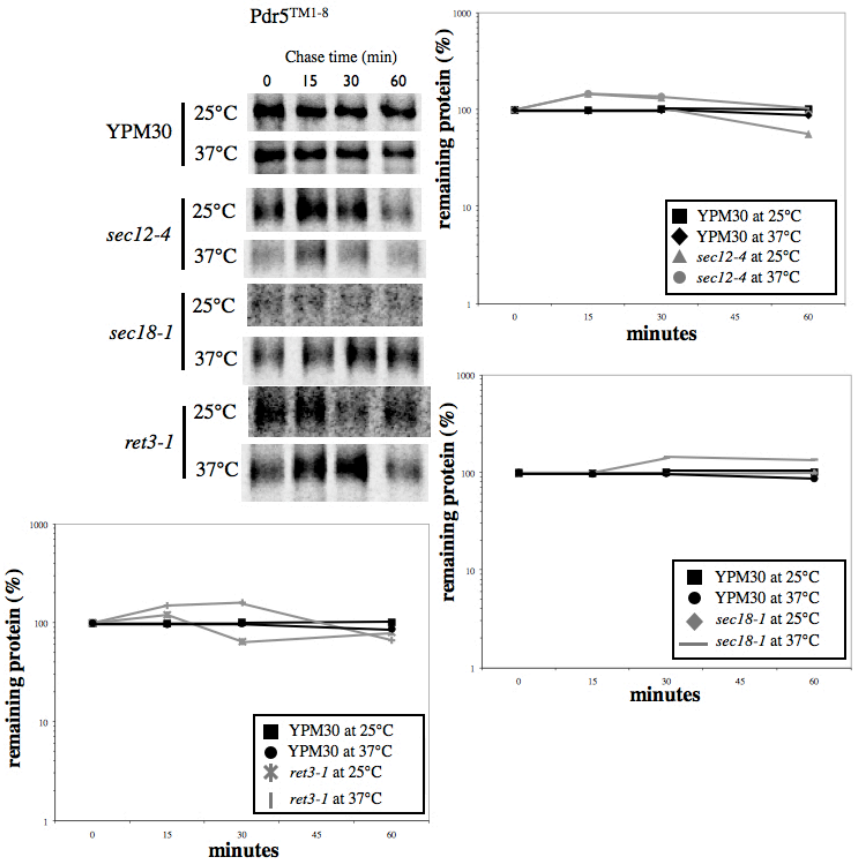

Figure 49. Role of Sec12p, Sec18p and Ret3p in Pdr5^{TM1-8} degradation. Pulse-chase analysis was carried out using wild-type (YPM30), *sec12-4*, *sec18-1* and *ret3-1* cells incubated at 25°C or 37°C. Protein remaining in percent is represented as a function of time. See Figure 13 for detailed experimental conditions.

9.3. Vacuolar and ER-associated degradation of Pdr5^{TM1-10}

A plasmid that expresses the C-terminally truncated form Pdr5^{TM1-10} lacking the last 2 TMSs was introduced into the wild-type parental BY4742 strain and the congenic *doa10Δ* and *hrd1Δ* null mutant strains. Appropriate transformants were selected and whole-cell extracts were analysed by Western blot using antibodies against Pdr5p (and Cdc48p as a control) to compare the steady-state amounts of the truncated ABC-transporter protein.

A 151-kDa band corresponding to the size of Pdr5^{TM1-10} was detected in exponential growing cells of the wild-type BY4742 strain and the congenic *doa10Δ* or *hrd1Δ* mutant strains (Figure 50). However, the 151-kDa band is no more detected in whole-cell extracts prepared from stationary phase cultures of BY4742 and *hrd1Δ* cells. A very faint band is seen with the *doa10Δ* cells, which might be explained by a higher amount of proteins loaded as judged from the increased signal seen with Cdc48p. In conclusion, Western blot analysis indicates that Pdr5^{TM1-10} is degraded as the cells enter the stationary phase of growth and this degradation is not impaired by the loss of Doa10p or Hrd1p, in a striking contrast to the results seen with Pdr5^{TM1-6} (see Figure 38).

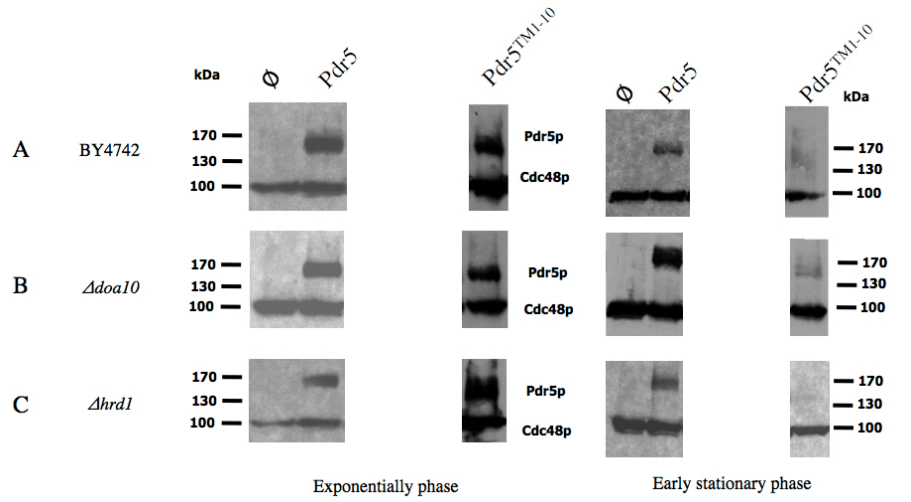

Figure 50. Expression of Pdr5^{TM1-10} in exponentially growing cells and during early stationary phase. Whole-cell extracts were prepared from exponential (OD_{600} 0.8-1, left panels) or early stationary (OD_{600} 1.6-2, right panels) phase cultures of BY4742 **(A)** and congenic *doa10Δ* **(B)** or *hrd1Δ* **(C)** strains. Cells were harvested by centrifugation and lysed with glass beads in the presence of protease inhibitors. An equal amount of whole-cell extract (10 µg) was analysed by SDS-PAGE and immunoblotting using antibodies against Pdr5p (1/2000 dilution) or Cdc48p (1/9000 dilution). The membrane was exposed to a Kodak XAR film for 30 sec (left panels) or left 16 h (right panels). Western blot analysis was repeated 2 times with independently prepared extracts giving similar results.

To further investigate the role of ERAD in Pdr5^{TM1-10} degradation, pulse-chase analysis were carried out using strains impaired in Doa10p and/or Hrd1p (n=2). The truncated ABC-transporter protein was degraded in the parental wild-type MHY501 strain with a half-life of 28 ± 5 min (Figure 51). Pdr5^{TM1-10} degradation was not altered by the loss of Doa10p ($t_{1/2}$ of 25 ± 4 min) or Hrd1p ($t_{1/2}$ of 17 ± 4 min). However, the loss of the two Ub-ligases resulted in stabilization of Pdr5^{TM1-10} ($t_{1/2}$ > 60 min). These results indicate that Pdr5^{TM1-10} is targeted for proteasomal degradation via the ERAD-C or the ERAD-L pathways as no degradation was observed in strains lacking Doa10p or Hrd1p.

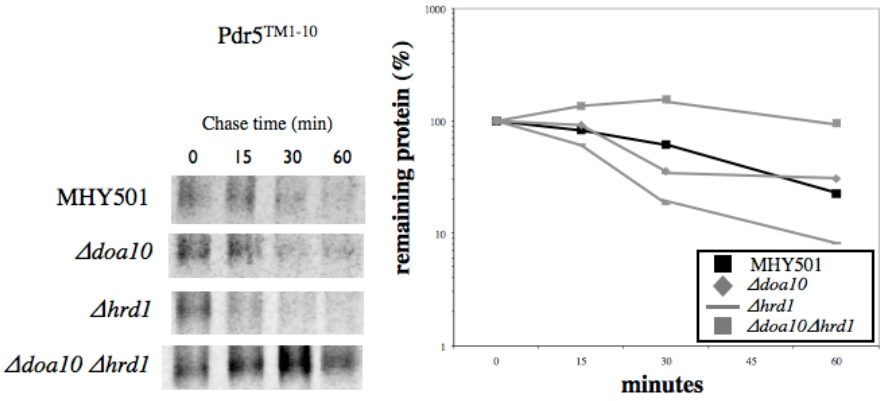

Figure 51. Pulse-chase analysis of Pdr5^{TM1-10} in mutant MHY501 cells impaired in ER Ub-ligases Doa10p and/or Hrd1p. Pulse-chase analysis were carried out using wild-type (MHY501), *doa10Δ*, *hrd1Δ*, and *doa10Δ hrd1Δ* cells. Protein remaining in percent is represented as a function of time. See Figure 13 for detailed experimental conditions.

The contribution of either pathway functioning independently one from another for ERADication of Pdr5^{TM1-10} contrasts with the requirement of the ERAD-C pathway alone for Pdr5^{TM1-6} degradation and the cooperation between the two pathways for Pdr5^{L183P}, Pdr5^{C1427Y} and Pdr5$^{L183P+C1427Y}$ degradation.

To test the possibility that Pdr5^{TM1-10} is degraded in the vacuole, a BY4742 strain deleted for the *PEP4* gene was transformed with a plasmid expressing the truncated Pdr5p variant and the turnover of Pdr5^{TM1-10} was determined by pulse-chase analysis (n=3). As shown in Figure 52, the rate of Pdr5^{TM1-10} degradation is decreased in *pep4Δ* cells ($t_{1/2}$ = 45 ± 5 min), compared to wild-type cells ($t_{1/2}$ = 22 ± 5 min). In a striking contrast, Pdr5^{TM1-10} is not stabilized in BY4742 cells lacking Doa10p ($t_{1/2}$ of 24 ± 5 min) or Hrd1p ($t_{1/2}$ of 28 ± 4 min) as shown previously (n=3). Figure 52 also shows that deletion of the *DER1* gene had no effect on Pdr5^{TM1-10} degradation ($t_{1/2}$ of 18 ± 3 min ; n=3), supporting the view that the ERAD-L pathway is not the major pathway targeting Pdr5^{TM1-10} for degradation.

Taken together, these results indicate that Pdr5^{TM1-10} is degraded by the proteasome via the ERAD pathway and in the vacuole.

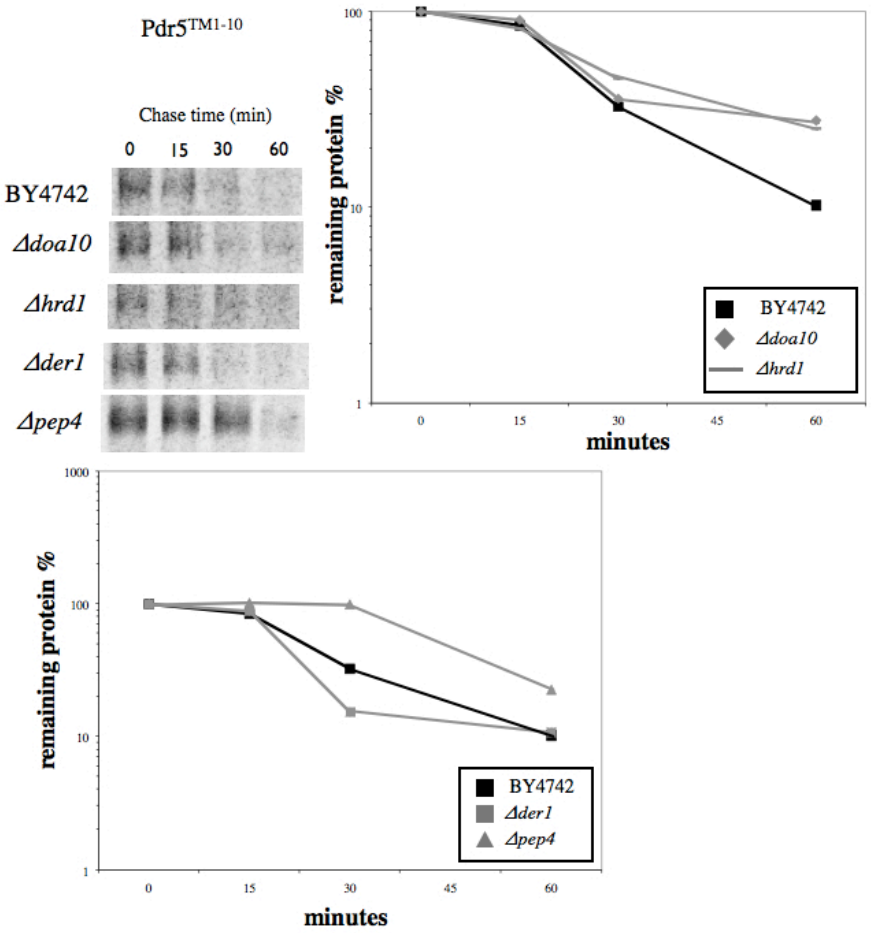

Figure 52. Proteasomal and vacuolar degradation of Pdr5^{TM1-10}. Pulse-chase analysis were carried out using wild-type (BY4742), *doa10Δ*, *hrd1Δ*, *der1Δ* and *pep4Δ* mutant cells. Protein remaining in percent is represented as a function of time. See Figure 13 for detailed experimental conditions.

Subcellular localization of the truncated Pdr5^{TM1-10} form in wild-type (BY4742, MHY501) cells, was determined by fluorescence microscopy using a GFP protein fusion (Figure 53). Mutant strains impaired in Doa10p and/or Hrd1p, and in Pep4p were also examined to determine whether these mutations influence the subcellular localization of Pdr5^{TM1-10}. The *pep4Δ* strain was also transformed with a plasmid expressing the Pdr5-GFP protein fusion as a control.

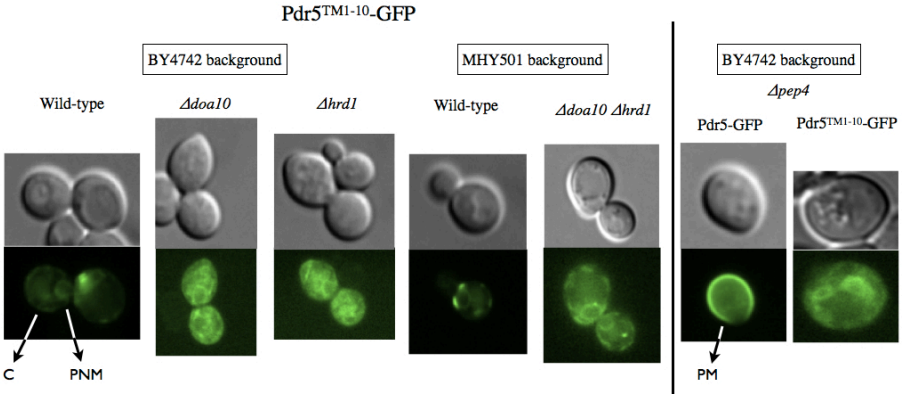

Figure 53. Localization of Pdr5^{TM1-10}-GFP in mutant strains impaired in ERAD and vacuolar degradation. Fluorescence microscopy-based images of wild-type (BY4742), *doa10Δ*, *hrd1Δ* and *pep4Δ* cells and of wild-type (MHY501), *doa10Δ hrd1Δ* cells expressing Pdr5^{TM1-10}-GFP. Around 50% of the cells examined showed no fluorescence signal. Pdr5-GFP was expressed in *pep4Δ* cells as a control and around 90% of the cells examined showed a fluorescence signal. PNM, ER-perinuclear membrane ; C, cortical ER ; PM, plasma membrane.

The truncated Pdr5^{TM1-10} form is localized in the ER-perinuclear membrane and cortical ER in wild-type BY4742 cells (Figure 53). The distribution of Pdr5^{TM1-10} into these compartments is not altered by the loss of Hrd1p and Doa10p, alone or in combination. The localization of Pdr5^{TM1-10} in *pep4Δ*

cells is difficult to interpret as the fluorescence signal is diffuse. Even though we found that Pep4p is implicated in Pdr5^{TM1-10} degradation, its loss may not alter the subcellular localization of the truncated variant in *pep4Δ* cells as we found that the distribution of Pdr5^{TM1-10} into the ER compartments is not altered by the loss of the ERAD pathway (Hrd1p and Doa10p). Co-localization with ER and vacuolar marker will be required to elucidate the subcellular localization of Pdr5^{TM1-10} in *pep4Δ* cells. Stronger fluorescence was observed in the *pep4Δ*, *hdr1Δ* and *doa10Δ* mutant strains compared to the wild-type BY4742 parental strain. We have no explanation for this difference.

The degradation of Pdr5^{TM1-10} in the vacuole implies a transit via the secretory pathway. A plasmid expressing Pdr5^{TM1-10} was introduced in the *sec12-4* and *sec18-1* mutant strains and the congenic wild-type parental strain to analyse the role of the early secretory pathway in Pdr5^{TM1-10} degradation. The role of retrograde Golgi-to-ER transport was also studied by using a *ret3-1* mutant strain (Figure 54).

The *sec12* and *sec18* mutant cells showed a decreased degradation of Pdr5^{TM1-10} at 37°C ($t_{1/2}$ > 60 min), compared to the wild-type YPM30 cells ($t_{1/2}$ = 11 ± 8 min) (n=2). Pdr5^{TM1-10} is rapidly degraded in *sec12-4* ($t_{1/2}$ = 26 ± 6 min), *sec18-1* ($t_{1/2}$ = 21 ± 5 min) and wild-type cells ($t_{1/2}$ = 11 ± 6 min) at 25°C (n=2). The inactivation of Ret3p at 37°C has no effect on Pdr5^{TM1-10} degradation ($t_{1/2}$ = 14 ± 7 min versus 14 ± 9 min at 25°C) (n=2). These results indicate that ER-to-Golgi transport and membrane fusion between the

vesicles and the Golgi are involved in the degradation of Pdr5^{TM1-10}. In contrast, the retrograde transport seems to be not required.

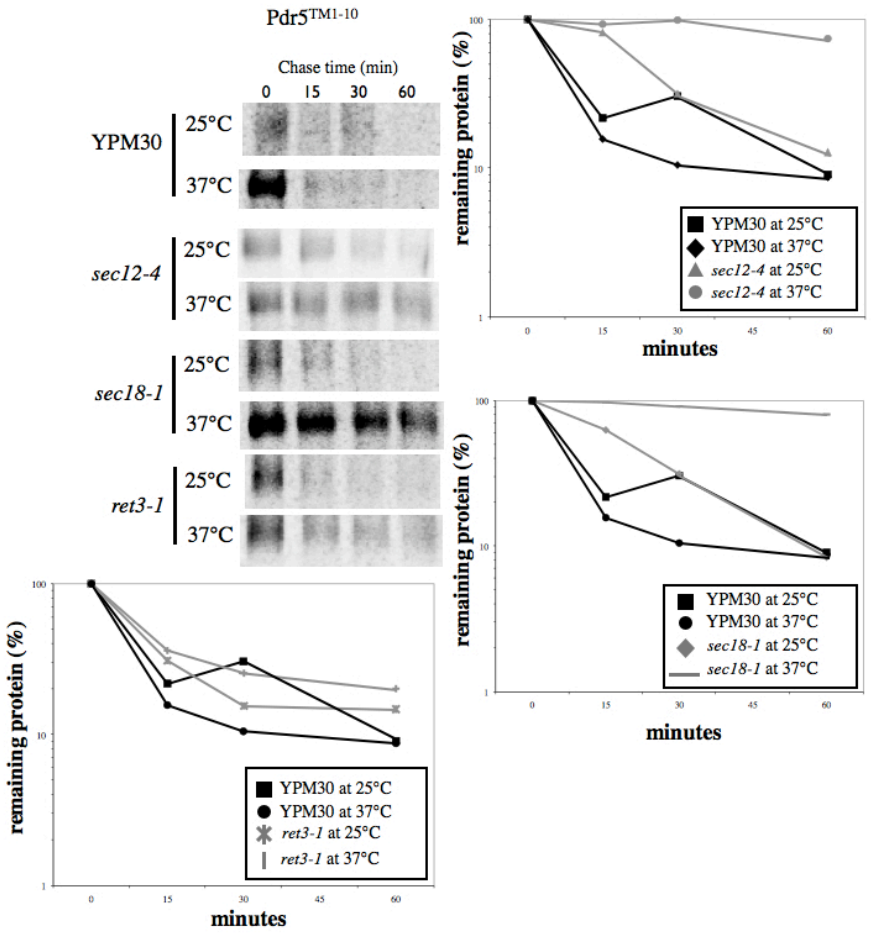

Figure 54. Role of Sec12p, Sec18p and Ret3p in Pdr5^{TM1-10} degradation. Pulse-chase analysis were carried out using wild-type (YPM30), *sec12-4*, *sec18-1* and *ret3-1* cells incubated at 25°C or 37°C. Protein remaining in percent is represented as a function of time. See Figure 13 for detailed experimental conditions.

As the inactivation of Sec12p results in Pdr5^{TM1-10} stabilization, we analysed the effect of the *sec12* mutation on the localization of Pdr5^{TM1-10} in the ER-perinuclear membrane and cortical ER by fluorescence microscopy using a GFP protein fusion (Figure 55).

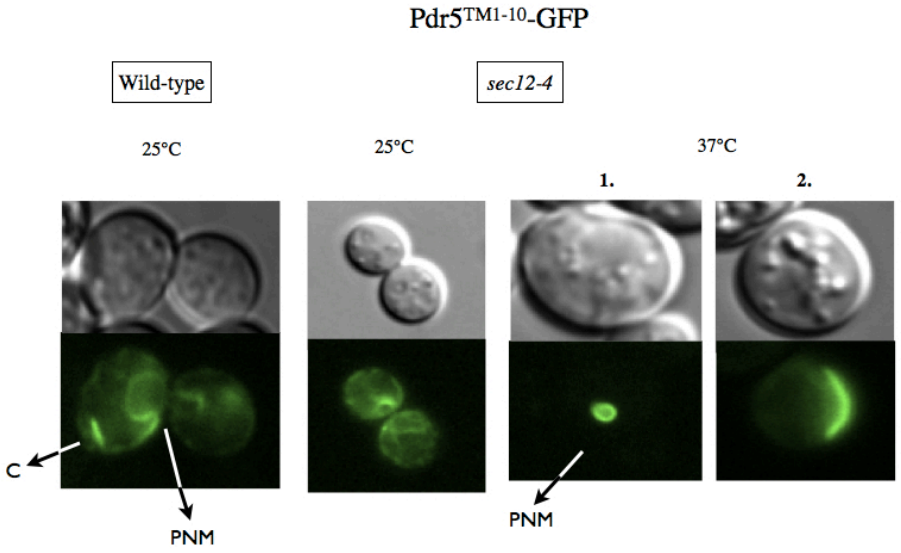

Figure 55. Role of Sec12p in localization of Pdr5^{TM1-10}-GFP. Fluorescence microscopy-based images of wild-type (YPM30) and *sec12-4* cells expressing Pdr5^{TM1-10}-GFP at 25°C and 37°C. Around 50% of the cells examined showed no fluorescence signal. PNE, ER-perinuclear membrane ; C, cortical ER.

Pdr5^{TM1-10}-GFP was found in the ER-perinuclear membrane and cortical ER in *sec12-4* mutant cells and the wild-type (YPM30) cells at 25°C (Figure 55). 30 min after the *sec12-4* cells were transferred to 37°C, fluorescence was detected in the ER-perinuclear membrane, but not in the cortical ER (panel 1). The different signal shown in panel 2 might result from a

difference in focal planes or correspond to asymmetry in the localization in the nuclear membrane.

In conclusion, the results of the fluorescence microscopy analysis indicate that the loss of Sec12p had an effect on the subcellular localization of $Pdr5^{TM1\text{-}10}$ even though the truncated form is located in the ER. This result suggests that $Pdr5^{TM1\text{-}10}$ transit via the early secretory pathway to reach the vacuole for its degradation.

10. Response of the UPR pathway to the expression of Pdr5p variants

The ERAD pathway is sufficient to degrade misfolded or unfolded proteins under normal growth conditions. Under stress conditions, accumulation of unfolded proteins in the lumen of the ER induces a signaling pathway called UPR, which increases the ER folding capacity. To determine whether the mutated and truncated forms of Pdr5p induces the UPR pathway, we used the reporter pUPRLacZ plasmid. This plasmid contains the *E. coli lacZ* region coding for β-galactosidase which has been cloned under the control of a minimal promoter region from the *PNC1* (nicotinamidase) gene fused to the unfolded response element (UPRE) from the *KAR2* promoter region. The suitability of the $P_{UPRE::PNC1}$::*lacZ* gene fusion to measure transcriptional activation of the UPR pathway was confirmed by incubating the *PDR1 pdr5Δ* (FYMK1/1) and the *PDR1-3 pdr5Δ* (FYM26/8-5077) strains in the presence of tunicamycin, an inhibitor of N-glycosylation (Travers et al. 2000), known to induce the accumulation of misfolded proteins. The *PDR1-3* strain was used to observe the effect of *PDR1-3* mutation on the UPR pathway. It has been shown that the presence of the *PDR1-3* stimulates the expression of proteasomal subunits (Owsianik et al. 2002) and phospholipids biosynthesis genes (Chang et al. 2002), which may protect the cells from an accumulation of unfolded proteins.

As shown in Figure 56, the incubation of *pdr5Δ* cells containing *PDR1* or *PDR1-3* in the presence of tunicamycin result in a ≈ 30-fold increase in β-

galactosidase activity (≃ 79 and 72 nmol.min^{-1}.mg^{-1}), compared to untreated cells (≃ 2,5 nmol.min^{-1}.mg^{-1}).

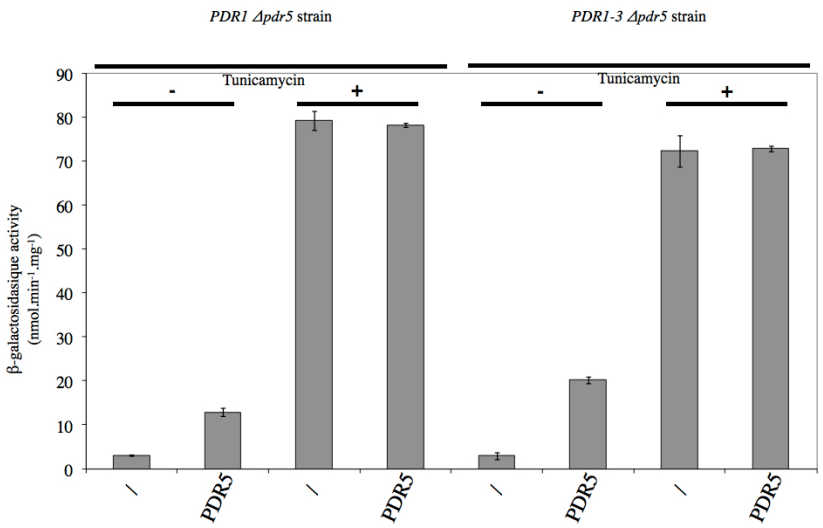

Figure 56. Tunicamycin-mediated induction of the UPR pathway. The *PDR1 pdr5Δ* (FYMK1/1) and *PDR1-3 pdr5Δ* (FYMK26/8-5077) strains were transformed with pUPRLACZ and a plasmid containing or lacking *PDR5*. Appropriate transformants were incubated at 28°C for 6h in the presence (+) or absence (-) of 1 µg/mL of tunicamycin before whole-cell extracts were prepared and β-galactosidase activity measured. Values of β-galactosidasic activity (nmol.min^{-1}.mg^{-1}) are means +/- standard deviation obtained with 4 whole-cell extracts prepared from different clones.

We introduced a high copy *PDR5* plasmid in these strains to determine whether overexpression of Pdr5p induces the UPR. As shown in Figure 56, levels of β-galactosidase activity increased to ≃ 12 nmol.min^{-1}.mg^{-1} in *PDR1 pdr5Δ* cells to ≃ 20 nmol.min^{-1}.mg^{-1} in *PDR1-3 pdr5Δ* cells. The Pdr5 overexpression induces the UPR although the levels seen are lower than those seen in the presence of tunicamycin (≃ 72-78 nmol.min^{-1}.mg^{-1}). The

overexpression of *PDR5* indirectly activates the UPR as the increase in the amount of the long-lived membrane protein may result in a protein trafficking jam in the secretory pathway, therefore increasing the ER load. Note that in the presence of tunicamycin, a slight reduction of UPR response for Pdr5p was observed in the *PDR1-3* strain compared to the *PDR1* strain.

Plasmids expressing the mutated and the truncated forms of Pdr5p were introduced in the *PDR1 pdr5Δ* and *PDR1-3 pdr5Δ* strains. Whole-cells extracts were prepared from appropriate transformants and β-galactosidase activity measured.

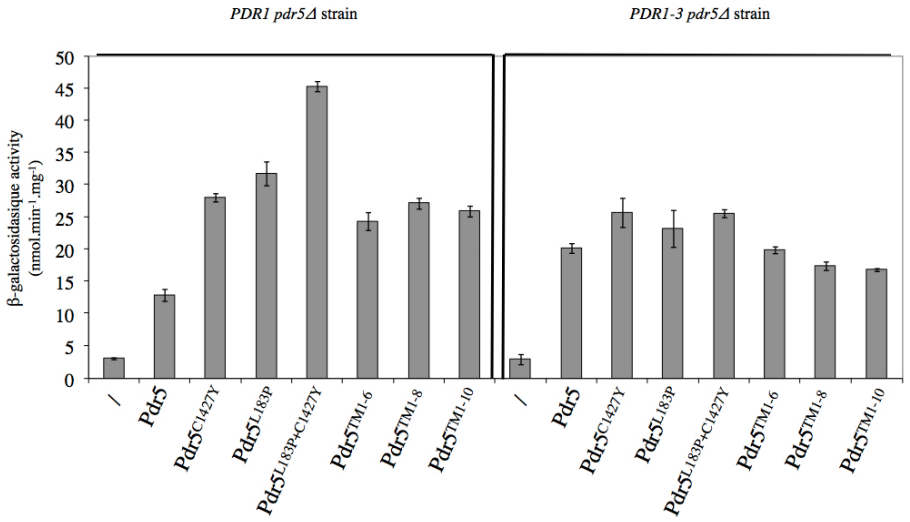

Figure 57. Stimulation of the UPR pathway by mutated and truncated forms of Pdr5p. The *PDR1 pdr5Δ* (FYMK1/1) **(A)** and *PDR1-3 pdr5Δ* (FYMK26/8-5077) **(B)** strains were transformed with pUPRLACZ and plasmids expressing the indicated mutated forms of Pdr5p. Whole-cell extracts were prepared and β-galactosidase activity measured. Values of β-galactosidasic activity ($nmol.min^{-1}.mg^{-1}$) are means +/- standard deviation obtained with 4 whole-cell extracts prepared from different clones.

Compared to the wild-type version, Pdr5^{L183P}, Pdr5^{C1427Y} and Pdr5$^{L183P+C1427Y}$ expressed in *PDR1* cells give a 3-4 fold increase in β-galactosidase activity (Figure 57, left panel). The truncated forms, however, give a smaller increase in the levels of β-galactosidase activity (≃ 1.5-fold).

The stimulation of the UPR pathway by Pdr5^{TM1-8} is the only evidence for a folding or a trafficking default for this stable variant. We easily understand that the misfolded luminal domain of Pdr5^{C1427Y} and Pdr5$^{L183P+C1427Y}$ triggers the UPR pathway through the binding of Kar2p. It is much harder to understand how the misfolded cytosolic domain of Pdr5^{L183P} induces the UPR pathway. As Kar2p and Ire1p are not required for the degradation of Pdr5^{C1427Y} (Plemper et al. 1998) and Pdr5^{L183P} (de Thozee et al. 2007) respectively, the simplest explanation for the UPR induction is an indirect effect. The expression of the mutated Pdr5 forms may saturate the ERAD and/or secretory pathways, resulting in decreased degradation of misfolded secretory proteins and increased ER stress loading. This hypothesis could explain the fact that Pdr5$^{L183P+C1427Y}$ gives a ≃ 1.5-fold increase in β-galactosidase activity in *PDR1* cells compared to Pdr5^{L183P} and Pdr5^{C1427Y} as the presence of both mutations could have a combinaison of direct and indirect effects on the UPR stimulation.

Expression of the Pdr5 variants results in a smaller UPR induction in the *PDR1-3* strain compared to the *PDR1* strain, the difference being significant for Pdr5$^{L183P+C1427Y}$ (2-fold decrease). The UPR decrease could be explain by the stimulation of the expression of proteasomal subunits (Owsianik et al. 2002) and phospholipids biosynthesis genes (Chang et al. 2002), which may

protect the cells from an accumulation of unfolded proteins as mentioned before.

An other point we want to discuss is the lack of correlation between the UPR activation and the formation of intracellular vesicles/ERACs. $Pdr5^{L183P}$, $Pdr5^{L183P+C1427Y}$ and $Pdr5^{TM1-6}$ accumulate in intracellular structures believed to correspond to ERACs, on the basis of studies showing similar topology in cells expressing mutated Ste6 (Huyer et al. 2004a) and heterologously-expressed CFTR (Kiser et al. 2001). These intracellular vesicles/ERACs are not seen in cells expressing $Pdr5^{C1427Y}$, $Pdr5^{TM1-8}$ and $Pdr5^{TM1-10}$ despite the UPR induction. The lack of correlation between the UPR pathway and ERACs has previously been reported in studies analysing various Ste6 mutated versions (Huyer et al. 2004a).

Discussion and perspectives

The main objective of the doctoral work was to ascertain the veracity of the widely accepted ERAD model featuring how misfolded membrane proteins are targeted for degradation by the proteasome. Depending of the localization of the mutated domain in the ER lumen or the cytosol, misfolded proteins are degraded via different pathways (Carvalho et al. 2006; Vashist et al. 2001; Vashist and Ng 2004). To ascertain the ERAD model which was established with engineered fusion proteins, we generated three mutated forms of Pdr5p, a well-characterised plasma membrane ABC-transporter protein. Pdr5^{L183P} has a mutation in a cytosolic loop, Pdr5^{C1427Y} has a mutation in a ER luminal loop and Pdr5$^{L183P+C1427Y}$ contains both mutations. We also generated C-terminally truncated forms of Pdr5p that lack 2-6 TMSs to investigate the presence of specific sequences (degrons) that target the variants for degradation by the proteasome, via the ERAD pathway, and not for vacuolar degradation. According to the current ERAD model, Pdr5^{L183P} is predicted to be ubiquitylated by the ER Ub-ligase Doa10p and transported back to the proteasome in a Der1p- and Sec61p-independent process (ERAD-C pathway). In contrast, Pdr5^{C1427Y} is predicted to be ubiquitylated by Hrd1p and the degradation requires Der1p and/or Sec61p (ERAD-L pathway). As the ERAD-C pathway predominates the ERAD-L pathway, Pdr5$^{L183P+C1427Y}$ is predicted to be addressed to the ERAD-C pathway for proteasome-mediated degradation. Here we show that Pdr5^{L183P}, Pdr5^{C1427Y} and Pdr5$^{L183P+C1427Y}$ are stabilized in mutant strains impaired in Doa10p or Hrd1p. This result indicates a cooperation between ER Ub-ligases. Therefore, the conclusions drawn from studies on engineered modular proteins cannot be generalized to a yeast endogenous ERAD substrate.

We start the discussion by summarizing the results we obtained with the truncated variants as they might be explained by the current ERAD model.

1. Degradation of Pdr5^{TM1-6}

The only substrate that fits the ERAD model is Pdr5^{TM1-6} which is degraded through the ERAD-C pathway (Doa10p).

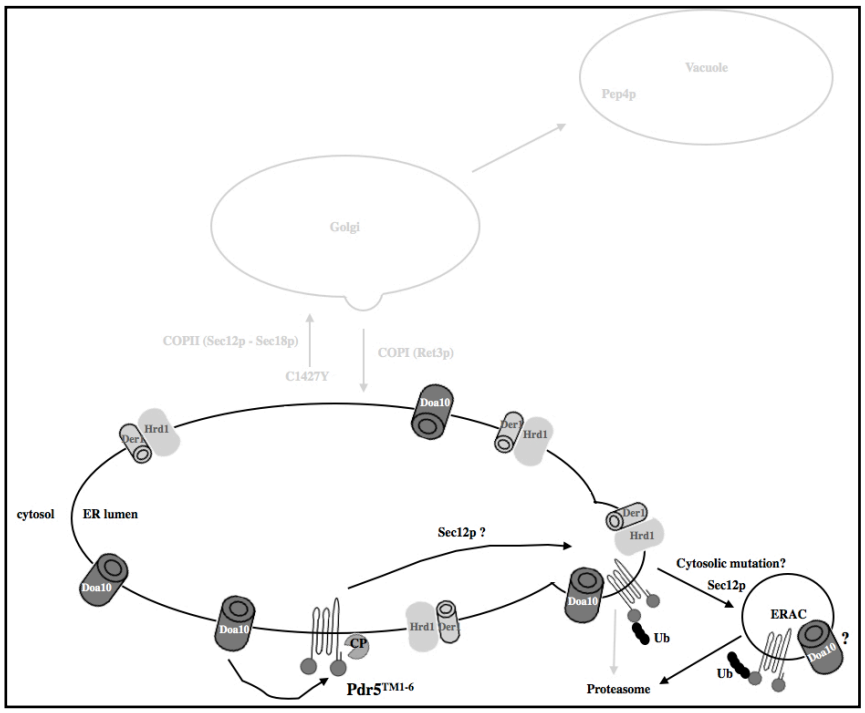

Figure 1. ERAD of Pdr5^{TM1-6}. The proteins and subcellular compartments responsible for degradation are in dark grey. Ubiquitylation of Pdr5^{TM1-6} is mediated by Doa10p only. The ubiquitylated ABC-transporter protein is delivered to specific ER subcompartments in a Sec12p-dependent manner. It is not known whether intracellular vesicles form a plate-form for the 26S proteasome or a last-chance compartment where misfolded proteins are sorted out the secretory pathway and the Ub-proteasome system and are given more trials for proper folding. The identity of the chaperone proteins (CP) involved remains to be determined. Ub, ubiquitin.

In the scheme shown in Figure 1, the misfolded variant is recognized by cytosolic chaperones, the nature of which remains to be determined, and addressed to Doa10p for ubiquitylation, probably through interaction between the Ub-ligase and the protein chaperones.

A second possibility is the binding of Doa10p to the C-terminal NBD2 of Pdr5^{TM1-6}, which is no more anchored to the membrane and is freely accessible (Figure 2). The multiple TMSs of Doa10p may constitute a channel (Kreft et al. 2006; Swanson et al. 2001) through which Pdr5^{TM1-6} is removed from the ER membrane by the Cdc48p-Ufd1p-Npl4p complex (not shown in Figures 1 and 2).

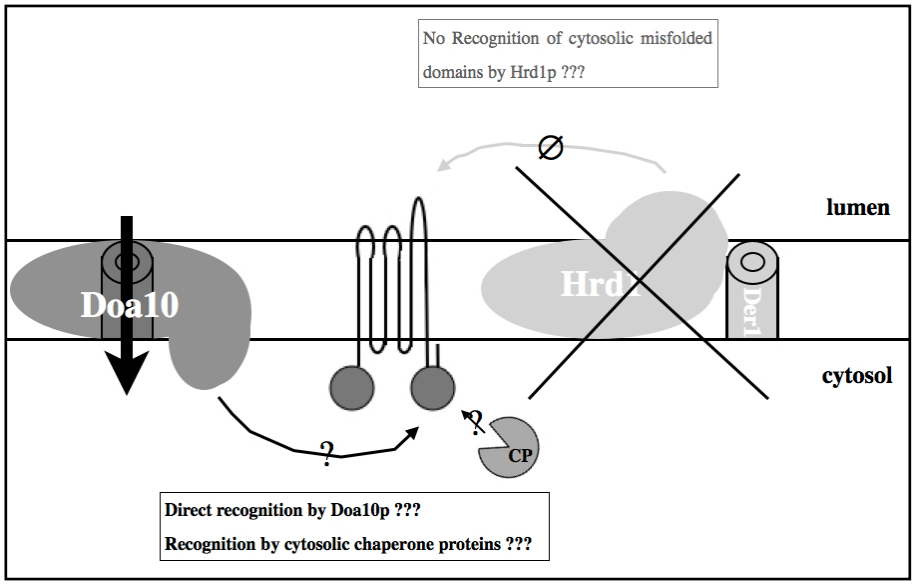

Figure 2. Mechanisms responsible for the recognition of Pdr5^{TM1-6} by Doa10p. The NBD2 domain of Pdr5^{TM1-6} may bind directly to cytosolic chaperones that interact with Doa10p. It is also possible that NBD2 binds directly to a region of Doa10p that protrudes into the cytosol. Hrd1p might lack such a protruding recognition site, explaining why the Ub-ligase is not active on Pdr5^{TM1-6}.

Pdr5^{TM1-6} degradation is dependent of Sec12p, but not of Sec18p or Ret3p. This result indicates that the function of Sec12p in the ERAD pathway is independent of its function in ER-to-Golgi transport. Pdr5^{TM1-6} contains the ERE motif at position 1163, which resembles the di-acidic (D/E-x-D/E) motif recognized by the COPII coat components. Therefore the lack of stabilizing effect of the *sec18* mutation is not explained by impaired ER-to-Golgi transport of Pdr5^{TM1-6}.

A study on heterologously expressed CFTR has shown that COPII machinery components Sec12p, Sec23p and Sec13p are implicated in the sequestration and degradation of the mammalian ABC-transporter (Fu and Sztul 2003). As CFTR is stabilized in a *sec12* mutant strain, but not in a *sec18* mutant strain, Fu and Sztul (2003) made the proposition that the COPII machinery plays a specific role in the ERAD pathway, in addition to the well-characterized function in the early secretory pathway and ER-to-Golgi transport. The molecular mechanisms underlying the new function of Sec12p remains to be determined.

The proposition made by Fu and Sztul (2003) is supported by our results on Pdr5^{TM1-6}. As Pdr5^{TM1-6} variant accumulates in ER and intracellular vesicles and is stabilized in a *sec12* mutant strain, but not in a *sec18* mutant strain, a specific role of COPII machinery to reach the ER subcompartments is plausible.

Note that the distribution of Pdr5^{TM1-6} seems to combine those seen with Pdr5^{L183P} (or Pdr5$^{L183P+C1427Y}$) and Pdr5^{TM1-8} (or Pdr5^{TM1-10}).

Formation of intracellular vesicles (ERACs) could be a «characteristic» of misfolded proteins with a cytosolic mutation as ERACs were seen for

$Pdr5^{TM1-6}$, $Pdr5^{L183P}$ and $Pdr5^{L183P+C1427Y}$ (this work; de Thozee et al. 2007) in addition to Ste6* and Pma1-D378N (de Kerchove d'Exaerde et al. 1995; Harris et al. 1994; Huyer et al. 2004a; Loayza et al. 1998; Supply et al. 1993; Wright et al. 1988).

Further truncations of $Pdr5^{TM1-6}$ that lack 82 ($Pdr5^{1157}$) and 196 ($Pdr5^{1043}$) residues from the C-terminus result in long-lived variants located in the ER ($t_{1/2}$ of 120 min (extrapolation) and 50 min respectively; de Thozee et al. 2007). In comparison the half-life of $Pdr5^{TM1-6}$ is 9 ± 3 min. Western blot analysis showed that, unlike $Pdr5^{TM1-6}$, the shortest variants are detected in exponentially growing cells. If differences in the strains and expression system used are not considered, we can predict the presence of a degron in the region consisting of residues 1157-1239. It is possible that $Pdr5^{1157}$ and $Pdr5^{1043}$ are not recognized as misfolded proteins and could simply lack a ER export signal that was removed by deletion.

2. Degradation of $Pdr5^{TM1-8}$

The fusion of TMS7 and TMS8 to the C-terminus of $Pdr5^{TM1-6}$ leads to the stabilization of the ABC-transporter. One possibility is that the resulting $Pdr5^{TM1-8}$ variant is properly folded. Another possibility is that $Pdr5^{TM1-8}$ is a misfolded variant, yet the degron present in $Pdr5^{TM1-6}$ is masked by TMS7 and TMS8 and no more accessible to Doa10p. Fluorescence microscopy analysis shows that $Pdr5^{TM1-8}$ is localized in the ER-perinuclear envelope and cortical ER. The failure of $Pdr5^{TM1-8}$ to reach the plasma membrane can

be explained by the deletion of a C-terminal addressing signal that acts downstream of the step requiring Sec12p as the signal is different from that seen in *sec12* mutant cells expressing Pdr5p at 37°C. Pdr5^{TM1-8} was found in a punctuated structure in the *sec12* cells at 37°C. On the other hand, Pdr5^{TM1-8} may get stuck in the ER due to the activation of the quality control system on the basis of the stimulation of the UPR.

3. Degradation of Pdr5^{TM1-10}

The fusion of TMS9 and TMS10 to the C-terminus of Pdr5^{TM1-8} results in instability of the resulting variant (Figure 3). The most likely explanation for this result is the presence of an additional degron in the region consisting of residues 1317-1375. Another possibility is that the degron present in Pdr5^{TM1-6} is unmasked in Pdr5^{TM1-10}. This second possibility seems unlikely as Hrd1p, in addition to Doa10p, is involved in the degradation of Pdr5^{TM1-10}.

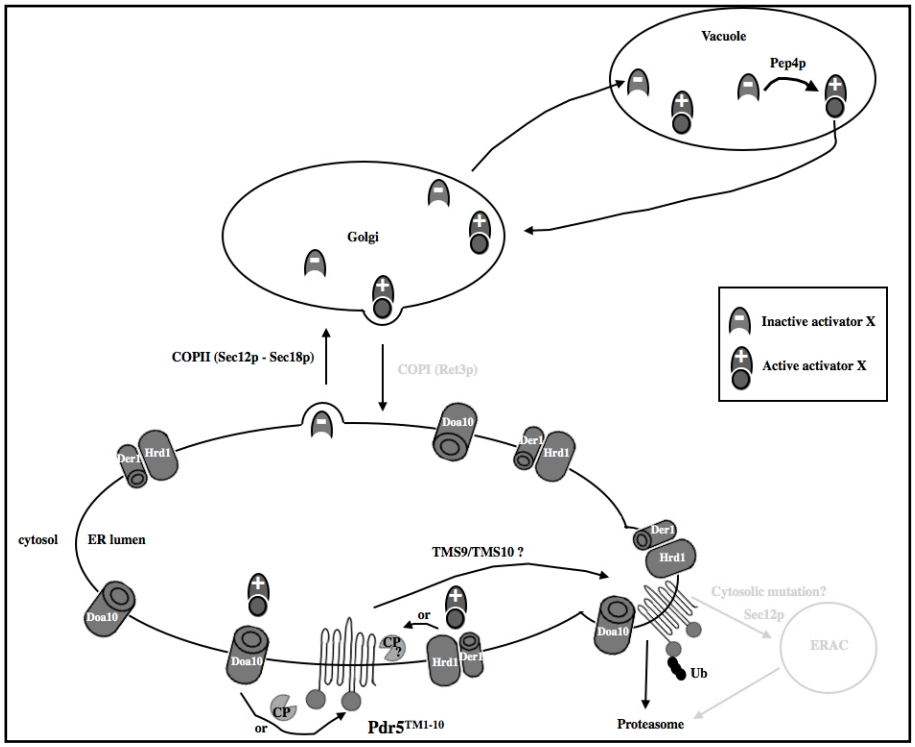

Figure 3. Degradation of Pdr5^{TM1-10} requires proteolytic components of the ER and vacuole. The proteins and subcellular compartments responsible for degradation are in dark grey. The truncated form is stabilized by mutations impairing vacuolar proteases (*pep4*) and early secretory pathway (*sec12*, *sec18*). Proteasome-mediated degradation requires Doa10p or Hrd1p, but not Der1p. Expression of Pdr5^{TM1-10} does not result in the formation of ERACs. Also shown is a hypothetical Ub-ligase activator X, the activity of which requires Pep4p. The identity of the chaperone proteins (CP) involved remains to be determined.

In the simple model shown in Figure 4, Doa10p binds to the degron present in Pdr5^{TM1-6} and/or to a new degron present in the residues 1317-1375, whereas Hrd1p (or luminal chaperones and other subunits of the Hrd1p complex) binds to the misfolded luminal loop connecting TMS9 to TMS10 or to the second truncated TMD. Arteaga et al. (2006) showed that, in mammals, degradation of Serum-and-glucocorticoid-induced kinase 1 (Sgk1) containing a cytosolic hydrophobic motif was mediated by Hrd1p. Therefore, Hrd1p may recognize a cytoplasmic misfolded region at least in mammals. Such an evidence is missing in yeast.

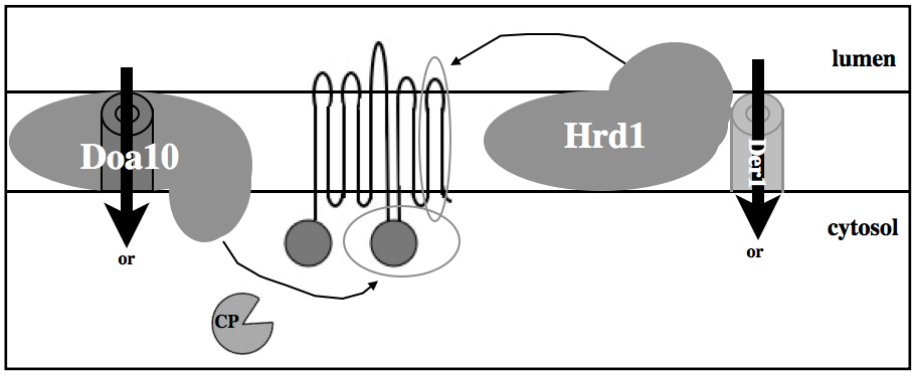

Figure 4. Degradation signals of Pdr5^{TM1-10}. Doa10p and/or cytosolic chaperone proteins could recognize a degron in Pdr5^{TM1-10}. Hrd1p could bind to misfolded luminal loop connecting TMS9 to TMS10 or to the second truncated TMD. CP, chaperone proteins.

Der1p is not required for the degradation of Pdr5^{TM1-10}, so the retro-translocon function could be fulfilled by Doa10p. This hypothesis can be easily tested by analysing the effect of the *DER1* deletion in a strain lacking Doa10p. A stabilization of Pdr5^{TM1-10} in a *der1Δ doa10Δ* mutant strain

would confirm that the mutated form of Pdr5p is retro-translocated through Der1p, in the absence of Doa10p.

Decreased turnover of Pdr5^{TM1-10} in cells deleted for the *PEP4* gene indicates that this variant might be targeted to the vacuole for degradation. To our knowledge, this would be the first example of a membrane protein that requires the proteasome and the vacuole for elimination. Pdr5^{TM1-10} stabilization in cells deleted for Doa10p and Hrd1p does not support a direct role of the vacuole proteases except if the delivery of Pdr5^{TM1-10} to the vacuole is impaired by the Ub ligases loss. However, ER loading stress conditions have been shown to induce the UPR, which in turn activates ER-to-vacuole transport and vacuolar degradation of CPY* (Spear and Ng 2003). Therefore our results could be more easily explained by an indirect effect of the *PEP4* deletion on the secretory pathway or by the requirement of a factor, the function of which is impaired in *pep4*Δ cells (Figure 3). The first explanation assumes that the loss of Pep4p, through accumulation of cargo proteins in the ER and Golgi apparatus, induces the UPR pathway. Pdr5^{TM1-10} is delivered more rapidly to the COPII vesicles and therefore escapes ERADication. The first explanation is not plausible as the UPR pathway is induced with all mutated/truncated variants and only Pdr5^{TM1-10} shows a decrease turnover in *pep4Δ* cells. The second explanation assumes a hypothetical activator of Doa10p or Hrd1p, which is no longer active or available in cells lacking Pep4p, either the activation of factor X requires some proteolytic maturation or the availability of factor X is reduced due to the increased activity of ER-to-Golgi transport.

4. Degradation of Pdr5$^{L183P+C1427Y}$

Pdr5$^{L183P+C1427Y}$ variant, with luminal and cytosolic mutations, is targeted for proteasomal degradation via the ERAD-L and –C pathways in contradiction with the ERAD model that predicts the predominance of the ERAD-C pathway over the ERAD-L pathway. In a striking contrast to the truncated Pdr5^{TM1-10} variant, neither Doa10p nor Hrd1p is dispensable as the loss of one Ub-ligase impairs the function of the other. Interestingly, Pdr5$^{L183P+C1427Y}$ accumulates in ERACs and the degradation requires Der1p. This result argues against the hypothesis of a single retrograde channel and agrees well with recent data that more than one protein may claim the responsibility of the transport to the cytoplasm. The results can be explained if we assume that the full-length ABC-transporter is too large or contains too many TMSs to be efficiently retro-translocated through the channel formed by Doa10p. However, the lesion site and the folding defect could be a determinant point for the channel choice. The requirement for Der1p also explains the stabilizing effect of the *HRD1* deletion alone, for we can easily imagine that the loss of Hrd1p impairs the function or membrane orientation of the retro-translocon (Figure 5). The stabilizing effect of the *DOA10* deletion alone is more difficult to explain, especially in regard to Pdr5^{TM1-10}, although this effect is in a good agreement with the study on a chimerical form of Ste6p with misfolded domains on both sides of the ER membrane (KSS in Figure 11 of Introduction) (Vashist and Ng 2004).

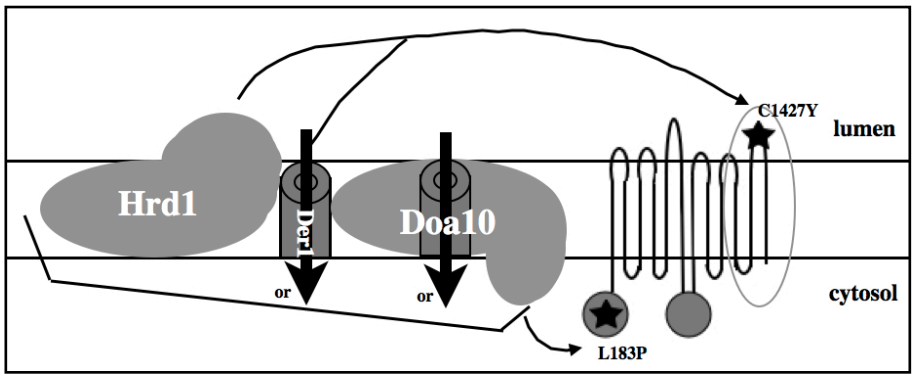

Figure 5. Degradation of Pdr5$^{L183P+C1427Y}$ is impaired by the loss of either Hrd1p or Doa10p. Neither Ub-ligases are dispensable, indicating that they are not interchangeable. The size and the number of TMSs of the full-length ABC transporter, the magnitude of the folding defects caused by the L183P and C1427Y substitutions or the domain accessibility to components of each machinery may explained the difference in the ways that the ERAD-L and ERAD-C pathways cooperate for degradation of Pdr5$^{L183P+C1427Y}$.

5. Degradation of Pdr5^{L183P} and Pdr5^{C1427Y}

In a striking contrast to the predictions based on the current ERAD model, neither Doa10p nor Hrd1p is dispensable for the degradation of Pdr5^{L183P} and Pdr5^{C1427Y}. Thus both Ub-ligases are required for the degradation of a membrane protein with a misfolded cytosolic domain and both Ub-ligases mediate ubiquitylation of a membrane proteins with a misfolded luminal domain. The same conclusion can be drawn from the works of Huyer et al. (2004a) and Nakatsukasa et al. (2008), showing partial stabilization of Ste6-Q-1249-X in cells lacking Doa10p, and complete stabilization in cells lacking Doa10p and Hrd1p.

We cannot ruled out the possibility that the L183P substitution influences the correct folding of the TMDs, thereby activating the Hrd1p complex and, reciprocally, that the mutation of the cysteine residue at position 1427 impairs the insertion of the last TMS inside the ER membrane and the correct orientation of the C-terminus, thereby activating Doa10p.

An other possibility based on the study of Arteaga et al. (2006) suggest that Hrd1 complex may recognize a cytosolic misfolded region.

A more likely possibility is the recognition of the misfolded Pdr5^{L183P} form by cytosolic components of the quality control system preventing glycosylation (still a matter of controversy) and therefore activating the ERAD-L pathway, via the lectin-like protein Yos9p. This possibility could be tested by analysing the effect of a *KAR2* deletion on the degradation of Pdr5^{L183P} even though this deletion has no effect on Pdr5^{C1427Y} degradation (Plemper et al. 1998). Note that Plemper et al. (1998) showed that Der1p was not implicated in the degradation of Pdr5^{C1427Y}, in contrast to our results.

6. Protein sorting according to misfolded domain location

Pulse-chase analysis showed that all the mutated Pdr5p forms generated in this work are stabilized by the inactivation of Sec12p. The role of this small GTPase in the ERAD pathway has been discussed for $Pdr5^{TM1-6}$. Then we investigated the implication of ER-to-Golgi transport by analysing the effect of the inactivation of Sec18p on the degradation of the Pdr5p variants and found that $Pdr5^{C1427Y}$ and $Pdr5^{L183P+C1427Y}$ were stabilized, whereas $Pdr5^{L183P}$ was not. $Pdr5^{TM1-10}$ is not considered as the stabilizing effect of the *sec12* mutation may be linked to the effect of the *pep4* mutation.

The results for $Pdr5^{C1427Y}$ and $Pdr5^{L183P}$ fit the current ERAD model. $Pdr5^{C1427Y}$ with a misfolded luminal domain requires ER-to-Golgi transport (an hallmark of the ERAD-L pathway), whereas $Pdr5^{L183P}$ with a cytosolic misfolded domain does not (Figure 6).

The results for $Pdr5^{L183P+C1427Y}$ are different from those expected, it shows a requirement of ER-to-Golgi transport although the ERAD model says that it should show the characteristics of an ERAD-C substrate since the ERAD-C checkpoint precedes the ERAD-L checkpoint (Figure 6).

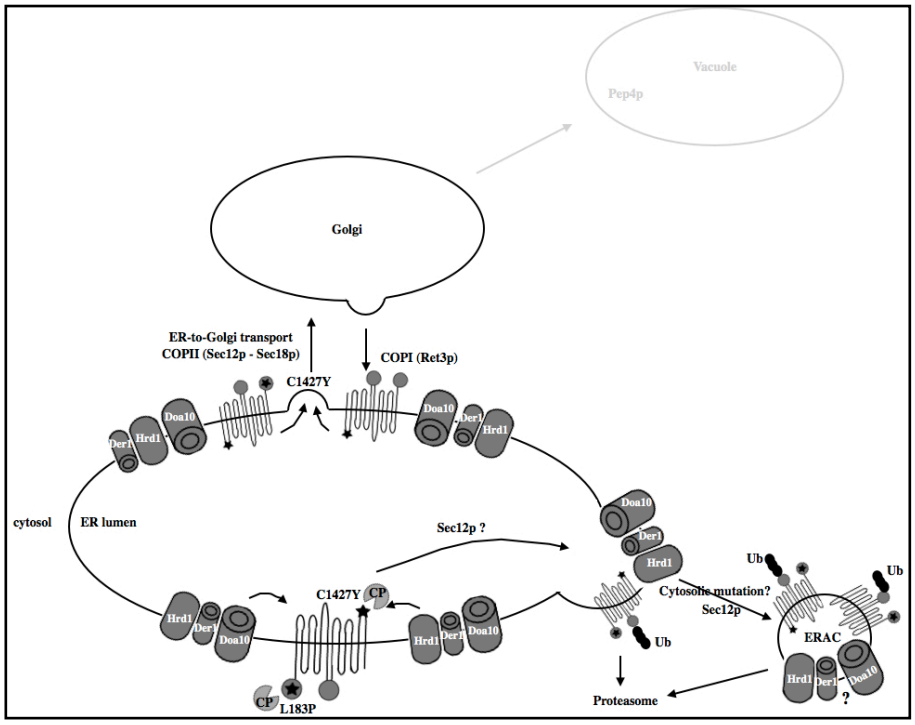

Figure 6. Distinct ER protein sorting mechanisms according to localization of the misfolded domain. The proteins and subcellular compartments responsible for degradation are in dark grey. Doa10p and Hrd1p target Pdr5^{L183P}, Pdr5^{C1427Y} and Pdr5$^{L183P+C1427Y}$ for proteasome-dependent degradation. The reason why ER-to-Golgi transport is required for the degradation of Pdr5^{C1427Y} and Pdr5$^{L183P+C1427Y}$ is unknown. A simple explanation is the requirement for Golgi chaperones that help to unfold ERAD-L substrates before proteasomal degradation. Pdr5^{L183P} and Pdr5$^{L183P+C1427Y}$ are delivered to the ERACs, via the ERAD-C pathway. ERACs may concentrate ER chaperones (Kar2p) that help to unfold ERAD-C substrates, in collaboration with the cytosolic chaperones. The identity of the chaperone proteins (CP) involved remains to be determined. Ub, ubiquitin.

Figure 7 summarizes the results reported here and the study by de Thozee et al. (2007).

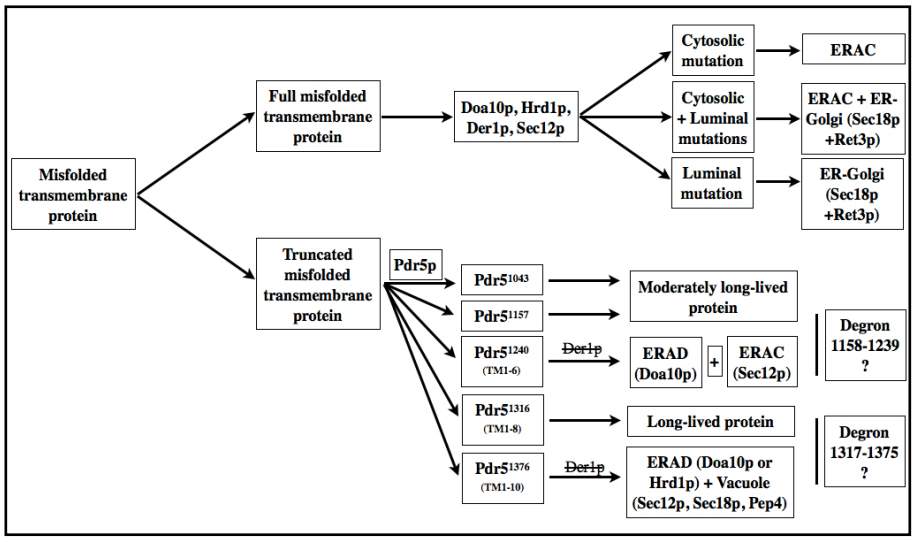

Figure 7. Degradation of mutated and truncated forms of Pdr5p. Full-length Pdr5p with a misfolded domain requires Doa10p, Hrd1p, Der1p and Sec12p for degradation, independently of the localization of the misfolded domain. A cytosolic mutation predominates a luminal mutation with respect to the ER subcompartment accumulating the Pdr5p variant. Mutated forms with a luminal misfolded domain requires ER-to-Golgi transport (Sec18p) and a luminal mutation was found to be dominant over a cytosolic mutation. Analysis of the truncated forms led to the identification of C-terminal degrons. $Pdr5^{TM1\text{-}6}$ is the only variant not requiring Hrd1p. Der1p does not seem to be required for the retro-translocation of the truncated proteins as it could be substituted by Doa10p.

7. Perspectives

A recent study using a real-time imaging approach and heterolously-expressed CFTR as an ERAD substrate has shown that ERACs co-localize with a pre-autophagosomal marker and are temporally and spatially adjacent to the vacuolar compartment (Fu and Sztul 2009). These results indicate that the proteasomal and autophagic pathways function together to eliminate the proteins which are misfolded. It would be interesting to analyze the effects of *atg1* or *atg6* mutations impairing autophagy on the degradation of the Pdr5p variants which induce the formation of ERACs.

Western blot analysis of whole-cell extracts fractionated by sucrose gradient centrifugation is required to show the plasma membrane localization of Pdr5^{TM1-8}. The same strategy would be useful to determine unambiguously the localization of the other Pdr5p variants (Golgi, ER or vacuole) using whole-cell extracts prepared from a *doa10*Δ *hrd1*Δ strain.
Anti-Kar2p antibodies could be used to confirm that ERACs and other internal compartments accumulating Pdr5^{TM1-6} are derived from the ER.

Western blot and pulse-chase analysis of the various GFP fusions constructed in this work will enable us to determine whether the protein fusions behave like the mutated Pdr5p forms.

The biochemical characterization requires purification of the mutated Pdr5p forms and therefore their stabilization in mutant strains impaired in the *doa10Δ hrd1Δ* strain. It would also be also interesting to determine whether

the L183P and C1427Y mutations modify protein folding, through analysis of protein's susceptibility to trypsin cleavage.

We do not know whether Pdr5^{TM1-10} reaches the plasma membrane where it is redirected to the vacuole, as shown for the wild-type version (Egner and Kuchler 1996), or whether Pdr5^{TM1-10} is sorted out of the Golgi apparatus and transported directly to the vacuole. To determine which pathway is used by the truncated variant, the GFP protein version should be observed in mutant strains impaired in endocytosis or ALP and CPY pathways. Pulse-chase analysis should also be carry out using these mutant strains.

To understand the regulator mechanism underlaying Pdr5^{TM1-10} degradation, it will be interesting to carry out pulse-chase analysis of the truncated variant in *pep4Δ hrd1Δ* and *pep4Δ doa10Δ* strains.

Pdr5^{TM1-6} degradation is independent of the retro-translocon, Der1p, suggesting that Pdr5^{TM1-6} is transported to the cytosol through a channel formed by Doa10p or the Sec61p translocon. A *sec61-3* mutant strain which has no effect on translocation could be used to test the role of Sec61p in retro-translocation of Pdr5^{TM1-6}. The *sec61-3* mutant strain could be used to analyze the degradation of mutated Pdr5 forms to establish a correlation between the position of the mutated residue, domain misfolded and the channel used.

It would be interesting to determine the minimal region of Doa10 which is involved in the recognition and /or the ubiquitylation of Pdr5^{TM1-6}. We could

generate progressive deletions of Doa10p or used a strategy based on domain swapping between Doa10p and Hrd1p.

It will be interesting to investigate the role of Hrd1p on truncated proteins lacking 1, 3 or 5 TMSs degradation to establish an ERAD model for truncated proteins.

Mutations in the ERE motif at position 1163 which resembles the di-acidic (D/E-x-D/E) motif recognized by the COPII coat components could be done to investigate the role of this motif in ER-to-Golgi transport.

Additional pulse-chase analysis are required to determine the role of the quality control system in the degradation of the various Pdr5p variants and to identify the chaperone proteins involved. We should also assess the role of other ERAD components, including the ER E2s (Ubc1p, Ubc6p, Ubc7p), the proteasome (subunit Cim3p), the translocon Sec61p subunit, Cdc48p and Usa1p (a protein of the Hrd1p complex).

Material and Methods

1. Strains and media

1.1. *Escherichia coli*

Escherichia coli DH5α strain (F^-, 80d*lacZΔM15* Δ(*lacZYA-argF*) U169, *rec*A1, *end*A1, *gyr*A96, *thi*-1, *hsd*R17(r_{K^-}, m_{K^-}), *sup*E44, *rel*A1, *deo*R) was used for plasmid maintenance and amplification during the various cloning and sequencing steps. Bacteria were cultured at 37 °C in Luria-Bertani (LB) medium (1% (w/v) bactotryptone, 0.5% (w/v) yeast extract and 1% (w/v) NaCl) supplemented with 150 μg/mL ampicilin (Roche) for selection of plasmids containing the β-lactamase gene (bla) confering ampicillin resistance. Ampicillin is an inhibitor of transpeptidase, which is required for bacterial cell wall. Solid media were supplemented with 2% (w/v) Bacto agar.

1.2. *Saccharomyces cerevisiae*

Saccharomyces cerevisiae strains used in this study are listed in Table 1. Yeast transformation was performed by using the lithium acetate method as described by Chen et al. (1992) (ONE STEP buffer: Li Ac 0.2 M, PEG (3500) 40%, DTT 100 mM).

Table 1 : *Saccharomyces cerevisiae* strains used in this study.

Strain	Genotype	Source
BY4742	*MATα his3Δ1 leu2Δ0 lys2Δ0 ura3Δ0*	Euroscarf

Strain	Genotype	Source
Y12409	BY4742 *MATα his3Δ1 leu2Δ0 lys2Δ0 ura3Δ0 pdr5Δ::KANMX4*	Euroscarf
Y17299	BY4742 *MATα his3Δ1 leu2Δ0 lys2Δ0 ura3Δ0 doa10Δ::KANMX4*	Euroscarf
Y11704	BY4742 *MATα his3Δ1 leu2Δ0 lys2Δ0 ura3Δ0 hrd1Δ::KANMX4*	Euroscarf
YBR201w	*BY4742 MAT α his3Δ1 leu2Δ0 lys2Δ0 ura3Δ0 YBR201w::kanMX4 (YBR201 = der1 gene)*	Euroscarf
YPL154c	*BY4742 MATα his3Δ1 leu2Δ0 lys2Δ0 ura3Δ0 YPL154c::kanMX4 (YPL154 = pep4 gene)*	Euroscarf
YPM30	*MATa his4 leu2 ura3 lys2 bar1*	Morsomme Pierre
YPM366	*MATa leu2 ura3 his4 bar1 sec18-1*	Morsomme Pierre
RHY1491	*MATa his4 ura3 leu2 lys2 bar1 sec12-4*	Funato and Riezman, 2001
FLY89	*MATa his3 ura3 leu2 trp1 ret3-1 suc2-Δ9*	Morsomme Pierre
FY1679-28C	*MATa his3 ura3 leu2 trp1*	Wilson *et al*., 1996
FYMK1/1	*MATa his3 ura3 leu2 trp1 pdr5Δ1::hisG*	Kolaczkowski *et al*., 1996
FYM26/8-5C	*MATa his3 ura3 leu2 trp1 pdr1-3*	Pety de Thozée *et al*., 2007
FYMK26/8-5077	*MATa his3 ura3 leu2 trp1 pdr5Δ1::hisG pdr1-3*	Pety de Thozée *et al*., 2007
MHY500	*MATa his3Δ200 leu2-3,112 ura3-52 lys2-801 trp1-1 gal2*	Hochstrasser, M. (Yale University, USA)
MHY501	*MATα his3Δ200 leu2-3,112 ura3-52 lys2-801 trp1-1 gal2*	Hochstrasser, M. (Yale University, USA)

Strain	Genotype	Source
MHY1631	*MATa his3Δ200 leu2-3,112 ura3-52 lys2-801 trp1-1 doa10-Δ1::HIS3*	Hochstrasser, M. (Yale University, USA)
MHY1669	*MATa his3Δ200 leu2-3,112 ura3-52 lys2-801 trp1-1 hrd1Δ::LEU2*	Hochstrasser, M. (Yale University, USA)
MHY1703	*MATa his3Δ200 leu2-3,112 ura3-52 lys2-801 trp1-1 doa10-Δ1::HIS3 hrd1Δ::LEU2*	Hochstrasser, M. (Yale University, USA)

Yeast strains were grown in rich YD medium containing 2% (w/v) Bacto-yeast extract and 2% (w/v) glucose or minimal SD medium containing 2% (w/v) glucose and 0.7% (w/v) yeast nitrogen base without amino acids and supplemented with lysine, uracil, leucine, histidine and tryptophan as required. Solid media were supplemented with 2% (w/v) Bacto-agar.

2. DNA constructs and oligonucleotides

Plasmids and oligonucleotides used in this study are listed in Tables 2 and 3. Plasmids pCPX2 and pCP2μU, which respectively contains *PDR5* and *pdr5-107*, were cut with *Mlu*I and *Xho*I and ligated to appropriate PCR DNA fragments to generate plasmids pRS426-pdr5-207 (C1427Y substitution) and pRS426-pdr5-307 (double L183P+C1427Y substitution). To generate these PCR DNA fragments, two PCR reactions were carried out. The first PCR introduced *Mlu*I restriction site at the 5' extremity and the Cys1427Tyr substitution at the 3' end by using the S10 oligonucleotide and the DownMutC1427Y mutagenic primer. The second PCR generated a

DNA fragment containing the Cys1427Tyr substitution at the 5' end and a *Xho*I restriction site at the 3' end by using the UpMutC1427Y mutagenic primer and the DownSpeITerm oligonucleotide. The amplicons were mixed with oligonucleotides S10 and DownSpeITerm to amplify *Mlu*I/*Xho*I fragment containing the engineered mutation. DNA sequencing revealed the absence of undesirable mutations.

Plamids expressing various GFP fusions (pUG35*-PDR5 ; pUG35*-pdr5-107 ; pUG35*-pdr5-207 ; pUG35*-pdr5-307 ; pUG35*-PDR5-1240 ; pUG35*-PDR5-1316 ; pUG35*-PDR5-1376) were constructed by PCR. The GFP proteins were fused to the carboxy-terminus of the mutated/ truncated proteins. A DNA linker was generated by annealing the oligonucleotides Linker Up XhoI and Linker Down XhoI and cutting with *Xba*I and *Spe*I. The resulting DNA fragment was then ligated to *Xba*I/*Spe*I-cut pUG35 plasmid to generate the pUG35* plasmid. Note that a *Kpn*I restriction site was present in the linker for verification of the correct insertion. Also, a *Xho*I site was added to the DNA linker to introduce the *PDR5* gene by PCR amplification. PCR fragments containing the wt or the mutated alleles of *PDR5* were generated using oligonucleotides PDR5 XhoI before Start and PDR5 before STOP SpeI for the full length proteins or oligonucleotides PDR5 XhoI before Start, Pdr5 1240 SpeI, Pdr5 1316 SpeI and Pdr5 1376 SpeI for the truncated variants. The various PCR products were cut with *Xho*I and *Spe*I and ligated to the pUG35* plasmid also cut with *Xho*I and *Spe*I. The resulting plasmids were analysed to check for the absence of undesirable mutations.

Table 2 : Plasmids used in this study.

Plasmid name	Description	Source
pRS426	*URA3*, 2µm, *amp*^{R}, ori	Christianson *et al*., 1992
pCPX2	pRS426::PDR5	Pety de Thozée *et al*., 2007
pCP2µU	pRS426::pdr5-107 (L183P substitution in *PDR5* gene)	Pety de Thozée *et al*., 2007
pUG35	ARS-CEN6, *URA3*, *amp*^{R}, ori, pMET25-yEGFP3	Guldener, U. and Hegermann, J.H.
pRS426-pdr5-207	pRS426::pdr5-207 (C1427Y substitution in *PDR5* gene)	This work
pRS426-pdr5-307	pRS426::pdr5-307 (L183P + C1427Y substitutions in *PDR5* gene)	This work
pRS315-UPRE lacZ	*LEU2*, 2µm, *amp*^{R}, ori, *PNC1* modified (with Kar2-UPRE) - *lacZ*	Pety de Thozée *et al*., 2007
pRS426-PDR5-1240	pRS426::PDR5-1240 (truncated form of *PDR5* gene, minus 6TMSs, Pdr5^{TM1-6})	Roy A., Master thesis work, 2008
pRS426-PDR5-1316	pRS426::PDR5-1316 (truncated form of *PDR5* gene, minus 4 TMSs, Pdr5^{TM1-8})	Roy A., Master thesis work, 2008
pRS426-PDR5-1376	pRS426::PDR5-1376 (truncated form of *PDR5* gene, minus 2 TMSs, Pdr5^{TM1-10})	Roy A., Master thesis work, 2008
pUG35*	ARS-CEN6, *URA3*, *amp*^{R}, ori, pMET25-yEGFP3 + linker with *XhoI* and *KpnI* restriction sites	This work
pUG35*-PDR5	pUG35*::PDR5 (wild-type *PDR5* gene)	This work
pUG35*-pdr5-207	pUG35*::pdr5-207 (C1427Y substitution in *PDR5* gene)	This work
pUG35*-pdr5-107	pUG35*::pdr5-107 (L183P substitution in *PDR5* gene)	This work

Plasmid name	Description	Source
pUG35*-pdr5-307	pUG35*::pdr5-307 (L183P + C1427Y substitutions in *PDR5* gene)	This work
pUG35*-PDR5-1240	pUG35*::PDR5-1240 (truncated form of *PDR5* gene, minus 6TMSs, $Pdr5^{TM1-6}$)	This work
pUG35*-PDR5-1316	pUG35*::PDR5-1316 (truncated form of *PDR5* gene, minus 4TMSs, $Pdr5^{TM1-8}$)	This work
pUG35*-PDR5-1376	pUG35*::PDR5-1376 (truncated form of *PDR5* gene, minus 2TMSs, $Pdr5^{TM1-10}$)	This work

Table 3 : Oligonucleotides used in this study.

Oligos name	Oligos sequence (5'->3')	Used of the primers
Avt Doa10	GCTGTCATCGAGGTTAGAGG	Verification of the *DOA10* gene deletion
Down Doa10	CCATTCTATCATCCATCATG	Verification of the *DOA10* gene deletion
Avt Hrd1	CCCGTAATTCTCCCTGCTCC	Verification of *HRD1* gene deletion
Down Hrd1	GGCTGAGATTGATCAGACTC	Verfication of *HRD1* gene deletion
Avt der1	TACAGCAGAGATTTCGTCAC	Verification of *DER1* gene deletion
Apr der1	ACATTTGAGACAGGTTCTTC	Verification of *DER1* gene deletion
UpMutC1427Y	GGTATGACATATGGGCAGTACATG	Construction of the plasmid pRS426-pdr5-207 ($Pdr5^{C1427Y}$)

Oligos name	Oligos sequence (5'->3')	Used of the primers
DownMutC1427Y	CATGTACTGCCCATATGTCATACCGG	Construction of the plasmid pRS426-pdr5-207 ($Pdr5^{C1427Y}$)
S10	CTTCAAAGCAGGAACCTC	Construction of the plasmids pRS426-pdr5-207 ($Pdr5^{C1427Y}$) and pRS426-pdr5-307 ($Pdr5^{L183P+C1427Y}$)
DownSpeITermi	CCACTAGTAATAAGGCCTATATGAG	Construction of the plasmids pRS426-pdr5-207 (Pdr5C1427Y) and pRS426-pdr5-307 (Pdr5L183P+C1427Y)
PDR5 XbaI before Start	GCTCTAGAAGTCACGCAAAGTTGCAAAC	Construction of the plasmids pUG35-pdr5-207 ($Pdr5^{C1427Y}$) and pUG35-pdr5-307 ($Pdr5^{L183P+C1427Y}$)
PDR5 before STOP SpeI	CTAGACTAGTTTTCTTGGAGAGTTTACC	Construction of the plasmids pUG35*-PDR5, pUG35*-pdr5-207 ($Pdr5^{C1427Y}$), pUG35*-pdr5-107 ($Pdr5^{L183P}$) and pUG35*-pdr5-307 ($Pdr5^{L183P+C1427Y}$)
Pdr5 1240 STOP Sp (6tm)	CTAGACTAGTTTACGAGGTTCCTGCTTTGA	Construction of the plasmid pRS426-PDR5-1240
Pdr5 1316 STOP Sp (8tm)	CTAGACTAGTTTATGCAGACGCGTTGGAGTA	Construction of the plasmid pRS426-PDR5-1316
Pdr5 1376 STOP Sp (10tm)	CTAGACTAGTTTATGGGGTAGTCATAACAC	Construction of the plasmid pRS426-PDR5-1376
Pdr5 1240 SpeI	CTAGACTAGTCGAGGTTCCTGCTTTGA	Construction of the plasmid pUG35*-PDR5-1240
Pdr5 1316 SpeI	CTAGACTAGTTGCAGACGCGTTGGAGTA	Construction of the plasmid pUG35*-PDR5-1316

Oligos name	Oligos sequence (5'->3')	Used of the primers
Pdr5 1376 SpeI	CTAGACTAGTTGGGGTAGTCATA ACAC	Construction of the plasmid pUG35*-PDR5-1376
PDR5 XhoI before Start	CCGCTCGAGTAGACAAAAATGC CCGAGGCC	Construction of GFP plasmids
Linker Up XhoI	CTAGAAATCGCCTCGAGGGTACC ACAGAGACTAGTG	Part of the insert in pUG35 to create pUG35*
Linker Down XhoI	AATTCACTAGTCTCTGTGGTACC CTCGAGGCGATTT	Part of the insert in pUG35 to create pUG35*
Km	CAGTTCAGTCGCATTACGAG	Verification of deleted genes
pUG35 bef	CTTCTGGCATGGCAGACTTG	Verification of *PDR5* gene insert for GFP constructs
pUG35 aft	TACAGGGTCGTCAGATACAT	Verification of *PDR5* gene insert for GFP constructs
Avt pep4	TATCTCACCCTACTGTATTCATA	Verification of *PEP4* gene deletion
Apr pep4	CTAAAACTGAGGACAAGATGGT	Verification of *PEP4* gene deletion
Act1 Up	ACTCTCCCATAACCTCCTAT	Amplification of *ACT1* gene for RNA probe
Act1 Down	TTACGGACATCGACATCACA	Amplification of *ACT1* gene for RNA probe

3. Antibodies

Anti-Pdr5p antisera were obtained from rabbits immunised against a small central peptide of Pdr5p (Decottignies et al. 1999). The production of rabbit anti-Pdr5p antiserum is described in de Thozee et al. (2007). A 198-bp

DNA fragment of the *PDR5* gene encoding residues Arg819 to Thr884 was amplified by PCR and cloned into the pGEX-KT plasmid cleaved with *BamH*I and *Eco*RI. After checking for the correct *PDR5* DNA sequence, the GST-Pdr5 fusion protein was produced in *E. coli* and used to immunize rabbits. Antibodies against Pma1p and Cdc48p were described by Capieaux et al. (1993) and Decottignies et al. (1999) respectively.

4. Drug resistance assays

Drugs resistance was assayed by growing cells in liquid and solid media. 7-µl samples from overnight cultures grown in SD medium (OD_{600} of 0.7-1) were spotted onto SD medium containing various concentrations of cycloheximide (0.01-1.5 µg/ML), itraconazole (0.05-6 µg/mL) and Rhodamine 6G (5-200 µg/mL). These plates were incubated at 28°C for 3 days for the determination of the minimal inhibitory concentrations (MICs). Fifty percent inhibitory concentration (IC50) values were determined by inoculating 50 mL of SD medium containing various concentrations of cycloheximide and itraconazole to an initial OD_{600} of 0.05. The cultures were incubated at 28°C until the cells transformed with pCPx2 *PDR5* plasmid reached an OD_{600} of 0.8-1. OD_{600} value of each culture were measured and expressed in percentage as a function of the drug concentration.

5. Protein analysis

5.1. Preparation of yeast whole-cell extracts

Yeast cells were grown in SD medium supplemented with uracil and amino acids required to an OD_{600} value of 0.5-0.7 (early exponential phase), 0.8-1 (exponential phase), 1.6-2 (early stationary phase) and 2.2-2.5 (late stationary phase). The cells were harvested by centrifugation for 5 min at 3000 rpm (Allegra X-22R centrifuge, C0650 rotor), resuspended in 1 mL of water and centrifuged for 15 sec at 14000 rpm (Eppendorf centrifuge 5417C). The supernatant was removed and the cellular pellet resuspended in 0.2 mL of lysis buffer (25 mM Tris, 5 mM EDTA, pH 7.5) supplemented with protease inhibitors (2 µg/mL) (leupetin, aprotinin, antipain, pepstatin and chymostatin) and 1 mM PMSF (Sigma). 0.2 mL of glass beads were added and the cells were lysed by vigorous vortexing (3.5 min with a 15 sec cooling period, every 30 sec). After addition of the Laemmli buffer (2% SDS, 80 mM Tris-HCl, 10% glycerol, 0.005% bromophenol blue, 1% DTT, urea 9M, pH 6.8) protein samples were agitated twice for 30 sec, incubated at 56 °C for 15 min, and centrifuged for 5 min at 14000 rpm (Eppendorf centrifuge 5417C) to remove cell debris.

5.2. Protein quantification

Protein concentration was determined by the Bradford method, which is based on the binding of Coomassie Blue G-250 (Sigma) to proteins. 0 to 15 µg of bovine serum albumin (BSA, Sigma) (stock solution at 2 mg/mL) was

used as a standard. Water was added to a final volume of 100 µL. 1 mL of the Bradford solution (100 mg Coomassie Blue G-250, 100 mL EtOH 100%, 100 mL of orthophosphoric acid, 800 mL of water) was added to a final volume of 1.1 mL. The same procedure was used for samples containing unknown protein amount. OD_{595} was measured after 15 min of incubation at room temperature.

5.3. Proteins separation and detection

5.3.1. SDS-polyacrylamide gel electrophoresis (PAGE)

Proteins were incubated at 56°C for 15 min in the Laemmli buffer (80 mM Tris-HCl, 2% (w/v) SDS, 10% (w/v) glycerol, 1% (w/v) DTT, 0.005% bromophenol blue, urea 9 M, pH 6.8) and separated onto a 8% (w/v) SDS-polyacrylamide gel. Electrophoresis was carried out at 80 V for 3-4 h for analysis of total extracts or at 60 V for 16 h for pulse-chase analysis. The migration buffer consists of 25 mM Tris, 192 mM glycine, 1 mM Na_2EDTA and 0.1% (w/v) SDS. A 8-mL stacking gel was composed of 1 mL 40% acrylamide/bis-acrylamide 29:1, 1 mL of 0.5 mM Tris-HCl pH 6.8, 80 µL 10% SDS, 80 µL 10% APS, 8 µL TEMED and 5.8 mL of water (final acrylamide concentration of the stacking gel : 5%). A 15-mL running gel was composed of 3 mL 40% acrylamide/bis-acrylamide 29:1, 3.8 mL of 1.5 mM Tris-HCl pH 8.8, 150 µL 10% SDS, 150 µL 10% APS, 9 µL TEMED and 7.9 mL of water (final acrylamide concentration of the running gel : 8%).

5.3.2 Western blot

Proteins and prestained protein marker (Fermentas) separated by SDS-PAGE were transferred onto a nitrocellulose membrane at 100 V for 1 h in a solution composed of 30 mM Tris, 240 mM glycine, 20% (v/v) methanol and 0.02% SDS. Electrotransfer was done with the BIO-RAD «wet» transfer system. After transfer, the membrane was incubated at room temperature for 30 min in a TBS (Tris-buffered saline) buffer (50 mM Tris-HCl, 150 mM NaCl, pH 7.5) supplemented with 3% (w/v) of powder milk and 0.5% (w/v) of Tween20. After three 5-min washings in the TBS buffer, the membrane was incubated for 2-3 h in TBS buffer supplemented with 0.5% (w/v) of powder milk, 0.1% (w/v) Tween20 and the specific primary antibodies (Anti-Pdr5p, dilution 1/2000; Anti-Cdc48p, dilution 1/9000). After washing twice for 10 min in TBS buffer, the membrane was incubated for 1 h with secondary anti-rabbit peroxidase-coupled antibodies (dilution 1/50000). After four 5-min washings in TBS buffer, the antigen-antibodies complexes were detected by the enhanced chemiluminescence (Roche). Antibodies bound on the membrane were removed by incubating the membrane with 0.5 M NaOH for 5 min and then washed 5 min with the TBS buffer.

6. RNA

6.1. RNA extraction

20 mL of minimal medium were inoculated with overnight precultures and incubated at 28 °C until an OD_{600} of 0.6-1 (exponential phase). The growth medium was removed by centrifugation at 3000 rpm for 5 min (Allegra centrifuge X-22R, rotor C0650) and the pellet cell was washed with 1 mL of water and was resuspended in 600 µL of TES buffer (10 mM Tris-HCl, 10 mM EDTA, 0.5% SDS, pH 7.5). Proteins and lipids were denatured by the addition of 400 µL of phenol and incubation at 65°C for 30 to 60 min with occasional short mixing. The tubes were then left on ice for 5 min and centrifuged for 5 min at 14000 rpm (Eppendorf centrifuge 5417C) at 4°C. The aqueous phase was transferred to a new tube and 400 µL of chloroform were added. The mixture was agitated briefly and centrifuged for 5 min at 14000 rpm (Eppendorf centrifuge 5417C) at 4°C. The aqueous phase was transferred into a new tube and the nucleic acids were precipitated by the addition of 40 µL of 3 M Na acetate pH 5.3 and 1 mL 100% cold ethanol. The mixture was centrifuged for 5 min at 14000 rpm (Eppendorf centrifuge 5417C) at 4°C. The supernatant was removed and the RNA pellet was washed with 1.1 mL 70% cold ethanol. The mixture was centrifuged at 14000 rpm (Eppendorf centrifuged 5417C) for 5 min at 4°C. The pellet was dried, resuspended in 50 µL of water and stored at -80°C.

6.2. RNA quantification

2 µL of RNA sample were added to 998 µL of water (dilution 1/500). OD_{260} was measured to determine the RNA concentration. (1 OD corresponds to a concentration of 40 $\mu g.mL^{-1}$). The presence of proteins was estimated by measuring the OD_{280}. Purified nucleic acids are expected to show an OD_{260}/OD_{280} ratio of 1.75-2.1. OD_{230} indicates the presence of polysaccharides and polyphenol. Pure nucleic acids are expected to show an OD_{260}/OD_{230} ratio above 2.

6.3. Northern blot

Mixture of 30-40 µg of RNA, 50% formamide, 3.5 µL formaldehyde and 2 µL of 1X MOPS electrophoresis migration buffer (0.2 M MOPS, 50 mM Na acetate pH 7, 1mM EDTA) for a final volume of 20 µL were incubated at 65°C for 15 min and then left on ice for 5 min. 2 µL of loading buffer (50% glycerol, 10 mM EDTA, 0.25% (w/v) bromophenol blue, 0.25% (w/v) xylene cyanol FF) were added before the samples were loaded on a 1.5% agarose formaldehyde gel (6.5% (v/v) formaldehyde, 1.5% (w/v) agarose, 8 mL of 10x MOPS buffer, 72 mL water). The electrophoresis was realized in a 1X MOPS migration solution at 45-60 V for 3-4 h. After migration the gel was rinsed with water to remove formaldehyde. Capillary transfer of RNA to Hybond-N^+ nylon membranes (Amersham Biosciences, Buckinghamshire, UK) for 16 h was followed by 5 min washes using a 6X SSC buffer (Stock solution of 20X SSC is 3 M NaCl, 300 mM sodium citrate, pH 7). The nylon membrane was dried at room temperature for 30 min, then at 70°C for

2 h between 2 Whatman papers. The nylon membrane was incubated 2 min in a 6X SSC buffer and then at 42°C for 2 h in a prehybridation buffer [(50% (v/v) formamide, 0.5% (w/v) SDS, 100 µg/mL denatured herring sperm DNA, 5X Denhart's (0.1% (w/v) Ficoll (Sigma), 0.1% (w/v) polyvinylpyrrolidone (UCB), 0.1% (w/v) BSA), 6X SSPE (Stock solution 20X SSPE: 3.6 M NaCl, 200 mM $NaH_2PO_4.H_2O$, 25 mM EDTA, pH 7.4)]. Hybridization was carried out at 42°C for 19 h in the prehybridation buffer containing radiolabelled DNA probes. The probe was a fragment of *PDR5* that had been amplified by PCR and radiolabelled with the «Rediprime II Random Prime Labelling System» (Amersham, Biosciences) using [^{32}P]α-dCTP (3000Ci/mmol, Perkin Elmer) and purified on a « Micro Biospin chromatography column » (Bio-Rad). After hybridization, the membrane was washed once with 200 mL of 2X SSC, 0.1% SDS for 5 min at room temperature, once with 200 mL of 2X SSC, 0.1% SDS for 15 min at room temperature, once with 200 mL of 0.1X SSC, 0.5% SDS for 30-60 min at 37°C with gentle agitation and once with 200 mL of 0.1X SSC, 0.5% SDS for 30-60 min at 65°C with gentle agitation. The membrane was then briefly washed with 200 mL of 0.1X SSC at room temperature. The excess liquid was removed. The membrane was exposed to a PhosphorImager screen and band intensity was determined by using the Pharos F Molecular Imager System (Bio-Rad). The probe was removed by incubating the membrane in a solution of 0.5% SDS at 70°C for 30 min with a short agitation and washed once with 6X SSC for 2 min. As a control of the amount of RNA loaded, the membrane was hybridized with a PCR fragment from the actin gene (*ACT1)*.

7. Pulse-Chase analysis

Cultures were inoculated with overnight cultures in SD medium and incubated at the appropriate temperature until an OD_{600} of 0.5-1.0. 10 ml of cells were harvested, resuspended in 400 µl of SD, incubated at the permissive (25°C-28°C) or the restrictive (37°C) temperature and metabolically labeled by adding 15-20 µl of Pro-Mix L-[^{35}S] labelling mix (Perkin Elmer) for 10-15 min (pulse). The cells were centrifuged to remove the uncorporated label, resuspended in 400 µl of SD medium containing 10 mM L-methionine and 0.2 mg/mL cycloheximide (chase medium) and incubated at 25°C-28°C or 37°C for 15, 30, 60 or 90 min (chase). Samples (100µl) were withdrawn at various times and transferred to a cryotube containing 400 µl of glass beads and 400 µl of lysis buffer (50 mM Hepes, 5 mM EDTA, pH 7.5) containing protease inhibitors (2 µg/mL) and 1 mM PMSF. The cells were lysed by vigorous agitation (3.5 min with a 15 sec cooling period, every 30 sec). SDS was then added to a final concentration of 0.5%, and the mixture was again agitated (2 x 30 sec with a 15 sec cooling interval). The lysates were clarified by centrifugation at 14.000 rpm for 15 min in a Eppendorf 5417C centrifuge (4°C). The lysates were diluted 4 times with immunoprecipitation buffer (50 mM Hepes pH 7.5, 5 mM EDTA pH 8.0, 150 mM NaCl, 1% Triton X-100) supplemented with protease inhibitors (2 µg/mL) and 1 mM PMSF. 2 µl of polyclonal anti-Pdr5p antibodies were added to the supernant and incubated at 4°C for 2 h with agitation. 20 µl of a 50% (v/v) suspension of protein A-agarose beads (Roche) were added and the mixture was incubated at 4°C for 1 h. The immune complexes bound to the protein A-agarose beads were washed 3-4

times with immunoprecipitation buffer containing 0.1% SDS, resuspended in 20 µl of 3-fold concentrated Laemmli sample buffer (SDS 2%, Tris 80 mM pH 6.8, glycerol 10%, bromophenol blue 0.005%, DTT 1%, Urea 9 M) and incubated at 56°C for 15 min. After centrifugation for 5 min at 14.000 rpm at room temperature in a Eppendorf centrifuge 5417C to pellet the beads, immunoprecipitate fractions were subjected to SDS-PAGE (8% polyacrylamide gel). The gel was fixed, dried and the relative intensity of the Pdr5p bands at each time point was quantified by phosphor imaging, using the Pharos FX Molecular Imager System (Bio-Rad).

8. β-galactosidase activity measurements

Yeast cells grown in 6-10 mL of SD medium (OD_{600} 0.5-1.0) were collected, washed with cold water and resuspended in 250 µl of lysis buffer (glycerol 20%, Tris-HCl 100 mM pH 8.0, PMSF 1 mM, DTT 1 mM). The cells were agitated with 200 µl of glass beads for 5 min with a 15 sec cooling period every 1 min. 150 µl of cold lysis buffer were added to the tubes. After a 10 sec agitation, the tubes were centrifuged at 20.000g for 10 min at 4°C. Protein concentration of the supernantant was determined by the Bradford Method. β-galactosidase activity was measured using the chromogenic substrate o-nitrophenyl-β-D-galactopyranoside (ONPG, Sigma). 100 µl of the supernantant were added to 900 µl of buffer Z (60 mM Na_2HPO_4, 40 mM NaH_2PO_4, 10 mM KCl, 1 mM $MgSO_4$, 50 mM β-mercaptoethanol, pH 7.0) and pre-incubated at 30°C for 5 min. The enzymatic reaction was started by adding 200 µl of ONPG (4 mg/mL in buffer Z). Time to develop yellow colour was measured before stopping the reaction by the addition of 500 µl

of 1 M Na_2CO_3 solution. OD_{420} was determined spectrometrically and β-galactosidase specific activity was calculed according to the following formula:

[OD_{420} nm x 1.7] / [4.5 x protein concentration x extract volume x time of the reaction x width of the cuve]

OD_{420} nm is the absorbance of o-nitrophenol at 420 nm. The factor 1.7 represent the total reaction volume (mL). The factor 4.5 represents the o-nitrophenol millimolar extinction coefficient ($mL.\mu mol^{-1}.cm^{-1}$), which is the absorbance of 1 mM o-nitrophenol solution. Protein concentration is expressed in mg/mL. Extract volume is the volume assayed (mL). Time of the reaction is expressed in min. The width of the cuve is 1 cm. β-galactosidase specific activity is expressed in μmol of o-nitrophenol produced per minute per milligram of protein.

9. Fluorescence microscopy

Exponential phase cultures (OD_{600} 0.5-1) of yeast strains expressing various Pdr5-GFP fusion were analysed by epifluorescence microscopy, using a DMR (Leica) microscope and a 100x oil immersion objective. Excitation was obtained with a mercury HBO 103 w/2 lamp (OSRAM) and observation was performed using a GFP filter (Leica, excitation path 470/40 nm, emission path 525/50 nm). The images were taken with a DC200 camera (Leica) and analysed with the Leica IM1000 sofware. Observation of temperature resistant and sensitive strains were done at 28°C and 25°C respectively. Temperature sensitive cells were also incubated at 37°C for 30-60 min before fluorescence microscopy analysis.

References

Abolmaali, S., et al. (2008), 'Engineered bakers yeast as a sensitive bioassay indicator organism for the trichothecene toxin deoxynivalenol', *J Microbiol Methods,* 72 (3), 306-12.

Ahner, A. and Brodsky, J. L. (2004), 'Checkpoints in ER-associated degradation: excuse me, which way to the proteasome?', *Trends Cell Biol,* 14 (9), 474-8.

Alam, S. L., et al. (2004), 'Ubiquitin interactions of NZF zinc fingers', *EMBO J,* 23 (7), 1411-21.

Ang, X. L. and Harper, J. W. (2004), 'Interwoven ubiquitination oscillators and control of cell cycle transitions', *Sci STKE,* 2004 (242), pe31.

Arendt, C. S. and Hochstrasser, M. (1997), 'Identification of the yeast 20S proteasome catalytic centers and subunit interactions required for active-site formation', *Proc Natl Acad Sci U S A,* 94 (14), 7156-61.

Arteaga, M. F., et al. (2006), 'An amphipathic helix targets serum and glucocorticoid-induced kinase 1 to the endoplasmic reticulum-associated ubiquitin-conjugation machinery', *Proc Natl Acad Sci U S A,* 103 (30), 11178-83.

Awasthi, S., et al. (2001), 'New roles for the Snp1 and Exo84 proteins in yeast pre-mRNA splicing', *J Biol Chem,* 276 (33), 31004-15.

Bachmair, A., Finley, D., and Varshavsky, A. (1986), 'In vivo half-life of a protein is a function of its amino-terminal residue', *Science,* 234 (4773), 179-86.

Balzi, E., et al. (1987), 'The multidrug resistance gene PDR1 from Saccharomyces cerevisiae', *J Biol Chem,* 262 (35), 16871-9.

--- (1994), 'PDR5, a novel yeast multidrug resistance conferring transporter controlled by the transcription regulator PDR1', *J Biol Chem,* 269 (3), 2206-14.

Barlowe, C., et al. (1994), 'COPII: a membrane coat formed by Sec proteins that drive vesicle budding from the endoplasmic reticulum', *Cell,* 77 (6), 895-907.

Bartel, B., Wunning, I., and Varshavsky, A. (1990), 'The recognition component of the N-end rule pathway', *EMBO J,* 9 (10), 3179-89.

Bauer, B. E., Wolfger, H., and Kuchler, K. (1999), 'Inventory and function of yeast ABC proteins: about sex, stress, pleiotropic drug and heavy metal resistance', *Biochim Biophys Acta,* 1461 (2), 217-36.

Bays, N. W., et al. (2001a), 'HRD4/NPL4 is required for the proteasomal processing of ubiquitinated ER proteins', *Mol Biol Cell,* 12 (12), 4114-28.

--- (2001b), 'Hrd1p/Der3p is a membrane-anchored ubiquitin ligase required for ER-associated degradation', *Nat Cell Biol,* 3 (1), 24-9.

Beck, R., et al. (2009), 'The COPI system: molecular mechanisms and function', *FEBS Lett,* 583 (17), 2701-9.

Bernales, S., Schuck, S., and Walter, P. (2007), 'ER-phagy: selective autophagy of the endoplasmic reticulum', *Autophagy,* 3 (3), 285-7.

Bethune, J., et al. (2006), 'Coatomer, the coat protein of COPI transport vesicles, discriminates endoplasmic reticulum residents from p24 proteins', *Mol Cell Biol,* 26 (21), 8011-21.

Biederer, T., Volkwein, C., and Sommer, T. (1996), 'Degradation of subunits of the Sec61p complex, an integral component of the ER membrane, by the ubiquitin-proteasome pathway', *EMBO J,* 15 (9), 2069-76.

--- (1997), 'Role of Cue1p in ubiquitination and degradation at the ER surface', *Science,* 278 (5344), 1806-9.

Bissinger, P. H. and Kuchler, K. (1994), 'Molecular cloning and expression of the Saccharomyces cerevisiae STS1 gene product. A yeast ABC transporter conferring mycotoxin resistance', *J Biol Chem,* 269 (6), 4180-6.

Bock, J. B., et al. (2001), 'A genomic perspective on membrane compartment organization', *Nature,* 409 (6822), 839-41.

Bolhuis, H., et al. (1997), 'Mechanisms of multidrug transporters', *FEMS Microbiol Rev,* 21 (1), 55-84.

Bonifacino, J. S. and Glick, B. S. (2004), 'The mechanisms of vesicle budding and fusion', *Cell,* 116 (2), 153-66.

Boscoboinik, D., et al. (1990), 'Dimerization of the P-glycoprotein in membranes', *Biochim Biophys Acta,* 1027 (3), 225-8.

Bouige, P., et al. (2002), 'Phylogenetic and functional classification of ATP-binding cassette (ABC) systems', *Curr Protein Pept Sci,* 3 (5), 541-59.

Braun, B. C., et al. (1999), 'The base of the proteasome regulatory particle exhibits chaperone-like activity', *Nat Cell Biol,* 1 (4), 221-6.

Braun, S., et al. (2002), 'Role of the ubiquitin-selective CDC48(UFD1/NPL4) chaperone (segregase) in ERAD of OLE1 and other substrates', *EMBO J,* 21 (4), 615-21.

Brodsky, J. L. (1996), 'Post-translational protein translocation: not all hsc70s are created equal', *Trends Biochem Sci,* 21 (4), 122-6.

Brodsky, J. L. and McCracken, A. A. (1997), 'ER-associated and proteasomemediated protein degradation: how two topologically restricted events came together', *Trends Cell Biol,* 7 (4), 151-6.

Bruderer, R. M., Brasseur, C., and Meyer, H. H. (2004), 'The AAA ATPase p97/ VCP interacts with its alternative co-factors, Ufd1-Npl4 and p47, through a common bipartite binding mechanism', *J Biol Chem,* 279 (48), 49609-16.

Bukau, B., Weissman, J., and Horwich, A. (2006), 'Molecular chaperones and protein quality control', *Cell,* 125 (3), 443-51.

Byrd, J. C., et al. (1982), 'Glycoprotein synthesis in yeast. Identification of Man8GlcNAc2 as an essential intermediate in oligosaccharide processing', *J Biol Chem,* 257 (24), 14657-66.

Cai, H., Reinisch, K., and Ferro-Novick, S. (2007), 'Coats, tethers, Rabs, and SNAREs work together to mediate the intracellular destination of a transport vesicle', *Dev Cell,* 12 (5), 671-82.

Caldwell, S. R., Hill, K. J., and Cooper, A. A. (2001), 'Degradation of endoplasmic reticulum (ER) quality control substrates requires transport between the ER and Golgi', *J Biol Chem,* 276 (26), 23296-303.

Campagnolo, N ; Ghislain, M (2010), 'ER-associated Degradation and Its Involvment in Human Disease: Insights from Yeast.', *ProteinReviews,* 13, 341-64.

Capieaux, E., et al. (1993), 'Overexpression in Escherichia coli and purification of an ATP-binding peptide from the yeast plasma membrane H(+)-ATPase', *J Biol Chem,* 268 (29), 21895-900.

Carvajal, E., et al. (1997), 'Molecular and phenotypic characterization of yeast PDR1 mutants that show hyperactive transcription of various ABC multidrug transporter genes', *Mol Gen Genet,* 256 (4), 406-15.

Carvalho, P., Goder, V., and Rapoport, T. A. (2006), 'Distinct ubiquitin-ligase complexes define convergent pathways for the degradation of ER proteins', *Cell,* 126 (2), 361-73.

Chang, G. (2003), 'Structure of MsbA from Vibrio cholera: a multidrug resistance ABC transporter homolog in a closed conformation', *J Mol Biol,* 330 (2), 419-30.

Chang, G. and Roth, C. B. (2001), 'Structure of MsbA from E. coli: a homolog of the multidrug resistance ATP binding cassette (ABC) transporters', *Science,* 293 (5536), 1793-800.

Chang, H. J., Jones, E. W., and Henry, S. A. (2002), 'Role of the unfolded protein response pathway in regulation of INO1 and in the sec14 bypass mechanism in Saccharomyces cerevisiae', *Genetics,* 162 (1), 29-43.

Chapman, R., Sidrauski, C., and Walter, P. (1998), 'Intracellular signaling from the endoplasmic reticulum to the nucleus', *Annu Rev Cell Dev Biol,* 14, 459-85.

Chen, D. C., Yang, B. C., and Kuo, T. T. (1992), 'One-step transformation of yeast in stationary phase', *Curr Genet,* 21 (1), 83-4.

Chen, L. and Madura, K. (2002), 'Rad23 promotes the targeting of proteolytic substrates to the proteasome', *Mol Cell Biol,* 22 (13), 4902-13.

Chen, P. and Hochstrasser, M. (1996), 'Autocatalytic subunit processing couples active site formation in the 20S proteasome to completion of assembly', *Cell,* 86 (6), 961-72.

Chen, P., et al. (1993), 'Multiple ubiquitin-conjugating enzymes participate in the in vivo degradation of the yeast MAT alpha 2 repressor', *Cell,* 74 (2), 357-69.

Christianson, T. W., et al. (1992), 'Multifunctional yeast high-copy-number shuttle vectors', *Gene,* 110 (1), 119-22.

Cole, S. P., et al. (1992), 'Overexpression of a transporter gene in a multidrug-resistant human lung cancer cell line', *Science,* 258 (5088), 1650-4.

Cox, J. S. and Walter, P. (1996), 'A novel mechanism for regulating activity of a transcription factor that controls the unfolded protein response', *Cell,* 87 (3), 391-404.

Dassa, E. and Bouige, P. (2001), 'The ABC of ABCS: a phylogenetic and functional classification of ABC systems in living organisms', *Res Microbiol,* 152 (3-4), 211-29.

de Kerchove d'Exaerde, A., et al. (1995), 'Functional complementation of a null mutation of the yeast Saccharomyces cerevisiae plasma membrane H(+)-ATPase by a plant H(+)-ATPase gene', *J Biol Chem,* 270 (40), 23828-37.

de Thozee, C. P., et al. (2007), 'Subcellular trafficking of the yeast plasma membrane ABC transporter, Pdr5, is impaired by a mutation in the N-terminal nucleotide-binding fold', *Mol Microbiol,* 63 (3), 811-25.

Deak, P. M. and Wolf, D. H. (2001), 'Membrane topology and function of Der3/Hrd1p as a ubiquitin-protein ligase (E3) involved in endoplasmic reticulum degradation', *J Biol Chem,* 276 (14), 10663-9.

Decottignies, A. and Goffeau, A. (1997), 'Complete inventory of the yeast ABC proteins', *Nat Genet,* 15 (2), 137-45.

Decottignies, A., Owsianik, G., and Ghislain, M. (1999), 'Casein kinase I-dependent phosphorylation and stability of the yeast multidrug transporter Pdr5p', *J Biol Chem,* 274 (52), 37139-46.

Decottignies, A., Evain, A., and Ghislain, M. (2004), 'Binding of Cdc48p to a ubiquitin-related UBX domain from novel yeast proteins involved in intracellular proteolysis and sporulation', *Yeast,* 21 (2), 127-39.

Decottignies, A., et al. (1994), 'Solubilization and characterization of the overexpressed PDR5 multidrug resistance nucleotide triphosphatase of yeast', *J Biol Chem,* 269 (17), 12797-803.

--- (1998), 'ATPase and multidrug transport activities of the overexpressed yeast ABC protein Yor1p', *J Biol Chem,* 273 (20), 12612-22.

DeLaBarre, B. and Brunger, A. T. (2003), 'Complete structure of p97/valosin-containing protein reveals communication between nucleotide domains', *Nat Struct Biol,* 10 (10), 856-63.

Delahodde, A., Delaveau, T., and Jacq, C. (1995), 'Positive autoregulation of the yeast transcription factor Pdr3p, which is involved in control of drug resistance', *Mol Cell Biol,* 15 (8), 4043-51.

Delaveau, T., et al. (1994), 'PDR3, a new yeast regulatory gene, is homologous to PDR1 and controls the multidrug resistance phenomenon', *Mol Gen Genet,* 244 (5), 501-11.

Denic, V., Quan, E. M., and Weissman, J. S. (2006), 'A luminal surveillance complex that selects misfolded glycoproteins for ER-associated degradation', *Cell,* 126 (2), 349-59.

DeRisi, J., et al. (2000), 'Genome microarray analysis of transcriptional activation in multidrug resistance yeast mutants', *FEBS Lett,* 470 (2), 156-60.

Diederichs, K., et al. (2000), 'Crystal structure of MalK, the ATPase subunit of the trehalose/maltose ABC transporter of the archaeon Thermococcus litoralis', *EMBO J,* 19 (22), 5951-61.

Dreveny, I., et al. (2004), 'Structural basis of the interaction between the AAA ATPase p97/VCP and its adaptor protein p47', *EMBO J,* 23 (5), 1030-9.

Egner, R. and Kuchler, K. (1996), 'The yeast multidrug transporter Pdr5 of the plasma membrane is ubiquitinated prior to endocytosis and degradation in the vacuole', *FEBS Lett,* 378 (2), 177-81.

Egner, R., Bauer, B. E., and Kuchler, K. (2000), 'The transmembrane domain 10 of the yeast Pdr5p ABC antifungal efflux pump determines both substrate specificity and inhibitor susceptibility', *Mol Microbiol,* 35 (5), 1255-63.

Egner, R., et al. (1998), 'Genetic separation of FK506 susceptibility and drug transport in the yeast Pdr5 ATP-binding cassette multidrug resistance transporter', *Mol Biol Cell,* 9 (2), 523-43.

Ellgaard, L. and Helenius, A. (2003), 'Quality control in the endoplasmic reticulum', *Nat Rev Mol Cell Biol,* 4 (3), 181-91.

Elsasser, S., et al. (2002), 'Proteasome subunit Rpn1 binds ubiquitin-like protein domains', *Nat Cell Biol,* 4 (9), 725-30.

Enenkel, C., et al. (1994), 'PRE3, highly homologous to the human major histocompatibility complex-linked LMP2 (RING12) gene, codes for a yeast proteasome subunit necessary for the peptidylglutamyl-peptide hydrolyzing activity', *FEBS Lett,* 341 (2-3), 193-6.

Ernst, R., et al. (2008), 'A mutation of the H-loop selectively affects rhodamine transport by the yeast multidrug ABC transporter Pdr5', *Proc Natl Acad Sci U S A,* 105 (13), 5069-74.

Fassio, A. and Sitia, R. (2002), 'Formation, isomerisation and reduction of disulphide bonds during protein quality control in the endoplasmic reticulum', *Histochem Cell Biol,* 117 (2), 151-7.

Ferreira-Pereira, A., et al. (2003), 'Three-dimensional reconstruction of the Saccharomyces cerevisiae multidrug resistance protein Pdr5p', *J Biol Chem,* 278 (14), 11995-9.

Finger, A., Knop, M., and Wolf, D. H. (1993), 'Analysis of two mutated vacuolar proteins reveals a degradation pathway in the endoplasmic reticulum or a related compartment of yeast', *Eur J Biochem,* 218 (2), 565-74.

Friedlander, R., et al. (2000), 'A regulatory link between ER-associated protein degradation and the unfolded-protein response', *Nat Cell Biol,* 2 (7), 379-84.

Frohlich, K. U., et al. (1991), 'Yeast cell cycle protein CDC48p shows full-length homology to the mammalian protein VCP and is a member of a protein family involved in secretion, peroxisome formation, and gene expression', *J Cell Biol,* 114 (3), 443-53.

Fu, L. and Sztul, E. (2003), 'Traffic-independent function of the Sar1p/COPII machinery in proteasomal sorting of the cystic fibrosis transmembrane conductance regulator', *J Cell Biol,* 160 (2), 157-63.

--- (2009), 'ER-associated complexes (ERACs) containing aggregated cystic fibrosis transmembrane conductance regulator (CFTR) are degraded by autophagy', *Eur J Cell Biol,* 88 (4), 215-26.

Funakoshi, M., et al. (2002), 'Budding yeast Dsk2p is a polyubiquitin-binding protein that can interact with the proteasome', *Proc Natl Acad Sci U S A,* 99 (2), 745-50.

Funato, K. and Riezman, H. (2001), 'Vesicular and nonvesicular transport of ceramide from ER to the Golgi apparatus in yeast', *J Cell Biol,* 155 (6), 949-59.

Galan, J. M., et al. (1996), 'Ubiquitination mediated by the Npi1p/Rsp5p ubiquitin-protein ligase is required for endocytosis of the yeast uracil permease', *J Biol Chem,* 271 (18), 10946-52.

Gardner, R. G. and Hampton, R. Y. (1999), 'A 'distributed degron' allows regulated entry into the ER degradation pathway', *EMBO J,* 18 (21), 5994-6004.

Gardner, R. G., et al. (2000), 'Endoplasmic reticulum degradation requires lumen to cytosol signaling. Transmembrane control of Hrd1p by Hrd3p', *J Cell Biol,* 151 (1), 69-82.

Gauss, R., Sommer, T., and Jarosch, E. (2006a), 'The Hrd1p ligase complex forms a linchpin between ER-lumenal substrate selection and Cdc48p recruitment', *EMBO J,* 25 (9), 1827-35.

Gauss, R., et al. (2006b), 'A complex of Yos9p and the HRD ligase integrates endoplasmic reticulum quality control into the degradation machinery', *Nat Cell Biol,* 8 (8), 849-54.

Giaever, G., et al. (2002), 'Functional profiling of the Saccharomyces cerevisiae genome', *Nature,* 418 (6896), 387-91.

Gnann, A., Riordan, J. R., and Wolf, D. H. (2004), 'Cystic fibrosis transmembrane conductance regulator degradation depends on the lectins Htm1p/EDEM and the Cdc48 protein complex in yeast', *Mol Biol Cell,* 15 (9), 4125-35.

Golin, J., Ambudkar, S. V., and May, L. (2007), 'The yeast Pdr5p multidrug transporter: how does it recognize so many substrates?', *Biochem Biophys Res Commun,* 356 (1), 1-5.

Golin, J., et al. (2000), 'Chemical specificity of the PDR5 multidrug resistance gene product of Saccharomyces cerevisiae based on studies with tri-n-alkyltin chlorides', *Antimicrob Agents Chemother,* 44 (1), 134-8.

--- (2003), 'Studies with novel Pdr5p substrates demonstrate a strong size dependence for xenobiotic efflux', *J Biol Chem,* 278 (8), 5963-9.

Groll, M., et al. (1997), 'Structure of 20S proteasome from yeast at 2.4 A resolution', *Nature,* 386 (6624), 463-71.

Gross, E., et al. (2006), 'Generating disulfides enzymatically: reaction products and electron acceptors of the endoplasmic reticulum thiol oxidase Ero1p', *Proc Natl Acad Sci U S A,* 103 (2), 299-304.

Grosshans, B. L., Ortiz, D., and Novick, P. (2006), 'Rabs and their effectors: achieving specificity in membrane traffic', *Proc Natl Acad Sci U S A,* 103 (32), 11821-7.

Hampton, R. Y. (2002), 'ER-associated degradation in protein quality control and cellular regulation', *Curr Opin Cell Biol,* 14 (4), 476-82.

--- (2003), 'IRE1: a role in UPREgulation of ER degradation', *Dev Cell,* 4 (2), 144-6.

Hampton, R. Y., Gardner, R. G., and Rine, J. (1996), 'Role of 26S proteasome and HRD genes in the degradation of 3-hydroxy-3-methylglutaryl-CoA reductase, an integral endoplasmic reticulum membrane protein', *Mol Biol Cell,* 7 (12), 2029-44.

Harris, S. L., et al. (1994), 'Dominant lethal mutations in the plasma membrane H (+)-ATPase gene of Saccharomyces cerevisiae', *Proc Natl Acad Sci U S A,* 91 (22), 10531-5.

Hein, C., et al. (1995), 'NPl1, an essential yeast gene involved in induced degradation of Gap1 and Fur4 permeases, encodes the Rsp5 ubiquitin-protein ligase', *Mol Microbiol,* 18 (1), 77-87.

Helliwell, S. B., Losko, S., and Kaiser, C. A. (2001), 'Components of a ubiquitin ligase complex specify polyubiquitination and intracellular trafficking of the general amino acid permease', *J Cell Biol,* 153 (4), 649-62.

Hicke, L. and Riezman, H. (1996), 'Ubiquitination of a yeast plasma membrane receptor signals its ligand-stimulated endocytosis', *Cell,* 84 (2), 277-87.

Higgins, C. F. and Linton, K. J. (2004), 'The ATP switch model for ABC transporters', *Nat Struct Mol Biol,* 11 (10), 918-26.

Hiller, M. M., et al. (1996), 'ER degradation of a misfolded luminal protein by the cytosolic ubiquitin-proteasome pathway', *Science,* 273 (5282), 1725-8.

Hirata, D., et al. (1994), 'Saccharomyces cerevisiae YDR1, which encodes a member of the ATP-binding cassette (ABC) superfamily, is required for multidrug resistance', *Curr Genet,* 26 (4), 285-94.

Hirsch, C., Gauss, R., and Sommer, T. (2006), 'Coping with stress: cellular relaxation techniques', *Trends Cell Biol,* 16 (12), 657-63.

Hirsch, C., et al. (2004), 'Yeast N-glycanase distinguishes between native and non-native glycoproteins', *EMBO Rep,* 5 (2), 201-6.

Hitchcock, A. L., et al. (2001), 'The conserved npl4 protein complex mediates proteasome-dependent membrane-bound transcription factor activation', *Mol Biol Cell,* 12 (10), 3226-41.

Hitt, R. and Wolf, D. H. (2004a), 'Der1p, a protein required for degradation of malfolded soluble proteins of the endoplasmic reticulum: topology and Der1-like proteins', *FEMS Yeast Res,* 4 (7), 721-9.

--- (2004b), 'DER7, encoding alpha-glucosidase I is essential for degradation of malfolded glycoproteins of the endoplasmic reticulum', *FEMS Yeast Res,* 4 (8), 815-20.

Hochstrasser, M. (1996), 'Ubiquitin-dependent protein degradation', *Annu Rev Genet,* 30, 405-39.

Hoof, T., et al. (1994), 'Cystic fibrosis-type mutational analysis in the ATP-binding cassette transporter signature of human P-glycoprotein MDR1', *J Biol Chem,* 269 (32), 20575-83.

Hopfner, K. P., et al. (2000), 'Structural biology of Rad50 ATPase: ATP-driven conformational control in DNA double-strand break repair and the ABC-ATPase superfamily', *Cell,* 101 (7), 789-800.

Hoseki, J., Ushioda, R., and Nagata, K. (2010), 'Mechanism and components of endoplasmic reticulum-associated degradation', *J Biochem,* 147 (1), 19-25.

Hsu, V. W. and Yang, J. S. (2009), 'Mechanisms of COPI vesicle formation', *FEBS Lett,* 583 (23), 3758-63.

Huibregtse, J. M., et al. (1995), 'A family of proteins structurally and functionally related to the E6-AP ubiquitin-protein ligase', *Proc Natl Acad Sci U S A,* 92 (11), 5249.

Hung, L. W., et al. (1998), 'Crystal structure of the ATP-binding subunit of an ABC transporter', *Nature,* 396 (6712), 703-7.

Huyer, G., et al. (2004a), 'A striking quality control subcompartment in Saccharomyces cerevisiae: the endoplasmic reticulum-associated compartment', *Mol Biol Cell,* 15 (2), 908-21.

--- (2004b), 'Distinct machinery is required in Saccharomyces cerevisiae for the endoplasmic reticulum-associated degradation of a multispanning membrane protein and a soluble luminal protein', *J Biol Chem,* 279 (37), 38369-78.

Jakob, C. A., et al. (1998), 'Degradation of misfolded endoplasmic reticulum glycoproteins in Saccharomyces cerevisiae is determined by a specific oligosaccharide structure', *J Cell Biol,* 142 (5), 1223-33.

--- (2001), 'Htm1p, a mannosidase-like protein, is involved in glycoprotein degradation in yeast', *EMBO Rep,* 2 (5), 423-30.

Jarosch, E., et al. (2002), 'Protein dislocation from the ER requires polyubiquitination and the AAA-ATPase Cdc48', *Nat Cell Biol,* 4 (2), 134-9.

Johnson, P. R., et al. (1998), 'Degradation signal masking by heterodimerization of MATalpha2 and MATa1 blocks their mutual destruction by the ubiquitin-proteasome pathway', *Cell,* 94 (2), 217-27.

Jungwirth, H. and Kuchler, K. (2006), 'Yeast ABC transporters-- a tale of sex, stress, drugs and aging', *FEBS Lett,* 580 (4), 1131-8.

Kaganovich, D., Kopito, R., and Frydman, J. (2008), 'Misfolded proteins partition between two distinct quality control compartments', *Nature,* 454 (7208), 1088-95.

Katzmann, D. J., et al. (1996), 'Multiple Pdr1p/Pdr3p binding sites are essential for normal expression of the ATP binding cassette transporter protein-encoding gene PDR5', *J Biol Chem,* 271 (38), 23049-54.

--- (1994), 'Transcriptional control of the yeast PDR5 gene by the PDR3 gene product', *Mol Cell Biol,* 14 (7), 4653-61.

--- (1995), 'Expression of an ATP-binding cassette transporter-encoding gene (YOR1) is required for oligomycin resistance in Saccharomyces cerevisiae', *Mol Cell Biol,* 15 (12), 6875-83.

Kihara, A. and Igarashi, Y. (2004), 'Cross talk between sphingolipids and glycerophospholipids in the establishment of plasma membrane asymmetry', *Mol Biol Cell,* 15 (11), 4949-59.

Kim, I., Mi, K., and Rao, H. (2004), 'Multiple interactions of rad23 suggest a mechanism for ubiquitylated substrate delivery important in proteolysis', *Mol Biol Cell,* 15 (7), 3357-65.

Kiser, G. L., et al. (2001), 'Expression and degradation of the cystic fibrosis transmembrane conductance regulator in Saccharomyces cerevisiae', *Arch Biochem Biophys,* 390 (2), 195-205.

Kispal, G., et al. (1999), 'The mitochondrial proteins Atm1p and Nfs1p are essential for biogenesis of cytosolic Fe/S proteins', *EMBO J,* 18 (14), 3981-9.

Klionsky, D. J. (2007), 'Autophagy: from phenomenology to molecular understanding in less than a decade', *Nat Rev Mol Cell Biol,* 8 (11), 931-7.

Knop, M., et al. (1996), 'Der1, a novel protein specifically required for endoplasmic reticulum degradation in yeast', *EMBO J,* 15 (4), 753-63.

Koegl, M., et al. (1999), 'A novel ubiquitination factor, E4, is involved in multiubiquitin chain assembly', *Cell,* 96 (5), 635-44.

Kolaczkowska, A. and Goffeau, A. (1999), 'Regulation of pleiotropic drug resistance in yeast', *Drug Resist Updat,* 2 (6), 403-14.

Kolaczkowska, A., et al. (2002), 'Functional dissection of Pdr1p, a regulator of multidrug resistance in Saccharomyces cerevisiae', *Mol Genet Genomics,* 267 (1), 96-106.

Kolaczkowski, M., et al. (1998), 'In vivo characterization of the drug resistance profile of the major ABC transporters and other components of the yeast pleiotropic drug resistance network', *Microb Drug Resist,* 4 (3), 143-58.

--- (1996), 'Anticancer drugs, ionophoric peptides, and steroids as substrates of the yeast multidrug transporter Pdr5p', *J Biol Chem,* 271 (49), 31543-8.

Kolling, R. and Hollenberg, C. P. (1994), 'The ABC-transporter Ste6 accumulates in the plasma membrane in a ubiquitinated form in endocytosis mutants', *EMBO J,* 13 (14), 3261-71.

Kopito, R. R. (1997), 'ER quality control: the cytoplasmic connection', *Cell,* 88 (4), 427-30.

Kostova, Z. and Wolf, D. H. (2003), 'For whom the bell tolls: protein quality control of the endoplasmic reticulum and the ubiquitin-proteasome connection', *EMBO J,* 22 (10), 2309-17.

Kovalchuk, A. and Driessen, A. J. (2010), 'Phylogenetic analysis of fungal ABC transporters', *BMC Genomics,* 11, 177.

Kozutsumi, Y., et al. (1989), 'Identification of immunoglobulin heavy chain binding protein as glucose-regulated protein 78 on the basis of amino acid sequence, immunological cross-reactivity, and functional activity', *J Cell Sci Suppl,* 11, 115-37.

Kralli, A., Bohen, S. P., and Yamamoto, K. R. (1995), 'LEM1, an ATP-binding-cassette transporter, selectively modulates the biological potency of steroid hormones', *Proc Natl Acad Sci U S A,* 92 (10), 4701-5.

Krebs, M. P., et al. (2004), 'Quality control of integral membrane proteins', *Trends Biochem Sci,* 29 (12), 648-55.

Kreft, S. G., Wang, L., and Hochstrasser, M. (2006), 'Membrane topology of the yeast endoplasmic reticulum-localized ubiquitin ligase Doa10 and comparison with its human ortholog TEB4 (MARCH-VI)', *J Biol Chem,* 281 (8), 4646-53.

Lamers, M. H., et al. (2000), 'The crystal structure of DNA mismatch repair protein MutS binding to a G x T mismatch', *Nature,* 407 (6805), 711-7.

Lenk, U., et al. (2002), 'A role for mammalian Ubc6 homologues in ER-associated protein degradation', *J Cell Sci,* 115 (Pt 14), 3007-14.

Leon, S., Erpapazoglou, Z., and Haguenauer-Tsapis, R. (2008), 'Ear1p and Ssh4p are new adaptors of the ubiquitin ligase Rsp5p for cargo ubiquitylation and sorting at multivesicular bodies', *Mol Biol Cell,* 19 (6), 2379-88.

Li, Z. S., et al. (1996), 'The yeast cadmium factor protein (YCF1) is a vacuolar glutathione S-conjugate pump', *J Biol Chem,* 271 (11), 6509-17.

Linton, K. J. and Higgins, C. F. (2007), 'Structure and function of ABC transporters: the ATP switch provides flexible control', *Pflugers Arch,* 453 (5), 555-67.

Liu, H. Y., et al. (2001), 'Characterization of CAF4 and CAF16 reveals a functional connection between the CCR4-NOT complex and a subset of SRB proteins of the RNA polymerase II holoenzyme', *J Biol Chem,* 276 (10), 7541-8.

Loayza, D., et al. (1998), 'Ste6p mutants defective in exit from the endoplasmic reticulum (ER) reveal aspects of an ER quality control pathway in Saccharomyces cerevisiae', *Mol Biol Cell,* 9 (10), 2767-84.

Locher, K. P., Lee, A. T., and Rees, D. C. (2002), 'The E. coli BtuCD structure: a framework for ABC transporter architecture and mechanism', *Science,* 296 (5570), 1091-8.

Loo, T. W. and Clarke, D. M. (1996), 'Inhibition of oxidative cross-linking between engineered cysteine residues at positions 332 in predicted transmembrane segments (TM) 6 and 975 in predicted TM12 of human P-glycoprotein by drug substrates', *J Biol Chem,* 271 (44), 27482-7.

--- (1997a), 'Identification of residues in the drug-binding site of human P-glycoprotein using a thiol-reactive substrate', *J Biol Chem,* 272 (51), 31945-8.

--- (1997b), 'Drug-stimulated ATPase activity of human P-glycoprotein requires movement between transmembrane segments 6 and 12', *J Biol Chem,* 272 (34), 20986-9.

Lubelski, J., Konings, W. N., and Driessen, A. J. (2007), 'Distribution and physiology of ABC-type transporters contributing to multidrug resistance in bacteria', *Microbiol Mol Biol Rev,* 71 (3), 463-76.

Lupas, A., Koster, A. J., and Baumeister, W. (1993), 'Structural features of 26S and 20S proteasomes', *Enzyme Protein,* 47 (4-6), 252-73.

Mahe, Y., et al. (1996), 'The ATP-binding cassette multidrug transporter Snq2 of Saccharomyces cerevisiae: a novel target for the transcription factors Pdr1 and Pdr3', *Mol Microbiol,* 20 (1), 109-17.

Mamnun, Y. M., Schuller, C., and Kuchler, K. (2004), 'Expression regulation of the yeast PDR5 ATP-binding cassette (ABC) transporter suggests a role in cellular detoxification during the exponential growth phase', *FEBS Lett,* 559 (1-3), 111-7.

Mamnun, Y. M., et al. (2002), 'The yeast zinc finger regulators Pdr1p and Pdr3p control pleiotropic drug resistance (PDR) as homo- and heterodimers in vivo', *Mol Microbiol,* 46 (5), 1429-40.

Marshall, J., et al. (1994), 'Stoichiometry of recombinant cystic fibrosis transmembrane conductance regulator in epithelial cells and its functional reconstitution into cells in vitro', *J Biol Chem,* 269 (4), 2987-95.

Martens, J. A., et al. (1996), 'Transcriptional activation by yeast PDR1p is inhibited by its association with NGG1p/ADA3p', *J Biol Chem,* 271 (27), 15884-90.

Mayer, A., Wickner, W., and Haas, A. (1996), 'Sec18p (NSF)-driven release of Sec17p (alpha-SNAP) can precede docking and fusion of yeast vacuoles', *Cell,* 85 (1), 83-94.

Mazon, M. J., Eraso, P., and Portillo, F. (2007), 'Efficient degradation of misfolded mutant Pma1 by endoplasmic reticulum-associated degradation requires Atg19 and the Cvt/autophagy pathway', *Mol Microbiol,* 63 (4), 1069-77.

McCracken, A. A. and Brodsky, J. L. (2003), 'Evolving questions and paradigm shifts in endoplasmic-reticulum-associated degradation (ERAD)', *Bioessays,* 25 (9), 868-77.

McGrath, J. P. and Varshavsky, A. (1989), 'The yeast STE6 gene encodes a homologue of the mammalian multidrug resistance P-glycoprotein', *Nature,* 340 (6232), 400-4.

Medicherla, B., et al. (2004), 'A genomic screen identifies Dsk2p and Rad23p as essential components of ER-associated degradation', *EMBO Rep,* 5 (7), 692-7.

Metzger, M. B., et al. (2008), 'Degradation of a cytosolic protein requires endoplasmic reticulum-associated degradation machinery', *J Biol Chem,* 283 (47), 32302-16.

Meusser, B., et al. (2005), 'ERAD: the long road to destruction', *Nat Cell Biol,* 7 (8), 766-72.

Meyer, H. H., et al. (2000), 'A complex of mammalian ufd1 and npl4 links the AAA-ATPase, p97, to ubiquitin and nuclear transport pathways', *EMBO J,* 19 (10), 2181-92.

Meyers, S., et al. (1992), 'Interaction of the yeast pleiotropic drug resistance genes PDR1 and PDR5', *Curr Genet,* 21 (6), 431-6.

Michaelis, S. and Berkower, C. (1995), 'Sequence comparison of yeast ATP-binding cassette proteins', *Cold Spring Harb Symp Quant Biol,* 60, 291-307.

Moody, J. E., et al. (2002), 'Cooperative, ATP-dependent association of the nucleotide binding cassettes during the catalytic cycle of ATP-binding cassette transporters', *J Biol Chem,* 277 (24), 21111-4.

Moussatova, A., et al. (2008), 'ATP-binding cassette transporters in Escherichia coli', *Biochim Biophys Acta,* 1778 (9), 1757-71.

Naito, M. and Tsuruo, T. (1992), 'Functionally active homodimer of P-glycoprotein in multidrug-resistant tumor cells', *Biochem Biophys Res Commun,* 185 (1), 284-90.

Nakatsukasa, K. and Brodsky, J. L. (2008), 'The recognition and retrotranslocation of misfolded proteins from the endoplasmic reticulum', *Traffic,* 9 (6), 861-70.

Nakatsukasa, K., et al. (2008), 'Dissecting the ER-associated degradation of a misfolded polytopic membrane protein', *Cell,* 132 (1), 101-12.

--- (2001), 'Mnl1p, an alpha -mannosidase-like protein in yeast Saccharomyces cerevisiae, is required for endoplasmic reticulum-associated degradation of glycoproteins', *J Biol Chem,* 276 (12), 8635-8.

Neuber, O., et al. (2005), 'Ubx2 links the Cdc48 complex to ER-associated protein degradation', *Nat Cell Biol,* 7 (10), 993-8.

Neyfakh, A. A. (2002), 'Mystery of multidrug transporters: the answer can be simple', *Mol Microbiol,* 44 (5), 1123-30.

Ng, W., et al. (2007), 'Characterization of the proteasome interaction with the Sec61 channel in the endoplasmic reticulum', *J Cell Sci,* 120 (Pt 4), 682-91.

Nishikawa, S. I., et al. (2001), 'Molecular chaperones in the yeast endoplasmic reticulum maintain the solubility of proteins for retrotranslocation and degradation', *J Cell Biol,* 153 (5), 1061-70.

Nita-Lazar, M. and Lennarz, W. J. (2005), 'Pkc1p modifies CPY* degradation in the ERAD pathway', *Biochem Biophys Res Commun,* 332 (2), 357-61.

Norgaard, P., et al. (2001), 'Functional differences in yeast protein disulfide isomerases', *J Cell Biol,* 152 (3), 553-62.

Normington, K., et al. (1989), 'S. cerevisiae encodes an essential protein homologous in sequence and function to mammalian BiP', *Cell,* 57 (7), 1223-36.

Obmolova, G., et al. (2000), 'Crystal structures of mismatch repair protein MutS and its complex with a substrate DNA', *Nature,* 407 (6805), 703-10.

Ogawa, A., et al. (1998), 'Role of ABC transporters in aureobasidin A resistance', *Antimicrob Agents Chemother,* 42 (4), 755-61.

Owsianik, G., Balzi l, L., and Ghislain, M. (2002), 'Control of 26S proteasome expression by transcription factors regulating multidrug resistance in Saccharomyces cerevisiae', *Mol Microbiol,* 43 (5), 1295-308.

Park, S., et al. (2005), 'Ufd1 exhibits the AAA-ATPase fold with two distinct ubiquitin interaction sites', *Structure,* 13 (7), 995-1005.

Peng, J., et al. (2003), 'A proteomics approach to understanding protein ubiquitination', *Nat Biotechnol,* 21 (8), 921-6.

Peyroche, A., Paris, S., and Jackson, C. L. (1996), 'Nucleotide exchange on ARF mediated by yeast Gea1 protein', *Nature,* 384 (6608), 479-81.

Pilon, M., Schekman, R., and Romisch, K. (1997), 'Sec61p mediates export of a misfolded secretory protein from the endoplasmic reticulum to the cytosol for degradation', *EMBO J,* 16 (15), 4540-8.

Piper, P., et al. (1998), 'The pdr12 ABC transporter is required for the development of weak organic acid resistance in yeast', *EMBO J,* 17 (15), 4257-65.

Plemper, R. K. and Wolf, D. H. (1999), 'Endoplasmic reticulum degradation. Reverse protein transport and its end in the proteasome', *Mol Biol Rep,* 26 (1-2), 125-30.

Plemper, R. K., et al. (1998), 'Endoplasmic reticulum degradation of a mutated ATP-binding cassette transporter Pdr5 proceeds in a concerted action of Sec61 and the proteasome', *J Biol Chem,* 273 (49), 32848-56.

--- (1997), 'Mutant analysis links the translocon and BiP to retrograde protein transport for ER degradation', *Nature,* 388 (6645), 891-5.

--- (1999), 'Genetic interactions of Hrd3p and Der3p/Hrd1p with Sec61p suggest a retro-translocation complex mediating protein transport for ER degradation', *J Cell Sci,* 112 (Pt 22), 4123-34.

Pohl, A., Devaux, P. F., and Herrmann, A. (2005), 'Function of prokaryotic and eukaryotic ABC proteins in lipid transport', *Biochim Biophys Acta,* 1733 (1), 29-52.

Rabinovich, E., et al. (2002), 'AAA-ATPase p97/Cdc48p, a cytosolic chaperone required for endoplasmic reticulum-associated protein degradation', *Mol Cell Biol,* 22 (2), 626-34.

Rape, M., et al. (2001), 'Mobilization of processed, membrane-tethered SPT23 transcription factor by CDC48(UFD1/NPL4), a ubiquitin-selective chaperone', *Cell,* 107 (5), 667-77.

Ravid, T. and Hochstrasser, M. (2008), 'Diversity of degradation signals in the ubiquitin-proteasome system', *Nat Rev Mol Cell Biol,* 9 (9), 679-90.

Ravid, T., Kreft, S. G., and Hochstrasser, M. (2006), 'Membrane and soluble substrates of the Doa10 ubiquitin ligase are degraded by distinct pathways', *EMBO J,* 25 (3), 533-43.

Reyes, C. L. and Chang, G. (2005), 'Structure of the ABC transporter MsbA in complex with ADP.vanadate and lipopolysaccharide', *Science,* 308 (5724), 1028-31.

Richly, H., et al. (2005), 'A series of ubiquitin binding factors connects CDC48/p97 to substrate multiubiquitylation and proteasomal targeting', *Cell,* 120 (1), 73-84.

Riordan, J. R., et al. (1985), 'Amplification of P-glycoprotein genes in multidrug-resistant mammalian cell lines', *Nature,* 316 (6031), 817-9.

Rogers, B., et al. (2001), 'The pleitropic drug ABC transporters from Saccharomyces cerevisiae', *J Mol Microbiol Biotechnol,* 3 (2), 207-14.

Ron, D. and Walter, P. (2007), 'Signal integration in the endoplasmic reticulum unfolded protein response', *Nat Rev Mol Cell Biol,* 8 (7), 519-29.

Rose, M. D., Misra, L. M., and Vogel, J. P. (1989), 'KAR2, a karyogamy gene, is the yeast homolog of the mammalian BiP/GRP78 gene', *Cell,* 57 (7), 1211-21.

Rumpf, S. and Jentsch, S. (2006), 'Functional division of substrate processing cofactors of the ubiquitin-selective Cdc48 chaperone', *Mol Cell,* 21 (2), 261-9.

Saris, N., et al. (1997), 'The Hsp70 homologue Lhs1p is involved in a novel function of the yeast endoplasmic reticulum, refolding and stabilization of heat-denatured protein aggregates', *J Cell Biol,* 137 (4), 813-24.

Sato, K. and Nakano, A. (2007), 'Mechanisms of COPII vesicle formation and protein sorting', *FEBS Lett,* 581 (11), 2076-82.

Schafer, A. and Wolf, D. H. (2009), 'Sec61p is part of the endoplasmic reticulum-associated degradation machinery', *EMBO J,* 28 (19), 2874-84.

Schuberth, C., et al. (2004), 'Shp1 and Ubx2 are adaptors of Cdc48 involved in ubiquitin-dependent protein degradation', *EMBO Rep,* 5 (8), 818-24.

Schuller, C., et al. (2004), 'Global phenotypic analysis and transcriptional profiling defines the weak acid stress response regulon in Saccharomyces cerevisiae', *Mol Biol Cell,* 15 (2), 706-20.

Scott, D. C. and Schekman, R. (2008), 'Role of Sec61p in the ER-associated degradation of short-lived transmembrane proteins', *J Cell Biol,* 181 (7), 1095-105.

Selkoe, D. J. (2003), 'Folding proteins in fatal ways', *Nature,* 426 (6968), 900-4.

Shamu, C. E. and Walter, P. (1996), 'Oligomerization and phosphorylation of the Ire1p kinase during intracellular signaling from the endoplasmic reticulum to the nucleus', *EMBO J,* 15 (12), 3028-39.

Shamu, C. E., Cox, J. S., and Walter, P. (1994), 'The unfolded-protein-response pathway in yeast', *Trends Cell Biol,* 4 (2), 56-60.

Sidrauski, C., Chapman, R., and Walter, P. (1998), 'The unfolded protein response: an intracellular signalling pathway with many surprising features', *Trends Cell Biol,* 8 (6), 245-9.

Simonics, T., et al. (2000), 'Isolation and molecular characterization of the carboxy-terminal pdr3 mutants in Saccharomyces cerevisiae', *Curr Genet,* 38 (5), 248-55.

Sitia, R. and Braakman, I. (2003), 'Quality control in the endoplasmic reticulum protein factory', *Nature,* 426 (6968), 891-4.

Soetens, O., De Craene, J. O., and Andre, B. (2001), 'Ubiquitin is required for sorting to the vacuole of the yeast general amino acid permease, Gap1', *J Biol Chem,* 276 (47), 43949-57.

Soszynski, M., et al. (1998), 'Radiation inactivation suggests that human multidrug resistance-associated protein 1 occurs as a dimer in the human erythrocyte membrane', *Arch Biochem Biophys,* 354 (2), 311-6.

Spang, A., et al. (2001), 'The ADP ribosylation factor-nucleotide exchange factors Gea1p and Gea2p have overlapping, but not redundant functions in retrograde transport from the Golgi to the endoplasmic reticulum', *Mol Biol Cell,* 12 (4), 1035-45.

Spear, E. D. and Ng, D. T. (2003), 'Stress tolerance of misfolded carboxypeptidase Y requires maintenance of protein trafficking and degradative pathways', *Mol Biol Cell,* 14 (7), 2756-67.

--- (2005), 'Single, context-specific glycans can target misfolded glycoproteins for ER-associated degradation', *J Cell Biol,* 169 (1), 73-82.

Springael, J. Y., et al. (1999), 'NH4+-induced down-regulation of the Saccharomyces cerevisiae Gap1p permease involves its ubiquitination with lysine-63-linked chains', *J Cell Sci,* 112 (Pt 9), 1375-83.

Strickland, E., et al. (2000), 'Recognition of misfolding proteins by PA700, the regulatory subcomplex of the 26 S proteasome', *J Biol Chem,* 275 (8), 5565-72.

Subba Rao, G., Bachhawat, A. K., and Gupta, C. M. (2002), 'Two-hybrid-based analysis of protein-protein interactions of the yeast multidrug resistance protein, Pdr5p', *Funct Integr Genomics,* 1 (6), 357-66.

Supply, P., et al. (1993), 'Proliferation of intracellular structures upon overexpression of the PMA2 ATPase in Saccharomyces cerevisiae', *J Biol Chem,* 268 (26), 19744-52.

Suzuki, T., et al. (2000), 'PNG1, a yeast gene encoding a highly conserved peptide:N-glycanase', *J Cell Biol,* 149 (5), 1039-52.

Swanson, R., Locher, M., and Hochstrasser, M. (2001), 'A conserved ubiquitin ligase of the nuclear envelope/endoplasmic reticulum that functions in both ER-associated and Matalpha2 repressor degradation', *Genes Dev,* 15 (20), 2660-74.

Takeuchi, S. (2006), 'Molecular cloning, sequence, function and structural basis of human heart 150 kDa oxygen-regulated protein, an ER chaperone', *Protein J,* 25 (7-8), 517-28.

Taxis, C., et al. (2003), 'Use of modular substrates demonstrates mechanistic diversity and reveals differences in chaperone requirement of ERAD', *J Biol Chem,* 278 (38), 35903-13.

Travers, K. J., et al. (2000), 'Functional and genomic analyses reveal an essential coordination between the unfolded protein response and ER-associated degradation', *Cell,* 101 (3), 249-58.

Triana-Alonso, F. J., Chakraburtty, K., and Nierhaus, K. H. (1995), 'The elongation factor 3 unique in higher fungi and essential for protein biosynthesis is an E site factor', *J Biol Chem,* 270 (35), 20473-8.

Tyers, M. and Jorgensen, P. (2000), 'Proteolysis and the cell cycle: with this RING I do thee destroy', *Curr Opin Genet Dev,* 10 (1), 54-64.

Van Den Hazel, H. B., Kielland-Brandt, M. C., and Winther, J. R. (1996), 'Review: biosynthesis and function of yeast vacuolar proteases', *Yeast,* 12 (1), 1-16.

van den Hazel, H. B., et al. (1999), 'PDR16 and PDR17, two homologous genes of Saccharomyces cerevisiae, affect lipid biosynthesis and resistance to multiple drugs', *J Biol Chem,* 274 (4), 1934-41.

Vashist, S. and Ng, D. T. (2004), 'Misfolded proteins are sorted by a sequential checkpoint mechanism of ER quality control', *J Cell Biol,* 165 (1), 41-52.

Vashist, S., et al. (2001), 'Distinct retrieval and retention mechanisms are required for the quality control of endoplasmic reticulum protein folding', *J Cell Biol,* 155 (3), 355-68.

Walter, J., et al. (2001), 'Sec61p-independent degradation of the tail-anchored ER membrane protein Ubc6p', *EMBO J,* 20 (12), 3124-31.

Wang, E. J., et al. (2000), 'Cooperativity in the inhibition of P-glycoprotein-mediated daunorubicin transport: evidence for half-of-the-sites reactivity', *Arch Biochem Biophys,* 383 (1), 91-8.

Ward, C. L., Omura, S., and Kopito, R. R. (1995), 'Degradation of CFTR by the ubiquitin-proteasome pathway', *Cell,* 83 (1), 121-7.

Werner, E. D., Brodsky, J. L., and McCracken, A. A. (1996), 'Proteasome-dependent endoplasmic reticulum-associated protein degradation: an unconventional route to a familiar fate', *Proc Natl Acad Sci U S A,* 93 (24), 13797-801.

Wilcox, L. J., et al. (2002), 'Transcriptional profiling identifies two members of the ATP-binding cassette transporter superfamily required for sterol uptake in yeast', *J Biol Chem,* 277 (36), 32466-72.

Willer, M., Forte, G. M., and Stirling, C. J. (2008), 'Sec61p is required for ERAD-L: genetic dissection of the translocation and ERAD-L functions of Sec61P using novel derivatives of CPY', *J Biol Chem,* 283 (49), 33883-8.

Wolfger, H., Mamnun, Y. M., and Kuchler, K. (2004), 'The yeast Pdr15p ATP-binding cassette (ABC) protein is a general stress response factor implicated in cellular detoxification', *J Biol Chem,* 279 (12), 11593-9.

Wolfger, H., et al. (1997), 'The yeast ATP binding cassette (ABC) protein genes PDR10 and PDR15 are novel targets for the Pdr1 and Pdr3 transcriptional regulators', *FEBS Lett,* 418 (3), 269-74.

Wright, R., et al. (1988), 'Increased amounts of HMG-CoA reductase induce "karmellae": a proliferation of stacked membrane pairs surrounding the yeast nucleus', *J Cell Biol,* 107 (1), 101-14.

Ye, Y., Meyer, H. H., and Rapoport, T. A. (2001), 'The AAA ATPase Cdc48/p97 and its partners transport proteins from the ER into the cytosol', *Nature,* 414 (6864), 652-6.

Young, L., et al. (2001), 'Role of the ABC transporter Mdl1 in peptide export from mitochondria', *Science,* 291 (5511), 2135-8.

2006

Département de biologie appliquée et des productions agricoles

N°71. Muratori Frédéric, Reconnaissance des facteurs cuticulaires de l'hôte et conséquences sur l'exploitation des colonies par le parasitoïde de pucerons, *Aphidius rhopalosiphi* (Hymenoptera: Aphidiinae) (Promoteurs : Hance Th., Maraite H.)

N°72. Condori Ali Paulino Bruno, Analyse comparative et modélisation de la croissance et du développement de tubercules andins dans les Andes en Bolivie. (Promoteur : Ledent J-F.)

N°75. Doucet Diane, Development of a model and similarities with a benyvirus. (Promoteur Bragard C.)

N°76. Nkwembe Unsital Guy-Bernard, La problématique de la pauvreté des ménages agricoles ruraux et urbains dans la périphérie de la ville de Kinshasa. Essai d'analyse du phénomène et de ses implications sur la sécurité alimentaire. (Promoteurs : Wautelet J-M., Gaspart F.)

N°78. Ndayiragjie Alexis, Relations entre métabolisme des polyamines et la résistance au stress salin chez le riz (*Oryza sativa* L.). (Promoteurs : Bertin P., Lutts S.)

N°80. Secheli Ringot Diana, Risk analysis of ochratoxin A and developpement of a decontamination procedure based on the biosorption of ochratoxin A onto yeast industry derivatives. (Promoteur : Larondelle Y.)

N°82. Abboudi Tarik, The indispensable amino acid requirements for maintenance in Atlantic salmon fry. (Promoteurs : Larondelle Y., Rollin X.)

N°83. Martins da Silva Evaldo, Polyphenols from the Amazonian plant *Inga edulis*: process optimization for the production of purified extracts with high antioxidant capacity. (Promoteur : Collin S.)

N°84. Fadlaoui Aziz, Modélisation bioéconomique de la conservation des ressources génétiques animales. (Promoteurs : Baret Ph., Roosen J.)

N°85. Kambale Valimunzigha Charles, Étude du comportement physiologique et agronomique de la tomate (*Solanum lycopersicum* L.) en réponse à un stress hydrique précoce. (Promoteurs : Kinet J-M., Ledent J-F.)

N°86. Lepoint Pascale, Speciation within the African Coffee Wilt Pathogen. (Promoteur : Maraite H.)

N°88. Mushagalusa Nachigera Gustave, Competitive relationships in potato/maize intercropping: involvement of root system architecture (Promoteurs : Draye X., Ledent F.)

N°89. Nyamangyoku Ishibwela Obedi, Ferrous iron toxicity: Mechanisms of resistance and impact on nutrient elements at the vegetative stage in cultivated rices (*Oryza sativa* L., *Oryza glaberrima* Steud and interspecific hybrids) (Promoteurs : Ledent J-F., Bertin P.)

Département de chimie appliquée et des bio-industries

N°73. Pety de Thozée Cédric, Implication of the ER quality control in the degradation of the yeast plasma membrane Pdr5 ^{L183P} ABC transporter. (Promoteur : Ghislain M.)

N°79. Gurdak Elzbieta, Supramolecular organization of collagen layers adsorbed on polymers. (Promoteurs : Rouxhet P., Dupont Ch.)

N°87. Janssens Xavier, Monitoring and predicting elusive species colonisation : Application to the otter in the Cévennes National Park (France). (Promoteurs : Baret Ph., Defourny P.)

Département des sciences du milieu et de l'aménagement du territoire

N°74. Kayitakire François, Forest stand characterisation using very high resolutions satellite remote sensing. (Promoteur : Defourny P.)

N°77. Van der Velde Marijn, Agricultural and climatic impacts on the groundwater resources of a small island: measuring and modelling water and solute transport in soil and groundwater on Tongatapu. (Promoteurs : Vanclooster M., Clothier B.)

N°81. Degen Thomas, Dynamique initiale de la végétation herbacée et de la régénération ligneuse dans le cas de trouées, au sein d'une hêtraie (*Luzulo-Fagetum*). (Promoteurs : Devillez F., Jacquemart A-L.)

2007

Département de biologie appliquée et des productions agricoles

N°97, De Dorlodot Sophie, Root system architecture : a genetic analysis in rice. (Promoteur : Draye X.)

N°99, Daoui Khalid**,** Recherche de stratégies d'amélioration de l'efficience d'utilisation du phosphore chez la fève (*Vicia faba* L.) dans les conditions d'agriculture pluviale au Maroc. (Promoteur : Ledent J-F.)

N°101, Vanloqueren, Gaëtan, Penser et gérer l'innovation en agriculture à l'heure du génie génétique . Contribution d'une approche systémique d'innovations scientifiques dans deux filières agroalimentaires wallonnes pour l'évaluation, la gestion et les politiques d'innovation. (Promoteur : Baret Ph.)

N°109, Pairon, Marie, Ecology and population genetics of an invasive forest tree species: *Prunus serotina* Ehrh. (Promoteurs : Jacquemart A-L., Devillez F.)

N°111, Manyonga, Madika, Modelling the competition for light in maize (*Zea mays* L.)/bean (*Phaseolus vulgaris* L.) intercropping with three-dimensional approach. (Promoteur : Ledent J-F.)

N°115, Silva de Souza, Jesus Nazareno, Etude des propriétés antioxydantes *in vitro* d'extraits de feuilles de *Byrsonima crassifolia* et *Inga edulis* et caractérisation partielle des composés phénoliques. (Promoteurs : Larondelle Y., Rogez H.)

N°116, Colinet, Hervé, Une approche écologique et biochimique de la résistance au froid chez un parasitoïde de puceron *Aphidius colemani* (Hymenoptera: Aphidiinae). (Promoteur : Boivin G.)

Département de chimie appliquée et des bio-industries

N°90. Eyers Laurent, Characterization of bacterial populations of 2,4,6-trinitrotoluene (TNT) contaminated soils and isolation of a *Pseudomonas aeruginosa* strain with TNT denitration activities. (Promoteur : Agathos S.)

N°91. Dupré de Boulois, Hervé, Role of arbuscular mycorrhizal fungi on the accumulation of radiocaesium by plants. (Promoteur : Declerck S.)

N°92. Crouzet, Jérôme, Expression pattern, ectopic expression and gene silencing of two *Nicotiana* Pleiotropic Drug Resistance transporters. (Promoteur : Boutry M.)

N°93, Drugmand, Jean-Christophe, Characterization of Insect Cell Lines Is Required for Appropriate Industrial Processes. (Promoteur : Bastin G.)

N°94, De La Providencia, Ivan Enrique, Contribution of Anastomosis and Hyphal Healing Mechanism to the Extraradical Mycelium Architecture of Arbuscular Mycorrhizal Fungi. (Promoteurs : Corbisier A-M., Declerck S.)

N°95, Sebari, Karima, Optimisation de la gestion conjointe des ressources en eau de surface et des ressources en eau souterraines dans une région semi aride - la Vallée du Drâa. (Promoteur : Vanclooster M.)

N°100, Vandermeeren Caroline, Quaternary Structure and Regulation of the *Nicotiana plumbaginifolia* Plasma Membrane Proton Pump ATPase. (Promoteur : Boutry M.)

N°102, Morales Belpaire Isabel, Fate of the active form of proteins in selected environmental matrices. Investigation with green fluorescent protein, β-glucosidase, and amyloid fibrils in wastewater sludges, biofilms and soils. (Promoteur : Gerin P.)

N°103, Trombik Tomasz, Characterization of two Pleiotropic Drug Resistance transporters from *Nicotiana plumbaginifolia*. (Promoteur : Boutry M.)

N°104, Callemien, Delphine, Use of new methodologies to study phenolic compounds through beer storage. (Promoteur : Collin S.)

N°106, Van der Auwera, Géraldine, pAW63: A molecular wanderer in the *Bacillus cereus* gene pool. (Promoteur : Mahillon J.)

N°107, Mateos Pedrero, Cecilia, Synthesis and characterization of Rh supported on Ti-modified oxides: catalytic activity in the partial oxidation of methane. (Promoteur : Ruiz P.)

N°108, Voets, Liesbeth, Role of arbuscular mycorrhizal networks on plant interconnection and carbon transfer. (Promoteurs : Declerck S., Strullu D.G.)

N°110, Jerkovic, Vesna, Découverte du resvératrol dans les houblons. Impact de la variété, de l'année de récolte et du conditionnement en vue de la préparation d'extraits polyphénoliques enrichis en stilbènes. (Promoteur : Delvaux B.)

N°112, Dekeyser, Caroline, Elaboration and evaluation of nanostructured surfaces for the control of cell behavior. (Promoteurs : Marchand J., Rouxhet P.)

N°113, Nonckreman, Cristèle, Design of materials with nanostructured surface to improve hemocompatibility. (Promoteurs : Rouxhet P., Dupont Ch.)

N°114, Caillou, Samuel, Protein Adsorption: from Interfacial Interactions to Enzyme Activity. (Promoteurs : Gerin P., Rouxhet P.)

Département des sciences du milieu et de l'aménagement du territoire

N°96, Lefèvre Isabelle, Investigation of three Mediterranean plant species suspected to accumulate and tolerate high cadmium and zinc levels: morphological,

physiological and biochemical characterization under controlled conditions. (Promoteurs : Delvaux B., Lutts S.)

N°98, Desclée, Baudouin, Automated object-based change detection for forest monitoring by satellite remote sensing: applications in temperate and tropical regions. (Promoteurs : Bogaert P., Defourny P.)

N°105, André, Frédéric, Influence of the heterogeneity of canopy structure on the spatio-temporal variability of atmospheric deposition within a mixed oak-beech stand. (Promoteur : Ponette Q.)

2008

Département de biologie appliquée et des productions agricoles

N°120, Chirinos Gallardo, Rosana Sonia, Polyphenols from the Andean mashua (*Tropaeolum tuberosum*) tuber: Evaluation of genotypes, extraction, chemical characterization and antioxidant properties. (Promoteurs : Larondelle Y., Campos D.)

N°126, Romier Béatrice, Modulation of intestinal inflammation by polyphenols. (Promoteurs : Larondelle Y., Schneider Y-J.)

N°130, Vaïanopoulos Céline, Widespread occurrence of soil-borne mosaic viruses in Belgium. Preferential associations of *Polymyxa graminis* and mosaic viruses on cereals. (Promoteurs : Bragard C., Legrève A.)

N°131, Tran Thi Nang Thu, Nutritional value of sesame oil cake and lysine utilization efficiency in plant protein-based diets for rainbow trout. (Promoteurs : Larondelle Y., Rollin X.)

N°134, Ngirente Edouard, Les marchés agricoles intérieurs et les mutations agro-économiques en milieu rural rwandais. Application à la filière pomme de terre. (Promoteurs : Gaspart F., Wautelet J-M.)

N°139, Gilbert Valérie, Genetic and pathogenic diversity of *Pseudomonas syringae* isolates associated with diseases on Belgian fruit trees. (Promoteurs : Maraite H., Bultreys A.)

N°141, Delpierre Matthieu, A Non-cooperative Approach to Rural Development Issues. (Promoteur : Gaspart F.)

N°142, André Christelle, Evaluation of Andean potato cultivars as a source of dietary antioxidants. (Promoteurs : Larondelle Y., Bvers D.)

N°145, Bodin Noëlie, Nutritional and interspecies effects on the estimation of threonine and lysine requirements in salmonid fry with a highlight on methodological impacts. (Promoteurs : Larondelle Y., Rollin X.)

N°147, Pissard Audrey, Structure and genetic diversity of two Andean tuber crops, oca (*Oxalis tuberosa* Mol.) and mashua (*Tropaeolum tuberosum* R.&P.): influence of the mode of conservation and of the agronomic and biological characteristics. (Promoteur : Bertin P.)

Département de chimie appliquée et des bio-industries

N° 117, Zelazny Enric, Regulation of maize aquaporin trafficking to the plasma membrane. (Promoteur : Chaumont F.)

N°122, Bobik Krzysztof, The two major tobacco plasma membrane H^+-ATPases, PMA2 and PMA4 are differentially phosphorylated on their penultimate threonine. (Promoteur : Boutry M.)

N° 123, Cabana Hubert, Elimination des perturbateurs endocriniens nonylphénol, bisphénol A et triclosan à l'aide de laccase de Coriolopsis polyzona. C. (Promoteurs : Agathos S., Peter Jones J.)

N°129, Srasra Mondher, Preparation and characterization of new basic catalyst by nitridation of Y zeolites. (Promoteurs : Delsarte S., Gaigneaux E.)

N°132, De Palmenaer Daniel, Genomic portrayal of IS*4* family –Modular insertion sequences, mobile insertion cassettes and overall family snapshot. (Promoteur : Mahillon J.)

N°133, Delannoy Mélanie, Identification of peptidases in the *Nicotiana tabacum* leaf intercellular fluid. (Promoteurs : Boutry M., Navarre C.)

N°135, Manente Myriam, Rta1, a yeast plasma membrane protein which confers resistance to fungicides. (Promoteur : Ghislain M.)

N°137, Hachez Charles, The expression pattern and activity of *Zea mays* plasma membrane aquaporins highlight their central role in the control of the cell membrane water permeability. (Promoteur : Chaumont F.)

N°146, Soria Miguel Angel, Etude des paramètres gouvernant les performances catalytiques d'AlPO, AlGaPO et GaPO purs et en présence de vanadium dans l'ammoxydation du propane. (Promoteurs : Gaigneaux E., Ruiz P.)

Département des sciences du milieu et de l'aménagement du territoire

N°118, Van Cauwenbergh Nora, Expert and local knowledge in decision support for natural resource management. (Promoteur : Ahlers R.)

N°119, Henriet Céline, Silicon in banana (*Musa* spp.): a soil-plant system approach.C. (Promoteur : Delvaux B.)

N°121, Tidjani Adamou Didier, Erosion éolienne dans le Damagaram Est (Sud-Est du Niger) : Paramétrisation, quantification et moyens de lutte. (Promoteurs : Bielders Ch., Ambouta K.J.M.)

N°124, Akponikpe Pierre Bienvenu Irénikatché, Millet response to water and soil fertility management in the Sahelian Niger: experiments and modeling Erosion éolienne dans le Damagaram Est (Sud-Est du Niger) : Paramétrisation, quantification et moyens de lutte. (Promoteurs : Bielders Ch., Gérard B.)

N°125, Vancutsem Christelle, Revisiting satellite time series compositing for earth observation applications. (Promoteur : Defourny P.)

N°127, Opfergelt Sophie, Silicon cycle in the soil-plant system: biogeochemical tracing using Si isotopes. (Promoteurs : Delveux B., André L.)

N°128, de Araujo Marinho Filho Eduardo Celsio, Economics of Hunger: Several Methods, Levels and Scales. (Promoteurs : Defourny P., Gaspart F.)

N°136, Saqalli Mehdi, Populations, Farming systems & Social transitions in Sahelian Niger: An Agent-based modeling approach. (Promoteurs : Defourny P., Bielders Ch.)

N°138, Lucau-Danila Cozmin Catalin, LAI retrieval from SAR remote sensing for crop monitoring at regional scale. (Promoteur : Defourny P.)

N°140, Iboukassene Soraya, Dynamique de la végétation des forêts à *Quercus suber* anthropisées du Nord-Est de l'Algérie (Parc National d'El-Kala). (Promoteur : Devillez)

N°143, Fasbender Dominique, Bayesian data fusion in environmental sciences : Theory and applications. (Promoteur : Bogaert P.)

N°144, Hoang Thi Thai, Hoa, Soil characteristics, cropping patterns, and use of organic resources in the coastal sandy area of Thua Thien Hue province, Central Vietnam. (Promoteur : Dufey J.)

2009

N°148, Pokrzywa Wojcieh, Targeting of the yeast Sna3p and Sna4p to the endosomal pathway depends on their interaction with ubiquitin ligase Rsp5p (Promoteur: Morsomme P. / février 2009)

N°149, de Lespinay Alexis, Study of seed priming mechanisms of three plant species used in revegetation of industrial sites (Promoteurs : Lutts S., Declerck S. / mai 2009)

N°150, Hoton Florence, Insights into the Ecology and Genetic Diversity of Cereulide-producing Bacillus cereus strains (Promoteur : Mahillon J. / mai 2009)

N°151, Fornelos Martins Nadine, GIL01 and relatives, a new generation of tectiviruses infecting the *Bacillus cereus* group (Promoteur : Mahillon J. / mai 2009)

N°152, Marghadi Saïd, Intégration des méthodes d'aide à la décision dans l'aménagement multifonctionnel des forêts au Maroc (Promoteurs : Devillez F., Farcy Ch. / juillet 2009)

N°153, Harahagazwe Dieudonné, Heat tolerance assessment of the potato crop: evaluation of CIP clones in the lowlands of Burundi (Promoteurs: Ledent J-F., Rusuku G. / août 2009)

N°154, Godet Marie, Survey of filamentous fungi and development of molecular tools for their rapid and accurate identification, in advanced life support systems like the International Space Station (Promoteurs: Declerck S., Munaut F. / septembre 2009)

N°155, Verbelen Claire, Nanoscale probing of the mycobacterial cell wall (Promoteur: Dufrêne Y. / octobre 2009)

N°156, Gaidashova Svetlana, Effect of plant parasitic nematodes and arbuscular mycorrhizal fungi on banana (*Musa* spp.) in the East African highland cropping systems (Promoteurs: Declerck S., De Waele D. / octobre 2009)

N°157, Gyuricza Veronika, Influence of arbuscular mycorrhizal fungi on the uptake and accumulation of radiocesium by plants and on its redistribution between plants (Promoteur: Declerck S. / novembre 2009)

N°158, Stenuit Benoît, Biological Degradation of 2,4,6-Trinitrotoluene (TNT): Bioprospecting for TNT-Denitrating Bacteria and Deciphering of Multiple TNT Denitration Pathways (Promoteur : Agathos S. / octobre 2009)

N°159, De Muynck Benoit, Expression of a functional antibody in *Nicotiana tabacum* plants and culture cells: analysis of proteolytic products and identification of putative extracellular peptidases involved (Promoteurs: Boutry M., Navarre C. / décembre 2009)

N°160, Mattern Samuel, Mapping and source identification of groundwater pollution by nitrate: Theory and application to the Brusselian sand groundwater body (Promoteur: Bogaert P. / décembre 2009)

N°161, Mehrvar Mohsen, Harahagazwe, Dieudonné, Diversity of soil-borne sugar beet viruses in Iran (Promoteur: Bragard C. / novembre 2009)

2010

N°162, Radoux Julien, Updating lan cover maps by GIS-driven analysis of very high resolution satellite images (Promoteur: Defourny P. / 13 janvier 2010)

N°163, Cochonneau Daphné, Characterization of yeast polymerase gamma mutations associated with human disorders (Promoteur: Foury F. / 24 mars 2010)

N°164, Obsomer Valérie Daphné, Multiscale environmental analysis and prediction for insects vector of disease : Application to malaria vectors in Southest Asia (Promoteur: Defourny P. / 7 mai 2010)

N°165, Lebrun Anne-Sophie, Towards functional and structural characterization of maize ZmSIP proteins belonging to a divergent aquaporin subfamily (Promoteur: Chaumont F. / 8 mars 2010)

N°166, Kalonda Mbulu Gabriel, Analyse de la transmission des prix internationaux des produits agricoles sur les marchés des pays ACP (Promoteur: Henry de Frahan B. / 15 mars 2010)

N°167, Fiamohe Rose, Facteur determinant les échanges de produits vivriers au Bénin : Rôle des institutions de marché (Promoteur : Henry de Frahan B. / 20 avril 2010)

N°168, Hochstenbach Jean-François, The yeast proteolipid Pmp3p is a new component of the plasma membrane microdomains associated with the eisosomes (Promoteur : Morsomme P. / 4 mai 2010)

N°169, Laloy Eric, Measuring and modeling the impact of intercrop management on plotscale runoff and erosion in a continuous maize cropping system (Promoteur : Bielders C. / 31 mai 2010)

N°170, Debecker Damien, MoO3-based heterogeneous catalysts for the metathesis of propene (Promoteur : Gaigneaux E. / 28 mai 2010)

N°171, Cornelis Jean-Thomas, Impact of tree species on silicon cycling in temperate soil-tree systems (Promoteur : Delvaux B. / 25 mai 2010)

N°172, Bontemps Sophie, Towards an automated satellite-based alarm system for global forest monitoring (Promoteur : Defourny P. / 17 juin 2010)

$t_{1/2}$ (min)	wt BY4742	doa10Δ BY4742	hrd1Δ BY4742	der1Δ BY4742	pep4Δ BY4742	MHY501	doa10Δ MHY501	hrd1Δ MHY501	doa10Δ hrd1Δ MHY501	YPM30 25°C	YPM30 37°C	sec12 YPM30 25°C	sec12 YPM30 37°C	sec18 YPM30 25°C	sec18 YPM30 37°C	ret3 YPM30 25°C	ret3 YPM30 37°C
Pdr5	> 60	> 60	> 60	> 60	> 60	> 60	> 60	> 60	> 60	> 60	> 60	> 60	> 60	> 60	> 60	> 60	> 60
$Pdr5^{C1427Y}$	25 ± 4	> 60	> 60	> 60	25 ± 5	26 ± 4	> 60	> 60	> 60	29 ± 5	30 ± 6	9 ± 3	> 60	16 ± 3	> 60	11 ± 2	> 60
$Pdr5^{L1183P}$	33 ± 5	> 60	> 60	> 60	22 ± 4	38 ± 8	> 60	> 60	> 60	24 ± 3	26 ± 6	12 ± 5	> 60	24 ± 5	26 ± 6	9 ± 4	15 ± 3
$Pdr5^{L1183P-C1427Y}$	8 ± 3	> 60	> 60	> 60	8 ± 3	23 ± 4	> 60	> 60	> 60	11 ± 3	17 ± 4	16 ± 6	> 60	7 ± 4	> 60	16 ± 6	> 60
$Pdr5^{TM1-4}$	9 ± 3	> 60	4 ± 2	4 ± 1	7 ± 3	8 ± 3	> 60	16 ± 3	> 60	13 ± 5	6 ± 2	7 ± 4	> 60	6 ± 2	11 ± 5	7 ± 4	8 ± 5
$Pdr5^{TM1-8}$	> 60	> 60	> 60	> 60	> 60	> 60	> 60	> 60	> 60	> 60	> 60	> 60	> 60	> 60	> 60	> 60	> 60
$Pdr5^{TM1-12}$	22 ± 5	24 ± 5	28 ± 4	18 ± 3	45 ± 5	28 ± 5	25 ± 4	17 ± 4	> 60	11 ± 6	11 ± 8	26 ± 6	> 60	21 ± 5	> 60	14 ± 9	14 ± 7